

Zoonotic negative-sense RNA viruses

Edited by

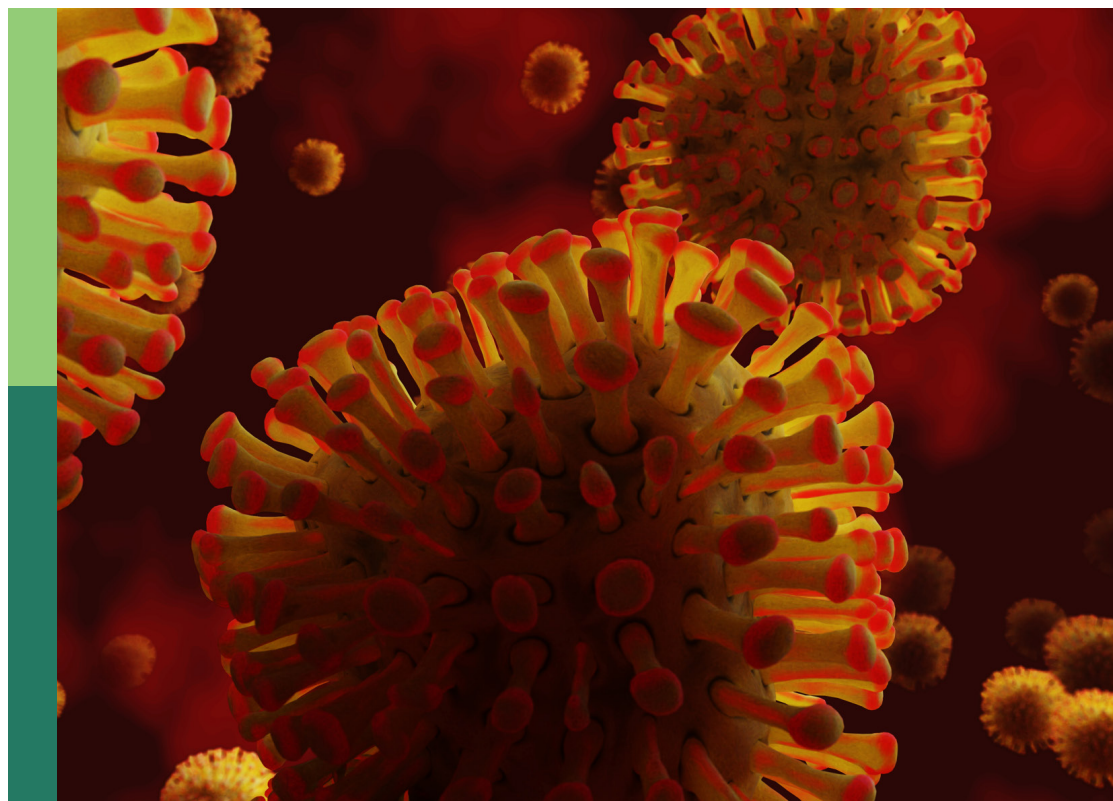
Jasmina M. Luczo and Sarah J. Edwards

Published in

Frontiers in Veterinary Science

Frontiers in Immunology

Frontiers in Virology



FRONTIERS EBOOK COPYRIGHT STATEMENT

The copyright in the text of individual articles in this ebook is the property of their respective authors or their respective institutions or funders. The copyright in graphics and images within each article may be subject to copyright of other parties. In both cases this is subject to a license granted to Frontiers.

The compilation of articles constituting this ebook is the property of Frontiers.

Each article within this ebook, and the ebook itself, are published under the most recent version of the Creative Commons CC-BY licence. The version current at the date of publication of this ebook is CC-BY 4.0. If the CC-BY licence is updated, the licence granted by Frontiers is automatically updated to the new version.

When exercising any right under the CC-BY licence, Frontiers must be attributed as the original publisher of the article or ebook, as applicable.

Authors have the responsibility of ensuring that any graphics or other materials which are the property of others may be included in the CC-BY licence, but this should be checked before relying on the CC-BY licence to reproduce those materials. Any copyright notices relating to those materials must be complied with.

Copyright and source acknowledgement notices may not be removed and must be displayed in any copy, derivative work or partial copy which includes the elements in question.

All copyright, and all rights therein, are protected by national and international copyright laws. The above represents a summary only. For further information please read Frontiers' Conditions for Website Use and Copyright Statement, and the applicable CC-BY licence.

ISSN 1664-8714
ISBN 978-2-8325-4589-8
DOI 10.3389/978-2-8325-4589-8

About Frontiers

Frontiers is more than just an open access publisher of scholarly articles: it is a pioneering approach to the world of academia, radically improving the way scholarly research is managed. The grand vision of Frontiers is a world where all people have an equal opportunity to seek, share and generate knowledge. Frontiers provides immediate and permanent online open access to all its publications, but this alone is not enough to realize our grand goals.

Frontiers journal series

The Frontiers journal series is a multi-tier and interdisciplinary set of open-access, online journals, promising a paradigm shift from the current review, selection and dissemination processes in academic publishing. All Frontiers journals are driven by researchers for researchers; therefore, they constitute a service to the scholarly community. At the same time, the *Frontiers journal series* operates on a revolutionary invention, the tiered publishing system, initially addressing specific communities of scholars, and gradually climbing up to broader public understanding, thus serving the interests of the lay society, too.

Dedication to quality

Each Frontiers article is a landmark of the highest quality, thanks to genuinely collaborative interactions between authors and review editors, who include some of the world's best academicians. Research must be certified by peers before entering a stream of knowledge that may eventually reach the public - and shape society; therefore, Frontiers only applies the most rigorous and unbiased reviews. Frontiers revolutionizes research publishing by freely delivering the most outstanding research, evaluated with no bias from both the academic and social point of view. By applying the most advanced information technologies, Frontiers is catapulting scholarly publishing into a new generation.

What are Frontiers Research Topics?

Frontiers Research Topics are very popular trademarks of the *Frontiers journals series*: they are collections of at least ten articles, all centered on a particular subject. With their unique mix of varied contributions from Original Research to Review Articles, Frontiers Research Topics unify the most influential researchers, the latest key findings and historical advances in a hot research area.

Find out more on how to host your own Frontiers Research Topic or contribute to one as an author by contacting the Frontiers editorial office: frontiersin.org/about/contact

Zoonotic negative-sense RNA viruses

Topic editors

Jasmina M. Luczo – CSIRO Australian Centre for Disease Preparedness, Australia

Sarah J. Edwards – Commonwealth Scientific and Industrial Research Organisation (CSIRO), Australia

Citation

Luczo, J. M., Edwards, S. J., eds. (2024). *Zoonotic negative-sense RNA viruses*.

Lausanne: Frontiers Media SA. doi: 10.3389/978-2-8325-4589-8

Table of contents

04	Editorial: Zoonotic negative-sense RNA viruses Sarah J. Edwards and Jasmina M. Luczo
07	South American H4N2 influenza A virus improved replication in chicken trachea after low number of passages Lucas M. Ferreri, Silvia Carnaccini, Valeria Olivera, Ariel Pereda, Daniela Rajao and Daniel R. Perez
14	Detection of intercontinental reassortant H6 avian influenza viruses from wild birds in South Korea, 2015 and 2017 Ji-Yun Kim, Sun-Hak Lee, Da-Won Kim, Dong-Wook Lee, Chang-Seon Song, Dong-Hun Lee and Jung-Hoon Kwon
20	Chimeric H5 influenza virus-like particle vaccine elicits broader cross-clade antibody responses in chickens than in ducks Jaekeun Park, Chang-Seon Song, David Hyunjung Chung, Sangyong Choi, Junghoon Kwon, Sungsu Youk and Dong-Hun Lee
28	Age is a determinant factor in the susceptibility of domestic ducks to H5 clade 2.3.2.1c and 2.3.4.4e high pathogenicity avian influenza viruses Sun-Hak Lee, Jiho Lee, Jin-Yong Noh, Jei-Hyun Jeong, Jun-Beom Kim, Jung-Hoon Kwon, Sungsu Youk, Chang-Seon Song and Dong-Hun Lee
36	Comparative analysis of PB2 residue 627E/K/V in H5 subtypes of avian influenza viruses isolated from birds and mammals Kelsey Briggs and Darrell R. Kapczynski
44	Natural hosts and animal models for Rift Valley fever phlebovirus Yuqing Xu, Xiao Wang, Lu Jiang, Yixuan Zhou, Yihan Liu, Fei Wang and Leiliang Zhang
55	Oral mucosa immunity: ultimate strategy to stop spreading of pandemic viruses Hyesun Jang, Michele Matsuoka and Marcelo Freire
69	classLog: Logistic regression for the classification of genetic sequences Michael A. Zeller, Zebulun W. Arendsee, Gavin J.D. Smith and Tavis K. Anderson
78	Development and characterization of an immortalized swine respiratory cell line for influenza A virus research Peter J. Neasham, Vasilis C. Pliasis, J. Fletcher North, Celeste Johnson, S. Mark Tompkins and Constantinos S. Kyriakis
88	Influenza virus immune imprinting dictates the clinical outcomes in ferrets challenged with highly pathogenic avian influenza virus H5N1 Ivette A. Nuñez, Hyesun Jang, Ying Huang, Alyson Kelvin and Ted M. Ross



OPEN ACCESS

EDITED AND REVIEWED BY

Michael Kogut,
United States Department of Agriculture,
United States

*CORRESPONDENCE

Jasmina M. Luczo
✉ jasmina.luczo@csiro.au

RECEIVED 11 February 2024

ACCEPTED 19 February 2024

PUBLISHED 01 March 2024

CITATION

Edwards SJ and Luczo JM (2024) Editorial:
Zoonotic negative-sense RNA viruses.
Front. Vet. Sci. 11:1384858.
doi: 10.3389/fvets.2024.1384858

COPYRIGHT

© 2024 Edwards and Luczo. This is an open-access article distributed under the terms of the [Creative Commons Attribution License \(CC BY\)](#). The use, distribution or reproduction in other forums is permitted, provided the original author(s) and the copyright owner(s) are credited and that the original publication in this journal is cited, in accordance with accepted academic practice. No use, distribution or reproduction is permitted which does not comply with these terms.

Editorial: Zoonotic negative-sense RNA viruses

Sarah J. Edwards¹ and Jasmina M. Luczo^{2*}

¹Health and Biosecurity, Australian Centre for Disease Preparedness, Commonwealth Scientific and Industrial Research Organisation, Geelong, VIC, Australia, ²Australian Animal Health Laboratory, Australian Centre for Disease Preparedness, Commonwealth Scientific and Industrial Research Organisation, Geelong, VIC, Australia

KEYWORDS

negative-sense RNA viruses, zoonotic viruses, one health, pathogenesis of infection, host pathogen interactions, host response to infection

Editorial on the Research Topic

Zoonotic negative-sense RNA viruses

Zoonotic negative-sense RNA viruses pose a major threat to animal and human health and have caused numerous significant outbreaks, including the 1918 Spanish influenza pandemic (1), the 2009 swine influenza pandemic (2), Ebola virus outbreaks (3), Rift Valley fever virus outbreaks (4), and the H5 highly pathogenic avian influenza virus (HPAIV) panzootic (5). The World Health Organization list of priority pathogens includes numerous negative-sense viruses that pose a significant public health threat due to their epidemic potential and lack of medical countermeasures. As part of outbreak preparedness frameworks, it is crucial to understand factors that contribute to the emergence, maintenance, infection, and spill-over of zoonotic negative-sense viruses.

The aim of this Research Topic was to provide novel insights into zoonotic negative-sense RNA virus biology, disease pathogenesis, host response to infection and countermeasures to mitigate the impact of these viruses.

Currently, H5 goose/Guangdong (gs/Gd)-lineage subclade 2.3.4.4b HPAIVs are causing widespread outbreaks globally. Concerningly, mammal-to-mammal transmission was reported in late 2022 (6). A well-known mammalian adaption of avian influenza viruses (AIVs) is the polymerase basic 2 E627K which enables AIV polymerases to use human ANP32 proteins to replicate (7–9). Briggs and Kapczynski performed a comparative analysis of PB2 E627K/V in H5 AIVs and described low prevalence of E627K in non-gs/Gd-lineages (American, 0.25%; Eurasian 1.03%) and a higher prevalence in the gs/Gd-lineage (range: 0.0–11.7%). In the evolutionary successful H5 gs/Gd-lineage HPAIV subclade 2.3.4.4b, E627K prevalence is 1.0%, suggesting the majority of subclade 2.3.4.4b H5 HPAIVs detected remain adapted to replication in avian species. Notably, E627K was present in 39.1% of human origin H5 AIV sequences, suggesting a non-exclusive requirement.

Vaccination of poultry is considered crucial to protect both animal and public health (10). Park et al. characterized the immunogenicity of a chimeric virus-like particle (VLP) vaccine co-expressing haemagglutinin from gs/Gd-lineage H5 clade 1 and clade 2 (subclade 2.3.2.1c) HPAIVs. The chimeric VLP vaccine elicited a broader antibody response compared to the monovalent VLP vaccine in chickens and ducks. Overall, the VLP vaccine elicited higher and broader serum HI responses in chickens compared to ducks. This VLP vaccine platform enables differentiating infected from vaccinated individuals, making it a valuable tool for the eradication of AIV in poultry whilst

ensuring food security. Importantly, vaccination of older ducks will be crucial for HPAIV control, as [Lee et al.](#) demonstrated that, whilst young ducks are highly susceptible to severe HPAIV disease and shed higher titres of virus, older ducks do not display clinical disease signs or mortality despite shedding high titres of virus. This highlights the potential for older ducks to maintain and spread HPAIV in the absence of clinical disease signs and suggests that vaccination programs should be targeted toward older ducks.

Another critical area of pandemic preparedness is the development of H5 vaccines for public health. [Nuñez et al.](#) demonstrated that immune imprinting with group 1 influenza A viruses (IAVs) (H1N1, H2N3), but not group 2 (H3N2), elicited complete protection following challenge with group 1 H5N1 HPAIV. H3 (group 2) infection of H1 (group 1)-imprinted ferrets did not abrogate protection from H5 HPAIV challenge. Conversely, H5 Hu-COBRA 2 VLP or H5 recombinant HA vaccination of H3 imprinted ferrets afforded protection against H5 HPAIV challenge. Group 1 pdmH1N1 recombinant HA vaccination of H3 pre-immune ferrets elicited partial protection against H5 HPAIV challenge. This study describes group 1 IAVs eliciting cross-reactive protection against heterologous H5 HPAIV challenge and can inform public health vaccination strategies. Complementary to this, the review by [Jang et al.](#) of oral mucosal immunity discusses the importance of eliciting sterilizing immunity at the oral mucosa to control transmission of respiratory viruses of pandemic concern. Strategies to improve the induction of sterilizing oral mucosal immunity, including novel mucosal vaccines and adjuvants and delivery systems, were reviewed with current barriers and opportunities described.

Avian influenza viruses are maintained in wild birds and continue to evolve and spread globally. [Kim et al.](#) described the detection of Eurasian H6 viruses in South Korea that harbor North American-lineage internal genes, highlighting continual intercontinental spread of AIVs and the need for continued surveillance. The wild bird origin H6 viruses displayed minimal infectivity in chickens, suggesting they were poorly adapted to chickens. Interestingly, [Ferreri et al.](#) demonstrated that wild bird-origin H4N2 AIV minimally passaged in chickens acquired increased fitness as evidenced by wider tissue tropism and longer duration of shedding in experimentally infected chickens. This highlights the continued evolution and adaptation potential of AIVs.

Swine IAVs (sIAVs) pose a significant threat to human and swine populations globally. Notably, the pdmH1N1 sIAV emerged in swine from a reassortment event between a triple reassortant sIAV (harboring gene segments from human IAV, sIAV, and AIV) and a Eurasian avian-like sIAV (2). [Zeller et al.](#) developed classLog, a general-purpose machine learning classifier to assign taxonomic classifications to virus sequence data without the need to infer evolutionary history. sIAV H1N1 haemagglutinin and Porcine Reproductive and Respiratory Syndrome virus ORF5 datasets were used to validate the classifiers. A classLog classifier trained on a sIAV dataset with 12 features (0.5% of features) and 0% sequence degradation (perfect sequence quality) was 100% accurate. At 10% sequence degradation, 121 features (5% of features) were needed to achieve 100% accuracy. At 20 and

30% sequence degradation, 243 features (10% of features) resulted in 100 and 93% accuracy, respectively. Uncoupling of inference of viral evolutionary history and virus classification increases the rapidity of classification with high accuracy. Importantly, this pipeline can be applied to real time genomic classification in the field. [Neasham et al.](#) developed an immortalized swine bronchial respiratory cell line for characterization and risk assessment of sIAVs in a relevant host cell line. The immortalized respiratory cell line was primarily of epithelial origin and maintained epithelial morphology, expressed a-2,3- and a-2,6-linked sialic acid receptors, was permissive to sIAVs and human IAVs, and was functionally immunocompetent, as evidenced by cytokine production.

Finally, [Xu et al.](#) undertook a review of Rift Valley fever phlebovirus (RVFV) with a focus on natural hosts and the pathogenesis of RVFV in animal models of infection.

Collectively, this Research Topic highlighted current research activities on zoonotic negative-sense RNA viruses. It is critical to understand viral evolution, infection dynamics, and the host response to infection to inform pandemic preparedness frameworks and develop effective diagnostic tools and countermeasures to combat these viruses.

Author contributions

SE: Writing—review & editing, Conceptualization. JL: Writing—original draft, Writing—review & editing, Conceptualization.

Funding

The author(s) declare no financial support was received for the research, authorship, and/or publication of this article.

Acknowledgments

We thank the editors, authors, and reviewers that contributed to this Research Topic.

Conflict of interest

The authors declare that the research was conducted in the absence of any commercial or financial relationships that could be construed as a potential conflict of interest.

Publisher's note

All claims expressed in this article are solely those of the authors and do not necessarily represent those of their affiliated organizations, or those of the publisher, the editors and the reviewers. Any product that may be evaluated in this article, or claim that may be made by its manufacturer, is not guaranteed or endorsed by the publisher.

References

1. Taubenberger JK, Reid AH, Krafft AE, Bijwaard KE, Fanning TG. Initial genetic characterization of the 1918 “Spanish” influenza virus. *Science*. (1997) 275:1793–6. doi: 10.1126/science.275.5307.1793
2. Smith GJD, Vijaykrishna D, Bahl J, Lycett SJ, Worobey M, Pybus OG, et al. Origins and evolutionary genomics of the 2009 swine-origin H1N1 influenza A epidemic. *Nature*. (2009) 459:1122–5. doi: 10.1038/nature08182
3. Jacob ST, Crozier I, Fischer WA, Hewlett A, Kraft CS, Vega MaDL, et al. Ebola virus disease. *Nat Rev Dis Prim*. (2020) 6:13. doi: 10.1038/s41572-020-0147-3
4. Linthicum KJ, Britch SC, Anyamba A. Rift Valley fever: an emerging mosquito-borne disease. *Annu Rev Entomol*. (2016) 61:395–415. doi: 10.1146/annurev-ento-010715-023819
5. Who One Health High Level Expert Panel. *The Panzootic Spread of Highly Pathogenic Avian Influenza H5N1 Sublineage 2.3.4.4b: a Critical Appraisal of One Health Preparedness and Prevention*. (2023). Available online at: <https://cdn.who.int/media/docs/default-source/one-health/ohhlep/panzootic-spread-of-highly-pathogenic-avian-influenza.pdf> (accessed January 22, 2024).
6. Agüero M, Monne I, Sánchez A, Zecchin B, Fusaro A, Ruano MJ, et al. Highly pathogenic avian influenza A(H5N1) virus infection in farmed minks, Spain, October 2022. *Eurosurveillance*. (2023) 28:2300001. doi: 10.2807/1560-7917.ES.2023.28.3.2300001
7. Long JS, Giotis ES, Moncorgé O, Frise R, Mistry B, James J, et al. Species difference in ANP32A underlies influenza A virus polymerase host restriction. *Nature*. (2016) 529:101–4. doi: 10.1038/nature16474
8. Sheppard CM, Goldhill DH, Swann OC, Staller E, Penn R, Platt OK, et al. An influenza A virus can evolve to use human ANP32E through altering polymerase dimerization. *Nat Commun*. (2023) 14:6135. doi: 10.1038/s41467-023-41308-4
9. Staller E, Sheppard CM, Neasham PJ, Mistry B, Peacock TP, Goldhill DH, et al. ANP32 proteins are essential for influenza virus replication in human cells. *J Virol*. (2019) 93:19. doi: 10.1128/JVI.00217-19
10. Mumford E, Bishop J, Hendrickx S, Embarek PB, Perdue M. Avian influenza H5N1: risks at the human-animal interface. *Food Nutr Bull*. (2007) 28:S357–63. doi: 10.1177/15648265070282S215



OPEN ACCESS

EDITED BY

Jasmina M. Luczo,
CSIRO Australian Centre for Disease
Preparedness, Australia

REVIEWED BY

Lynn Nazareth,
Australian Animal Health Laboratory (CSIRO),
Australia
Stacey Lynch,
Commonwealth Scientific and Industrial
Research Organisation (CSIRO), Australia

*CORRESPONDENCE

Daniel R. Perez
✉ dperez1@uga.edu

PRESENT ADDRESS

Lucas M. Ferreri,
Department of Microbiology and Immunology,
School of Medicine,
Emory University,
Atlanta, GA, United States

RECEIVED 08 March 2023

ACCEPTED 03 May 2023

PUBLISHED 31 May 2023

CITATION

Ferreri LM, Carnaccini S, Olivera V, Pereda A,
Rajao D and Perez DR (2023) South American
H4N2 influenza A virus improved replication in
chicken trachea after low number of passages.
Front. Vet. Sci. 10:1182550.
doi: 10.3389/fvets.2023.1182550

COPYRIGHT

© 2023 Ferreri, Carnaccini, Olivera, Pereda,
Rajao and Perez. This is an open-access article
distributed under the terms of the [Creative
Commons Attribution License \(CC BY\)](#). The
use, distribution or reproduction in other
forums is permitted, provided the original
author(s) and the copyright owner(s) are
credited and that the original publication in this
journal is cited, in accordance with accepted
academic practice. No use, distribution or
reproduction is permitted which does not
comply with these terms.

South American H4N2 influenza A virus improved replication in chicken trachea after low number of passages

Lucas M. Ferreri^{1,2†}, Silvia Carnaccini¹, Valeria Olivera²,
Ariel Pereda³, Daniela Rajao¹ and Daniel R. Perez^{1*}

¹Department of Population Health, Poultry Diagnostic and Research Center, College of Veterinary Medicine, University of Georgia, Athens, GA, United States, ²Instituto de Virología CICVyA, Instituto Nacional de Tecnología Agropecuaria (INTA), Castelar, Buenos Aires, Argentina, ³Programa Nacional de Sanidad Animal, Instituto Nacional de Tecnología Agropecuaria (INTA), Castelar, Buenos Aires, Argentina

Introduction of influenza A viruses (FLUAV) into poultry from waterfowl is frequent, producing economic burden and increasing the probability of human infections. We have previously described the presence of FLUAV in wild birds in Argentina with unique evolutionary trajectories belonging to a South American lineage different from the North American and Eurasian lineages. Adaptability of this South American lineage FLUAV to poultry species is still poorly understood. In the present report, we evaluated the capacity of an H4N2 FLUAV from the South American lineage to adapt to chickens after low number of passages. We found that five mutations were acquired after five passages in 3-days-old chickens. These mutations produced a virus with better infectivity in *ex vivo* trachea explants but overall lower infection in lung explants. Infection of 3-week-old chickens persisted for a longer period and was detected in more tissues than the parental virus, suggesting adaptation of the H4N2 influenza A virus to chicken.

KEYWORDS

influenza A virus, adaptation, subtype H4N2, poultry, waterfowl

Introduction

Influenza A viruses (FLUAV) from waterfowl are of global concern. Multiple pandemics have occurred as the product of genetic exchange between FLUAV circulating in humans and the avian reservoir (1). FLUAV contains eight gene segments, two of which encode for the surface glycoproteins hemagglutinin and neuraminidase (HA and NA, respectively). The other six for the internal gene cassette, comprised by the set of polymerases, PB2, PB1 and PA, the nucleoprotein NP, the matrix segment M and NS, which encodes for nonstructural proteins. While HA and NA are responsible for the entrance to and exit from the cell, the internal genes perform replication, innate immune evasion, and physical support among other functions. The 18 HA and 11 NA subtypes of FLUAV are classified by their antigenic properties whereas the internal gene cassettes are divided by their origin. Three major lineages of avian FLUAV internal genes have been described: Eurasian, North American, and South American lineages (2).

Among the most prevalent FLUAV circulating in waterfowls, the H4 subtype has been detected frequently in domestic avian species across Asia, Europe, and North America since it was first isolated from a duck in 1956, highlighting its wide distribution (3). Furthermore, some

H4s have been shown to infect mice (4–6), pigs (7), and marine mammals (8) without prior adaptation, indicating ability to switch hosts between avian and mammalian species.

Chicken (*Gallus gallus domesticus*) meat and eggs are among the most consumed animal-based proteins, making this species widely distributed worldwide. Chickens are risen in large numbers and found at high densities within commercial farms, a scenario that increases the probability of virus transmission and adaptation upon new introductions. Chickens can be infected with a broad range of FLUAV and can act as intermediate species between waterfowl and mammalian hosts (9, 10). Studies showed that farmers, workers, and veterinarians in the poultry industry are at higher risk of infection with zoonotic FLUAVs, including H4 viruses (11, 12).

In the present work, we evaluated the adaptability of a H4N2 influenza A virus, from the South American lineage isolated from silver teal (*Anas versicolor*) in Argentina. We found that mutations were acquired after five passages, and that, even though absent or at low frequency in nature, they conferred better replication *in vivo*. Furthermore, we show fitness improvement in the trachea but not in the lungs, suggesting that the acquired substitutions were positively selected. Overall, we show that the H4 subtype from the South American lineage isolated from wild birds requires only a few passages to adapt to chicken.

Materials and methods

Viruses and cells

The isolation of the duck A/silver teal/Argentina/CIP051-32/2011 (H4N2) virus (32/H4N2) has been previously described (2). The P5Ch32/H4N2 virus was sequenced from lung and trachea homogenates after five passages of 32/H4N2 in 3-days-old chickens. Viruses 32/H4N2 and P5Ch32/H4N2 were produced by reverse genetics as previously described (13) and stocks were generated in 10-day-old embryonated chicken eggs. Madin-Darby canine kidney cells (MDCK cells) were used for either titration by tissue culture infectious dose 50 (TCID₅₀) or plaque assay. Read out for TCID₅₀ was performed by Reed and Muench as previously described (14).

Chickens and housing

Specific-pathogen-free (SPF) White Leghorn (*Gallus gallus domesticus*) embryonated eggs (Rosenbusch S.A. CABA, Argentina) were purchased, incubated, and hatched in an automatic incubator (Yonar, CABA, Argentina). Groups were housed separately in sterilized isolators for chickens under negative pressure conditions (Allentown CH8ISOL) with food and water *ad libitum* throughout the experiments. Animal care was performed in accordance with the approved protocols of the National Institute of Agricultural Technology Ethics Committee (INTA, Argentina; protocols numbers 26/2013 and 44/2014).

Serial lung passages in 3-days-old chicken

Serial lung passages started with the infection of three 3-days-old chicken inoculated intratracheally with 1×10^6 TCID₅₀/bird of allantoic fluid in PBS. At 3 dpi, the chickens were sacrificed, whole

lungs were collected; lung homogenates were prepared with a mortar and sterile sea sand. The pool of lung homogenates from passage 1 was used to infect animals in passage 2. From passage 2 to 4, the lung homogenate with the lowest Ct value was used to inoculate the next group of chickens. The homogenates were resuspended in 5 mL of PBS with antibiotics penicillin 10,000 IU/mL, streptomycin 5 mg/mL, gentamicin Sulfate 1 mg/mL, kanamycin sulfate 700 µg/mL and amphotericin B 10 µg/mL (Sigma Chemical Co, St. Louis, MO, United States), clarified by centrifugation at 1,500 rpm for 20 min at 4°C and store at –80°C until used. Inoculum for serial passages were obtained using 100 µL of clarified lung homogenates from the bird with lowest Ct values. The number of birds per group varied from 3 to 5 based on availability of SPF embryonated eggs at the time of the experiments. Birds were observed daily for clinical signs of infection and general well-being. Experiments were carried out under BSL-3 conditions with investigators wearing appropriate protective equipment and compliant with animal care approved protocols of the National Institute of Agricultural Technology Ethics Committee (INTA, Argentina; protocols numbers 26/2013 and 44/2014).

Infection of 3-weeks old chicken

To assess infectivity of the 32/H4N2 virus, two experiments of four 3-week-old chickens were performed. Chickens were inoculated with 1×10^6 TCID₅₀/bird of allantoic fluid diluted in PBS. Sampling was performed by swabbing trachea and cloaca at 2, 3 and 4 dpi. Two chickens were euthanized at 3 and 4 dpi for lung tissue collection. Lung homogenates for virus detection were prepared as described above. For inoculation with the P5Ch32/H4N2 virus, we performed one experiment with eight chickens. Chickens were also inoculated with 1×10^6 TCID₅₀/bird of allantoic fluid diluted in PBS. Sampling was performed by swabbing trachea and cloaca at 2, 3 and 4 dpi. Four chickens were euthanized at 3 and 4 dpi for lung tissue collection. Lung homogenates for virus detection were prepared as described above.

Detection by qRT-PCR

The viral RNA was extracted from 140 µL of either lung homogenates or tracheal swabs using a QIAamp Viral RNA Mini Kit (Qiagen Inc.). Viral cDNA was prepared with random hexamers using a High Capacity cDNA Archive kit (Applied Biosystems, Foster City, CA, United States). FLUAV detection was done by real-time reverse transcriptase PCR (RT-qPCR) using TaqMan Universal PCR Master Mix (Applied Biosystems) directed to the matrix (M) gene described elsewhere (15). The PCR reaction was performed on an ABI Prism 7,500 SDS (Applied Biosystems). Samples with a CT value of less than or equals to 38 were considered positives.

Sequencing

Total RNA was extracted using the QIAamp viral RNA, Mini kit (Qiagen, Valencia, CA, United States) according to manufacturer's instructions. Reverse transcription was carried out with the uni-12 primer (5'-AGCAAAAGCAAAGG-3') and AMV reverse transcriptase (Promega, Madison, WI, United States). PCR

amplification was performed using specific primers. The PCR products were sequenced using BigDye-Terminator protocol V3.1 (Applied Biosystems, Foster City, CA, United States).

Plaque assay and plaque size measurement

Six-well plates with confluent Madin-Darby canine kidney cells were infected with either 32/H4N2 or P5Ch32/H4N2 in PBS. After 1 h of adsorption, the monolayer was washed twice and overlay with agar media (2 × MEM media, Gibco, ThermoFisher Scientific, Waltham, MA, United States), L-glutamine (4 mM; VWR, Radnor, PA, United States), sodium bicarbonate (0.3%; VWR), BSA (0.5%; Sigma), HEPES (30 mM; Lonza, Basel, Switzerland), 0.8% agar (Oxoid, ThermoFisher Scientific), 1% DEAE dextran [ThermoFisher Scientific, 1 µg/ml TPCK-treated trypsin (Sigma)]. After 48 h, cells were fixed with 4% formaldehyde and stained with crystal violet (Sigma). Size of plaques were manually measure using Fiji ImageJ2 version 2.9.0/1.53 t.

Lung and trachea explants

Lungs and tracheas were used for explant studies (16, 17). Tissues were obtained from 3-weeks old SPF White Leghorn chickens. Using aseptic technique, the tracheas were dissected from the animal, and washed with wash media (PBS containing Penicillin (200 U/mL), Streptomycin (200 µg/mL), Amphotericin B (25 µg/mL)). Tracheal rings of equal width (0.5 cm of length) were infected with 10^4 TCID₅₀/mL of virus for 1 h at 37°C and 5% CO₂. Afterwards, explants were washed 5 × in wash media. Trachea explants were placed on an air-liquid interface supported by a gauze pedestal of approximately 1 cm² embedded in Trachea explant media 250 mL DMEM/F12, no phenol, 250 mL RPMI, no phenol, Penicillin (200 U/mL), Streptomycin (200 µg/mL), Amphotericin B (0.1 µg/mL), Gentamicin (0.2 µg/mL), Glutamine (0.3 ng/mL), 5 mL 100 × amino acids (ThermoFisher Scientific) in 12-well plates (ThermoFisher Scientific), and incubated for 72 h at 37°C and 5% CO₂.

For lung explants, the desired lobes were dissected from the birds and washed 5 × with Lung explant media (500 mL M199, no phenol), Penicillin (200 U/mL), Streptomycin (200 µg/mL), Amphotericin B (0.1 µg/mL), Gentamicin (0.2 µg/mL), 5 mL Vitamin supplement (ATCC), 5 mL 100 × amino acids (ThermoFisher Scientific), 5 mL ITS 100 × (Insulin, Transferrin, Selenium; ThermoFisher Scientific), Hydrocortisone (0.5 µg/ml). Pieces of lungs were obtained using 4 mm biopsy punches (VWR). Infection and cultivation of lung explants was done as with trachea explants. Collection of supernatants from kinetic growth experiments in both types of explants was done adding 200 µL of tissue-specific media before collecting 200 µL of media containing the virus. Titration was performed by TCID₅₀ as described above.

Statistical methods

Plaque size comparison between the 32/H4N2 virus and the P5Ch32/H4N2 virus was done by two sample unpaired t-test. For evaluating significance for growth kinetics in explants, Welch two sample t-test was used. All tests were performed in rstatix (version 0.7.2), from R version 4.1.3.

Results

Low fitness of 32/H4N2 in 3-weeks-old chickens

We evaluated infection capacity of the duck isolate A/silver teal/Argentina/CIP051-32/2011(H4N2; 32/H4N2) in 3-weeks-old chickens (*Gallus gallus domesticus*). Two groups of four chickens produced infection detectable only at 2 days post inoculation (dpi; Table 1).

Low number of passages of the 32/H4N2 virus in chickens resulted in mutations with differential fitness

To evaluate the adaptability of the 32/H4N2 virus to chicken, we performed five passages of lung homogenates in 3-days-old chickens (18). Initially, three chickens were inoculated with 1×10^6 TCID₅₀. Lung homogenates from the bird with the lowest Ct value were used to perform the serial passages (Figure 1). No overt clinical signs were observed. We characterized phenotypically and genetically the virus from the bird with the lowest Ct value in the passage 5 group (P5Ch32/H4N2 virus).

Sequencing the P5Ch32/H4N2 virus from lung and trachea homogenates revealed the same amino acid substitutions in both organs: NA N402K, PB2 K663E, PA V432I, NP L226I, and M1 V80I (Figure 2). We then evaluated the presence of these molecular markers in nature, which would help understanding their fitness in different hosts. We evaluated internal genes from all subtypes and N2 NA regardless of its HA subtype association. The PA V432I mutation was present at ~8% of FLUAV sequences detected in avian hosts and at 1% in mammalian hosts. The NA N402K mutation was detected at ~0.05% of N2 FLUAV sequences detected in mammalian hosts and the M1 V80I mutation was present at >5% of FLUAV sequences in mammalian species (Figure 3).

The size of a plaque produced by cytopathic effect is a direct measurement of fitness *in vitro*. We compared the size of plaques to evaluate whether the mutations acquired after passages in young chickens resulted in fitness differences (Figure 4). While the wild type

TABLE 1 The P5Ch32/H4N2 virus is detected for longer and in more tissues in 3-weeks old chicken than the parental 32/H4N2 virus.

Tissue	Virus	Days post infection		
		2	3	4
Trachea	32/H4N2	33.1 (4) 31.5 (4)	<i>bld</i> (4/4)	<i>bld</i> (2/2)
	P5Ch32/H4N2	31.75 (8)	28.78 (8)	26.67 (4)
Cloaca	32/H4N2	<i>bld</i> (4/4)	<i>bld</i> (4/4)	<i>bld</i> (2/2)
	P5Ch32/H4N2	<i>bld</i> (8)	28.34 (8)	31.2 (4)
Lung	32/H4N2	<i>na</i>	<i>bld</i> (2/2)	<i>bld</i> (2/2)
	P5Ch32/H4N2	<i>na</i>	30.35 (4)	<i>bld</i> (4)

Values for the infection with the 32/H4N2 virus represent two experiments of four chickens whereas values for the infection with the P5Ch32/H4N2 virus represent one experiment of eight chickens. Numbers show mean Ct values from samples whereas values between brackets show number of birds from which the mean Ct values were calculated. Trachea and cloaca were sampled by swabbing whereas lungs represent homogenates. "*bld*" = below limit of detection. "*na*" = not assessed.

32/H4N2 virus produced large plaques, the P5Ch32/H4N2 virus produced pinpoint plaques, demonstrating that the mutations associated with the P5Ch32/H4N2 virus had impacted its fitness *in vitro*.

The P5Ch32/H4N2 virus improved fitness in trachea

We infected trachea and lung explants, to evaluate whether the mutations present in the P5Ch32/H4N2 virus confer differential replication in these tissues. For the P5Ch32/H4N2 virus, replication in the lung decreased compared to the 32/H4N2 virus, but the

differences did not reach statistical significance (Figure 5). In the trachea, overall replication was improved for the P5Ch32/H4N2 virus, reaching statistical significance at 12 h post-infection (hpi). Even though between 24 and 36 hpi both viruses replicated at similar titers, at 48 and 72 hpi the P5Ch32/H4N2 virus maintained higher titers than the 32/H4N2 virus. Overall, these data suggest that the acquisition of the mutations after the passages conferred a replicative improvement in the trachea.

The P5Ch32/H4N2 virus improved fitness *In vivo*

Since the 32/H4N2 virus showed to be deficient to replicate in 3-week-old chickens, we assessed the capacity of the P5Ch32/H4N2 virus to produce infection in chickens of the same age. The group of birds infected with the P5Ch32/H4N2 virus tested positive for virus shedding until the last day evaluated, 4 dpi. Furthermore, virus was also detected in cloacal swabs at 3 and 4 dpi as well as in lung homogenates at 3 dpi (Table 1; Supplementary Table 1). Overall, these data showed that the P5Ch32/H4N2 virus had improved shedding and extended tissue tropism compared to its ancestral 32/H4N2 virus.

Discussion

Introduction and adaptation of viruses from their natural hosts are key for the establishment of novel viruses into new species. Wild waterfowls, from the order Anseriformes and Charadriiforms, are the natural host for FLUAV. Close contact of poultry with species from these two orders has been reported (22), helping disseminate FLUAV to domestic avian species and the consequent host switch for low and high pathogenicity FLUAV. In the present work, we aimed to evaluate

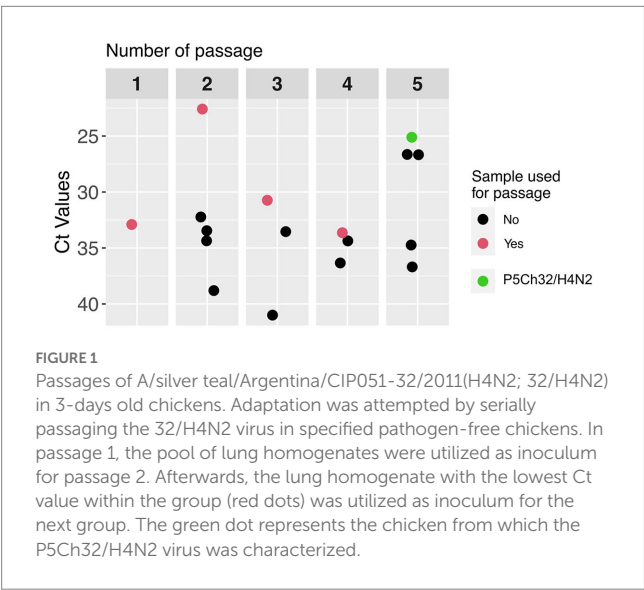


FIGURE 1 Passages of A/silver teal/Argentina/CIP051-32/2011(H4N2; 32/H4N2) in 3-days old chickens. Adaptation was attempted by serially passaging the 32/H4N2 virus in specified pathogen-free chickens. In passage 1, the pool of lung homogenates were utilized as inoculum for passage 2. Afterwards, the lung homogenate with the lowest Ct value within the group (red dots) was utilized as inoculum for the next group. The green dot represents the chicken from which the P5Ch32/H4N2 virus was characterized.

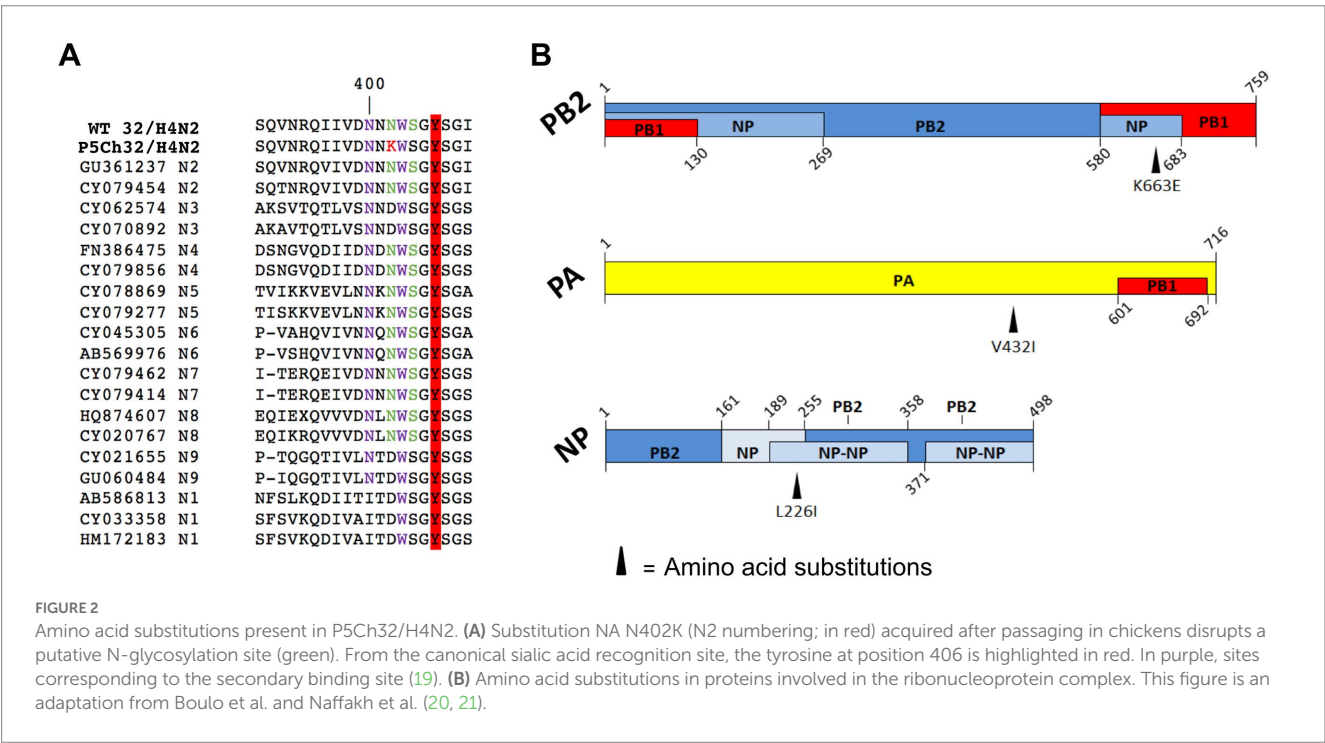


FIGURE 2 Amino acid substitutions present in P5Ch32/H4N2. (A) Substitution NA 402K (N2 numbering; in red) acquired after passaging in chickens disrupts a putative N-glycosylation site (green). From the canonical sialic acid recognition site, the tyrosine at position 406 is highlighted in red. In purple, sites corresponding to the secondary binding site (19). (B) Amino acid substitutions in proteins involved in the ribonucleoprotein complex. This figure is an adaptation from Boulo et al. and Naffakh et al. (20, 21).

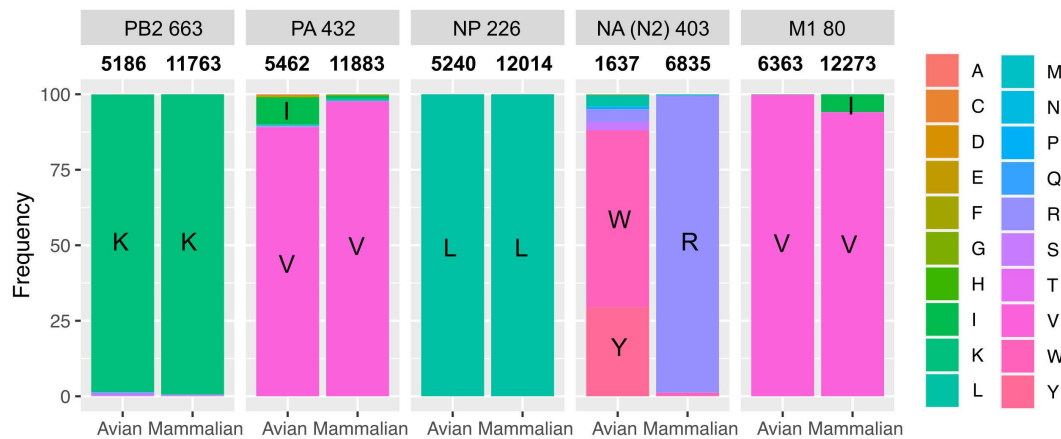


FIGURE 3

Absence of molecular markers from P5Ch32/H4N2 suggest fitness cost in nature. NCBI database was searched for NA N403K, PB2 K663E, PA V432I, NP L226I and, M1 V80I. Numbers between title of the panel and bar plots show the total number of sequences analyzed.

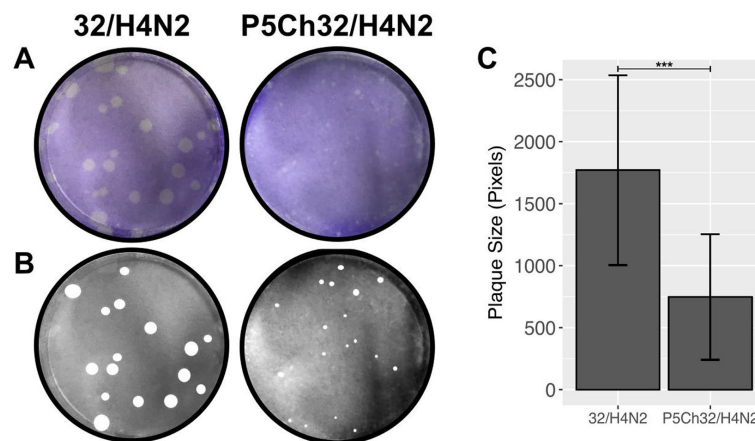


FIGURE 4

In vitro fitness differences conferred by mutations in P5Ch32/H4N2. Plaque size is indicative of fitness differences *in vitro*. Plaque formation from infection in Madin-Darby canine cells was evaluated after crystal violet staining (A). Plaques were manually measured (B) and total area of plaques was evaluated (C). Plaque size was statistically significant ($***p=0.000106$, two samples unpaired *t*-test). Bars represent the mean size of the plaques and bars, the standard deviation.

the adaptation of a H4N2 avian influenza virus from the South American lineage isolated from a wild bird. After five passages in young chickens, we found that the mutations acquired conferred a replicative advantage in 3-weeks-old chicken and in trachea explants suggesting that the passages promoted selection for infection in chicken.

The South American lineage represents a unique evolutionary clade with little information about its adaptability (2, 23, 24). Rimondi et al. (23) recently showed that 20 passages in 3-weeks old chickens produced 13 amino acid substitutions that conferred a South American H6N2 capacity to increase replication in chickens. Here, we found that five amino acid substitutions arose after only five passages in 3-days old chickens. This experimental setup allowed us to make the process of adaptation more efficient because young chickens do not have their innate immunity fully developed, lowering innate immune pressure (25). Moreover, a high number of passages increases the probability of mutations being fixed by chance interfering with the process of positive selection.

The mutations acquired after passages were present in NA, PB2, PA, NP, and M1 proteins. Even though at low frequency, NA N402K, PA V432I, and M1 V80I were found in viruses isolated from mammals suggesting that these viruses are capable of infecting species other than avian hosts. Conversely, the PA V432I mutation was found in ~8% of the avian and 1% in mammalian FLUAV sequences deposited in public databases. This reflects the capacity of viruses with the PA V432I substitution to infect mammals and birds.

The fact that 3 out of 5 mutations are present in the ribonucleoproteins is indicative of a process of adaptation that involves the replicative machinery of the virus. The mutation PB2 K663E falls in the 627 domain—a distinctive domain protruding from the polymerase core. The domain 627 was previously shown to play a role in the adaptation of avian viruses to mammals (26). Differences in the biology of infection from waterfowl to chicken is likely one of the main host restrictions since FLUAV replicate in the gastrointestinal tract in waterfowl whereas is mainly a respiratory infection in poultry.

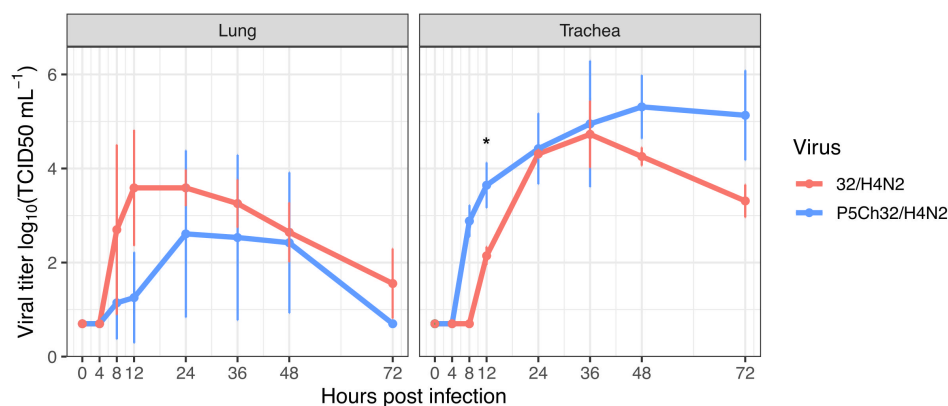


FIGURE 5

Trend of higher replication in chicken trachea upon infection with P5Ch32/H4N2 virus. While in lung explants the P5Ch32/H4N2 virus seemed to have a cost early in the infection at 12h post infection (No statistical significance), passages conferred better replication in trachea with statistical significance at 12hpi (* $p=0.02082$; Welch two sample t -test). Data represents two independent experiments with three replicates each. Dots represent the mean titer and bars represent their standard deviations.

Therefore, the mutations found in the proteins involved in the formation of the ribonucleoproteins may moderate efficiency of replication under these two different environments.

Another salient mutation is NA N402K. This mutation falls in a region of the protein that has the potential to disrupt a putative glycosylation site, and/or to modify the secondary binding site (19). Furthermore, site 406Y, which forms part of the primary sialic acid recognition site, is adjacent. This can have implications in the performance of the NA and the sialic acid species it recognizes. It has been shown that the epithelial cells from the respiratory tract of chickens contain both sialic acid in α 2,3 and α 2,6 conformation whereas the α 2,3 conformation is predominant in the gastrointestinal tract of waterfowl (9, 27–29). Therefore, mutations in either of the proteins involved in the recognition of these ligands are expected to change upon host switch. Which of these mutations are the ones responsible for the infection improvement in 3-weeks-old chickens and whether they confer transmission capacity warrants further research.

It has been shown that selective pressure acts differently across various anatomical sites within the infected individuals (30). In our experiment of adaptation, we utilized lung homogenates to make serial passages but, in the *ex vivo* infection, fitness gain was only detected in the trachea. This can be attributed to the use of intratracheal inoculation during the passages. We argue that even though viruses were homogenized and collected from the lungs, intratracheal inoculation allowed the virus populations produced in the lungs to be selected in the trachea. Furthermore, the P5Ch32/H4N2 virus was mainly detected in the trachea of infected chicken and its robust infection in the trachea explains further support the notion that the trachea acted as a compartment where selection occurred, creating fit populations therein (31, 32).

Poultry species have been proposed as intermediate hosts between waterfowl and humans (9, 10). Even though human infections by H4 subtypes of FLUAV are still limited, the fact that FLUAV evolve rapidly in poultry (33) in addition to the close contact of the human population with these birds, sets the conditions for spillovers, increasing the probability of the establishment of new viruses in the human population.

Data availability statement

Nucleotide genomic sequences from all Guatemalan viruses have been deposited at the NCBI Database under the following accession numbers OQ821651–OQ821658.

Ethics statement

The animal study was reviewed and approved by National Institute of Agricultural Technology Ethics Committee (INTA, Argentina) (protocols numbers 26/2013 and 44/2014).

Author contributions

LMF conception of the work, performed experiments, analyzed data, and wrote and edited the manuscript. SC and VO performed experiments. AP conception of the work and edited the manuscript. DR edited manuscript. DRP conception of the work, wrote and edited the manuscript. All authors contributed to the article and approved the submitted version.

Funding

This research was funded by a subcontract from the Center for Research on Influenza Pathogenesis (CRIP) to DRP under contract HHSN272201400008C from the National Institute of Allergy and Infectious Diseases (NIAID) Centers for Influenza Research and Surveillance (CEIRS). This research was also funded by the Instituto Nacional de Tecnología Agropecuaria (INTA; PNSA 1115052 and PNSA 1115056) to AP. This work was also supported by CONICET (Consejo Nacional de Investigación Científica y Técnicas) and CIC (Comisión de Investigaciones Científicas), through fellowships given to ML.

Conflict of interest

The authors declare that the research was conducted in the absence of any commercial or financial relationships that could be construed as a potential conflict of interest.

Publisher's note

All claims expressed in this article are solely those of the authors and do not necessarily represent those of their affiliated

organizations, or those of the publisher, the editors and the reviewers. Any product that may be evaluated in this article, or claim that may be made by its manufacturer, is not guaranteed or endorsed by the publisher.

Supplementary material

The Supplementary material for this article can be found online at: <https://www.frontiersin.org/articles/10.3389/fvets.2023.1182550/full#supplementary-material>

References

- Webster RG, Shortridge KF, Kawaoka Y. Influenza: interspecies transmission and emergence of new pandemics. *FEMS Immunol Med Microbiol.* (1997) 18:275–9. doi: 10.1111/j.1574-695X.1997.tb01056.x
- Rimondi A, Gonzalez-Reiche AS, Olivera VS, Decarre J, Castresana GJ, Romano M, et al. Evidence of a fixed internal gene constellation in influenza A viruses isolated from wild birds in Argentina (2006–2016). *Emerg Microbes Infect.* (2018) 7:194. doi: 10.1038/s41426-018-0190-2
- Donis RO, Bean WJ, Kawaoka Y, Webster RG. Distinct lineages of influenza virus H4 hemagglutinin genes in different regions of the world. *Virology.* (1989) 169:408–17. doi: 10.1016/0042-6822(89)90166-9
- Kang HM, Choi JG, Kim KI, Park HY, Park CK, Lee YJ. Genetic and antigenic characteristics of H4 subtype avian influenza viruses in Korea and their pathogenicity in quails, domestic ducks and mice. *J Gen Virol.* (2013) 94:30–9. doi: 10.1099/vir.0.046581-0
- Arai Y, Bui VN, Takeda Y, Trinh DQ, Nibuno S, Runstadler J, et al. Lung cytokine gene expression is correlated with increased severity of disease in a novel H4N8 influenza virus isolated from shorebirds. *J Vet Med Sci.* (2013) 75:1341–7. doi: 10.1292/jvms.13-0201
- Wu H, Peng X, Peng X, Cheng L, Lu X, Jin C, et al. Genetic characterization of natural reassortant H4 subtype avian influenza viruses isolated from domestic ducks in Zhejiang province in China from 2013 to 2014. *Virus Genes.* (2015) 51:347–55. doi: 10.1007/s11262-015-1245-2
- Karasin AI, Brown IH, Carman S, Olsen CW. Isolation and characterization of H4N6 avian influenza viruses from pigs with pneumonia in Canada. *J Virol.* (2000) 74:9322–7. doi: 10.1128/jvi.74.19.9322-9327.2000
- Capuano AM, Miller M, Stallknecht DE, Moriarty M, Plancarte M, Dodd E, et al. Serologic detection of subtype-specific antibodies to influenza A viruses in Southern Sea otters (*Enhydra lutris nereis*). *J Wildl Dis.* (2017) 53:906–10. doi: 10.7589/2017-01-011
- Kuchipudi SV, Nelli R, White GA, Bain M, Chang KC, Dunham S. Differences in influenza virus receptors in chickens and ducks: implications for interspecies transmission. *J Mol Genet Med.* (2009) 3:143–51. doi: 10.4172/1747-0862.1000026
- Blagodatski A, Trutneva K, Glazova O, Mityaeva O, Shevkova L, Kegeles E, et al. Avian influenza in wild birds and poultry: dissemination pathways, monitoring methods, and virus ecology. *Pathogens.* (2021) 10:630. doi: 10.3390/pathogens10050630
- Kayali G, Barbour E, Dbaibo G, Tabet C, Saade M, Shaib HA, et al. Evidence of infection with H4 and H11 avian influenza viruses among Lebanese chicken growers. *PLoS One.* (2011) 6:e26818. doi: 10.1371/journal.pone.0026818
- Kayali G, Ortiz EJ, Chorazy ML, Gray GC. Evidence of previous avian influenza infection among US Turkey workers. *Zoonoses Public Health.* (2010) 57:265–72. doi: 10.1111/j.1863-2378.2009.01231.x
- Sorrell EM, Wan H, Araya Y, Song H, Perez DR. Minimal molecular constraints for respiratory droplet transmission of an avian-human H9N2 influenza A virus. *Proc Natl Acad Sci U S A.* (2009) 106:7565–70. doi: 10.1073/pnas.0900877106
- Reed LJM. A simple method for estimating fifty percent endpoints. *Am J Hyg.* (1938) 27:493–7.
- Spackman E, Senne DA, Myers TJ, Bulaga LL, Garber LP, Perdue ML, et al. Development of a real-time reverse transcriptase PCR assay for type A influenza virus and the avian H5 and H7 hemagglutinin subtypes. *J Clin Microbiol.* (2002) 40:3256–60. doi: 10.1128/JCM.40.9.3256-3260.2002
- Lar RM, Cooley WA, Woodward MJ. The role of fimbriae and flagella in the adherence of avian strains of *Escherichia coli* O78:K80 to tissue culture cells and tracheal and gut explants. *J Med Microbiol.* (2000) 49:327–38. doi: 10.1099/0022-1317-49-4-327
- Nunes SF, Murcia PR, Tiley LS, Brown IH, Tucker AW, Maskell DJ, et al. An ex vivo swine tracheal organ culture for the study of influenza infection. *Influenza Other Respir Viruses.* (2010) 4:7–15. doi: 10.1111/j.1750-2659.2009.00119.x
- Hossain MJ, Hickman D, Perez DR. Evidence of expanded host range and mammalian-associated genetic changes in a duck H9N2 influenza virus following adaptation in quail and chickens. *PLoS One.* (2008) 3:e3170. doi: 10.1371/journal.pone.0003170
- Varghese JN, Colman PM, van Donkelaar A, Blick TJ, Sahasrabudhe A, McKimm-Breschkin JL. Structural evidence for a second sialic acid binding site in avian influenza virus neuraminidases. *Proc Natl Acad Sci U S A.* (1997) 94:11808–12. doi: 10.1073/pnas.94.22.11808
- Boulo S, Akarsu H, Ruigrok RW, Baudin F. Nuclear traffic of influenza virus proteins and ribonucleoprotein complexes. *Virus Res.* (2007) 124:12–21. doi: 10.1016/j.virusres.2006.09.013
- Naffakh N, Tomoiu A, Rameix-Welti MA, van der Werf S. Host restriction of avian influenza viruses at the level of the ribonucleoproteins. *Annu Rev Microbiol.* (2008) 62:403–24. doi: 10.1146/annurev.micro.62.081307.162746
- Velkers FC, Manders TTM, Vernooij JCM, Stahl J, Slaterus R, Stegeman JA. Association of wild bird densities around poultry farms with the risk of highly pathogenic avian influenza virus subtype H5N8 outbreaks in the Netherlands, 2016. *Transbound Emerg Dis.* (2021) 68:76–87. doi: 10.1111/tbed.13595
- Rimondi A, Olivera VS, Soria I, Parisi GD, Rumbo M, Perez DR. Few amino acid mutations in H6 influenza A virus from south American lineage increase viral replication efficiency in poultry. *Front Microbiol.* (2022) 13:953738. doi: 10.3389/fmicb.2022.953738
- Xu K, Ferreri L, Rimondi A, Olivera V, Romano M, Ferreyra H, et al. Isolation and characterization of an H9N2 influenza virus isolated in Argentina. *Virus Res.* (2012) 168:41–7. doi: 10.1016/j.virusres.2012.06.010
- Song B, Tang D, Yan S, Fan H, Li G, Shahid MS, et al. Effects of age on immune function in broiler chickens. *J Anim Sci Biotechnol.* (2021) 12:42. doi: 10.1186/s40104-021-00559-1
- Subbarao EK, London W, Murphy BR. A single amino acid in the PB2 gene of influenza A virus is a determinant of host range. *J Virol.* (1993) 67:1761–4. doi: 10.1128/JVI.67.4.1761-1764.1993
- Gambaryan A, Webster R, Matrosovich M. Differences between influenza virus receptors on target cells of duck and chicken. *Arch Virol.* (2002) 147:1197–208. doi: 10.1007/s00705-002-0796-4
- Gambaryan AS, Tuzikov AB, Bovin NV, Yamnikova SS, Lvov DK, Webster RG, et al. Differences between influenza virus receptors on target cells of duck and chicken and receptor specificity of the 1997 H5N1 chicken and human influenza viruses from Hong Kong. *Avian Dis.* (2003) 47:1154–60. doi: 10.1637/0005-2086-47.s3.1154
- Wan H, Perez DR. Quail carry sialic acid receptors compatible with binding of avian and human influenza viruses. *Virology.* (2006) 346:278–86. doi: 10.1016/j.virol.2005.10.035
- Lakdawala SS, Jayaraman A, Halpin RA, Lamirande EW, Shih AR, Stockwell TB, et al. The soft palate is an important site of adaptation for transmissible influenza viruses. *Nature.* (2015) 526:122–5. doi: 10.1038/nature15379
- Amato KA, Haddock LA 3rd, Braun KM, Meliopoulos V, Livingston B, Honce R, et al. Influenza A virus undergoes compartmentalized replication in vivo dominated by stochastic bottlenecks. *Nat Commun.* (2022) 13:3416. doi: 10.1038/s41467-022-31147-0
- Ganti K, Bagga A, Carnaccini S, Ferreri LM, Geiger G, Joaquin Caceres C, et al. Influenza A virus reassortment in mammals gives rise to genetically distinct within-host subpopulations. *Nat Commun.* (2022) 13:6846. doi: 10.1038/s41467-022-34611-z
- Fourment M, Holmes EC. Avian influenza virus exhibits distinct evolutionary dynamics in wild birds and poultry. *BMC Evol Biol.* (2015) 15:120. doi: 10.1186/s12862-015-0410-5



OPEN ACCESS

EDITED BY

Sarah J. Edwards,
Commonwealth Scientific and Industrial
Research Organisation (CSIRO), Australia

REVIEWED BY

Yousong Peng,
Hunan University, China
Ye Ge,
Guangdong Ocean University, China

*CORRESPONDENCE

Dong-Hun Lee
✉ donghunlee@konkuk.ac.kr
Jung-Hoon Kwon
✉ Junghoon.kwon@knu.ac.kr

[†]These authors contributed equally to this work
and share first authorship

RECEIVED 03 February 2023

ACCEPTED 10 May 2023

PUBLISHED 12 June 2023

CITATION

Kim J-Y, Lee S-H, Kim D-W, Lee D-W, Song C-S,
Lee D-H and Kwon J-H (2023) Detection of
intercontinental reassortant H6 avian influenza
viruses from wild birds in South Korea, 2015
and 2017.
Front. Vet. Sci. 10:1157984.
doi: 10.3389/fvets.2023.1157984

COPYRIGHT

© 2023 Kim, Lee, Kim, Lee, Song, Lee and
Kwon. This is an open-access article distributed
under the terms of the [Creative Commons
Attribution License \(CC BY\)](#). The use,
distribution or reproduction in other forums is
permitted, provided the original author(s) and
the copyright owner(s) are credited and that
the original publication in this journal is cited,
in accordance with accepted academic
practice. No use, distribution or reproduction is
permitted which does not comply with these
terms.

Detection of intercontinental reassortant H6 avian influenza viruses from wild birds in South Korea, 2015 and 2017

Ji-Yun Kim^{1†}, Sun-Hak Lee^{2†}, Da-Won Kim¹, Dong-Wook Lee¹,
Chang-Seon Song², Dong-Hun Lee^{3*} and Jung-Hoon Kwon^{1*}

¹College of Veterinary Medicine, Kyungpook National University, Daegu, Republic of Korea, ²Avian Disease Laboratory, College of Veterinary Medicine, Konkuk University, Seoul, Republic of Korea, ³Wildlife Health Laboratory, College of Veterinary Medicine, Konkuk University, Seoul, Republic of Korea

Avian influenza viruses (AIVs) in wild birds are phylogenetically separated in Eurasian and North American lineages due to the separated distribution and migration of wild birds. However, AIVs are occasionally dispersed between two continents by migratory wild birds flying across the Bering Strait. In this study, we isolated three AIVs from wild bird feces collected in South Korea that contain gene segments derived from American lineage AIVs, including an H6N2 isolated in 2015 and two H6N1 in 2017. Phylogenetic analysis suggests that the H6N2 virus had American lineage matrix gene and the H6N1 viruses had American lineage nucleoprotein and non-structural genes. These results highlight that novel AIVs have continuously emerged by reassortment between viruses from the two continents. Therefore, continuous monitoring for the emergence and intercontinental spread of novel reassortant AIV is required to prepare for a possible future outbreak.

KEYWORDS

influenza virus, reassortment, phylogenetic analysis, wild bird, South Korea

1. Introduction

Wild waterfowl are the natural hosts of avian influenza viruses (AIVs) (1). Because of the geographical barrier, AIVs are separated into two phylogenetic lineages, the Eurasian and American lineages (2). However, some migratory waterfowl (e.g., the Northern Pintail duck; *Anas acuta* and Greater White-fronted goose; *Anser albifrons*) move intercontinentally, causing genetic mixing between the two lineages of AIVs (3–8).

Previous surveillance studies on AIVs in wild birds provide evidence for the intercontinental exchange of AIVs. For example, the Eurasian H6 subtype AIV has been reported in North America since the 1990s and it replaced the prevailing North American H6 AIV (8). AIVs subtype H9N2, which contains six genes originating from North America, were simultaneously isolated in South Korea, China, and Alaska (5–7). In 2019, subtype H6N5 AIV carrying all eight gene segments from North American ancestors was detected in Mandarin duck in South Korea (4). In addition, the intercontinental spread of the highly pathogenic avian influenza (HPAI) virus from Eurasia to North America was detected in 2014 and 2021 (9, 10). Western Alaska, where migratory flyways of waterfowl overlap, is the location to encounter AIVs from Eurasian and North American lineages (3).

TABLE 1 Summary of viruses used in this study.

Virus name	GISAID accession #	Collection date	Province	Location coordinate
A/Mandarin duck/Korea/K15-68/2015(H6N2)	EPI_ISL_11110143	2015-11-11	Cheonsu bay	36°36'21"N 126°25'9"E
A/Greater white-fronted goose/Korea/K16-727-5/2017(H6N1)	EPI_ISL_11112483	2017-03-14	Ganghwa-gun	37°44'50"N 126°29'8"E
A/Greater white-fronted goose/Korea/K16-738/2017(H6N1)	EPI_ISL_11112543	2017-03-14	Ganghwa-gun	37°44'50"N 126°29'8"E

In the current study, we report three reassortant H6 viruses containing gene segments originating from North America. Complete genome sequencing and phylogenetic analysis were used to find the origin of each gene segment.

2. Materials and methods

We collected fresh fecal samples from wild bird habitats in South Korea for routine AIV surveillance during the fall migration and wintering seasons of wild waterfowl. In the 2015–2016 winter, we collected total of 1,896 fecal samples and in the 2016–2017 winter, we collected total of 8,096 fecal samples. Following as the previous study, fecal samples were examined for influenza A virus by real-time reverse transcription polymerase chain reaction (rRT-PCR) targeting the matrix (M) gene (11). Virus isolation was done using embryonated SPF chicken eggs. We found three reassortant H6 viruses containing gene segments originating from the American continent: A/Mandarin duck/Korea/K15-68/2015 (H6N2), A/Greater White-fronted goose/Korea/K16-727-5/2017 (H6N1), and A/Greater White-fronted goose/Korea/K16-738/2017 (H6N1) (designated as K15-68, K16-727-5, and K16-738, respectively). The date and location information of the isolated viruses is shown in Table 1. We sequenced full-length genomes of the isolates using the Illumina MiSeq system. We deposited the nucleotide sequences of each virus into the Global Initiative for Sharing All Influenza Data (GISAID) database (accession nos. EPI_ISL_11110143, EPI_ISL_11112483, and EPI_ISL_11112543, respectively). The host of each fecal sample positive for AIV was identified using a DNA barcoding technique, as previously described (12).

Comparative phylogenetic analysis of each gene was conducted to trace their origin. For phylogenetic analysis, all available sequences collected between 2010 and 2021 were downloaded from GISAID. To prevent the omission of intercontinental spread viruses during the subsampling process, we classified all downloaded sequences into two groups before subsampling: one containing the viruses isolated from Asia, Africa, and Europe and the other containing the viruses isolated from South and North America. We reduced the number of sequences in each gene segment of each group based on sequence identities of 97–99% using the program CD-HIT (13). Maximum-likelihood (ML) phylogenetic trees were constructed using a general time reversible (GTR) substitution model with 500 bootstrap replications in RAxML version 8.2.11 (14). We used BLAST¹ to search for

sequences with the highest identity to each virus for each gene segment.

To verify the result of the phylogenetic tree, we constructed time-scaled phylogenetic trees using BEAST version 1.10.4 (15). The GTR nucleotide substitution model and uncorrelated lognormal relaxed molecular clock model were used for constructing a time-scaled maximum clade credibility (MCC) tree. MCC trees were visualized using FigTree 1.4.2.²

To evaluate the pathogenicity of the viruses in chickens, a total of 15 three-week-old SPF chickens (Namdeok SPF, Korea) were divided into 3 groups (5 chickens/group). The chickens were inoculated with H6 LPAI viruses at $10^{6.0}$ EID₅₀ in a volume of 100ul by intranasal route. At 2-, 3-, 5-, and 7-days post-infection (dpi), oropharyngeal (OP) and cloacal (CL) swabs were collected from all chickens and examined for virus shedding using a quantitative real-time reverse transcription polymerase chain reaction (rRT-PCR) targeting the matrix gene, as described previously (11). For each virus, the standard curve was used to convert the Ct values into equivalent EID₅₀ titer. All chickens were monitored daily for clinical signs and mortality. Serum samples were collected for serological investigations including anti-NP ELISA (Bionote, Inc., Korea) and Hemagglutination inhibition (HI) testing for homologous HA-specific antibodies.

3. Results

We successfully obtained complete genome sequences of the K15-68, K16-727-5, and K16-738 viruses. Host species of K15-68 was identified as Mandarin duck, and K16-727-5 and K16-738 viruses' host were identified as Greater White-fronted goose using DNA barcoding. The genome sequences of K16-727-5 and K16-738 which were isolated on the same sample collection day were almost identical (NP: 99.936%, NS: 99.944%, and other 6 genes: 100%).

BLAST research indicated that the matrix (M) gene of K15-68 strain shared >99% nucleotide identity with the Guatemalan origin H14N3 subtype AIV. The nucleoprotein (NP) gene of K16-727-5 and K16-738 strains sharing 99.94% nucleotide identity with H9N6 subtype AIV isolated from Missouri, United States, and the nonstructural (NS) gene shared 98.31% nucleotide identity with Ohio, USA isolate (Table 2). All other segments showed >98% identity with the low-pathogenicity AIVs (LPAI) identified in South Korea, Japan, China, and Mongolia. Corresponding to the BLAST results, the ML and Bayesian phylogenetic analysis showed that the M gene of K15-68

¹ <https://blast.ncbi.nlm.nih.gov/Blast.cgi>

² <http://tree.bio.ed.ac.uk/software/figtree/>

TABLE 2 BLAST results of 8 gene segments of three viruses isolated in this study.

Virus	Gene	BLAST results		
		Strain	% Genetic identity	GenBank accession #
K15-68	PB2	A/duck/Hokkaido/201/2014(H1N1)	99.01%	LC339528.1
	PB1	A/waterfowl/Korea/S353/2016(H11N9)	99.83%	KX703017.1
	PA	A/waterfowl/Korea/S245/2016(H6N2)	99.60%	KX761368.1
	HA	A/wild bird/Jiangxi/P419/2016(H6N8)	98.34%	KX867857.1
	NP	A/waterfowl/Korea/S245/2016(H6N2)	99.74%	KX761370.1
	N2	A/duck/Miyazaki/CAD-1/2016(H4N2)	99.38%	LC415036.1
	M	A/blue-winged teal/Guatemala/CIP049H105-15/2011(H14N3)	99.42%	KJ195679.1
	NS	A/waterfowl/Korea/S245/2016(H6N2)	99.44%	KX761373.1
K16-727-5	PB2	A/waterfowl/Korea/S245/2016(H6N2)	99.36%	KX761366.1
	PB1	A/duck/Akita/51019/2017(H5N3)	98.88%	MK592459.1
	PA	A/Duck/Mongolia/782/2017(H7N3)	99.01%	MH744642.1
	HA	A/duck/Hunan/10.27_YYGK57B2-O/2016(mixed)	99.42%	MW108112.1
	NP	A/northern shoveler/Missouri/17OS4858/2017(H6N2)	99.94%	MK237594.1
	N1	A/wild waterfowl/Korea/F14-5/2016(H6N1)	99.65%	MH130116.1
	M	A/mallard/Netherlands/89/2017(H4N6)	99.42%	MK192396.1
	NS	A/Mallard/Ohio/18OS1894/2018(mixed)	98.31%	MT565511.1
K16-738	PB2	A/waterfowl/Korea/S245/2016(H6N2)	99.36%	KX761366.1
	PB1	A/duck/Akita/51019/2017(H5N3)	98.88%	MK592459.1
	PA	A/Duck/Mongolia/782/2017(H7N3)	99.01%	MH744642.1
	HA	A/duck/Hunan/10.27_YYGK57B2-O/2016(mixed)	99.42%	MW108112.1
	NP	A/northern shoveler/Missouri/17OS4858/2017(H6N2)	99.94%	MK237594.1
	N1	A/wild waterfowl/Korea/F14-5/2016(H6N1)	99.65%	MH130116.1
	M	A/mallard/Netherlands/89/2017(H4N6)	99.42%	MK192396.1
	NS	A/Mallard/Ohio/18OS1894/2018(mixed)	98.31%	MT565511.1

The American lineage strains were highlighted in bold.

K15-68, A/Mandarin duck/Korea/K15-68/2015(H6N2); K16-727-5, A/Greater white-fronted goose/Korea/K16-727-5/2017 (H6N1); K16-738, A/Greater white-fronted goose/Korea/K16-738/2017(H6N1). PB, polymerase basic protein polymerase basic gene; PA, polymerase acidic gene; HA, hemagglutinin gene; NP, nucleoprotein gene; NA, neuraminidase gene; M, matrix protein; NS, nonstructural protein.

and the NP and NS gene of K16-727-5 and K16-738 clustered with the American lineage wild bird AIVs and the rest of the gene segments were clustered with the Eurasian lineage wild bird AIVs (Figure 1; Supplementary Figures S1, S2). These results demonstrate that the three viruses were generated by reassortment between Eurasian and American AIVs.

The HA genes from H6N1 and H6N2 AIVs have some phylogenetic distance. Eurasian lineage H6 genes are divided into seven groups; ST339-like, W312-like, ST2853-like, HN573-like, South African-like, Taiwan-like, and Europe (Figure 1) (16). HN573-like is divided into three subgroups, subgroup 1 (mixed group), 2 (Eurasian group), and 3 (American group). All three isolates cluster with HN573-like, but with different subgroups (Supplementary Figure S1D). H6N2 belongs to subgroup 1 and H6N1 belongs to subgroup 2.

The amino acid changes related to the mammalian adaptation, including Q591K, E627K, and D701N mutations in PB2 (17), N137/

E190V/ G228S triad, and Q226L mutation in HA (H3 numbering) (18, 19), were not detected in the viruses isolated in this study. The NA stalk deletion, which has been associated with adaptation to gallinaceous hosts (20), was also not detected.

Three-week-old SPF chickens were inoculated with the H6 viruses to study their infectivity and virulence. During the 14-day experiment, no obvious clinical signs and no mortality were observed. Virus shedding through the OP and CL routes was detected during 3–7 dpi, but the detected amount of viruses was very low ($<10^{3.5}$ EID₅₀) (Table 2). For the chickens inoculated with K15-68 and K16-727-5 virus, mean shedding titers for both routes did not exceed $10^{1.0}$ EID₅₀ throughout the whole period of the experiment. Chickens inoculated with K16-738 showed a peak of OP shedding at 3 dpi and a peak of CL shedding at 7 dpi, with mean shedding titers of $10^{1.85}$ EID₅₀ and $10^{1.84}$ EID₅₀, respectively. Both HI and NP-specific antibodies were detected in two of five, one of five, and one of five chickens inoculated with K15-68, K16-727-5, and K16-768, respectively (Table 3).

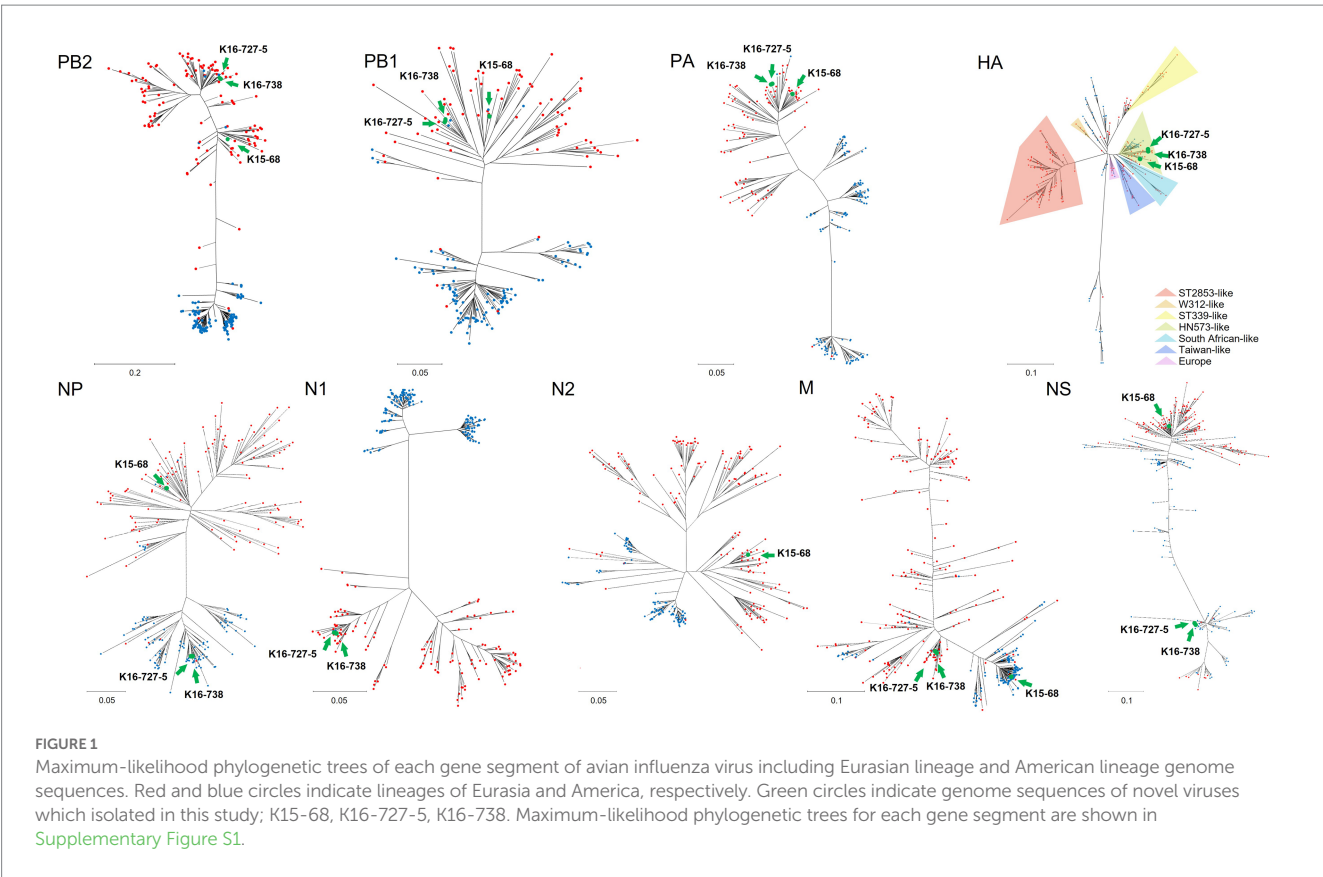


TABLE 3 Viral shedding and antibody responses of chickens inoculated with H6 avian influenza viruses.

viruses	No. of positive chickens/total chickens (Mean viral titer, log ₁₀ EID ₅₀ /ml±SD) ^c								Serology, no. of positive/total ^f	
	OP ^a				CL ^b				NP-ELISA ^d (Mean PI)	HI Assay ^e (Mean Titer)
	2 dpi	3 dpi	5dpi	7 dpi	2 dpi	3 dpi	5dpi	7 dpi		
K15-68 (H6N2)	0/5	3/5 (0.8±0.2)	4/5 (0.8±0.2)	5/5 (0.6±0.4)	0/5	0/5	3/5 (0.6±0.2)	2/5 (0.7±0.0)	2/5 (40.0)	2/5 (2 ⁴)
K16-727-5 (H6N1)	0/5	1/5 (1.5)	2/5 (0.9±0.2)	5/5 (0.5±0.0)	0/5	0/5	2/5 (0.7±0.1)	4/5 (1.0±0.3)	1/5 (11.6)	1/5 (2 ³)
K16-738 (H6N1)	0/5	4/5 (2.0±0.3)	3/5 (1.8±0.5)	4/5 (1.5±0.0)	1/5 (1.8)	2/5 (1.3±0.1)	3/5 (2.1±0.8)	3/5 (2.2±1.0)	1/5 (23.4)	1/5 (2 ⁷)

^aOP: Oropharyngeal swab.

^bCL: Cloacal swab.

^cPositive birds were indicated by real-time RT-PCR. Ct-value < 36 was considered as positive. Mean viral titer and standard deviation were calculated after converting the Ct values into equivalent EID₅₀ titer by using the standard curves for each virus.

^dAnti-influenza A nucleoprotein (NP)-specific antibody was analyzed using the commercially available multispecies competitive NP-ELISA Kit (Bionote, Korea). A percent inhibition (PI) value >50 was regarded as positive.

^eHI assay: hemagglutination inhibition assay. An HI titer ≥4 was regarded as positive.

^fSerum samples were collected from the birds at 14 days after the infection.

4. Discussion

In the current study, we report American-Eurasian reassortants H6N1 and H6N2 viruses isolated from two wild bird species, the Greater White-fronted goose and Mandarin duck. Since the first report of North American-Eurasian reassortant

AIVs detected from wild birds in South Korea in 2010 (21), North American lineage AIV gene segments have been detected continuously in South Korea (4, 21–23). Previous studies also detected multiple Eurasian lineage AIV genes in Alaska, indicating the bi-directional flow of AIV exchange between East Asia and North America (24).

Recently, intercontinental reassortants AIVs have been frequently detected (4, 6, 9, 21–23, 25, 26). The reason for the frequent discovery of intercontinental reassortants is not fully determined yet. We assume that climate change can be a factor in contributing to frequent exchange of AIVs between two continents. A previous study indicated that an abnormal climate in Africa might have contributed to the trans-continental introduction of HPAI H5Nx in Africa by migratory birds (27). The temperature of Alaska has increased since 2014 and it might affect the migration pattern of migratory birds and the ecology of AIVs in wild birds (28). On the other hand, Next-Generation Sequencing techniques have been widely used for AIV sequencing (23), and this high-throughput sequencing system would also contribute to the frequent detections of novel reassortants.

The reassortment of AIVs causes rapid changes in the biological characteristics of viruses and it could be a considerable threat to the poultry industry and public health (29). In 2014, in China, for example, human infection of AIV subtype H7N9 occurred by reassortment of AIVs in poultry and wild birds (30). In 2013, a case of human infection with subtype H6N1, AIV generated by reassortment carrying N137/E190V/G228S triad amino acid changes in HA, was reported in Taiwan (31). Although no mammalian adaptation mutation was detected in this study, the emergence of novel AIVs reassortants and the detection of mutation related to mammalian adaptation highlights the importance of wild bird surveillance in terms of the ‘One Health’ concept.

The viruses isolated in this study showed limited infectivity in chickens similar to other wild bird-origin H6 viruses tested in previous studies (32–35). These H6 viruses may be poorly adapted to chickens, but we assume that they possibly replicate in domestic waterfowl without prior adaptation which could lead to the spread and maintenance of H6 viruses in land-based poultry. Bahl et al. showed that the introduction and establishment of Eurasian H6 viruses in North America dramatically changed the evolutionary dynamics of the influenza virus in wild birds (36). Thus, genomic surveillance and *in vivo* pathobiology studies should be continued to monitor the evolution of reassortant H6 viruses and their host ranges.

Constant monitoring for AIVs in wild birds is essential to detect the introduction of new viruses and trace the dispersion path. Particularly, as a major wintering site for various wild birds (37), South Korea would be an important location for monitoring the intercontinental exchange of AIVs. Combined with recently developed sequencing technology, continuing monitoring of the intercontinental dispersion of AIVs would expand our knowledge of AIV ecology and epidemiology.

Data availability statement

The datasets presented in this study can be found in online repositories. The names of the repository/repositories and accession number(s) can be found in the article/Supplementary material.

Ethics statement

The animal study was reviewed and approved by Institutional Animal Care and Use Committee of Konkuk University.

Author contributions

C-SS, D-HL, and J-HK contributed to conception and design of the study. S-HL collected and analyzed samples and conducted an animal experiment. J-YK, D-WK, and D-WL organized data and performed genetic analysis. J-YK visualized data and wrote the first draft of the manuscript. S-HL wrote animal experiment sections. D-HL and J-HK revised final manuscript. All authors contributed to the article and approved the submitted version.

Funding

This research was funded by Kyungpook National University Research Fund, 2020.

Acknowledgments

The authors gratefully acknowledge the authors and submitting laboratories of the sequences from GISAID's EpiFlu (<https://www.gisaid.org/>) database. The GISAID acknowledgement tables for laboratory contributions are shown in Supplementary Table S1.

Conflict of interest

The authors declare that the research was conducted in the absence of any commercial or financial relationships that could be construed as a potential conflict of interest.

Publisher's note

All claims expressed in this article are solely those of the authors and do not necessarily represent those of their affiliated organizations, or those of the publisher, the editors and the reviewers. Any product that may be evaluated in this article, or claim that may be made by its manufacturer, is not guaranteed or endorsed by the publisher.

Supplementary material

The Supplementary material for this article can be found online at: <https://www.frontiersin.org/articles/10.3389/fvets.2023.1157984/full#supplementary-material>

References

1. Swayne DE. *Animal influenza*. 2nd ed. Ames: John Wiley and Sons, Inc (2017). 634 p.
2. Olsen B, Munster VJ, Wallensten A, Waldenström J, Osterhaus AD, Fouchier RA. Global patterns of influenza a virus in wild birds. *Science*. (2006) 312:384–8. doi: 10.1126/science.1122438
3. Pearce JM, Reeves AB, Ramey AM, Hupp JW, Ip HS, Bertram M, et al. Interspecific exchange of avian influenza virus genes in Alaska: the influence of trans-hemispheric migratory tendency and breeding ground sympatry. *Mol Ecol*. (2011) 20:1015–25. doi: 10.1111/j.1365-294X.2010.04908.x
4. Jeong S, Lee D-H, Kim Y-J, Lee S-H, Cho AY, Noh J-Y, et al. Introduction of avian influenza a (H6N5) virus into Asia from North America by wild birds. *Emerg Infect Dis*. (2019) 25:2138–40. doi: 10.3201/eid2511.190604
5. Lee D-H, Park J-K, Yuk S-S, Erdene-Ochir T-O, Kwon J-H, Lee J-B, et al. Complete genome sequence of a natural reassortant H9N2 avian influenza virus found in bean goose (*Anser fabalis*): direct evidence for virus exchange between Korea and China via wild birds. *Infect Genet Evol*. (2014) 26:250–4. doi: 10.1016/j.meegid.2014.06.007
6. Ramey AM, Reeves AB, Sonsthagen SA, TeSlaa JL, Nashold S, Donnelly T, et al. Dispersal of H9N2 influenza a viruses between East Asia and North America by wild birds. *Virology*. (2015) 482:79–83. doi: 10.1016/j.virol.2015.03.028
7. Wang B, Chen Q, Chen Z. Complete genome sequence of an H9N2 avian influenza virus isolated from egret in Lake Dongting wetland. *J Virol*. (2012) 86:11939. doi: 10.1128/JVI.02042-12
8. Zu Dohna H, Li J, Cardona CJ, Miller J, Carpenter TE. Invasions by Eurasian avian influenza virus H6 genes and replacement of its north American clade. *Emerg Infect Dis*. (2009) 15:1040–5. doi: 10.3201/eid1507.090245
9. Ip HS, Torchetti MK, Crespo R, Kohrs P, DeBruyn P, Mansfield KG, et al. Novel Eurasian highly pathogenic avian influenza a H5 viruses in wild birds, Washington, USA, 2014. *Emerg Infect Dis*. (2015) 21:886–90. doi: 10.3201/eid2105.142020
10. Bevins SN, Shriner SA, Cumbee JC Jr, Dilione KE, Douglass KE, Ellis JW, et al. Intercontinental movement of highly pathogenic avian influenza a (H5N1) clade 2.3.4.4 virus to the United States, 2021. *Emerg Infect Dis*. (2022) 28:1006–11. doi: 10.3201/eid2805.220318
11. Spackman E. Avian influenza virus detection and quantitation by real-time RT-PCR. *Methods Mol Biol*. (2020) 2123:137–48. doi: 10.1007/978-1-0716-0346-8_11
12. Hebert PDN, Stoeckle MY, Zemlak TS, Francis CM, Godfray C. Identification of birds through DNA barcodes. *PLoS Biol*. (2004) 2:e312. doi: 10.1371/journal.pbio.0020312
13. Li W, Godzik A. Cd-hit: a fast program for clustering and comparing large sets of protein or nucleotide sequences. *Bioinformatics*. (2006) 22:1658–9. doi: 10.1093/bioinformatics/btl1158
14. Stamatakis A. RAxML version 8: a tool for phylogenetic analysis and post-analysis of large phylogenies. *Bioinformatics*. (2014) 30:1312–3. doi: 10.1093/bioinformatics/btu033
15. Suchard MA, Lemey P, Baele G, Ayres DL, Drummond AJ, Rambaut A. Bayesian phylogenetic and phylodynamic data integration using BEAST 1.10. *Virus Evol*. (2018) 4:vey016. doi: 10.1093/ve/vey016
16. Everest H, Hill SC, Daines R, Sealy JE, James J, Hansen R, et al. The evolution, spread and global threat of H6Nx avian influenza viruses. *Viruses*. (2020) 12:673. doi: 10.3390/v12060673
17. Yamada S, Hatta M, Staker BL, Watanabe S, Imai M, Shinya K, et al. Biological and structural characterization of a host-adapting amino acid in influenza virus. *PLoS Pathog*. (2010) 6:e1001034. doi: 10.1371/journal.ppat.1001034
18. Maines TR, Chen L-M, Van Hoeven N, Tumpey TM, Blixt O, Belser JA, et al. Effect of receptor binding domain mutations on receptor binding and transmissibility of avian influenza H5N1 viruses. *Virology*. (2011) 413:139–47. doi: 10.1016/j.virol.2011.02.015
19. Liu WJ, Wu Y, Bi Y, Shi W, Wang D, Shi Y, et al. Emerging HxNy influenza a viruses. *Cold Spring Harb Perspect Med*. (2022) 12:a038406. doi: 10.1101/cshperspect.a038406
20. Li J, Dohna HZ, Cardona CJ, Miller J, Carpenter TE. Emergence and genetic variation of neuraminidase stalk deletions in avian influenza viruses. *PLoS One*. (2011) 6:e14722. doi: 10.1371/journal.pone.0014722
21. Lee D-H, Lee H-J, Lee Y-N, Park J-K, Lim T-H, Kim M-S, et al. Evidence of intercontinental transfer of north American lineage avian influenza virus into Korea. *Infect Genet Evol*. (2011) 11:232–6. doi: 10.1016/j.meegid.2010.09.012
22. Nguyen NM, Sung HW, Yun K-J, Park H, Yeo S-J. Genetic characterization of a novel north American-origin avian influenza a (H6N5) virus isolated from bean goose of South Korea in 2018. *Viruses*. (2020) 12:774. doi: 10.3390/v12070774
23. Lee D-H, Park J-K, Yuk S-S, Erdene-Ochir T-O, Kwon J-H, Lee J-B, et al. Complete genome sequence of a natural recombinant H9N2 influenza virus isolated from a white-fronted goose (*Anser albifrons*) in South Korea. *Genome Announc*. (2013) 1:e00149–13. doi: 10.1128/genomeA.00149-13
24. Reeves AB, Pearce JM, Ramey AM, Ely CR, Schmutz JA, Flint PL, et al. Genomic analysis of avian influenza viruses from waterfowl in western Alaska, USA. *J Wildl Dis*. (2013) 49:600–10. doi: 10.7589/2012-04-108
25. Lee D-H, Torchetti MK, Winker K, Ip HS, Song C-S, Swayne DE. Intercontinental spread of Asian-origin H5N8 to North America through Beringia by migratory birds. *J Virol*. (2015) 89:6521–4. doi: 10.1128/JVI.00728-15
26. González-Reiche AS, Morales-Betoulle ME, Alvarez D, Betoulle J-L, Müller ML, Sosa SM, et al. Influenza a viruses from wild birds in Guatemala belong to the north American lineage. *PLoS One*. (2012) 7:e32873. doi: 10.1371/journal.pone.0032873
27. Fusaro A, Zecchin B, Vrancken B, Abolnik C, Ademun R, Alassane A, et al. Disentangling the role of Africa in the global spread of H5 highly pathogenic avian influenza. *Nat Commun*. (2019) 10:1–13. doi: 10.1038/s41467-019-13287-y
28. Coggin JDP. *New Report Highlights Alaska's Last Five Years of Dramatic Climate Change* 2019. Available at: <https://www.climate.gov/news-features/understanding-climate/new-report-highlights-alaska%E2%80%99s-last-five-years-dramatic-climate>
29. Su S, Bi Y, Wong G, Gray GC, Gao GF, Li S. Epidemiology, evolution, and recent outbreaks of avian influenza virus in China. *J Virol*. (2015) 89:8671–6. doi: 10.1128/JVI.01034-15
30. Cui L, Liu D, Shi W, Pan J, Qi X, Li X, et al. Dynamic reassortments and genetic heterogeneity of the human-infecting influenza a (H7N9) virus. *Nat Commun*. (2014) 5:1–9. doi: 10.1038/ncomms4142
31. Wei S-H, Yang J-R, Wu H-S, Chang M-C, Lin J-S, Lin C-Y, et al. Human infection with avian influenza a H6N1 virus: an epidemiological analysis. *Lancet Respir Med*. (2013) 1:771–8. doi: 10.1016/S2213-2600(13)70221-2
32. Jackwood MW, Suarez DL, Hilt D, Pantin-Jackwood MJ, Spackman E, Woolcock P, et al. Biologic characterization of chicken-derived H6N2 low pathogenic avian influenza viruses in chickens and ducks. *Avian Dis*. (2010) 54:120–5. doi: 10.1637/8987-070909-ResNote.1
33. Lin W, Cui H, Teng Q, Li L, Shi Y, Li X, et al. Evolution and pathogenicity of H6 avian influenza viruses isolated from southern China during 2011 to 2017 in mice and chickens. *Sci Rep*. (2020) 10:1–12. doi: 10.1038/s41598-020-76541-0
34. Nam J-H, Kim E-H, Song D, Choi YK, Kim J-K, Poo H. Emergence of mammalian species-infectious and-pathogenic avian influenza H6N5 virus with no evidence of adaptation. *J Virol*. (2011) 85:13271–7. doi: 10.1128/JVI.05038-11
35. Yao Y, Wang H, Chen Q, Zhang H, Zhang T, Chen J, et al. Characterization of low-pathogenic H6N6 avian influenza viruses in Central China. *Arch Virol*. (2013) 158:367–77. doi: 10.1007/s00705-012-1496-3
36. Bahl J, Vijaykrishna D, Holmes EC, Smith GJ, Guan Y. Gene flow and competitive exclusion of avian influenza a virus in natural reservoir hosts. *Virology*. (2009) 390:289–97. doi: 10.1016/j.virol.2009.05.002
37. Moores N. South Korea's shorebirds: a review of abundance, distribution, threats and conservation status. *Stilt*. (2007) 50:62–72.



OPEN ACCESS

EDITED BY

Jasmina M. Luczo,
CSIRO Australian Centre for Disease
Preparedness, Australia

REVIEWED BY

Semmannan Kalaiyarasu,
ICAR-National Institute of High Security Animal
Diseases (ICAR-NIHSAD), India
Ivette Nunez,
Division of Clinical Research (NIAID/NIH),
United States

*CORRESPONDENCE

Dong-Hun Lee
✉ donghunlee@konkuk.ac.kr

[†]These authors have contributed equally to this work

RECEIVED 03 February 2023

ACCEPTED 31 May 2023

PUBLISHED 15 June 2023

CITATION

Park J, Song C-S, Chung DH, Choi S, Kwon J, Youk S and Lee D-H (2023) Chimeric H5 influenza virus-like particle vaccine elicits broader cross-clade antibody responses in chickens than in ducks.
Front. Vet. Sci. 10:1158233.
doi: 10.3389/fvets.2023.1158233

COPYRIGHT

© 2023 Park, Song, Chung, Choi, Kwon, Youk and Lee. This is an open-access article distributed under the terms of the [Creative Commons Attribution License \(CC BY\)](#). The use, distribution or reproduction in other forums is permitted, provided the original author(s) and the copyright owner(s) are credited and that the original publication in this journal is cited, in accordance with accepted academic practice. No use, distribution or reproduction is permitted which does not comply with these terms.

Chimeric H5 influenza virus-like particle vaccine elicits broader cross-clade antibody responses in chickens than in ducks

Jaekeun Park^{1,2†}, Chang-Seon Song^{1†}, David Hyunjung Chung³, Sangyong Choi⁴, Junghoon Kwon⁵, Sungsu Youk⁶ and Dong-Hun Lee^{1*}

¹College of Veterinary Medicine, Konkuk University, Seoul, South Korea, ²Department of Veterinary Medicine, Virginia-Maryland College of Veterinary Medicine, University of Maryland, College Park, MD, United States, ³Department of Pathobiology and Veterinary Sciences, University of Connecticut, Storrs, CT, United States, ⁴Department of Nutritional Sciences, University of Connecticut, Storrs, CT, United States, ⁵College of Veterinary Medicine, Kyungpook National University, Daegu, Republic of Korea, ⁶College of Medicine and Medical Research Institute, Chungbuk National University, Cheongju, Republic of Korea

Eurasian-lineage highly pathogenic avian influenza (HPAI) H5 viruses have spread throughout Asia, the Middle East, Europe, Africa, and most recently, North and South America. These viruses are independently evolving into genetically and antigenically divergent clades, and broad-spectrum vaccines protecting against these divergent clades are needed. In this study, we developed a chimeric virus-like particle (VLP) vaccine co-expressing hemagglutinins from two clades (clades 1 and 2.3.2.1) of HPAI H5 viruses and performed comparative cross-clade hemagglutination inhibition (HI) analysis in chickens and ducks. The chimeric VLP immunization induced a significantly broader spectrum of antibodies against various clades of HPAI H5 viruses than monovalent VLPs both in chickens and ducks. While the chimeric VLP led to broadened antibody responses in both species, significantly lower levels of HI antibodies were elicited in ducks than in chickens. Moreover, boost immunization failed to increase antibody responses in ducks regardless of the VLPs used, in contrast to chickens that showed significantly enhanced antibody responses upon boost immunization. These results suggest (1) the potential application of the chimeric VLP technology in poultry to help control HPAI H5 viruses by offering broader antibody responses against antigenically different strains and (2) possible obstacles in generating high levels of antibody responses against HPAI H5 viruses in ducks via vaccination, implying the need for advanced vaccination strategies for ducks.

KEYWORDS

highly pathogenic avian influenza virus, vaccine, virus like particle, insect cell, poultry, chicken, duck

1. Introduction

Highly pathogenic avian influenza (HPAI) viruses cause high mortality in Gallinaceous bird species. Since 1996, the Eurasian-origin A/goose/Guangdong/1/1996 (Gs/GD) lineage of HPAI H5Nx has caused outbreaks in poultry and wild birds around the world except for Antarctica and Australia (1). The Gs/GD lineage HPAI virus has evolved independently into 10 genetically and

antigenically distinct clades (from clades 0 to 9) and their subclades (2, 3), making it difficult to control them with vaccination in poultry. While the clade 2 viruses have widely spread and predominated in poultry residing in most parts of the world since 2005, the clade 1 viruses remained predominant in Southeast Asia (4, 5). Moreover, continuous human infections with the Gs/GD lineage HPAI H5 viruses in enzootic regions have often been fatal and raised concerns about potential human pandemics (6, 7).

To reduce economic losses in the poultry industry and the risk of human infection, vaccination of domestic poultry against HPAI H5 has been extensively utilized in various enzootic regions, including China, Egypt, Indonesia, and Vietnam (8). However, current vaccines have a critical limitation in that they cannot elicit broad-spectrum antibody responses against diverse clades of HPAI H5 viruses (9). Antigenic match between the vaccine strain and the locally circulating virus is thus a critical factor in achieving optimal vaccine efficacy and controlling the spread of HPAI H5 viruses. Indeed, an outbreak of antigenically distinct HPAI H5 strains in vaccinated poultry was reported to cause significant morbidity and mortality despite of vaccination (10). The decrease in vaccine efficacy is also experimentally demonstrated in heterologous challenge studies using chickens (11, 12) and domestic ducks (11, 13), necessitating the development of vaccines offering broad protection against different clades of H5 viruses.

Domestic ducks play a critical role in maintaining and transmitting HPAI H5 viruses to various host species, including poultry and wild birds (14, 15). Given their significant contribution to the epidemiology of HPAI, it is imperative to mitigate the risk of virus infection in domestic ducks through vaccination in order to control the spread of HPAI. Antigenically-matching vaccination has proven effective in protecting domestic ducks against infection and clinical signs following a homologous HPAI H5 virus challenge (16). Currently developed vaccines, however, have shown suboptimal protective efficacy in domestic ducks, allowing morbidity, mortality, and prolonged viral shedding upon challenges with antigenically distant HPAI H5 viruses (11, 13). Despite its importance, there has been a lack of development in vaccines aimed at providing broader immunity to domestic ducks against antigenically distant clades of HPAI H5 viruses. Virus-like particles (VLPs), which resemble infectious virus particles in structure and morphology, have been suggested as the new generation of vaccines against various viruses, including various influenza A viruses (17–20). In particular, chimeric influenza VLPs containing hemagglutinins (HAs) derived from multiple subtypes of influenza viruses were shown to provide protection from multiple subtypes of influenza viruses in ferrets (21). Recently, Kang et al. also demonstrated the protective efficacy of chimeric influenza VLPs expressing HAs of clade 2.3.2.1c and clade 2.3.4.4c HPAI H5 viruses in chickens (22). However, the potential of chimeric influenza VLPs has not been demonstrated in domestic ducks.

In this study, we generated chimeric VLPs simultaneously expressing antigenically remote HAs from clades 1 and 2 HPAI H5 viruses using the baculovirus expression vector system (BEVS). Our objective was to investigate the enhanced antibody responses elicited by the chimeric VLPs against four antigenically distant clades of HPAI H5N1 viruses. We conducted our investigations in two major poultry species: chickens and domestic ducks.

2. Materials and methods

2.1. Generation of recombinant baculoviruses

For cloning the full-length HA gene of clade 1 H5N1 virus, the HA gene of A/Vietnam/1194/2004 (H5N1) virus was chemically synthesized (Bioneer, Republic of Korea) without the multi-basic cleavage site (MBCS) sequence. For cloning the full-length HA gene of clade 2 H5N1 virus, viral RNA was extracted from A/mandarin duck/K10-483/2010 (H5N1, clade 2.3.2.1), the HA gene was amplified (23), and the MBCS was removed as previously described (24). The amplified HA gene from clade 1 or clade 2 virus was cloned into the vector pFastBac1 (Thermo Fisher, United States), and the resulting plasmids were designated as pFast_clade1 and pFast_clade2, respectively. The other pFastBac1 simultaneously containing both HA genes of clade 1 and clade 2 H5N1 viruses was constructed by cloning a *Sna*BI/*Hpa*I-digested fragment from pFast_clade 2 into the *Hpa*I-digested site of pFast_clade 1, and the resulting plasmid was designated as pFast_clade1 + 2. A plasmid containing an influenza matrix1 (M1) gene, designated as pFast_M1, was constructed by cloning the full-length M1 gene of A/Puerto Rico/8/1934 (H1N1) into the empty vector pFastBac1 (25). Using pFast_clade 1, pFast_clade 2, pFast_clade 1 + 2, and pFast_M1, recombinant baculovirus (rBV) encoding clade 1 HA gene, clade 2 HA gene, clade 1 and clade 2 HA genes, or influenza M1 gene was generated using a Bac-to-Bac BEVS (Thermo Fisher), and the resulting rBVs were designated as rBV_clade 1, rBV_clade 2, rBV_clade 1 + 2, or rBV_M1, respectively (Figure 1A). The titers of rBVs were measured by standard plaque assay using *Spodoptera frugiperda* (Sf9) insect cells.

2.2. Production and characterization of H5 VLPs and preparation of VLPs vaccines

For clade 1 H5 VLPs production, Sf9 cells were co-infected with rBV_clade1 and rBV_M1, both at a multiplicity of infection (MOI) of 5. For clade 2 H5 VLPs production, Sf9 cells were co-infected with rBV_clade2 and rBV_M1, both at an MOI of 5. For chimeric H5 VLPs production, Sf9 cells were co-infected with rBV_clade 1 + 2 and rBV_M1, both at an MOI of 5. After 72 h of infection, the culture medium containing VLPs (Figure 1B) was collected and clarified by low-speed centrifugation (2,000 × g, 30 min, 4°C) to remove large cell debris, and VLPs from the clarified supernatants were pelleted (30,000 × g, 1.5 h, 4°C). The pellet was resuspended in phosphate-buffered saline (PBS; pH 7.2), loaded onto a 20–50% (w/v) discontinuous sucrose density gradient, and ultra-centrifuged (150,000 × g, 1.5 h, 4°C) for purification. The bands positioned above the 50% sucrose density were collected. The total protein concentration of each H5 VLPs preparation was quantified using the Bradford protein assay kit (Pierce, United States) according to the manufacturer's instructions. Expression of the clade 1 and 2 HA as well as M1 proteins in each VLPs preparation was detected by Western blotting using mouse anti-clade 1 H5 monoclonal antibody (Median Diagnostics, Republic of Korea), mouse anti-clade 2 H5 monoclonal antibody (Bionote, Republic of Korea), and rabbit anti-M1 polyclonal antibodies (Immune Technology, United States), followed by incubation with horseradish peroxidase (HRP)-conjugated goat anti-mouse or

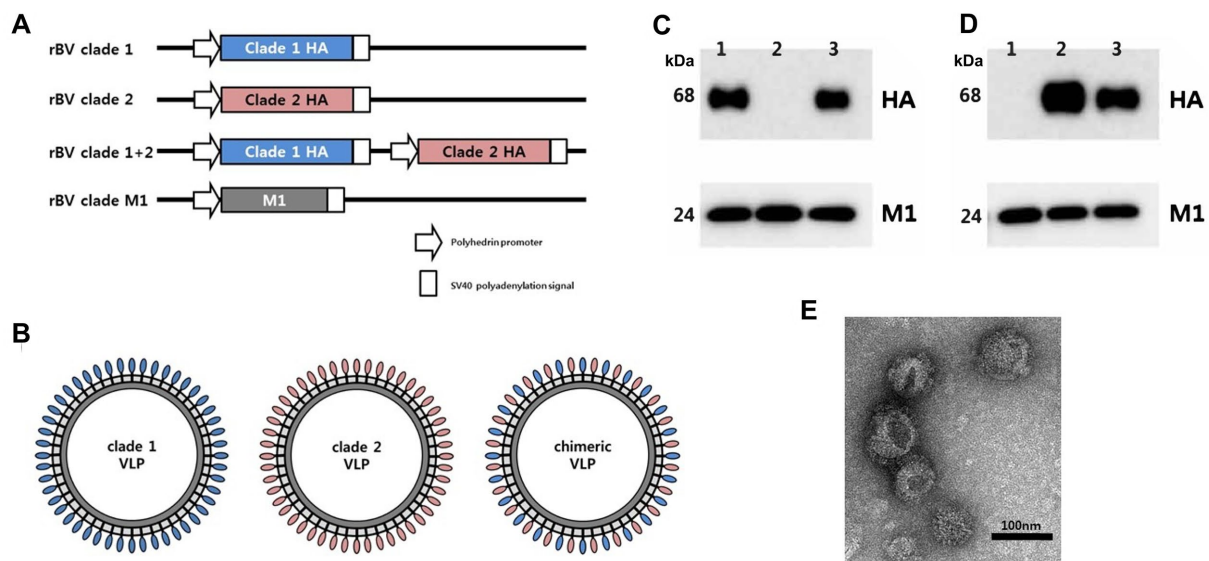


FIGURE 1

Preparation and characterization of chimeric H5 VLP vaccine containing hemagglutinin (HA) proteins from different clades of highly pathogenic avian influenza (HPAI) H5 viruses. (A) Recombinant baculoviruses (rBV) encoding clade 1 HA, clade 2 HA, or both clade 1 HA and clade 2 HA were used to infect Sf9 cells. Sf9 cells were co-infected with rBV encoding HA gene and rBV encoding influenza matrix 1 (M1) gene to generate (B) clade 1, clade 2, or clade 1+2 VLPs. Four micrograms of clade 1 VLP (lane 1), clade 2 VLP (lane 2), and chimeric VLP (lane 3) were characterized by Western blotting using (C) anti-clade 1 HA monoclonal antibody with anti-influenza M1 antibody or (D) anti-clade 2 monoclonal antibody with anti-influenza M1 antibody. HA and M1 are expected to be 68kDa and 28kDa, respectively. (E) Transmission electron microscope was used to take images of negative staining for the chimeric VLPs. Scale bar represents 100nm.

anti-rabbit IgG (AbD Serotec, United Kingdom). Four micrograms of each VLPs preparation were used per well for Western blotting. The presence of VLPs was observed by transmission electron microscopy (TEM; Tecnai G2 Spirit, FEI, Netherlands, installed at Korea Basic Science Institute) using a negative staining method. The H5 VLPs vaccines with final concentrations of 40 µg of VLPs/0.5 mL-dose were prepared by emulsifying each H5 VLPs collection in the oil adjuvant Montanide ISA70 (SEPPIC, France) at a ratio of 30:70 (v/v).

2.3. Immunization of animals and determination of serological immune responses

A total of 30 6-week-old SPF white leghorn chickens (Namduck Sanitec, Republic of Korea) and 30 5-week-old commercially available Pekin ducks (kindly provided by the Moran Food & Breeding Company, Republic of Korea) were divided into respective 3 groups (10 chickens per group and 9–10 ducks per group). Each group of chickens or ducks was intramuscularly immunized twice (three weeks apart) with clade 1, clade 2, or chimeric H5 VLPs vaccines (0.5 mL per animal). All the animals were confirmed for seronegativity before immunization using the hemagglutination inhibition (HI) test against different clades of H5N1 viruses as described below.

To determine the seronegativity of the animals before immunization and seroconversion after immunization, sera were collected from VLPs-vaccinated chickens and ducks before immunization and at 3 weeks after each immunization for cross-clade HI test using H5N1 viruses from different clades. H5N1 viruses containing HA genes, without MBCS

sequences, of A/Vietnam/1194/2004 (clade 1), A/Indonesia/5/2005 (clade 2.1), A/mandarin duck/K10-483/2010 (clade 2.3.2.1), or A/chicken/Korea/ES/2003 (clade 2.5) were generated using reverse genetics (RG) system as previously described (26). HI tests were performed according to the OIE standard method using 4 HA units of H5N1 viruses. To eliminate non-specific HI factors, 1 volume of duck serum was treated with 3 volumes of receptor-destroying enzyme (Denka Seiken Co., JAPAN) at 37°C for 16h followed by heat inactivation for 30 min at 56°C.

2.4. Statistical analysis

Dunn's multiple comparison test was used following Kruskal–Wallis test (non-parametric one-way ANOVA) to compare HI titers between groups (i.e., clade 1 VLPs vs. clade 2 VLPs vs. chimeric VLPs). A two-tailed non-parametric Mann–Whitney test was used to compare HI titers between two groups (i.e., prime vs. boost or chicken vs. duck). An HI titer of 2 was assigned to samples with undetected HI activity for statistical analyses. Log-transformed (base 2) HI titers were used for statistical analysis. Results with *p*-values <0.05 were considered statistically significant.

2.5. Ethics statement

All animal procedures performed in this study were reviewed and approved by the Institutional Animal Care and Use Committee (IACUC) of Konkuk University.

3. Results

3.1. Generation and characterization of chimeric H5 VLPs

The chimeric H5 VLPs containing both clade 1 and clade 2 HA were observed to be released into the culture supernatants (Figures 1C–E). Western blotting analysis showed the presence of both clade 1 (Figure 1C) and clade 2 (Figure 1D) H5 HAs from the chimeric VLP, while standard VLPs only possessed either clade 1 HA or clade 2 HA as expected. Matrix proteins were detected at comparable levels between VLPs (Figures 1C,D). The size of VLP particles was approximately 100 nm in diameter, while the morphology resembled influenza virion with spikes on the surface (Figure 1E). These results confirm the successful generation of the chimeric VLPs.

3.2. Antibody responses in chickens

The chimeric VLPs elicited broader antibody responses against multiple HPAI H5 viruses from different clades compared to the monovalent VLPs (Figures 2A,F). Both prime and boost immunization of chimeric VLPs induced significantly higher HI antibodies against clade 1 (Figures 2B,G) and clade 2.3.2 (Figures 2D,I) H5N1 viruses compared to each standard VLPs. For example, the levels of anti-clade 1 antibodies elicited by chimeric VLPs were significantly higher than

those induced by the monovalent clade 2.3.2 VLPs and comparable to those induced by monovalent clade 1 VLPs (Figures 2B,G). While the antibody response was moderate against the clade 2.1 (Figures 2C,H) and clade 2.5 viruses (Figures 2E,J) which are different from the HA clades incorporated in the chimeric VLPs, the chimeric VLP induced significantly higher anti-clade 2.5 antibodies compared to that induced by monovalent clade 2.3.2 VLP both after prime and boost immunization. These data show that the chimeric VLPs induce broader antibody responses against multiple HPAI H5 viruses from various clades compared to the monovalent VLPs.

3.3. Antibody responses in ducks

Similar to the results from chickens, the chimeric VLPs elicited broader antibody responses in ducks against multiple HPAI H5 viruses compared to the monovalent VLPs (Figures 3A,F). After both prime and boost immunization, the chimeric VLPs induced significantly higher HI antibody titers against clade 1 (Figures 3B,G) and clade 2.3.2 (Figures 3D,I) H5N1 viruses compared to each monovalent VLPs. For example, the levels of anti-clade 1 antibodies elicited by the chimeric VLPs were significantly higher than those induced by the monovalent clade 2.3.2 VLPs and comparable to those induced by the monovalent clade 1 VLPs (Figures 3B,G). The chimeric VLPs induced higher mean HI antibody titers against clade 2.1 (Figures 3C,H) and clade 2.5 (Figures 3E,J) H5N1 viruses compared

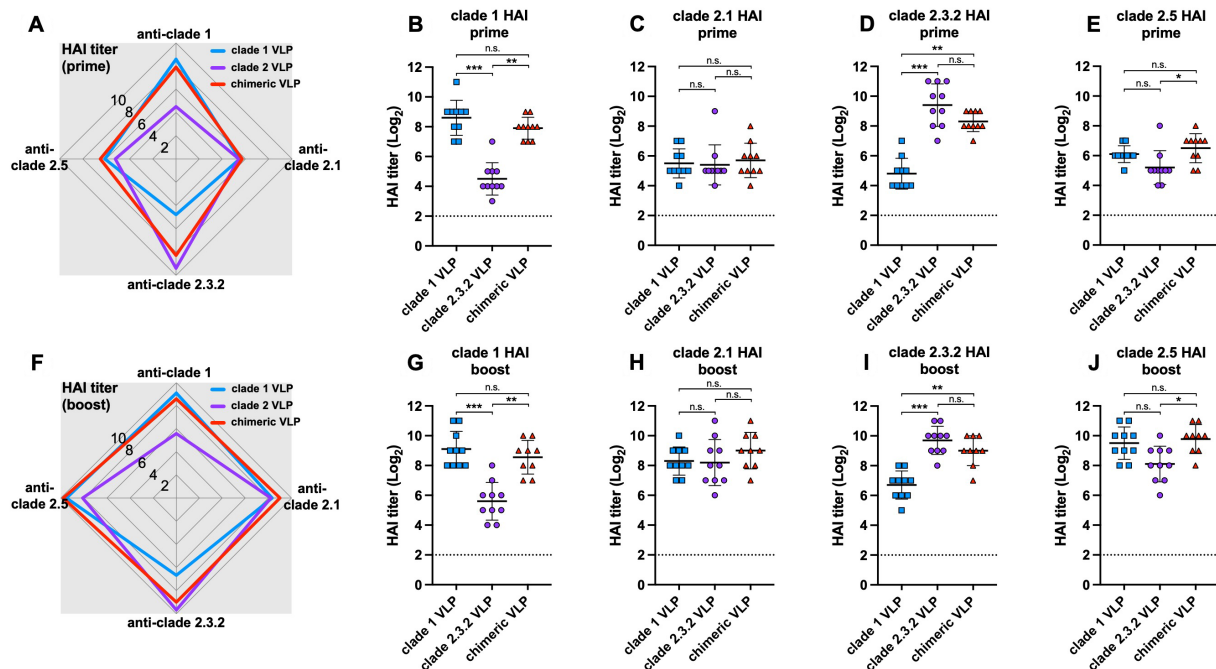


FIGURE 2

Antibody responses against chimeric H5 VLP vaccines in chickens. 6-week-old SPF chickens ($n=10$ per group) were immunized with clade 1, clade 2, or chimeric H5 VLP vaccines ($40 \mu\text{g}$ of VLP/ 0.5 mL dose). Serum HI titers against different clades of HPAI H5N1 viruses were determined using antigenically different H5N1 viruses 3 weeks after priming (A–E) and boosting (F–J). Radar charts show geometric mean serum HI titers (\log_2) from chickens immunized with clade 1 (blue), clade 2 (purple), or chimeric (red) H5 VLP vaccines against clade 1, 2.1, 2.3.2.1, and 2.5 H5N1 viruses. Each symbol in dot plots represents an individual animal. Horizontal lines and error bars in dot plots represent geometric mean serum HI titers and standard deviations, respectively. Dashed lines show the detection limit of the HI assay. An HI titer of 2 was assigned to samples with undetected HI activity for generating graphs and statistical analyses. Dunn's multiple comparison test was used following Kruskal–Wallis test (non-parametric one-way ANOVA) to compare HI titers between groups (* $p<0.05$, ** $p<0.01$, *** $p<0.001$, n.s. = not significant).

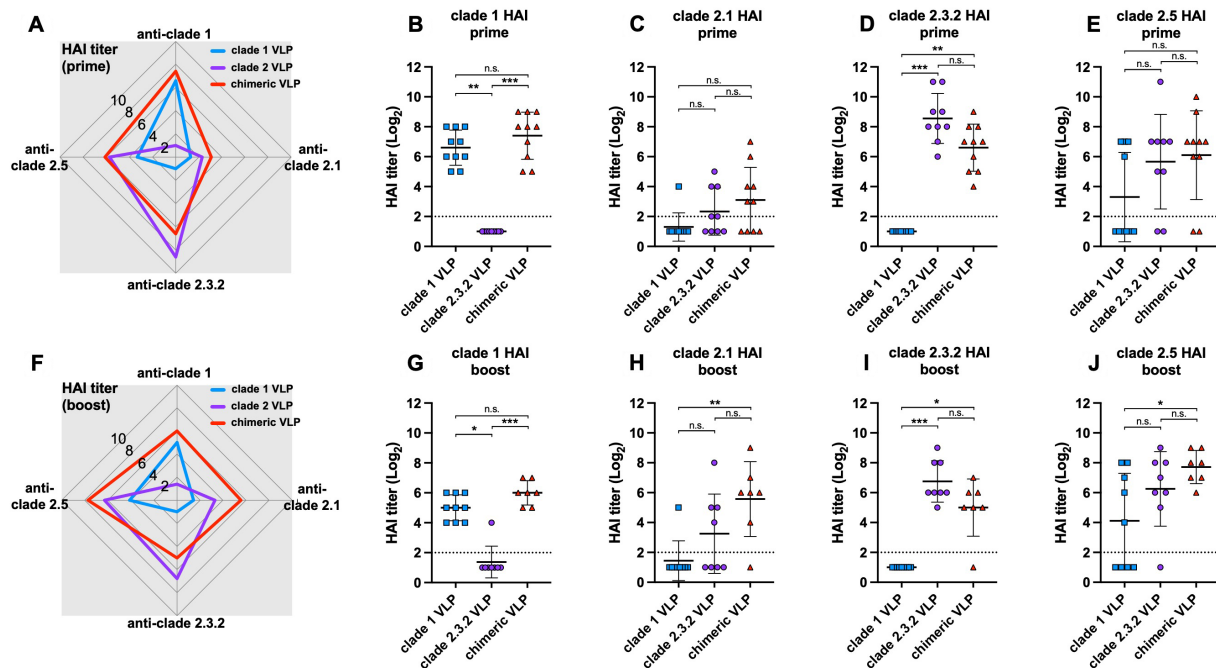


FIGURE 3

Antibody responses against chimeric H5 VLP vaccines in ducks. 5-week-old commercial ducks ($n=9-10$ per group) were immunized with clade 1, clade 2, or chimeric H5 VLP vaccines ($40\ \mu\text{g}$ of VLP/ $0.5\ \text{mL}$ dose). Serum HI titers against different clades of HPAI H5N1 viruses were determined using antigenically different H5N1 viruses 3 weeks after priming (A–E) and boosting (F–J). Radar charts show geometric mean serum HI titers (\log_2) from chickens immunized with clade 1 (blue), clade 2 (purple), or chimeric (red) H5 VLP vaccines against clade 1, 2.1, 2.3.2, and 2.5 H5N1 viruses. Each symbol in dot plots represents an individual animal. Horizontal lines and error bars in dot plots represent geometric mean serum HI titers and standard deviations, respectively. Dashed lines show the detection limit of the HI assay. An HI titer of 2 was assigned to samples with undetected HI activity for generating graphs and statistical analyses. Dunn's multiple comparison test was used following Kruskal–Wallis test (non-parametric one-way ANOVA) to compare HI titers between groups ($*p<0.05$, $**p<0.01$, $***p<0.001$, n.s. = not significant).

to each monovalent VLPs. Particularly, the chimeric VLPs induced significantly higher anti-clade 2.1 as well as anti-clade 2.5 antibodies compared to the monovalent clade 1 VLPs after the boost immunization (Figures 3H,J). These data suggest that the chimeric VLPs can induce broader antibody responses compared to the monovalent VLPs in ducks, in correspondence with the results from chickens. However, the induction of cross-reactive antibodies against heterologous HAs (i.e., clade 2.1 and clade 2.5) was lower than what was observed in chickens.

3.4. Comparison of antibody responses in chickens and ducks

The antibody responses in ducks were significantly narrower and lower than those in chickens throughout the study, regardless of the VLPs used and the number of immunizations. Except for the HI antibodies against the clade 2.5 HA, ducks generated significantly lower levels of antibody responses than chickens following the prime immunization with either monovalent clade 1 or clade 2 VLPs (Figures 4A,B) and the chimeric VLPs (Figure 4C). The differences were even greater following the boost immunization. Across all four clades of HAs, ducks generated significantly lower levels of antibody responses compared to chickens regardless of the VLPs used (Figures 4D–F). While boost immunization significantly broadened cross-clade antibody responses in chickens (Figures 5A–C), this effect

was not observed in ducks which did not show any increase in antibody responses upon the boost immunization (Figures 5D–F).

4. Discussion

In this study, we developed the chimeric influenza VLP vaccine containing HAs from two different clades of HPAI H5 viruses and performed a comparative evaluation of the vaccine's potential uses in chickens and ducks against the globally circulating Eurasian-lineage H5 HPAI viruses. Our chimeric H5 VLP vaccine incorporating HAs from clades 1 and 2 HPAI H5N1 viruses induced broader HI antibodies than monovalent VLPs in chickens and domestic ducks, indicating the potential for a broad protective efficacy against different clades of HPAI H5 viruses. We also showed that antibody responses to the VLPs in ducks were significantly narrower and lower than those in chickens, regardless of the type of antigens used and the number of immunizations, suggesting that more advanced vaccine or vaccination strategies would be required to elicit broad and robust antibody responses in ducks.

Although this study successfully demonstrated the potential of chimeric VLP technology to broaden antibody responses to multiple clades of HPAI H5 viruses in chickens and ducks, there are several limitations. Firstly, our comparison of antibody breadth between chickens and ducks was based solely on HI assays. Although HI titers generally correlate well with neutralizing titers and are widely accepted

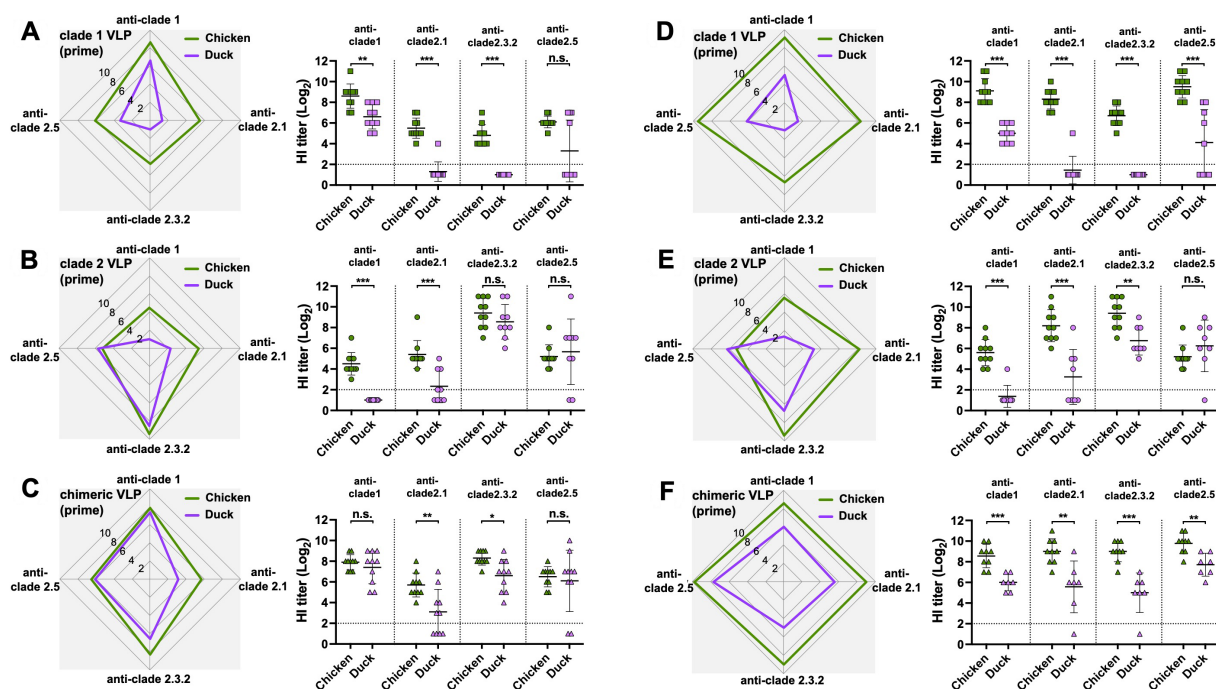


FIGURE 4

Comparison of the effect of VLP immunization on serum HI titers between chickens and ducks. The effect of VLP immunization on serum HI titers were compared between chickens and ducks using data from Figures 2, 3. The HI titers elicited by (A) clade 1, (B) clade 2, or (C) chimeric H5 VLP vaccines (40 μ g of VLP/0.5 mL dose) in SPF chickens (green) and commercial ducks (purple) were compared 3-weeks after priming. Similarly, the HI titers elicited by (D) clade 1, (E) clade 2, or (F) chimeric H5 VLP vaccines (40 μ g of VLP/0.5 mL dose) in SPF chickens (green) and commercial ducks (purple) were compared 3-weeks after boosting. HI titers against clade 1, 2.1, 2.3.2.1, and 2.5 H5N1 viruses were measured. Horizontal lines and error bars in dot plots represent geometric mean serum HI titers and standard deviations, respectively. Dashed lines show the detection limit of the HAI assay. An HI titer of 2 was assigned to samples with undetected HI activity for generating graphs and statistical analyses. A two-tailed nonparametric Mann–Whitney test was used for the comparison (* p <0.05, ** p <0.01, *** p <0.001, n.s. = not significant).

as indicators of influenza protection (27, 28), it is important to consider that different species may exhibit varying levels of neutralizing antibodies despite similar HI titers. While this study did not include neutralization assays, it is possible that such assays could provide higher sensitivity in assessing the level of protective antibodies in immunized animals and serve as better predictors of the broadened protective efficacy of the chimeric VLPs compared to HI assays. Secondly, the lack of challenge experiments in this study prevents us from determining whether the relatively low titers of HI antibodies in ducks would result in lower levels of protection against HPAI H5 viruses in ducks compared to chickens. Protection from viral infections is not solely determined by pre-existing immunity but is also influenced by host anti-viral responses and the susceptibility of hosts to different viral strains, which are factors that evolutionarily differentiate chickens and ducks. For example, RIG-I in ducks was shown to play a suppressive role in viral replication and initiate pro-inflammatory pathways involving type I interferon signals at the sites of infection and was suggested as one of the key pathways causing the differences in susceptibilities to avian influenza viruses between chickens and ducks (29). Therefore, it remains uncertain whether the generally lower HI titers following VLP immunization in ducks relative to chickens would result in lower levels of protection in ducks. In fact, studies by Webster et al. have demonstrated complete protection from HPAI H5N1 virus challenges in vaccinated ducks with HI titers much lower than those observed in chickens (30),

indicating that low HI antibody titers may not necessarily predict a lack of protection against HPAI viruses in domestic ducks. Ultimately, it is crucial to conduct challenge studies in both chickens and ducks, using multiple clades of HPAI H5 viruses, to confirm the broadened protective efficacy of the chimeric VLPs and to determine whether the lower HI titers in ducks correspond to a decrease in protective efficacy.

Both current and previous studies have demonstrated the chimeric VLPs as a promising vaccine platform to provoke enhanced protective efficacy against antigenically distant influenza viruses in chickens (22). While the effectiveness of chimeric VLPs may vary across poultry species against HPAI, the chimeric VLP vaccine platform remains a promising approach for controlling HPAI epidemics. Future studies will include comparative viral challenge experiments in order to gain further insights into broadly-protective vaccination, host species immunity, and the varying pathogenic mechanisms of AIVs in different poultry species.

The chimeric VLP vaccine developed in this study demonstrated the induction of a high level of broadly reacting HI antibodies against various H5 viruses in immunized chickens and similar but relatively lower responses in ducks. These findings suggest that the chimeric VLP technology holds promise as a platform for controlling the Gs/GD-lineage HPAI H5 viruses in poultry. In addition, since the VLPs have only HA and M1 proteins, it will allow differentiation of virus-infected birds from vaccinated birds by detecting antibodies to viral nucleocapsid, as we showed in our previous studies (17–19), which

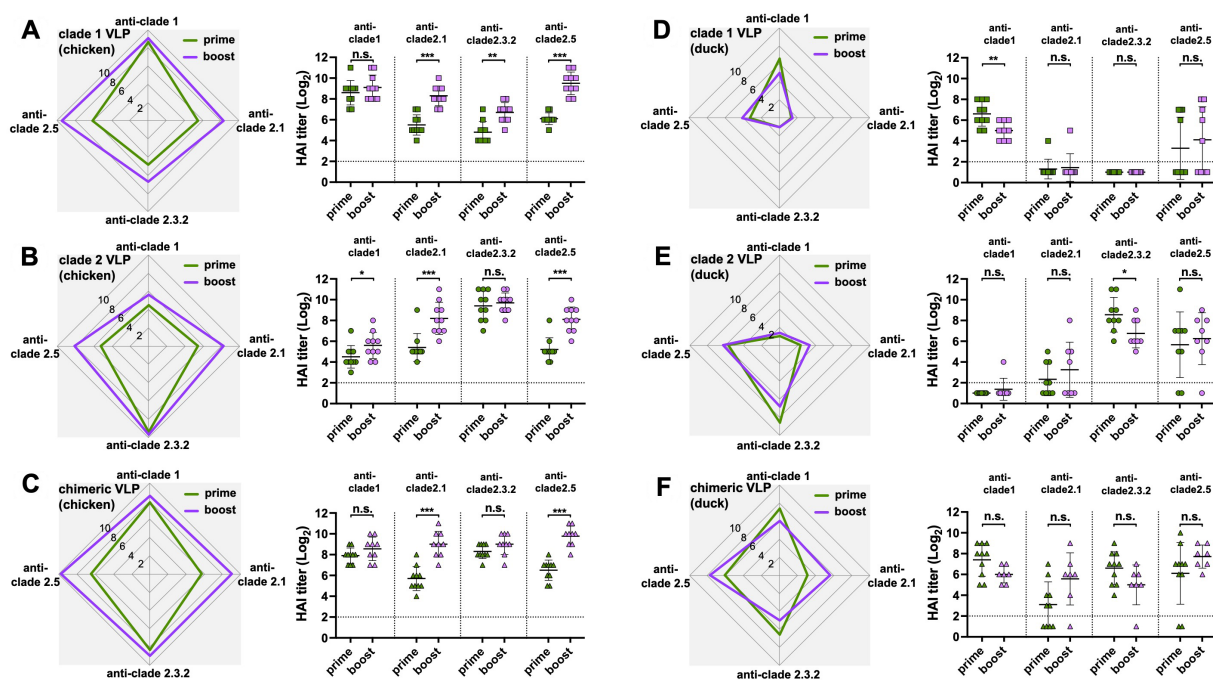


FIGURE 5

Boost-immunization significantly increased antibody responses in chickens but not in ducks. The effect of boost immunization on serum HI titers in chickens and ducks were investigated using data from Figures 2, 3. The boosting effect of (A) clade 1, (B) clade 2, or (C) chimeric H5 VLP vaccines (40 µg of VLP/0.5 mL-dose) in SPF chickens was investigated by comparing the serum HI titers between the primed and boosted serum HI titers against clade 1, 2.1, 2.3.2.1, and 2.5 H5N1 viruses. Similarly, the boosting effect of (D) clade 1, (E) clade 2, or (F) chimeric H5 VLP vaccines (40 µg of VLP/0.5 mL-dose) in commercial ducks was investigated by comparing the serum HI titers against different H5N1 viruses. Horizontal lines and error bars in dot plots represent geometric mean serum HI titers and standard deviations, respectively. Dashed lines show the detection limit of the HAI assay. An HI titer of 2 was assigned to samples with undetected HI activity for generating graphs and statistical analyses. A two-tailed nonparametric Mann–Whitney test was used for the comparison (* $p<0.05$, ** $p<0.01$, *** $p<0.001$, n.s. = not significant).

offers a promising strategy for differentiating infected from vaccinated animals.

Data availability statement

The raw data supporting the conclusions of this article will be made available by the authors, without undue reservation.

Ethics statement

The animal study was reviewed and approved by Institutional Animal Care and Use Committee (IACUC) of Konkuk University.

Author contributions

D-HL and C-SS: conceptualization and funding acquisition. D-HL and JP: methodology. JK, SY, D-HL, and JP: formal analysis. JK, SY, DC, JP, and SC: investigation. DC, JP, and SC: data curation. JP and D-HL: writing—original draft preparation. JK, SY, C-SS, DC, and SC: writing—review and editing. All authors have read and agreed to the published version of the manuscript.

Funding

D-HL is supported by Korea Institute of Planning and Evaluation for Technology in Food, Agriculture and Forestry (IPET) through Animal Disease Management Technology Development Program, funded by Ministry of Agriculture, Food and Rural Affairs (MAFRA) (grant number: 122057–2).

Conflict of interest

The authors declare that the research was conducted in the absence of any commercial or financial relationships that could be construed as a potential conflict of interest.

Publisher's note

All claims expressed in this article are solely those of the authors and do not necessarily represent those of their affiliated organizations, or those of the publisher, the editors and the reviewers. Any product that may be evaluated in this article, or claim that may be made by its manufacturer, is not guaranteed or endorsed by the publisher.

References

- Lee DH, Bertran K, Kwon JH, Swayne DE. Evolution, global spread, and pathogenicity of highly pathogenic avian influenza H5Nx clade 2.3.4.4. *J Vet Sci.* (2017) 18:269–0. doi: 10.4142/jvs.2017.18.S1.269
- Sonnberg S, Webby RJ, Webster RG. Natural history of highly pathogenic avian influenza H5N1. *Virus Res.* (2013) 178:63–77. doi: 10.1016/j.virusres.2013.05.009
- Donis RO, Smith GJ. Nomenclature updates resulting from the evolution of avian influenza a(H5) virus clades 2.1.3.2a, 2.2.1, and 2.3.4 during 2013–2014. *Influenza Other Respir Viruses.* (2015) 9:271–6. doi: 10.1111/irv.12324
- Thor SW, Nguyen H, Balish A, Hoang AN, Gustin KM, Nhung PT, et al. Detection and characterization of clade 1 Reassortant H5N1 viruses isolated from human cases in Vietnam during 2013. *PLoS One.* (2015) 10:e0133867. doi: 10.1371/journal.pone.0133867
- Le TH, Nguyen NT. Evolutionary dynamics of highly pathogenic avian influenza a(H5N1) HA clades and vaccine implementation in Vietnam. *Clin Exp Vacc Res.* (2014) 3:117–7. doi: 10.7774/cevr.2014.3.2.117
- Beigel JH, Farrar J, Han AM, Hayden FG, Hyer R, de Jong MD, et al. Avian influenza a (H5N1) infection in humans. *N Engl J Med.* (2005) 353:1374–85. doi: 10.1056/NEJMra052211
- Webby RJ, Webster RG. Are we ready for pandemic influenza? *Science.* (2003) 302:1519–22. doi: 10.1126/science.1090350
- Swayne DE, Spackman E, Pantin-Jackwood M. Success factors for avian influenza vaccine use in poultry and potential impact at the wild bird-agricultural interface. *EcoHealth.* (2014) 11:94–8. doi: 10.1007/s10393-013-0861-3
- Criado MF, Sá e Silva M, Lee DH, Salge CAL, Spackman E, Donis R, et al. Cross-protection by inactivated H5 Prepandemic vaccine seed strains against diverse goose/Guangdong lineage H5N1 highly pathogenic avian influenza viruses. *J Virol.* (2020) 94:e00720–20. doi: 10.1128/JVI.00720-20
- Salaheldin AH, Veits J, Abd el-Hamid HS, Harder TC, Devrishov D, Mettenleiter TC, et al. Isolation and genetic characterization of a novel 2.2.1.2a H5N1 virus from a vaccinated meat-turkeys flock in Egypt. *Virol J.* (2017) 14:48. doi: 10.1186/s12985-017-0697-5
- Pfeiffer J, Suarez DL, Sarmento L, To TL, Nguyen T, Pantin-Jackwood MJ. Efficacy of commercial vaccines in protecting chickens and ducks against H5N1 highly pathogenic avian influenza viruses from Vietnam. *Avian Dis.* (2010) 54:262–1. doi: 10.1637/8715-031909-Reg.1
- Kapczynski DR, Pantin-Jackwood MJ, Spackman E, Chrzastek K, Suarez DL, Swayne DE. Homologous and heterologous antigenic matched vaccines containing different H5 hemagglutinins provide variable protection of chickens from the 2014 U.S. H5N8 and H5N2 clade 2.3.4.4 highly pathogenic avian influenza viruses. *Vaccine.* (2017) 35:6345–53. doi: 10.1016/j.vaccine.2017.04.042
- Cha RM, Smith D, Shepherd E, Davis CT, Donis R, Nguyen T, et al. Suboptimal protection against H5N1 highly pathogenic avian influenza viruses from Vietnam in ducks vaccinated with commercial poultry vaccines. *Vaccine.* (2013) 31:4953–60. doi: 10.1016/j.vaccine.2013.08.046
- Gilbert M, Chaitaweessub P, Parakamawongsa T, Premasithira S, Tiensin T, Kalpravidh W, et al. Free-grazing ducks and highly pathogenic avian influenza. *Thailand Emerg Infect Dis.* (2006) 12:227–4. doi: 10.3201/eid1202.050640
- Kwon JH, Bahl J, Swayne DE, Lee YN, Lee YJ, Song CS, et al. Domestic ducks play a major role in the maintenance and spread of H5N8 highly pathogenic avian influenza viruses in South Korea. *Transbound Emerg Dis.* (2020) 67:844–1. doi: 10.1111/tbed.13406
- Pantin-Jackwood MJ, DeJesus E, Costa-Hurtado M, Smith D, Chrzastek K, Kapczynski DR, et al. Efficacy of two licensed avian influenza H5 vaccines against challenge with a 2015 U.S. H5N2 clade 2.3.4.4 highly pathogenic avian influenza virus in domestic ducks. *Avian Dis.* (2019) 63:90–6. doi: 10.1637/11895-050918-Reg.1
- Lee DH, Park JK, Lee YN, Song JM, Kang SM, Lee JB, et al. H9N2 avian influenza virus-like particle vaccine provides protective immunity and a strategy for the differentiation of infected from vaccinated animals. *Vaccine.* (2011) 29:4003–7. doi: 10.1016/j.vaccine.2011.03.067
- Lee DH, Park JK, Song CS. Progress and hurdles in the development of influenza virus-like particle vaccines for veterinary use. *Clin Exp Vacc Res.* (2014) 3:133–9. doi: 10.7774/cevr.2014.3.2.133
- Park JK, Lee DH, Youn HN, Kim MS, Lee YN, Yuk SS, et al. Protective efficacy of crude virus-like particle vaccine against HPAI H5N1 in chickens and its application on DIVA strategy. *Influenza Other Respir Viruses.* (2013) 7:340–8. doi: 10.1111/j.1750-2659.2012.00396.x
- Roldao A, Mellado MC, Castilho LR, Carrondo MJ, Alves PM. Virus-like particles in vaccine development. *Expert Rev Vaccines.* (2010) 9:1149–76. doi: 10.1586/erv.10.115
- Pushko P, Pearce MB, Ahmad A, Tretyakova I, Smith G, Belser JA, et al. Influenza virus-like particle can accommodate multiple subtypes of hemagglutinin and protect from multiple influenza types and subtypes. *Vaccine.* (2011) 29:5911–8. doi: 10.1016/j.vaccine.2011.06.068
- Kang YM, Cho HK, Kim JH, Lee SJ, Park SJ, Kim DY, et al. Single dose of multi-clade virus-like particle vaccine protects chickens against clade 2.3.2.1 and clade 2.3.4.4 highly pathogenic avian influenza viruses. *Sci Rep.* (2021) 11:13786. doi: 10.1038/s41598-021-93060-8
- Hoffmann E, Stech J, Guan Y, Webster RG, Perez DR. Universal primer set for the full-length amplification of all influenza A viruses. *Arch Virol.* (2001) 146:2275–89. doi: 10.1007/s007050170002
- Heckman KL, Pease LR. Gene splicing and mutagenesis by PCR-driven overlap extension. *Nat Protoc.* (2007) 2:924–2. doi: 10.1038/nprot.2007.132
- Park JK, Lee DH, Yuk SS, Tseren-Ochir EO, Kwon JH, Noh JY, et al. Virus-like particle vaccine confers protection against a lethal Newcastle disease virus challenge in chickens and allows a strategy of differentiating infected from vaccinated animals. *Clin. Vac. Immunol.* (2014) 21:360–5. doi: 10.1128/CVI.00636-13
- Lee DH, Park JK, Kwon JH, Yuk SS, Erdene-Ochir TO, Jang YH, et al. Efficacy of single dose of a bivalent vaccine containing inactivated Newcastle disease virus and reassortant highly pathogenic avian influenza H5N1 virus against lethal HPAI and NDV infection in chickens. *PLoS One.* (2013) 8:e58186. doi: 10.1371/journal.pone.0058186
- Molesti E, Wright E, Terregino C, Rahman R, Cattoli G, Temperton NJ. Multiplex evaluation of influenza neutralizing antibodies with potential applicability to in-field serological studies. *J Immunol Res.* (2014) 2014:457932:1–11. doi: 10.1155/2014/457932
- Benne CA, Kroon FP, Harmsen M, Tavares L, Kraaijeveld CA, de Jong JC. Comparison of neutralizing and hemagglutination-inhibiting antibody responses to influenza A virus vaccination of human immunodeficiency virus-infected individuals. *Clin Diagn Lab Immunol.* (1998) 5:114–7. doi: 10.1128/CDLI.5.1.114-117.1998
- Evseev D, Magor KE. Innate immune responses to avian influenza viruses in ducks and chickens. *Vet Sci.* (2019) 6. doi: 10.3390/vetsci6010005
- Webster RG, Webby RJ, Hoffmann E, Rodenberg J, Kumar M, Chu HJ, et al. The immunogenicity and efficacy against H5N1 challenge of reverse genetics-derived H5N3 influenza vaccine in ducks and chickens. *Virology.* (2006) 351:303–11. doi: 10.1016/j.virol.2006.01.044



OPEN ACCESS

EDITED BY

Jasmina M. Luczo,
CSIRO Australian Centre for Disease
Preparedness, Australia

REVIEWED BY

Hyesun Jang,
J. Craig Venter Institute (La Jolla), United States
Romain Volmer,
Ecole Nationale Vétérinaire de Toulouse
(ENVT), France

*CORRESPONDENCE

Dong-Hun Lee
✉ donghunlee@konkuk.ac.kr

[†]These authors have contributed equally to this work

RECEIVED 17 April 2023

ACCEPTED 03 July 2023

PUBLISHED 20 July 2023

CITATION

Lee S-H, Lee J, Noh J-Y, Jeong J-H, Kim J-B,
Kwon J-H, Youk S, Song C-S and Lee D-H
(2023) Age is a determinant factor in the
susceptibility of domestic ducks to H5 clade
2.3.2.1c and 2.3.4.4e high pathogenicity avian
influenza viruses.
Front. Vet. Sci. 10:1207289.
doi: 10.3389/fvets.2023.1207289

COPYRIGHT

© 2023 Lee, Lee, Noh, Jeong, Kim, Kwon,
Youk, Song and Lee. This is an open-access
article distributed under the terms of the
[Creative Commons Attribution License \(CC BY\)](https://creativecommons.org/licenses/by/4.0/).
The use, distribution or reproduction in other
forums is permitted, provided the original
author(s) and the copyright owner(s) are
credited and that the original publication in this
journal is cited, in accordance with accepted
academic practice. No use, distribution or
reproduction is permitted which does not
comply with these terms.

Age is a determinant factor in the susceptibility of domestic ducks to H5 clade 2.3.2.1c and 2.3.4.4e high pathogenicity avian influenza viruses

Sun-Hak Lee^{1†}, Jiho Lee^{1†}, Jin-Yong Noh^{1,2}, Jei-Hyun Jeong^{1,2},
Jun-Beom Kim^{1,2}, Jung-Hoon Kwon³, Sungsu Youk⁴,
Chang-Seon Song^{1,2} and Dong-Hun Lee^{5*}

¹Avian Disease Laboratory, College of Veterinary Medicine, Konkuk University, Seoul, Republic of Korea, ²KHAV Co., Ltd., Seoul, Republic of Korea, ³Laboratory of Veterinary Microbiology, College of Veterinary Medicine, Kyungpook National University, Daegu, Republic of Korea, ⁴Department of Microbiology, College of Medicine, Chungbuk National University, Cheongju-si, Republic of Korea, ⁵Wildlife Health Laboratory, College of Veterinary Medicine, Konkuk University, Seoul, Republic of Korea

High pathogenicity avian influenza (HPAI) is a viral disease with devastating consequences for the poultry industry worldwide. Domestic ducks are a major source of HPAI viruses in many Eurasian countries. The infectivity and pathogenicity of HPAI viruses in ducks vary depending on host and viral factors. To assess the factors influencing the infectivity and pathogenicity of HPAI viruses in ducks, we compared the pathobiology of two HPAI viruses (H5N1 clade 2.3.2.1c and H5N6 clade 2.3.4.4e) in 5- and 25-week-old ducks. Both HPAI viruses caused mortality in a dose-dependent manner (10^4 , 10^6 , and 10^8 EID₅₀) in young ducks. By contrast, adult ducks were infected but exhibited no mortality due to either virus. Viral excretion was higher in young ducks than in adults, regardless of the HPAI strain. These findings demonstrate the age-dependent mortality of clade 2.3.2.1c and clade 2.3.4.4e H5 HPAI viruses in ducks.

KEYWORDS

high pathogenicity avian influenza, clade 2.3.2.1c H5N1, clade 2.3.4.4e H5N6, age-related pathogenicity, duck

1. Introduction

Avian influenza viruses (AIVs), members of the genus Influenza virus A of the family Orthomyxoviridae, are divided into subtypes based on the surface glycoproteins hemagglutinin (HA, H1-H16) and neuraminidase (NA, N1-N9) (1). The natural reservoirs of most AIVs are wild aquatic birds, especially those of the orders Anseriformes (ducks, geese, and swans) and Charadriiformes (gulls, terns, and waders). They play a major role in the evolution, maintenance, and dissemination of AIVs (2). Most AIVs in natural hosts are low-pathogenic avian influenza (LPAI) viruses that cause little or no disease in natural hosts and Gallinaceous poultry (3). However, novel high pathogenicity avian influenza (HPAI) viruses arise following the adaptation of the H5 and H7 subtypes in domestic poultry and cause significant illness or death (4). Since the detection of A/Goose/Guangdong/1/1996(H5N1) (Gs/GD) in domestic poultry in southern China, the descendant viruses have evolved into 10 genetically distinct hemagglutinin (HA)

clades (0–9) (5). Along with prolonged circulation in poultry, the predominant subclades of clade 2 H5 viruses were replaced by an antigenically distinct subclade, followed by 2.2 (6) and 2.3.2.1 (7), and further evolved into three subclades, 2.3.2.1a, 2.3.2.1b, and 2.3.2.1c (8), mainly in China and Southeast Asia. Various HPAI subtypes bearing the genetic backbone of the Gs/GD lineage H5 clade 2.3.4.4 have been identified in domestic ducks since 2008 and have subsequently evolved into different subclades (9). Among them, clades 2.3.2.1c H5N1 and 2.3.4.4b H5NX HPAI spread intercontinentally via wild migratory birds, causing earlier intercontinental waves (waves 2 and 3a) and subsequent waves (waves 3b and 4), respectively (10).

Domestic ducks play a substantial role in the evolution, maintenance, and spread of Gs/GD HPAI. For example, novel genotypes of HPAI H5N1 in Bangladesh and HPAI H5N5 and H5N8 in China have been reported in domestic ducks, highlighting the role of domestic ducks as reassortment vessels for creating new genotypes of influenza viruses (11). Some studies have emphasized that domestic duck populations and transport could affect the prevalence and distribution of HPAI viruses, particularly in countries where ducks are the main food source. During the HPAI H5N1 outbreaks from 2007 to 2009 in South and Southeast Asia, the population of domestic ducks was the main factor delineating areas at risk of HPAI H5N1 spreading in domestic poultry (12). For the novel introduction of clade 2.3.4.4 H5N8 viruses that occurred in South Korea in 2014, wild waterfowl migration and domestic duck density have shaped the epidemiology of H5N8 viruses (13). Under the unique fattening duck production system known as ‘foie gras’ in southwest France, the trade-related transport of fattening ducks contributed to the 2016–2017 epizootic of HPAI H5N8 in France (14).

The clinical signs and mortality of HPAI viruses vary. In ducks, depending on various factors, including viral strains and pre-immune status. Some strains of HPAI viruses induce subclinical infection that can facilitate the spread and persistence of HPAI viruses (15–19). Mortality among ducks naturally infected with the HPAI virus was first reported in Italy (20), and Asian-origin H5N1 viruses have caused mortality in wild and domestic ducks (21). In contrast, different pathogenicities in ducks have been observed between distinct strains of HPAI viruses in several previous studies. The Hong Kong H5N1 HPAI isolates in 1997 caused limited pathogenicity in ducks (22), but the 2002 HPAI isolates caused increased mortality and systemic infections in ducks (23). Comparison studies showed differences in pathogenicity between two H5N1 HPAI isolates from Egypt in 2007 and 2008 (24) and two H5N6 HPAI isolates from Korea in 2016. However, host factors, especially age at infection, which possibly affects pathogenicity, have not been fully understood in recent clades of the HPAI virus. This study aimed to assess the factors influencing the infectivity and pathogenicity of HPAI viruses in ducks. We compared the pathobiology of two HPAI viruses (H5N1 clade 2.3.2.1c and H5N6 clade 2.3.4.4e) in 5- and 25-week-old ducks.

2. Materials and methods

2.1. Viruses

We used two HPAI viruses, A/duck/Korea/ES2/2016 (H5N6, ES2) clade 2.3.4.4e and A/chicken/Vietnam/NCVD-KA435/2013 (H5N1, KA435) clade 2.3.2.1c, for experimental infection. The viruses were

kindly provided by the Animal and Plant Quarantine Agency of Korea. Viruses were inoculated into 9–11 days old specific-pathogen-free embryonated chicken eggs, and allantoic fluids were harvested after 2–3 days of incubation at 37°C. The virus was aliquoted and stored in a –70°C deep freezer for further experiments. The titration endpoints for each virus were calculated using standard methods (25).

2.2. Animals

We used 37 five-week-old domestic ducks and 40 25-week-old domestic ducks obtained from the Moran Food & Breeding Company (Eum-Seong, Republic of Korea). All oropharyngeal and cloacal swabs were negative for influenza virus infection based on the real-time reverse transcription-polymerase chain reaction (rRT-PCR) (25). Before the viral challenge, all ducks were confirmed to be seronegative for anti-AIV antibodies using a commercial enzyme-linked immunosorbent assay (ELISA) kit (Bionote, Korea). All ducks used in this study were housed in self-contained isolation cages in a controlled environment at the ABSL-3 facility at Konkuk University to maintain biosafety and biosecurity barriers. All animal procedures were reviewed, approved, and supervised by the Institutional Animal Care and Use Committee (IACUC) (no. KU1840, KU18193), and the Institutional Biosafety Committee (No. KUIBC-2018-10, KUIBC-2019-05) at Konkuk University.

2.3. Experimental design

Five-week-old ($n=27$) and 25-week-old ($n=36$) ducks were divided into two groups. Each group was inoculated with the ES2 virus ($n=13$ for younger ducks and $n=14$ for older ducks) or the KA435 virus ($n=18$ for each age group). Six 5-week-old and eight 25-week-old ducks were used as negative controls. To evaluate the mean bird infectious dose (BID_{50}) and mean bird lethal dose (BLD_{50}), we divided each age group into three groups (4–6 ducks). Ducks were inoculated intranasally with 10^4 , 10^6 , or 10^8 50% egg infective doses (EID_{50}) of the viruses, hereafter referred to as low, medium, and high doses, respectively. Ducks were observed daily for clinical signs and mortality after the challenge for 14 days. To detect and quantify viral shedding, oropharyngeal and cloacal swabs were collected at 3, 5, 7, 10, and 14 day-post-challenge (dpc) and submerged in 1.5 ml PBS. Sera were collected from the birds 14 d after infection to verify seroconversion. A commercial competitive ELISA kit (Bionote, Korea) was used to detect anti-AIV antibodies targeting nucleocapsid protein (NP) according to the manufacturer's instructions. Ducks were considered infected if they were seroconverted by 14 dpc or had detectable viruses, along with clinical signs and mortality.

2.4. Clinical scoring

Clinical scores were determined by applying the IVPI scoring system on ducks (26, 27). Ducks were observed daily for 14 days post infection. Birds were scored 0 if healthy, 1 if sick, 2 if severely sick, and 3 if dead. Birds were considered ‘sick’ if one of the following signs was observed and considered ‘severely sick’ if more than one of the following signs were observed: respiratory involvement, depression,

diarrhea, cyanosis of the feet or mucosa, edema of face or head, and nervous signs. Clinical scores were calculated per group with an observation period of 10 days. When ducks were too sick or could not be urged to move, they were killed humanely and scored as dead.

2.5. Viral RNA quantification

Viral RNA from oropharyngeal and cloacal swabs was extracted from 200 μ L of the supernatant using the MagNA Pure 96 extraction system (Roche, Mannheim, Germany) according to the manufacturer's instructions. The extracted RNA was quantified by real-time reverse transcription-polymerase chain reaction using previously described protocols (28). The Ct values were converted into infectious units equivalent to EID₅₀/ml using a standard curve.

2.6. Statistical analysis

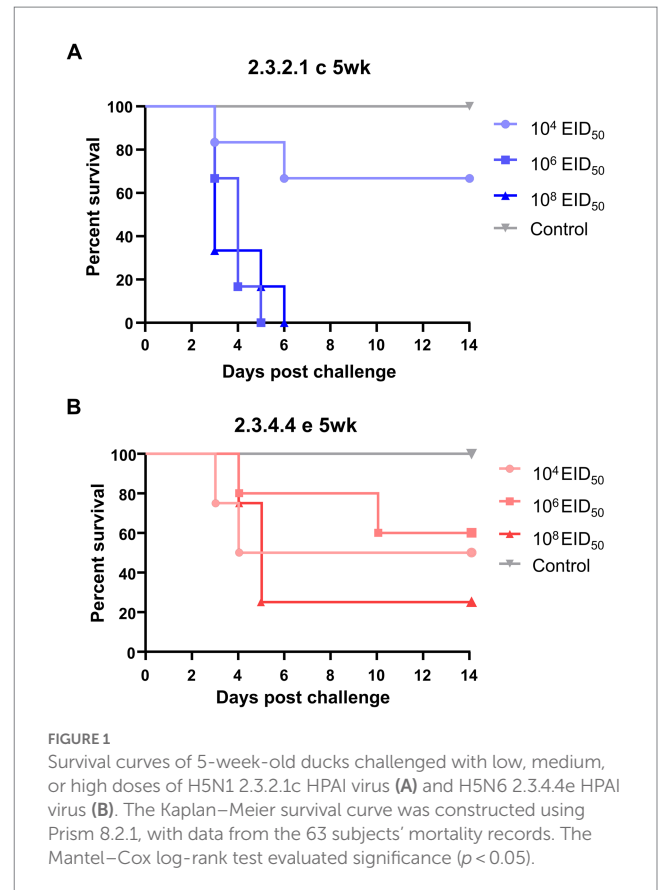
The Kaplan–Meier survival curve was constructed, and the Mantel–Cox log-rank test was used to compare the survival curves between the two age groups. An unpaired *t*-test was applied for normally distributed data; otherwise, the Mann–Whitney U test was used. All statistical analyses were performed using GraphPad Prism version 8.2.1 (GraphPad Software Inc., CA, USA). Statistical significance was set at $p \leq 0.05$.

3. Results

3.1. Infectivity, mortality, and clinical signs

None of the negative control ducks of either age exhibited viral shedding, seroconversion, or clinical signs (Figure 1). In the groups inoculated with the KA435 virus, all 5-week-old ducks died, except for four out of six ducks challenged with the low dose. None of the 5-week-old ducks had anti-AIV antibodies. All 5-week-old ducks in the medium- and high-dose challenge groups died within 6 days, with a mean death time (MDTs) of 3.8 days (Table 1). For the group infected with a low dose, two out of six ducks died within 6 days, and the MDT was 4 days. Ducks died before 4dpc did not show any clinical signs, while torticollis and incoordination started to appear after 4dpc on ducks that succumbed to death. The BID₅₀ and BLD₅₀ were 10^{4.5}EID₅₀. In contrast, none of the 25-week-old ducks challenged with the KA435 virus died while some ducks showed depression and respiratory involvement (Supplementary Figure 1A). Based on the serologic examination, all 25-week-old ducks challenged with the high-dose virus were seroconverted, followed by four out of six ducks in the medium-dose group and one out of six ducks in the low dose challenge group, resulting in a BID₅₀ dose of 10^{5.27}EID₅₀.

For the ES2 virus, the BLD₅₀ of 5-week-old ducks was 10^{5.26}EID₅₀, as three out of four ducks (high-dose), three out of five ducks (medium-dose), and two out of four ducks (low dose) died after the challenge. Severe clinical signs, such as incoordination and torticollis, were observed in the four out of eight ducks died from the infection (Supplementary Figure 1B). A few ducks challenged with the ES2 virus survived and seroconverted, resulting in a lower BID₅₀ ($< 10^{4.0}$ EID₅₀) than the BLD₅₀. The MDTs of the younger ducks challenged with a



high, medium, and low dose was 3.5, 6.7, and 4.7 days, respectively. Consistent with the KA435 virus, none of the 25-week-old ducks died after the challenge with the ES2 virus. No ducks showed incoordination or nervous signs, while six ducks showed depression or mild respiratory involvements. The morbidity rates of the high-, medium-, and low-dose challenge groups were 100% (five out of five ducks), 66.6% (four out of six ducks), and 16.6% (one out of six ducks), respectively, indicating that the BID₅₀ of the ES2 virus in 25-week-old ducks was 10^{5.27}EID₅₀.

The survival curves of different age groups inoculated with the same dose of the virus were compared using the log-rank test (Figure 1). The survival curves of the groups inoculated with high and medium doses of the KA435 virus showed significant differences ($p=0.001$ and $p=0.0014$, respectively, Figure 1A; Supplementary Figure 2) in the survival rate between 5-week-old and 25-week-old ducks. Adult ducks that received a high-dose of the ES2 virus were significantly less likely to exhibit mortality than young ducks with the same challenge dose and strain ($p=0.0148$, Supplementary Figure 2). In addition, the survival curves of groups inoculated with the same doses of KA435 and ES2 viruses were compared (Supplementary Figure 3). These data demonstrated significant differences between the two viruses only at medium doses using the log-rank test ($p=0.008$, Supplementary Figure 3). Young ducks inoculated with a medium-dose of the KA435 virus had a significantly lower estimate of survival than young ducks inoculated with the same dose of the ES2 virus. No statistically significant difference was observed between the survival curves for the other two doses.

TABLE 1 Mortality, morbidity, mean death time, BID₅₀, and BLD₅₀ of H5N1 clade 2.3.2.1C and H5N6 clade 2.3.4.4e in 5-week-old ducks and 25-week-old ducks.

Age	Virus strain	Dose ^a	Morbidity ^b	Mortality ^c	MDT ^d	BID ₅₀ ^e	BLD ₅₀ ^f
5-week-old	2.3.2.1c A/chicken/Vietnam/ NCVD-KA435/ 2013(H5N1)	High (10 ^{8.0} EID ₅₀)	6/6	6/6	3.8	10 ^{4.5} EID ₅₀	10 ^{4.5} EID ₅₀
		Medium (10 ^{6.0} EID ₅₀)	6/6	6/6	3.8		
		Low (10 ^{4.0} EID ₅₀)	2/6	2/6	4		
	2.3.4.4e A/duck/Korea/ES2/ 2016(H5N6)	High (10 ^{8.0} EID ₅₀)	4/4	3/4	4.7	<10 ^{4.0} EID ₅₀	10 ^{5.26} EID ₅₀
		Medium (10 ^{6.0} EID ₅₀)	5/5	3/5	6.7		
		Low (10 ^{4.0} EID ₅₀)	3/4	2/4	3.5		
25-week-old	2.3.2.1c A/chicken/Vietnam/ NCVD-KA435/ 2013(H5N1)	High (10 ^{8.0} EID ₅₀)	6/6	0/6	ND ^g	10 ^{5.27} EID ₅₀	>10 ^{8.0} EID ₅₀
		Medium (10 ^{6.0} EID ₅₀)	4/6	0/6	ND		
		Low (10 ^{4.0} EID ₅₀)	1/6	0/6	ND		
	2.3.4.4e A/duck/Korea/ES2/ 2016(H5N6)	High (10 ^{8.0} EID ₅₀)	5/5	0/5	ND	<10 ^{4.0} EID ₅₀	>10 ^{8.0} EID ₅₀
		Medium (10 ^{6.0} EID ₅₀)	4/5	0/5	ND		
		Low (10 ^{4.0} EID ₅₀)	4/4	0/4	ND		

^aDucks were inoculated intranasally with each dose of the viruses.^bNumber of infected ducks confirmed with viral shedding or seroconversion/number of inoculated ducks.^cNumber of dead ducks/number of inoculated ducks.^dMean death time in days.^e50% Bird infectious dose.^f50% Bird lethal dose.^gNot detectable.

3.2. Viral shedding

Oropharyngeal (OP) and cloacal (CL) swabs collected from virus-inoculated ducks at different time points were analyzed using quantitative rRT-PCR to measure viral shedding. The mean viral titer of OP swabs on each swab day was consistently higher than that of CL swabs for both viruses. In general, virus shedding peaked at 3 dpc and then gradually declined, regardless of the dose and virus strain, except for the 25-week-old ducks inoculated with a low dose of ES2. For high- and medium-dose groups inoculated with KA435, 5-week-old ducks shed more virus than 25-week-old ducks in both OP and CL routes at 3 dpc (Figure 2, $p < 0.001$ for OP-high, OP-medium, and CL-medium, and $p < 0.01$ for CL-high). Virus shedding was also higher in 5-week-old ducks challenged with high and medium doses of ES2 at 3 and 5 dpc (Figure 3; $p < 0.001$ for OP-high, medium at 3 dpc, and $p < 0.01$, for the others). Therefore, for the ducks that were confirmed to be infected, 5-week-old ducks shed significantly higher amounts of the virus *via* the OP and CL routes than 25-week-old ducks, regardless of the virus strain.

4. Discussion

Previous natural and experimental infection studies have shown that HPAI-infected wild and domestic waterfowls present no to mild clinical signs (15–19). For example, early Hong Kong H5N1 HPAI isolates from 1997 showed limited pathogenicity in ducks (22). However, the continuous evolution of HPAI viruses has increased their lethality in various bird species, including ducks. Many previous studies have demonstrated that HPAI viruses induce varied pathogenicities in ducks. Unlike the 1997 H5N1 HPAI isolates, the novel 2002 HPAI isolates caused systemic infection in ducks, with high

virus titers and pathology in multiple organs, causing neurological dysfunction and death (23). Mortality in wild and domestic ducks is caused by many Asian-origin HPAI H5N1 viruses (21). Recently, mass die-off cases of tufted ducks (*Aythya fuligula*) were reported in the Netherlands (29, 30) and Germany (31) from 2016 to 2017, and high wild bird mortality was observed in coastal and other water-rich areas of the Netherlands between October 2020 and June 2021 (32). In this study, the ES2 virus, which belongs to clade 2.3.4.4e, had a lower BID₅₀ and higher BLD₅₀ in 5-week-old ducks than KA435, which belongs to clade 2.3.2.1c HPAI clade. Recent studies have reported that the molecular changes associated with the unusual lethality of HPAI viruses in ducks are related to the PA and PB1 genes of the H5N1 virus (33), PA and NS genes of clade 2.3.4.4 H5N6 virus (34), and PB2, NP, and M genes of clade 2.3.4.4 H5N8 virus (35). However, the underlying mechanisms have not been identified.

Our data indicate that younger ducks are more susceptible to both the 2.3.2.1c and 2.3.4.4e challenge viruses. Our findings are consistent with those of other studies by Pantin-Jackwood et al. (36), Jang et al. (37), and Londt et al. (38), in that the younger the host age, the more severe the clinical signs and higher the mortality were observed, while variances existed in the degree of mortality rate and clinical signs in accordance with the strain challenge and age at infection. In other words, some strains of Gs/GD H5 HPAI viruses, such as A/chicken/Hong Kong/220/97 (H5N1), A/Egret/HK/757.2/02 (H5N1), A/Duck/Vietnam/218/05 (H5N1) (36), and A/Waterfowl/Korea/S57/2016 (H5N6) (37), showed age-dependent pathogenicity in ducks. Age-related pathogenicity of HPAI has also been reported in turkeys (39), wild ducks (ruddy ducks, lesser scaups) (40), and humans (41), but not in broiler chickens (42). In a previous study, the BID₅₀ and BLD₅₀ of the ES2 virus in 2-week-old ducks were 10^{3.0}EID₅₀ and 10^{4.0}EID₅₀, supporting the younger the duck is, the more vulnerable it is to the HPAI virus (34). The challenged ducks exhibited higher viral titers

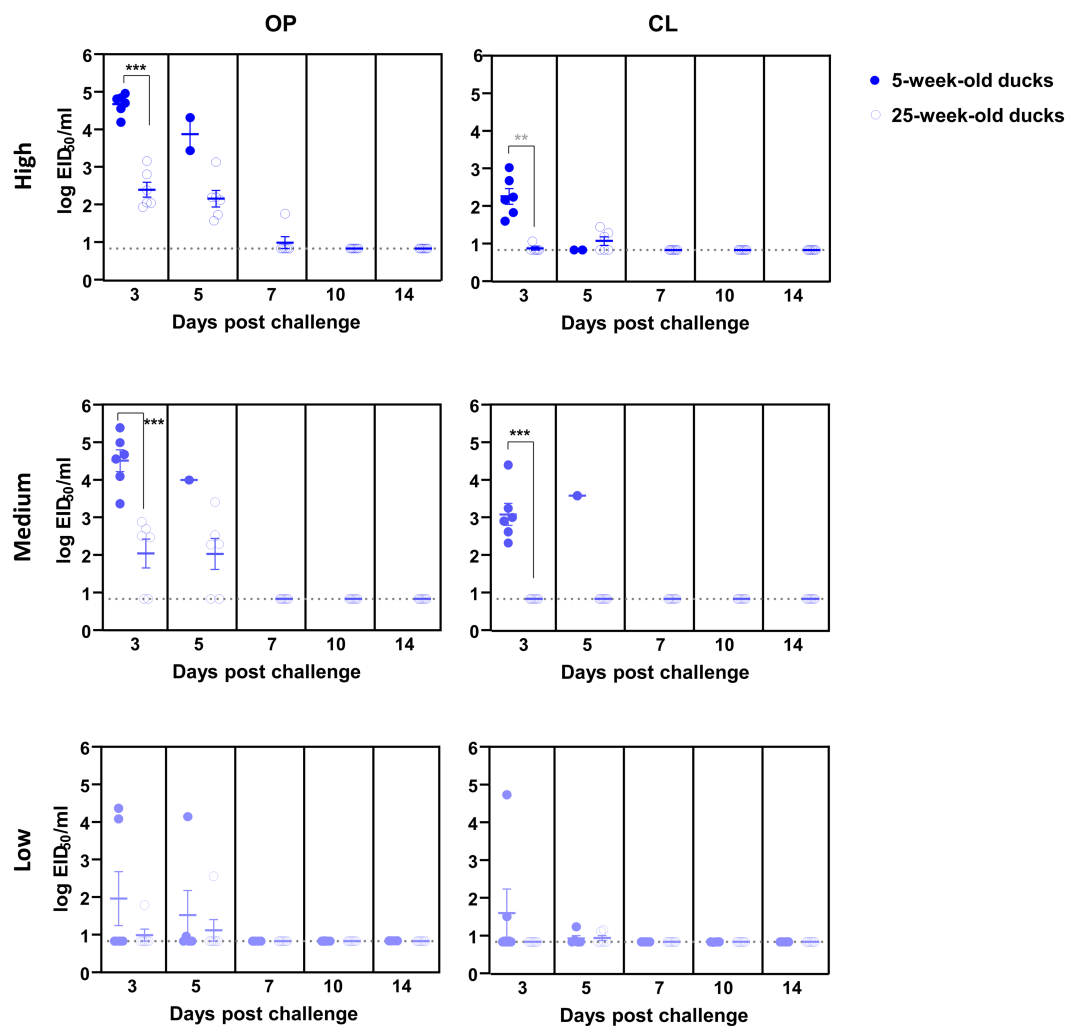


FIGURE 2

Oropharyngeal (OP) and cloacal (CL) virus shedding in 5- and 25-week-old ducks challenged with low, medium, or high doses of H5N1 2.3.2.1c HPAI virus. The dotted line indicates the detection limit ($10^{0.8345}$ EID₅₀ equivalent/0.1 ml). The middle line among circles indicates the mean value and error bars indicate standard deviation. The black asterisks indicate that statistical analyses were conducted using an independent samples t-test. The grey asterisks indicated that statistical analyses were conducted using a Mann–Whitney U Test (** $p < 0.01$; *** $p < 0.001$).

in the OP swabs than in the CL swabs in this study, consistent with previous studies using other HPAI viruses, including H5N1 viruses isolated in 2002 and 2004 (18), and H5N8 and H5N6 viruses isolated in South Korea in 2016 and 2017, respectively (19).

No mortality was observed in 25-week-old ducks, even at a high-dose of inoculation, but excreted viruses, suggesting that adult ducks could play a significant role in the maintenance and spread of HPAI viruses. Also, ducks that showed viral shedding did not show any clinical signs, indicating their role as a silent reservoir of the virus. Innate immunity and receptor distribution are suspected to be factors affecting age-dependent pathogenicity. Studies on Pekin ducks suggest that higher body temperature and upregulation of innate immune-related genes, including IFN- α , retinoic acid-inducible gene I (RIG-I), and IL-6 in spleens, could impact the age-related pathogenicity of several H5N1 HPAI viruses (36). In a pathogenicity study of the H5N6 HPAI virus isolated in South Korea in 2016, cell damage-related genes, such as CIDEA and ND2, and the immune response-related gene

NR4A3 were dramatically induced in the lungs of infected 2-week-old ducks compared with those in the lungs of 4-week-old ducks (37). Age-dependent α -2,6 sialic acid expression variations among minor poultry species have been observed in ducks, geese, and turkeys (43). In turkeys, sialic acid receptor patterns change with age, which can result in variations in viral replication and tissue tropism. As poultry species age, the migration of lymphocytes to peripheral mucosa-associated lymphoid tissue (MALT) increases (44), which could lead to mortality in younger ducks and a higher inflammatory response against HPAI viral replication. Based on these studies, it is reasonable to hypothesize that variations in viral pathogenicity may arise from differences in innate immunity, immune response-related gene expression, and receptor expression according to age. Consequently, analyzing these factors in poultry, including ducks of different ages, can provide crucial data for comprehending the responses to viral infections.

Other host and environmental factors can also affect duck pathogenicity. In the case of host factors, as presented in this study,

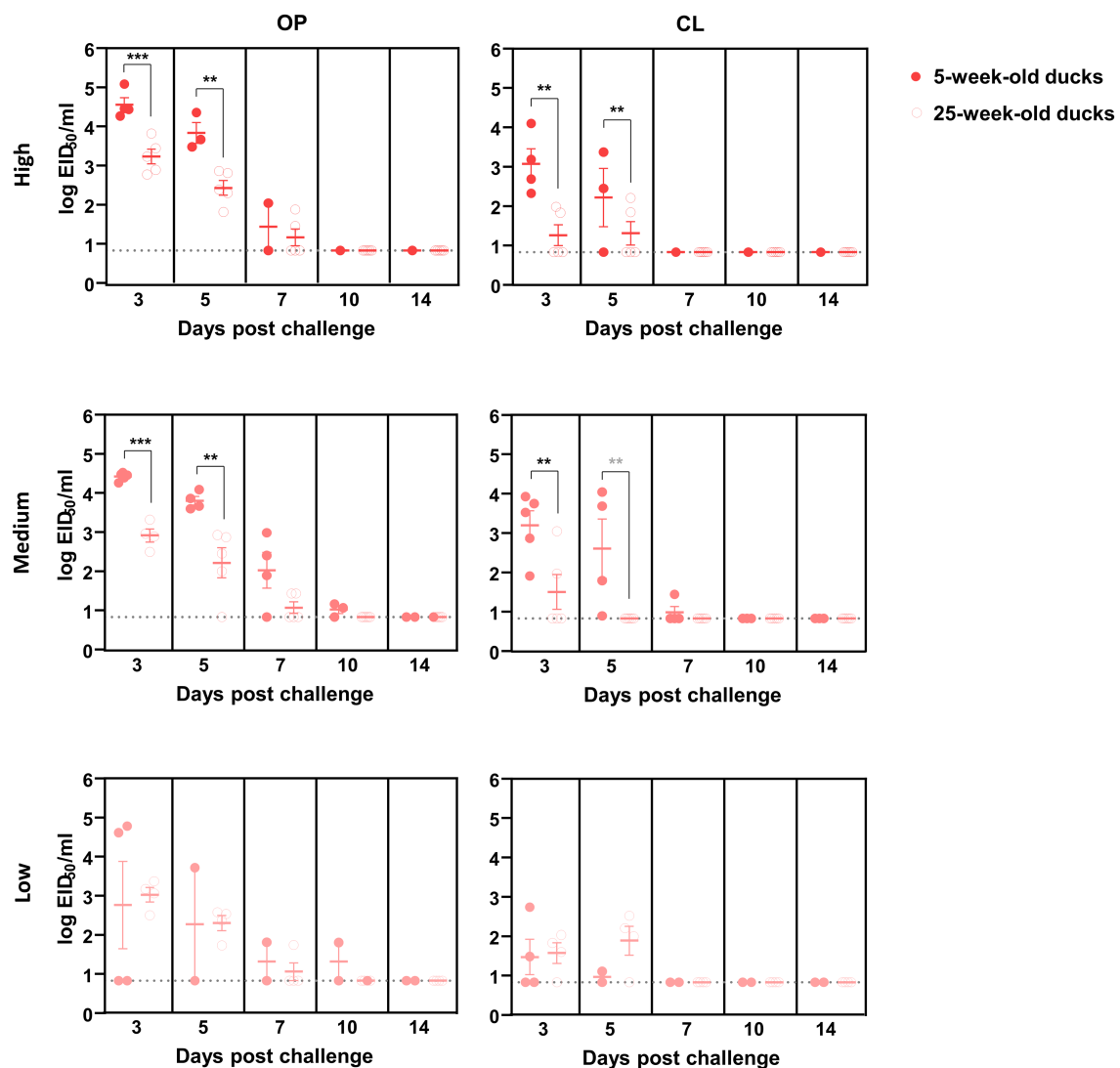


FIGURE 3

Oropharyngeal (OP) and cloacal (CL) virus shedding in 5- and 25-week-old ducks challenged with low, medium, or high doses of H5N6 2.3.4.4e HPAI virus. The dotted line indicates the detection limit ($10^{0.8345}$ EID₅₀ equivalent/0.1 ml). The middle line among circles indicates the mean value and error bars indicate standard deviation. The black asterisks indicated that statistical analyses were conducted using an independent samples *t*-test. The grey asterisks indicated that statistical analyses were conducted using a Mann–Whitney U Test (***p* < 0.01; ****p* < 0.001).

age at infection is a determinant factor for some strains in certain species; consistently, younger groups showed high pathogenicity (18, 36–40). The presentation of the disease also varied by virus strain and duck species, with Muscovy ducks being more vulnerable than Pekin ducks (45), and pre-existing immunity by commercial vaccination (46) or immunosuppressive viral infections (47). Co-infections with other respiratory pathogens could influence the outcome of infection, as seen in previous studies using the duck hepatitis virus (48) and other subtypes of LPAI viruses (49). Infections and pathogenicity could also be influenced by environmental factors, leading to higher virus concentrations and persistence, such as elevated virus levels due to ventilation and longer virus survival under favorable environmental conditions (50). Altogether, the pathogenicity of HPAI viruses depends on many factors, which could raise various patterns of disease, including the diverse onset of infections, clinical signs, and mortality. Further

studies should be conducted to investigate the pathogenicity and related factors of recently circulating viruses to understand the mechanisms of the disease.

The pathogenicity of HPAI can be influenced by a range of factors, including viral characteristics and environmental conditions, as well as host physiology and immune response. In this study, we investigated the impact of age on the pathogenicity of two clades of HPAI viruses in ducks, in terms of mortality, infectivity, and level of virus shedding. Our results showed that younger ducks exhibited higher pathogenicity, as evidenced by increased mortality rates and viral shedding, compared to older ducks. The results obtained in this study may help gain insight into age-related differences in the transmission dynamics and disease patterns of viruses. The contrasting survival between younger and older ducks suggests that silent infection and transmission can occur in older ducks, indicating that active surveillance and risk assessment should be carefully implemented in

aged ducks in the earlier stages of HPAI outbreaks to prevent them from spreading. In addition, since ducks can host a variety of avian influenza viruses as a natural reservoir species, older ducks with asymptomatic or mild infections can play a role in evolution of HPAIVs, potentially giving rise to new strains with altered pathogenicity or increased zoonotic potential. The precise mechanisms causing the higher virulence in young ducks remain unknown and warrant further investigation.

Data availability statement

The raw data supporting the conclusions of this article will be made available by the authors, without undue reservation.

Ethics statement

The animal study was reviewed and approved by Institutional Animal Care and Use Committee, Institutional Biosafety Committee.

Author contributions

JL, J-YN, J-HJ, and J-BK contributed to conceptualization, methodology, formal analysis, investigation, resources, and data curation. S-HL and JL wrote the first draft of the manuscript. S-HL, JL, J-HK, SY, and D-HL wrote review and editing. Project administration and funding acquisition were performed by JL, J-YN, J-HJ, J-BK, and C-SS. All authors contributed to the article and approved the submitted version.

References

- Tong S, Li Y, Rivailler P, Conrardy C, Castillo DAA, Chen L-M, et al. A distinct lineage of influenza A virus from bats. *Proc Natl Acad Sci.* (2012) 109:4269–74. doi: 10.1073/pnas.1116200109
- Stallknecht DE, Shane S. Host range of avian influenza virus in free-living birds. *Vet Res Commun.* (1988) 12:125–41. doi: 10.1007/BF00362792
- Gonzales JL, Elbers AR. Effective thresholds for reporting suspicions and improve early detection of avian influenza outbreaks in layer chickens. *Sci Rep.* (2018) 8:1–9. doi: 10.1038/s41598-018-26954-9
- Webster RG, Rott R. Influenza virus a pathogenicity: the pivotal role of hemagglutinin. *Cells.* (1987) 50:665–6. doi: 10.1016/0092-8674(87)90321-7
- Group E.W. Toward a unified nomenclature system for highly pathogenic avian influenza virus (H5N1). *Emerg Infect Dis.* (2008) 14:e1. doi: 10.3201/eid1407.071681
- Nagarajan S, Tosh C, Smith DK, Peiris JSM, Murugkar HV, Sridevi R, et al. Avian influenza (H5N1) virus of clade 2.3. 2 in domestic poultry in India. *PLoS One.* (2012) 7:e31844. doi: 10.1371/journal.pone.0031844
- Creanga A, Nguyen DT, Gerloff N, Do HT, Balish A, Nguyen HD, et al. Emergence of novel clade 2.3. 2.1 influenza A (H5N1) virus subgroups in Vietnam and detection of novel reassortants. *Virology.* (2013) 444:12–20. doi: 10.1016/j.virol.2013.06.005
- Bi Y, Chen J, Zhang Z, Li M, Cai T, Sharshov K, et al. Highly pathogenic avian influenza H5N1 clade 2.3. 2.1 c virus in migratory birds, 2014–2015. *Virol Sin.* (2016) 31:300–5. doi: 10.1007/s12250-016-3750-4
- Lee D-H, Bertran K, Kwon J-H, Swayne DE. Evolution, global spread, and pathogenicity of highly pathogenic avian influenza H5Nx clade 2.3. 4.4. *J Vet Sci.* (2017) 18:269–80. doi: 10.4142/jvs.2017.18.S1.269
- Lee DH, Criado MF, Swayne DE. Pathobiological origins and evolutionary history of highly pathogenic avian influenza viruses. *Cold Spring Harb Perspect Med.* (2021) 11:a038679. doi: 10.1101/cshperspect.a038679
- Gu M, Liu W, Cao Y, Peng D, Wang X, Wan H, et al. Novel reassortant highly pathogenic avian influenza (H5N5) viruses in domestic ducks, China. *Emerg Infect Dis.* (2011) 17:1060–3. doi: 10.3201/eid1706.101406
- Gilbert M, Newman SH, Takekawa JY, Loth L, Biradar C, Prosser DJ, et al. Flying over an infected landscape: distribution of highly pathogenic avian influenza H5N1 risk in South Asia and satellite tracking of wild waterfowl. *EcoHealth.* (2010) 7:448–58. doi: 10.1007/s10393-010-0672-8
- Hill SC, Lee Y-J, Song B-M, Kang H-M, Lee E-K, Hanna A, et al. Wild waterfowl migration and domestic duck density shape the epidemiology of highly pathogenic H5N8 influenza in the Republic of Korea. *Infect Genet Evol.* (2015) 34:267–77. doi: 10.1016/j.meegid.2015.06.014
- Guinat C, Artois J, Bronner A, Guérin JL, Gilbert M, Paul MC. Duck production systems and highly pathogenic avian influenza H5N8 in France, 2016–2017. *Sci Rep.* (2019) 9:6177. doi: 10.1038/s41598-019-42607-x
- Jeong S, Kwon J-H, Lee S-H, Kim Y-J, Jeong J-H, Park J-E, et al. Subclinical infection and transmission of clade 2.3. 4.4 H5N6 highly pathogenic avian influenza virus in mandarin duck (*Aix galericulata*) and domestic pigeon (*Columba livia domestica*). *Viruses.* (2021) 13:1069. doi: 10.3390/v13061069
- Kwon JH, Noh YK, Lee DH, Yuk SS, Erdene-Ochir TO, Noh JY, et al. Experimental infection with highly pathogenic H5N8 avian influenza viruses in the mandarin duck (*Aix galericulata*) and domestic pigeon (*Columba livia domestica*). *Vet Microbiol.* (2017) 203:95–102. doi: 10.1016/j.vetmic.2017.03.003
- Newman SH, Hill NJ, Spragens KA, Janies D, Voronkin IO, Prosser DJ, et al. Eco-virological approach for assessing the role of wild birds in the spread of avian influenza H5N1 along the central Asian flyway. *PLoS One.* (2012) 7:e30636. doi: 10.1371/journal.pone.0030636
- Pantin-Jackwood MJ, Swayne DE. Pathobiology of Asian highly pathogenic avian influenza H5N1 virus infections in ducks. *Avian Dis.* (2007) 51:250–9. doi: 10.1637/7710-090606R.1
- Park MJ, Cha RM, Kye SJ, Lee YN, Kim NY, Baek YG, et al. Pathogenicity of H5N8 high pathogenicity avian influenza virus in chickens and ducks from South Korea in 2020–2021. *Viruses.* (2021) 13:1903. doi: 10.3390/v13101903
- Capua I, Mutinelli F. Mortality in Muscovy ducks (*Cairina moschata*) and domestic geese (*Anser anser* var. domestica) associated with natural infection with a highly

Funding

This work was supported by the Korea Institute of Planning and Evaluation for Technology in Food, Agriculture, Forestry (IPET) through the Animal Disease Management Technology Development Program, funded by the Ministry of Agriculture, Food, and Rural Affairs (MAFRA) (grant number: 318032). This paper was supported by Konkuk University in 2022.

Conflict of interest

J-YN, J-HJ, J-BK and C-SS are employed by KHAV Co., Ltd..

The remaining authors declare that the research was conducted in the absence of any commercial or financial relationships that could be construed as a potential conflict of interest.

Publisher's note

All claims expressed in this article are solely those of the authors and do not necessarily represent those of their affiliated organizations, or those of the publisher, the editors and the reviewers. Any product that may be evaluated in this article, or claim that may be made by its manufacturer, is not guaranteed or endorsed by the publisher.

Supplementary material

The Supplementary material for this article can be found online at: <https://www.frontiersin.org/articles/10.3389/fvets.2023.1207289/full#supplementary-material>

- pathogenic avian influenza virus of H7N1 subtype. *Avian Pathol.* (2001) 30:179–83. doi: 10.1080/03079450120044597
21. Pantin-Jackwood MJ, Swayne D. Pathogenesis and pathobiology of avian influenza virus infection in birds. *Rev Sci Tech.* (2009) 28:113–36. doi: 10.20506/rst.28.1.1869
 22. Leigh Perkins LE, Swayne DE. Pathogenicity of a Hong Kong–origin H5N1 highly pathogenic avian influenza virus for emus, geese, ducks, and pigeons. *Avian Dis.* (2002) 46:53–63. doi: 10.1637/0005-2086(2002)046[0053:POAHKO]2.0.CO;2
 23. Sturm-Ramirez KM, Ellis T, Bousfield B, Bissett L, Dyrting K, Reh JE, et al. Reemerging H5N1 influenza viruses in Hong Kong in 2002 are highly pathogenic to ducks. *J Virol.* (2004) 78:4892–901. doi: 10.1128/JVI.78.9.4892-4901.2004
 24. Wasilenko J, Arafa A, Selim A, Hassan M, Aly M, Ali A, et al. Pathogenicity of two Egyptian H5N1 highly pathogenic avian influenza viruses in domestic ducks. *Arch Virol.* (2011) 156:37–51. doi: 10.1007/s00705-010-0813-y
 25. Swayne DE. *Laboratory manual for the isolation and identification of avian pathogens*. American Association of Avian Pathologists: University of Pennsylvania (1998).
 26. Spackman E. Avian influenza virus detection and quantitation by real-time RT-PCR. *Methods Mol Biol.* (2020) 2123:137–48. doi: 10.1007/978-1-0716-0346-8_11
 27. Cotec C. (2006). Diagnostic manual for avian influenza as provided for in council directive 2005/94/EC. Official Journal of the European Union.
 28. Grund C, Hoffmann D, Ulrich R, Naguib M, Schinköthe J, Hoffmann B, et al. A novel European H5N8 influenza A virus has increased virulence in ducks but low zoonotic potential. *Emerg Microb Infect.* (2018) 7:1–14. doi: 10.1038/s41426-018-0130-1
 29. Kleyheeg E, Slaterus R, Bodewes R, Rijks JM, Spierenburg MA, Beerens N, et al. Deaths among wild birds during highly pathogenic avian influenza A (H5N8) virus outbreak, the Netherlands. *Emerg Infect Dis.* (2017) 23:2050–4. doi: 10.3201/eid2312.171086
 30. Poen MJ, Bestebroer TM, Vuong O, Scheuer RD, Van Der Jeugd HP, Kleyheeg E, et al. Local amplification of highly pathogenic avian influenza H5N8 viruses in wild birds in the Netherlands, 2016 to 2017. *Eur Secur.* (2018) 23:17–00449. doi: 10.2807/1560-7917.ES.2018.23.4.17-00449
 31. Pohlmann A, Starick E, Harder T, Grund C, Höper D, Globig A, et al. Outbreaks among wild birds and domestic poultry caused by reassorted influenza A (H5N8) clade 2.3. 4.4 viruses, Germany, 2016. *Emerg Infect Dis.* (2017) 23:633–6. doi: 10.3201/eid2304.161949
 32. Engelsma M., Heutink R., Harders F., Germeraad E.A. And Beerens N. (2022). Multiple introductions of reassorted highly pathogenic avian influenza H5Nx viruses clade 2.3. 4.4 b causing outbreaks in wild birds and poultry in the Netherlands. *Microbiol Spect* 10:e0249921. doi: 10.1128/spectrum.02499-21.
 33. Hulse-Post D, Franks J, Boyd K, Salomon R, Hoffmann E, Yen H, et al. Molecular changes in the polymerase genes (PA and PB1) associated with high pathogenicity of H5N1 influenza virus in mallard ducks. *J Virol.* (2007) 81:8515–24. doi: 10.1128/JVI.00435-07
 34. Kwon JH, Noh JY, Jeong JH, Jeong S, Lee SH, Kim YJ, et al. Different pathogenicity of two strains of clade 2.3.4.4c H5N6 highly pathogenic avian influenza viruses bearing different PA and NS gene in domestic ducks. *Virology.* (2019) 530:11–8. doi: 10.1016/j.virol.2019.01.016
 35. Leyson CM, Youk S, Ferreira HL, Suarez DL, Pantin-Jackwood M. Multiple gene segments are associated with enhanced virulence of clade 2.3. 4.4 H5N8 highly pathogenic avian influenza virus in mallards. *J Virol.* (2021) 95:e00955–21. doi: 10.1128/JVI.00955-21
 36. Pantin-Jackwood MJ, Smith DM, Wasilenko JL, Cagle C, Shepherd E, Sarmiento L, et al. Effect of age on the pathogenesis and innate immune responses in Pekin ducks infected with different H5N1 highly pathogenic avian influenza viruses. *Virus Res.* (2012) 167:196–206. doi: 10.1016/j.virusres.2012.04.015
 37. Jang Y, Seo SH. Age-dependent lethality in ducks caused by highly pathogenic H5N6 avian influenza virus. *Viruses.* (2020) 12:591. doi: 10.3390/v12060591
 38. Londt BZ, Nunez A, Banks J, Alexander DJ, Russell C, Richard-Londt AC, et al. The effect of age on the pathogenesis of a highly pathogenic avian influenza (HPAI) H5N1 virus in Pekin ducks (*Anas platyrhynchos*) infected experimentally. *Influenza Other Respir Viruses.* (2010) 4:17–25. doi: 10.1111/j.1750-2659.2009.00116.x
 39. Carnaccini S, Santos JJS, Obadan AO, Pantin-Jackwood MJ, Suarez DL, Rajao DS, et al. Age-dependent pathogenesis of clade 2.3.4.4a H5N2 HPAIV in experimentally infected broad breasted white turkeys. *Vet Microbiol.* (2019) 231:183–90. doi: 10.1016/j.vetmic.2019.03.011
 40. Spackman E, Prosser DJ, Pantin-Jackwood MJ, Berlin AM, Stephens CB. The pathogenesis of clade 2.3. 4.4 H5 highly pathogenic avian influenza viruses in ruddy duck (*Oxyura jamaicensis*) and lesser scaup (*Aythya affinis*). *J Wildl Dis.* (2017) 53:832–42. doi: 10.7589/2017-01-003
 41. Poovorawan Y, Pyungporn S, Prachayangprecha S, Makkoch J. Global alert to avian influenza virus infection: from H5N1 to H7N9. *Pathog Glob Health.* (2013) 107:217–23. doi: 10.1179/2047773213Y.0000000103
 42. Bertran K, Lee D-H, Balzli C, Pantin-Jackwood MJ, Spackman E, Swayne DE. Age is not a determinant factor in susceptibility of broilers to H5N2 clade 2.3. 4.4 high pathogenicity avian influenza virus. *Vet Res.* (2016) 47:1–11. doi: 10.1186/s13567-016-0401-6
 43. Kimble B, Nieto GR, Perez DR. Characterization of influenza virus sialic acid receptors in minor poultry species. *Virol J.* (2010) 7:1–10. doi: 10.1186/1743-422X-7-365
 44. Schat KA, Kaspers B, Kaiser P. *Avian immunology*. USA: Elsevier Philadelphia (2014).
 45. Pantin-Jackwood M, Swayne DE, Smith D, Shepherd E. Effect of species, breed and route of virus inoculation on the pathogenicity of H5N1 highly pathogenic influenza (HPAI) viruses in domestic ducks. *Vet Res.* (2013) 44:62–11. doi: 10.1186/1297-9716-44-62
 46. Cha RM, Smith D, Shepherd E, Davis CT, Donis R, Nguyen T, et al. Suboptimal protection against H5N1 highly pathogenic avian influenza viruses from Vietnam in ducks vaccinated with commercial poultry vaccines. *Vaccine.* (2013) 31:4953–60. doi: 10.1016/j.vaccine.2013.08.046
 47. Sun S, Cui Z, Wang J, Wang Z. Protective efficacy of vaccination against highly pathogenic avian influenza is dramatically suppressed by early infection of chickens with reticuloendotheliosis virus. *Avian Pathol.* (2009) 38:31–4. doi: 10.1080/03079450802607504
 48. Mansour SM, Ali H, Elbakrey RM, El-Araby IE, Knudsen DE, Eid AA. Co-infection of highly pathogenic avian influenza and duck hepatitis viruses in Egyptian backyard and commercial ducks. *Int J Vet Sci Med.* (2018) 6:301–6. doi: 10.1016/j.ijvsm.2018.07.004
 49. Nickbakhsh S, Hall MD, Dorigatti I, Lycett SJ, Mulatti P, Monne I, et al. Modelling the impact of co-circulating low pathogenic avian influenza viruses on epidemics of highly pathogenic avian influenza in poultry. *Epidemics.* (2016) 17:27–34. doi: 10.1016/j.epidem.2016.10.005
 50. Zhao Y, Richardson B, Takle E, Chai L, Schmitt D, Xin H. Airborne transmission may have played a role in the spread of 2015 highly pathogenic avian influenza outbreaks in the United States. *Sci Rep.* (2019) 9:1–10. doi: 10.1038/s41598-019-47788-z



OPEN ACCESS

EDITED BY

Jasmina M. Luczo,
CSIRO Australian Centre for Disease
Preparedness, Australia

REVIEWED BY

Jeff Michael Butler,
Australian Animal Health Laboratory
(CSIRO), Australia
Zhiqiang Duan,
Guizhou University, China

*CORRESPONDENCE

Darrell R. Kapczynski
✉ darrell.kapczynski@usda.gov

RECEIVED 30 June 2023

ACCEPTED 08 August 2023

PUBLISHED 01 September 2023

CITATION

Briggs K and Kapczynski DR (2023) Comparative analysis of PB2 residue 627E/K/V in H5 subtypes of avian influenza viruses isolated from birds and mammals. *Front. Vet. Sci.* 10:1250952. doi: 10.3389/fvets.2023.1250952

COPYRIGHT

© 2023 Briggs and Kapczynski. This is an open-access article distributed under the terms of the [Creative Commons Attribution License \(CC BY\)](#). The use, distribution or reproduction in other forums is permitted, provided the original author(s) and the copyright owner(s) are credited and that the original publication in this journal is cited, in accordance with accepted academic practice. No use, distribution or reproduction is permitted which does not comply with these terms.

Comparative analysis of PB2 residue 627E/K/V in H5 subtypes of avian influenza viruses isolated from birds and mammals

Kelsey Briggs and Darrell R. Kapczynski*

Exotic and Emerging Avian Diseases Research Unit, Southeast Poultry Research Laboratory, U.S. National Poultry Research Center, Agricultural Research Service, Athens, GA, United States

Avian influenza viruses (AIVs) are naturally found in wild birds, primarily in migratory waterfowl. Although species barriers exist, many AIVs have demonstrated the ability to jump from bird species to mammalian species. A key contributor to this jump is the adaption of the viral RNA polymerase complex to a new host for efficient replication of its RNA genome. The AIV PB2 gene appears to be essential in this conversion, as key residues have been discovered at amino acid position 627 that interact with the host cellular protein, acidic nuclear phosphoprotein 32 family member A (ANP32A). In particular, the conversion of glutamic acid (E) to lysine (K) is frequently observed at this position following isolation in mammals. The focus of this report was to compare the distribution of PB2 627 residues from different lineages and origins of H5 AIV, determine the prevalence between historical and contemporary sequences, and investigate the ratio of amino acids in avian vs. mammalian AIV sequences. Results demonstrate a low prevalence of E627K in H5 non-Goose/Guangdong/1996-lineage (Gs/GD) AIV samples, with a low number of mammalian sequences in general. In contrast, the H5-Gs/GD lineage sequences had an increased prevalence of the E627K mutation and contained more mammalian sequences. An approximate 40% conversion of E to K was observed in human sequences of H5 AIV, suggesting a non-exclusive requirement. Taken together, these results expand our understanding of the distribution of these residues within different subtypes of AIV and aid in our knowledge of PB2 mutations in different species.

KEYWORDS

avian influenza virus, PB2, ANP32A, virus replication, wild birds, poultry

Introduction

Highly pathogenic (HP) avian influenza virus (AIV) outbreaks in domesticated poultry were rare prior to the 1990's (1, 2). However, in 1996, an HPAIV H5N1 was detected in a domesticated goose (A/Goose/Guangdong/1/1996) that crossed species barriers and was detected in humans in 1997 (3, 4). This AIV lineage created what we now know as the H5-Gs/GD lineage and is responsible for mortality in wild birds, poultry, mammals, and humans. The H5-Gs/GD lineage viruses have become adapted and distributed across the world via migratory waterfowl. This lineage has evolved into 10 genetically distinct clades (0–9) (1). Clade 2 versions of this lineage have become the most successful in terms of viral fitness and global distribution (1, 5, 6). The subclade 2.3.4 was first detected in 2008 in China and has continued to evolve into the current 2.3.4.4a-h viruses (1). The United States (U.S.) saw its first incursion of H5-Gs/GD lineage clade 2.3.4.4c viruses in 2014, which resulted in the deaths of over 47 million poultry, resulting in an estimated loss of 3.3 billion dollars

(1, 7). Many countries, including the U.S., are experiencing large-scale outbreaks from clade 2.3.4.4b viruses, which appear very adapted to migratory waterfowl based on their global spread over the past few years (8, 9).

One interest of this subclade is the adaption to other species (10–14). A well-described avian-to-mammalian genetic adaptation is an amino acid change in the PB2 protein at residue 627. Traditionally, avian sequences contain glutamate (E) at this position, while mammalian/human sequences contain a lysine (K) (15). It was originally thought that this residue played a role in the ability of PB2 to replicate at lower temperatures and provided an explanation for the inefficient replication of AIV in non-avian hosts (16). While the temperature may still play a role, more recent structural studies have determined that PB2 interacts with host protein acidic nuclear phosphoprotein 32 family member A (ANP32A) at residue 627, and this interaction is the driving force behind the E627K mutation (17, 18). The interaction is critical for the stabilization of the AIV polymerase complex (vPol), and the amino acid composition of ANP32A that surrounds residue 627 plays a major role in supporting AIV replication (18). However, other PB2 mutations have been found to support AIV replication in the absence of E627K, namely at positions 271, 590, and 591 (19–21).

Most avian ANP32A proteins encode an additional 33 amino acids (ANP32A₃₃) in between the two domains that are critical for AIV polymerase activity (22). The first four amino acids of the insert are a SUMO interacting motif (SIM) site that has been shown to increase the binding efficiency of ANP32A₃₃ with the vPol and is located directly above the PB2 627 residue (18, 23). The SIM site contains a mixture of acidic and basic residues, which provides the stabilization of the complex, and likely allows for replication with either a PB2 627E or K. The other 27 additional amino acids duplicated from exon 4 (amino acid residues 149–175) are believed to strengthen the interaction between vPol and ANP32A. Humans, mammals, and ratite species lack the 33 amino acid insertion (ANP32A_Δ), which results in a weaker interaction between ANP32A and the vPol leading to lower polymerase activity (17, 18, 23). The E627K mutation appears to compensate for the weaker interaction and helps to restore the vPol activity of AIV in hosts lacking ANP32A₃₃ (18, 23).

Avian ANP32A contains natural variations in splicing patterns that result in three major isoforms of the protein, whereas humans only carry the ANP32A_Δ isotype (22, 24). Chicken, turkey, and duck produce all three transcripts of ANP32A (ANP32A₃₃, ANP32₂₉ (lacking SIM), and ANP32A_Δ), but the ANP32A₃₃ isotype is the preferentially expressed isoform (approximately 65%). However, some species of wild waterfowl and other migratory birds express higher proportions of the human-like ANP32A (ANP32A_Δ) and the partial insertion that lacks the SIM site (ANP32₂₉), indicating that ANP32A expression is strongly associated with host range (22–24).

In this study, we investigate the number of submitted sequences containing PB2 627E, K, or V from H5 AIV. We compare the prevalence of sequences with 627K between non-Gs/GD and Gs/GD lineages and examine the ratio of sequences within the Gs/GD lineage. Finally, we examine residue specificity within the broad host range of clade 2 AIV, including current global 2.3.4.4 viruses.

Methods

Sequence analysis

All sequences were obtained from the Global Initiative on Sharing All Influenza Data (GISAID EPIFLU™) database (25). The search parameters on GISAID always included type A, H5, and required a complete segment of PB2. Other parameters, such as host(s) and clade(s) were chosen as needed. Downloaded datasets were aligned in Geneious Prime (Boston, MA) using a MUSCLE alignment. Only complete and correct PB2 protein sequences with coverage over residue 627 were used for analysis. Sequences that did not meet this criterion were discarded. Tables were created based on the number of PB2 sequences that matched the criteria set, such as host species, total number, amino acid residue, and clade. Totals were calculated by adding up each group in the table, and in some cases, the total does not represent the entire dataset. Very few sequences had 627 residues that were not glutamate (E), lysine (K), or valine (V), so they were not included in the analysis total. The percentage of K residues was obtained by dividing the number of K residues by the total of that group and then multiplying by 100. When a clade or subclade was chosen in the “clade” search panel, all subclades were included in the analysis, unless otherwise noted. Tables including a species section were chicken/turkey only, all other avian species (in addition to chicken/turkey), mammals (not including humans), and humans. It is important to note that all timespans listed in this report are based on the dataset used for analysis. They do not represent the exact circulation of those virus clades. The findings of this study are based on data from 125,996 PB2 sequences available on GISAID as of March 2023.

Results

Prevalence of 627K in non-A/Gs/GD/96 lineage H5Nx viruses

Using the GISAID “clade” search panel, we examined sequences that were not classified as part of the Gs/Gd lineage (25). The American-non-Gs/GD/96 (Am_non-GsGD) lineage had 789 complete PB2 sequences with 627 coverages, and the earliest viruses in the dataset were from Wisconsin, USA, in 1975. The subtypes in 1975 included H5N2, H5N6, and H5N1. The species in this lineage consisted of chicken/turkey (220), all other avian (567), mammalian (2), and human (0). Of the 789 sequences examined, only two had PB2 627K, the animals were a rhea and an emu (both from Texas, USA, 1993, H5N2). The percent of PB2 627K sequences for the Am_non-GsGD lineage was 0.25%. Unexpectedly, there were 17 chicken sequences with a V at position 627, which accounted for 2.15% of the total. They originated from an H5N2 isolation in Mexico in 2019 (Table 1, top).

For the Eurasian-non-Gs/GD/96 (Ea_non-GsGD) lineage, 390 sequences were examined. The earliest sequences were from Scotland in 1959 (H5N1). In this lineage, there were 46 chicken/turkey, 342 other avian, 2 mammals, and 0 human sequences. Of the 390 sequences, four had PB2 627K. All four sequences came from ostriches in South Africa in 2011 and 2015. The percentage of PB2 627K sequences from the Ea_non-GsGD

TABLE 1 Prevalence of PB2 627 E/K/V in non-A/Gs/GD/96 H5 lineage viruses.

Lineage	Species	Total numbers	627E	627K	627V	Percent 627E	Percent 627K
American-non-Gs/GD/96 (1975-present)	Chicken/Turkey	220	203	0	17	92.3	0
	Other Avian	567	564	2 ^a	0	99.5	0.4
	Mammalian	2	2	0	0	100.0	0
	Human	0	0	0	0	0	0
	Total	789	769	2	17	97.3	0.25
Eurasian-non-Gs/GD/96 (1959-present)	Chicken/Turkey	46	0	0	0	0	0
	Other Avian	342	338	4 ^b	0	98.8	1.2
	Mammalian	2	2	0	0	100.0	0
	Human	0	0	0	0	0	0
	Total	390	2	4	0	99.4	1.03

^a1 rhea and 1 emu.^b4 Four ostriches.

lineage was 1.03% (Table 1, bottom). Interestingly, there were only four mammalian sequences in the dataset within the two lineages. All four were H5N2 sequences from swine, two were from Mexico in 2014/2015, and two were from Korea in 2008 (Table 1). Based on the available data, the American and Eurasian lineages appear to have low mammalian/human spillover events and a low percentage of PB2 627K adaptations.

Prevalence of PB2 627K in A/Gs/GD/96 H5 lineage clades 0–9

Next, we examined the percentage of PB2 627K residues in clades 0–9 of the Gs/GD lineage, which began in 1996. PB2 sequence availability ranged from 17 to 10,734 sequences between the clades (Table 2). Clade 0 had 11.7% (7/60) PB2 sequences with 627K, which included an ostrich and six human samples. The dataset contained sequences from 1996 to 2008 (Table 2). Clade 1 had 395 sequences available, 39 of which had PB2 627K (9.9%), which consisted of 14 avian species, 24 mammalian/human species, and 1 unknown, and were sequenced from 1996 to 2014 (Table 2). Clade 2 had the most sequences available (10,734); of those, 738 contained PB2 627K and 16 contained a 627V. Clade 2 had 6.9% of total sequences with 627K; of those, 608 were avian and 130 were mammalian/human. Available clade 2 sequences ranged from 1996 to the present (Table 2). Clade 3 sequences contained 2.9% PB2 627K residues (6/206), 1 was from the environment and 5 were human cases. The sequences were collected from 1997 to 2015 (Table 2). Clade 6 (2002–2022) had two human cases with PB2 627K out of 33 total, making the percentage 6.1% (Table 2). Clade 7 had 2.5% sequences with PB2 627K, there were 2 avian samples out of 80 from 2002 to 2015 (Table 2). Clade 9 sequences ranged from 1997 to 2006; only 2 avian sequences had PB2 627K out of 49 total (4.1%) (Table 2). Clades 4, 5, and 8 had no sequences containing PB2 627K (Table 2). The overall average of PB2 627K in the Gs/GD lineage was 4.9%, which is 13x more than the Am_non-GsGd and 4.8x more than the Ea_non-GsGd lineages.

Prevalence of PB2 627K in A/Gs/GD/96 H5 lineage clade 2

To examine clade 2 more thoroughly, we determined the percent PB2 627K in subclades 2.1–2.5, based on available GISAID sequences (25). Clade 2.1 had a low proportion of avian sequences (34.6%) available compared to mammalian/human sequences (65.4%). All 19 (8.3%) sequences with PB2 627K in clade 2.1 were mammalian/human in origin (Table 3, top). The sequences from clade 2.1 were obtained between 2003 and 2015. Clade 2.2 was previously shown to have a high incidence of PB2 627K residues (20). We found that 92.1% of available PB2 sequences classified as clade 2.2 had 627K residue. Unexpectedly, 578 sequences with PB2 627K were from avian species, and only 36 were mammalian/human. Clade 2.2 sequences ranged from 1997 to 2017 in the dataset (Table 3, top). Clade 2.2 contributed to 83% (614/738) of the total clade 2 PB2 627K population (Table 2). Clade 2.3 (2003–present) has the largest total number of sequences available (9,797), although only 105 of them had PB2 627K. Of the sequences with 627K, 75 were mammalian/human and 30 were of avian origin. The total percentage of PB2 627K sequences for clade 2.3 was 1.1% (Table 3, top). Of note, only clade 2.3 contained PB2 627V sequences. The species containing PB2 627V were mixed, eight chickens, two other avians, three red foxes, one tiger, and one human. Clades 2.4 and 2.5 had low sample sizes, and none of the sequences contained PB2 627K residue. Additionally, the sequences available were only from 2003 to 2004 to 2003–2006, respectively (Table 3, top). The data indicate that the majority of PB2 627K sequences are from clade 2.2, not 2.3.

The most current and prevalent Gs/GD lineage viruses belong to clade 2.3.4.4 (1). We wanted to examine which species in subclades 2.3.4.4a–h had PB2 627K residue. Because the subclades 2.3.4.4d and 2.3.4.4f did not have “clade” options in the GISAID database, they were not included in the analysis (25). Clade 2.3.4.4a contained 1.2% (6/502) sequences with PB2 627K, including two avians and four humans among the species. Sequences in this clade were collected between 2012 and 2018 (Table 3, bottom). The 2.3.4.4b viruses are responsible for the current outbreak in the U.S. and have been reported in many countries (12, 25).

TABLE 2 Prevalence of PB2 627 E/K/V in A/Gs/GD/96 H5 lineage clades 0–9.

Clade	Total numbers	627E	627K	627V	Percent 627E	Percent 627K
0	60	53	7 ^a	0	88.3	11.7
1	395	356	39 ^b	0	90.1	9.9
2	10,734	9,996	738 ^c	15	93.1	6.9
3	206	200	6 ^d	0	97.1	2.9
4	18	18	0	0	100.0	0.0
5	22	22	0	0	100.0	0.0
6	33	31	2 ^e	0	93.9	6.1
7	80	78	2 ^f	0	97.5	2.5
8	17	17	0	0	100.0	0.0
9	49	47	2 ^g	0	95.9	4.1

^aClade 0—1 avian (ostrich) and 6 humans.

^bClade 1—14 avians (1 ostrich), 24 mammals/humans, 1 unknown.

^cClade 2—608 avian, 130 mammals/humans.

^dClade 3—1 environment, 5 humans.

^eClade 6—2 humans.

^fClade 7—2 avians.

^gClade 9—2 avians.

Of the 5,311 sequences analyzed from 2003 to the present, 53 had PB2 627K making the percentage only 1.0%. However, 48 of the 53 sequences were from 2021 to the present. Bird sequences containing 627K accounted for 23 of the 53 sequences and included chickens/turkeys, ducks, ratites, and common terns. There was a higher diversity of mammalian species containing PB2 627K in the 2.3.4.4b viruses, compared to all other groups analyzed. Most of the mammalian/human sequences in clades 2.1 and 2.2 were human, whereas the 2.3.4.4b sequences included 1 bear, 2 skunks, 3 cats, 2 ferrets, 1 raccoon, 14 foxes, 4 seals, 1 otter, and 2 humans (Tables 2, 3, bottom). Of note, the 2.3.4.4c sequences, which were responsible for the first outbreak of a Gs/GD lineage H5Nx virus in the U.S., did not have any sequences with PB2 627K (8). The dataset contained 1,056 samples and included sequences from 2014 to 2020 (Table 3, bottom). Three human samples (3/551) from 2.3.4.4e had PB2 627K from 2014 to 2018 (Table 3, bottom). Clade 2.3.4.4g (2014–2020) had the smallest sample size (84), and none of the sequences contained PB2 627K (Table 3, bottom). Finally, 2.3.4.4h had the highest percentage of PB2 627K sequences at 4.02% (15/373), spanning from 2014 to 2021. The sequences were from two chickens/turkeys, four minks, and nine humans (Table 3, bottom). Taken together, the data indicate that the current 2.3.4.4b viruses have a low overall percentage of PB2 627K sequences, but an increased propensity to infect multiple species.

Prevalence of PB2 627E/K/V in human sequences from different hemagglutinin subtypes

Finally, we examined the prevalence of PB2 627K in human AIV sequences with more common HA subtypes (26). First, the percent of PB2 627K in human sequences in subtypes (H1–H3) was examined. Interestingly, 95% of the H1 sequences sequenced

contained the avian-like PB2 627E. We only observed 4.7% of all H1 sequences demonstrating the PB2 627K residue. However, the majority of the 39,418 sequences examined were from the pandemic H1N1 (pdm09) lineage, which began in 2009 and was known to contain a PB2 segment from an avian North American virus (Table 4) (27). As expected, both the H2 and H3 sequences contained higher percentages of PB2 627K residues, with prevalence rates of 91.9% and 99.4%, respectively (Table 4). Next, we examined the proportion of PB2 627K in avian-adapted AIV subtypes (H5, H7, and H9). H5 viruses obtained from human samples contained 39.1% PB2 627K sequences (Table 4). Of the 1,207 human sequences classified as subtype H7, 851, or 70.4% contained a K at position 627 (Table 4). Finally, the H9 subtype contained only two human sequences with PB2 627K (Table 4). Interestingly, the H7 and H9 viruses contained a higher proportion of 627V residues, 2.7% and 36%, respectively. Apart from the pdm09 H1N1 viruses, the data illustrate that human-adapted viruses typically contain PB2 627K.

Discussion

This research aimed to compare the distribution of PB2 627 residues between avian and mammalian sequences in H5 from non-Gs/GD and Gs/GD lineages and determine the prevalence between previous subclades and current ones. The current clade 2.3.4.4b H5Nx AIVs have a global distribution and raise concerns about mammalian adaptations as recent isolations have occurred in domestic and peridomestic mammals (12, 28). In this study, we focused on one well-known avian-to-mammalian adaption residue, E627K/V, to determine if the 2.3.4.4 viruses have an increased propensity to mutate in that direction.

All sequences were obtained from GISAID, so the number of sequences was limited to what was available in the database. We chose GISAID because it contained the most sequences of

TABLE 3 Comparative prevalence of PB2 E/K/V in Gs/GD/96 H5 lineage clades 2.1–2.5 (Top) and distribution within various species in subclade 2.3.4.4 (Bottom).

Clade	Total numbers	Percent Avian sample	627E	627K	627V	Percent 627E	Percent 627K
2.1 ^a	228	34.6	209	19 ^d	0	91.7	8.3
2.2 ^b	667	94.2	53 ^e	614 ^f	0	7.9	92.1
2.3 ^c	9,797	92.4	9,672	105 ^g	15	98.7	1.1
2.4	16	100.0	16	0	0	100.0	0.0
2.5	26	100.0	26	0	0	100.0	0.0
Species		2.3.4.4a (502) ^l	2.3.4.4b (5,311)	2.3.4.4c (1,056)	2.3.4.4e (551)	2.3.4.4g (84)	2.3.4.4h (373)
Chicken/Turkey		0	16	0	0	0	2
Other Avian		2 ^h	7 ⁱ	0	0	0	0
Mammalian		0	28 ^j	0	0	0	4 ^k
Human		4	2	0	3	0	9
Percent 627E		98.8	99.0	100.0	99.5	100.0	96.0
Total with 627K		6	53	0	3	0	15
Percent 627K		1.2	1.0	0.0	0.5	0.0	4.0

^a2.1 includes 2.1.1, 2.1.2, 2.1.3, 2.1.3.1, 2.1.3.2, 2.1.3.2a, 2.1.3.2b, 2.1.3.3.^b2.2 includes 2.2, 2.2.1, 2.2.1.1, 2.2.1.1a, 2.2.1.2, 2.2.2, 2.2.2.1.^c2.3 includes 2.3.1, 2.3.2, 2.3.2.1, 2.3.2.1a, 2.3.2.1b, 2.3.2.1c, 2.3.3, 2.3.4, 2.3.4.1, 2.3.4.2, 2.3.4.3, 2.3.4.4, 2.3.4.4b, 2.3.4.4c, 2.3.4.4e, 2.3.4.4g, 2.3.4.4h.^d19 mammals/humans. Of mammals/humans (149), 12.8% have 627K.^e3 mammals and 50 avian.^f36 mammals/humans and 578 avians (4 ostriches).^g75 mammals/humans and 30 avians (1 emu, 2 rhea).^h1 cormorant and 1 pheasant.ⁱ2 rhea, 1 emu, 1 duck, 2 common terns, and 1 unknown avian.^j1 bear, 2 skunks, 3 cats, 2 ferrets, 1 raccoon, 14 foxes, 4 seals, and 1 otter.^k4 minks.^lTotal number of samples per 2.3.4.4 subclade.**TABLE 4** Prevalence of PB2 627 E/K/V from human sequences among different influenza hemagglutinin subtypes.

HxNx	Total numbers	627E	627K	627V	Percent 627E	Percent 627K
H1	39,418	37,559	1,855	4	95.3	4.7 ^a
H2	123	10	113	0	8.1	91.9
H3	71,994	419	71,560	15	0.6	99.4
H5	402	244	157	1	60.7	39.1
H7	1,207	323	851	33	26.8	70.4 ^b
H9	59	36	2	21	61.0	3.4

^aPandemic H1N1 (pdm09) contained PB2 from an avian North American virus.^bRecent H7N9 cases predominate sequences in this subtype.

current (2021–present) AIV, but it is possible that older strains were missed in the analysis because they were not added retroactively (prior to 2008) (25). AIV surveillance and reporting are not a standard practice in all countries; consequently, samples are limited to countries that do report, and this may contribute to the low dataset numbers and sample bias in some clades. Obtaining samples from only dead birds may also result in sampling bias, but it is not possible to tell whether samples were taken during active or passive surveillance.

In the non-Gs/GD lineage, the majority of sequences contained the 627E residue. We observed only six avian sequences that contained PB2 627K and they belonged to the Ratite family

(Ostrich, Rhea, Emu, Cassowary, and Kiwi) of birds (Table 1). Ratites were the only species of birds that contained PB2 627K residues in this group. Phylogenetic analysis of the ANP32A gene demonstrates that the Ratite family lacks the 33 amino acid insertion in exon 5 that most other avian species have, which presumably makes it more mammalian-like, and may explain why viruses isolated from these species select for 627K during replication (14, 22). Of further note is that both rhea and emu sequences from the Am_non-GsGD lineage contained multiple polybasic residues at the HA cleavage site, suggesting that they were HPAI viruses. In the EA_non-GsGD lineage, the two ostriches from 2011 contained an HPAI cleavage

sequence, whereas the two ostriches from 2015 contained an LPAI sequence.

Clade 2 is the most evolutionarily successful clade from the Gs/GD lineage of AIV based on the sample size and the number of subclades (Tables 2, 3) (1, 29). Within subclade 2, the proportion of avian and mammalian samples in clade 2.1 was unexpected. The largest portion of samples was human sequences from Indonesia, ranging from 2003 to 2015 (Table 3). Of note is the observation that most of the sequences in clade 2.2 containing 627K were of avian origin (Table 3). Clade 2.2 viruses were shown to be shed via the respiratory route in waterfowl rather than the typical cloacal route; therefore, it was proposed that clade 2.2 viruses maintained the 627K to compensate for the cooler temperature of the respiratory tract (20, 30, 31). Recently, a study using RNA-seq showed that some waterfowl, land fowl, and pelicans preferentially express a human-like ANP32A, which could also have contributed to a larger proportion of avian species containing 627K in clade 2.2, as there was no selective pressure to maintain 627E (22). Additionally, Long et al. found that the PB2 627K mutation did not affect pathogenesis or transmission in ducks, suggesting that mammalian adaption could be maintained in an avian species, which also supports the notion that there is little selection pressure to go from K627E (20). The clade 2.3 dataset was comprised of 17 subclades, including the current 2.3.4.4b viruses. Interestingly, 98.7% (9,672) of the 2.3 sequences contained a 627E residue despite only 92.4% (9,052) being of avian origin, demonstrating that non-avian species also maintained the 627E residue. This observation went both ways in that of the 105 clade 2.3 sequences demonstrating 627K, only 71.4% (75) were mammalian (Table 3).

Within clade 2.3.4, more than half of the PB2 627K sequences were in the clade 2.3.4.4b subclade (Tables 2, 3). There were 16 chicken/turkey species and 7 other avians that contained PB2 627K in clade 2.3.4.4b, this may indicate that the virus is spilling over from mammals into avians and maintaining the residue at the time of isolation. Several accounts of mammalian spillover events have occurred since the 2.3.4.4b viruses have become predominant and the diversity of species being infected is unprecedented (Table 3) (9, 12, 13, 32). Nevertheless, based on our data, the number of 2.3.4.4b mammalian sequences with PB2 627K is still lower than the sequences with a 627E. Interestingly, we found that five sea mammals (four seals and one otter) contained PB2 627K, whereas a recent study examined dolphin and sea lion sequences from Peru and found they contained a 627E. Leguia et al. also proposed that transmission between sea lions off the coast of Peru could be occurring rather than independent avian spillover events because of the massive die-offs being observed (28). More investigation is required to determine if mammal-to-mammal and mammal-to-avian transmission are occurring, and which residues are allowing for efficient replication of the virus.

Despite the fact that residue PB2 627 is almost exclusively a K or E in all influenza A viruses, a small portion contains a valine (V). A study by Chin et al. found that inducing random mutations at position 627 allowed for the 627V mutation when purified in a mammalian system but not in an avian system (33). This may indicate that the 627V mutations observed in all avian species were transmitted from a mammalian host (Tables 1–4). The study observed a slight reduction in replication compared to the 627K

mutation using the culture-adapted A/Puerto Rico/8/34 (H1N1) virus (33). However, a more recent study used the polymerase genes from an avian H5N1 (A/Muscovy duck/Vietnam/TY93/2007; clade 2.3.4) to rescue a virus containing the PB2 627V mutation. Taft et al. found that the 627V mutation had significantly increased viral replication in mammalian cell culture and virulence in mice that was comparable to the 627K virus (34). Additionally, Luk et al. found that an H7N9 virus containing PB2 627V was extremely fit and transmissible between chickens and mammals (35). The number of V residues in H5 sequences remains low; however, the H7 and H9 human cases had a considerable number of sequences containing a 627V, many of which are from recent years (Table 4).

The dependency of viral polymerases on host ANP32A is one factor in crossing host barriers exemplified by the propensity for AIV sequences to mutate to 627K in mammalian sequences (Tables 1–4) (23). The Gs/GD lineage viruses are commonly found in wild waterfowl and appear to transcribe higher rates of the human-like ANP32A, which may account for shifts in 627 residue specificity (23, 32). While PB2 627K is an established marker for mammalian adaption, it is not solely responsible for it (15, 27, 33). The pdm09 H1N1 viruses contained a PB2 627E, due to the avian origin of the segment but had other compensatory mutations that allowed for efficient replication in mammals and humans (19, 20, 36). As more mammalian species become infected by 2.3.4.4b AIV additional residues may yet be identified. It is known that efficient replication in a certain host requires adaption to the machinery within, and that adaption from one host species to another requires mutation and selection. In this study, we performed a differential analysis of PB2 residue 627 and demonstrated a non-exclusive requirement for conversion.

Data availability statement

The raw data supporting the conclusions of this article will be made available by the authors, without undue reservation.

Author contributions

KB and DK: conceptualization, methodology, formal analysis, writing—original draft and preparation, and writing—review and editing. All authors contributed to the article and approved the submitted version.

Funding

This study was supported by a USDA-NIFA grant # 2015-67015-22968 and a USDA-ARS CRIS grant # 6040-32000-062-00D.

Acknowledgments

The authors thank Ryan Sweeney for his excellent technical assistance. The authors gratefully acknowledge all data contributors, i.e., the authors and their originating laboratories responsible for obtaining the specimens and their submitting

laboratories for generating the genetic sequence and metadata and sharing via the GISAID Initiative, on which this research is based.

Conflict of interest

The authors declare that the research was conducted in the absence of any commercial or financial relationships that could be construed as a potential conflict of interest.

References

- Lee DH, Bertran K, Kwon JH, Swayne DE. Evolution, global spread, and pathogenicity of highly pathogenic avian influenza H5Nx clade 23.44. *J Vet Sci.* (2017) 18:269–80. doi: 10.4142/jvs.2017.18.S1.269
- Joseph U, Su YC, Vijaykrishna D, Smith GJ. The ecology and adaptive evolution of influenza A interspecies transmission. *Influenza Other Respi Viruses.* (2017) 11:74–84. doi: 10.1111/irv.12412
- Guo Y, Xu X, Wan X. Genetic characterization of an avian influenza A (H5N1) virus isolated from a sick goose in China. *Zhonghua Shi Yan He Lin Chuang Bing Du Xue Za Zhi.* (1998) 12:322–5.
- Wan X. Lessons from emergence of A/goose/Guangdong/1996-like H5N1 highly pathogenic avian influenza viruses and recent influenza surveillance efforts in southern China. *Zoonoses Public Health.* (2012) 59:32–42. doi: 10.1111/j.1863-2378.2012.01497.x
- Claas EC, de Jong JC, van Beek R, Rimmelzwaan GF, Osterhaus AD. Human influenza virus A/HongKong/156/97 (H5N1) infection. *Vaccine.* (1998) 16:977–8. doi: 10.1016/S0264-410X(98)00005-X
- Alkie TN, Lopes S, Hisanaga T, Xu W, Suderman M, Koziuk J, et al. A threat from both sides: Multiple introductions of genetically distinct H5 HPAI viruses into Canada via both East Asia-Australasia/Pacific and Atlantic flyways. *Virus Evolut.* (2022) 8:veac077. doi: 10.1093/ve/veac077
- Kapczynski DR, Sylte MJ, Killian ML, Torchetti MK, Chrzastek K, Suarez DL. Protection of commercial turkeys following inactivated or recombinant H5 vaccine application against the 2015 US H5N2 clade 2.3.44 highly pathogenic avian influenza virus. *Vet Immunol Immunopathol.* (2017) 191:74–9. doi: 10.1016/j.vetimm.2017.08.001
- Final Report for the 2014–2015 Outbreak of Highly Pathogenic Avian Influenza (HPAI) in the United States, in USDA APHIS HPAI Response. Riverdale, MD: United States Department of Agriculture. (2016). p. 59.
- 2022–2023 Confirmations of Highly Pathogenic Avian Influenza in Commercial and Backyard Flocks. Avian Influenza. (2023). Available online at: <https://www.aphis.usda.gov/aphis/ourfocus/animalhealth/animal-disease-information/avian/avian-influenza/hpai-2022/2022-hpai-commercial-backyard-flocks> (accessed April 11, 2023).
- Kaplan BS, Webby RJ. The avian and mammalian host range of highly pathogenic avian H5N1 influenza. *Virus Res.* (2013) 178:3–11. doi: 10.1016/j.virusres.2013.09.004
- Claas EC, Osterhaus AD, Van Beek R, De Jong JC, Rimmelzwaan GF, Senne DA, et al. Human influenza A H5N1 virus related to a highly pathogenic avian influenza virus. *Lancet.* (1998) 351:472–7. doi: 10.1016/S0140-6736(97)11212-0
- Elsmo EJ, Wunschmann A, Beckmen KB, Broughton-Neiswanger LB, Buckles EL, Ellis J, et al. Pathology of natural infection with highly pathogenic avian influenza virus (H5N1) clade 2.3.4.4 b in wild terrestrial mammals in the United States in 2022. *bioRxiv.* (2023) 2023:03. doi: 10.1101/2023.03.10.532068
- Klopfleisch R, Wolf PU, Wolf C, Harder T, Starick E, Niebuhr M, et al. Encephalitis in a stone marten (*Martes foina*) after natural infection with highly pathogenic avian influenza virus subtype H5N1. *J Comp Pathol.* (2007) 137:155–9. doi: 10.1016/j.jcpa.2007.06.001
- Shinya K, Makino A, Ozawa M, Kim JH, Sakai-Tagawa Y, Ito M, et al. Ostrich involvement in the selection of H5N1 influenza virus possessing mammalian-type amino acids in the PB2 protein. *J Virol.* (2009) 83:13015–8. doi: 10.1128/JVI.01714-09
- Subbarao EK, London W, Murphy BR. A single amino acid in the PB2 gene of influenza A virus is a determinant of host range. *J Virol.* (1993) 67:1761–4. doi: 10.1128/jvi.67.4.1761-1764.1993
- Massin P, van der Werf S, Naffakh N. Residue 627 of PB2 is a determinant of cold sensitivity in RNA replication of avian influenza viruses. *J Virol.* (2001) 75:5398–404. doi: 10.1128/JVI.75.11.5398-5404.2001
- Long JS, Giotis ES, Moncorgé O, Frise R, Mistry B, James J, et al. Species difference in ANP32A underlies influenza A virus polymerase host restriction. *Nature.* (2016) 529:101–4. doi: 10.1038/nature16474
- Carrique L, Fan H, Walker AP, Keown JR, Sharps J, Staller E, et al. Host ANP32A mediates the assembly of the influenza virus replicase. *Nature.* (2020) 587:638–43. doi: 10.1038/s41586-020-2927-z
- Mehle A, Doudna JA. Adaptive strategies of the influenza virus polymerase for replication in humans. *Proc Natl Acad Sci.* (2009) 106:21312–6. doi: 10.1073/pnas.0911915106
- Long JS, Howard WA, Núñez A, Moncorgé O, Lycett S, Banks J, et al. The effect of the PB2 mutation 627K on highly pathogenic H5N1 avian influenza virus is dependent on the virus lineage. *J Virol.* (2013) 87:9983–96. doi: 10.1128/JVI.01399-13
- Mok CK, Yen HL, Yu MY, Yuen KM, Sia SF, Chan MC, et al. Amino acid residues 253 and 591 of the PB2 protein of avian influenza virus A/H9N2 contribute to mammalian pathogenesis. *J Virol.* (2011) 85:9641–5. doi: 10.1128/JVI.00702-11
- Baker SF, Ledwith MP, Mehle A. Differential splicing of ANP32A in birds alters its ability to stimulate RNA synthesis by restricted influenza polymerase. *Cell Rep.* (2018) 24:2581–8. doi: 10.1016/j.celrep.2018.08.012
- Domingues P, Hale BG. Functional insights into ANP32A-dependent influenza A virus polymerase host restriction. *Cell Reports.* (2017) 20:2538–46. doi: 10.1016/j.celrep.2017.08.061
- Domingues P, Eletto D, Magnus C, Turkington HL, Schmutz S, Zagordi O, et al. Profiling host ANP32A splicing landscapes to predict influenza A virus polymerase adaptation. *Nat Commun.* (2019) 10:3396. doi: 10.1038/s41467-019-11388-2
- Elbe S, Buckland-Merrett G. Data, disease and diplomacy: GISAID's innovative contribution to global health. *Global challenges.* (2017) 1:33–46. doi: 10.1002/gch2.1018
- Mänz B, Schwemmler M, Brunotte L. Adaptation of avian influenza A virus polymerase in mammals to overcome the host species barrier. *J Virol.* (2013) 87:7200–9. doi: 10.1128/JVI.00980-13
- Long JS, Mistry B, Haslam SM, Barclay WS. Host and viral determinants of influenza A virus species specificity. *Nat Rev Microbiol.* (2019) 17:67–81. doi: 10.1038/s41579-018-0115-z
- Leguia M, Garcia-Glaessner A, Munoz-Saavedra B, Juarez D, Barrera P, Calvo-Mac C, et al. Highly pathogenic avian influenza A (H5N1) in marine mammals and seabirds in Peru. *bioRxiv.* (2023) 4:2023–03. doi: 10.1101/2023.03.03.531008
- Li YT, Su YC, Smith GJ. H5Nx viruses emerged during the suppression of H5N1 virus populations in poultry. *Microbiology Spectrum.* (2021) 9:e01309–21. doi: 10.1128/Spectrum.01309-21
- Löndt BZ, Nunez A, Banks J, Nili H, Johnson LK, Alexander DJ. Pathogenesis of highly pathogenic avian influenza A/turkey/Turkey/1/2005 H5N1 in Pekin ducks (*Anas platyrhynchos*) infected experimentally. *Avian Pathology.* (2008) 37:619–27. doi: 10.1080/03079450802499126
- Wasilenko JL, Arafa AM, Selim AA, Hassan MK, Aly MM, Ali A, et al. Pathogenicity of two Egyptian H5N1 highly pathogenic avian influenza viruses in domestic ducks. *Arch Virol.* (2011) 156:37–51. doi: 10.1007/s00705-010-0813-y
- Rijks JM, Hesselink H, Lollinga P, Wesselman R, Prins P, Weesendorp E, et al. Highly pathogenic avian influenza A (H5N1) virus in wild red foxes, the Netherlands, 2021. *Emerg Infect Dis.* (2021) 27:2960. doi: 10.3201/eid2711.211281

Publisher's note

All claims expressed in this article are solely those of the authors and do not necessarily represent those of their affiliated organizations, or those of the publisher, the editors and the reviewers. Any product that may be evaluated in this article, or claim that may be made by its manufacturer, is not guaranteed or endorsed by the publisher.

33. Chin AW, Li OT, Mok CK, Ng MK, Peiris M, Poon LL. Influenza A viruses with different amino acid residues at PB2-627 display distinct replication properties in vitro and in vivo: revealing the sequence plasticity of PB2-627 position. *Virology*. (2014) 468:545–55. doi: 10.1016/j.virol.2014.09.008
34. Taft AS, Ozawa M, Fitch A, Depasse JV, Halfmann PJ, Hill-Batorski L, et al. Identification of mammalian-adapting mutations in the polymerase complex of an avian H5N1 influenza virus. *Nat Commun*. (2015) 6:7491. doi: 10.1038/ncomms8491
35. Luk GS, Leung CY, Sia SF, Choy KT, Zhou J, Ho CC, et al. Transmission of H7N9 influenza viruses with a polymorphism at PB2 residue 627 in chickens and ferrets. *J Virol*. (2015) 89:9939–51. doi: 10.1128/JVI.01444-15
36. Bussey KA, Bousse TL, Desmet EA, Kim B, Takimoto T. PB2 residue 271 plays a key role in enhanced polymerase activity of influenza A viruses in mammalian host cells. *J Virol*. (2010) 84:4395–406. doi: 10.1128/JVI.02642-09



OPEN ACCESS

EDITED BY

Sarah J. Edwards,
Commonwealth Scientific and Industrial
Research Organisation (CSIRO), Australia

REVIEWED BY

Petrus Jansen Van Vuren,
Australian Animal Health Laboratory (CSIRO),
Australia
Velmurugan Balaraman,
Kansas State University, United States

*CORRESPONDENCE

Leiliang Zhang
✉ armzhang@hotmail.com

RECEIVED 13 July 2023

ACCEPTED 06 October 2023

PUBLISHED 19 October 2023

CITATION

Xu Y, Wang X, Jiang L, Zhou Y, Liu Y,
Wang F and Zhang L (2023) Natural hosts and
animal models for Rift Valley fever phlebovirus.
Front. Vet. Sci. 10:1258172.
doi: 10.3389/fvets.2023.1258172

COPYRIGHT

© 2023 Xu, Wang, Jiang, Zhou, Liu, Wang and
Zhang. This is an open-access article
distributed under the terms of the [Creative
Commons Attribution License \(CC BY\)](#). The
use, distribution or reproduction in other
forums is permitted, provided the original
author(s) and the copyright owner(s) are
credited and that the original publication in this
journal is cited, in accordance with accepted
academic practice. No use, distribution or
reproduction is permitted which does not
comply with these terms.

Natural hosts and animal models for Rift Valley fever phlebovirus

Yuqing Xu^{1,2,3}, Xiao Wang^{2,3}, Lu Jiang^{2,3}, Yixuan Zhou^{2,3},
Yihan Liu^{2,3}, Fei Wang^{2,4} and Leiliang Zhang^{1,2,3*}

¹Department of Clinical Laboratory Medicine, The First Affiliated Hospital of Shandong First Medical University and Shandong Provincial Qianfoshan Hospital, Jinan, China, ²Medical Science and Technology Innovation Center, Shandong First Medical University, Shandong Academy of Medical Sciences, Jinan, China, ³Department of Pathogen Biology, School of Clinical and Basic Medical Sciences, Shandong First Medical University and Shandong Academy of Medical Sciences, Jinan, China, ⁴School of Laboratory Animal and Shandong Laboratory Animal Center, Shandong First Medical University and Shandong Academy of Medical Sciences, Jinan, China

Rift Valley fever phlebovirus (RVFV) is a zoonotic mosquito-transmitted arbovirus, presenting a serious threat to humans and animals. Susceptible hosts are of great significance for the prevention of RVFV. Appropriate animal models are helpful to better understand the onset and development of diseases, as well as the control measures and vaccine research. This review focuses on the role of animal hosts in the maintenance of the virus, and summarizes the host range of RVFV. We list some common animal models in the process of RVFV research, which would provide some important insights into the prevention and treatment of RVFV, as well as the study of Rift Valley fever (RVF) pathogenesis and vaccines.

KEYWORDS

RVFV, RVF, zoonotic, natural host, animal model

1. Introduction

Rift Valley fever phlebovirus (RVFV) was initially isolated from ruminants in the Rift Valley region of Kenya in 1930 (1), and since then, it has been known to cause periodic outbreaks in Africa. In September 2000, RVF spread to Saudi Arabia and Yemen through the trade of RVFV-infected animals. Subsequently, from 2007 to 2022, RVF outbreaks were reported in over 20 countries, including Tanzania, Kenya, South Africa, Madagascar, and Mauritania, spanning a period of 15 years.¹

RVFV belongs to the *Phlebovirus* genus in the *Phenuiviridae* family of Bunyavirales. It is an enveloped virus with a spherical shape (2). Similar to other bunyaviruses, RVFV possesses a single-stranded RNA genome that consists of three segments: large (L), medium (M), and small (S). The L segment encodes RNA-dependent RNA polymerase, the M segment encodes structural glycoproteins Gn and Gc, and the S segment encodes nucleoprotein (N) and a non-structural protein called NSs (2). NSs is considered the main virulence factor, and its deletion results in decreased infectivity of RVFV (3). The interaction between NSs and the host general transcription factor IIH (TFIIH, a multiprotein complex involved in both eukaryotic transcription and DNA repair) plays a crucial role in RVFV virulence. TFIIH is composed of 10 subunits, which can be divided into two functional complexes: the core complex (XPB, XPD, p62, p52, p44, p34, and p8/TTD-A) and the CDK-activated kinase (CAK) complex (CDK 7,

¹ <https://wahis.woah.org/#/event-management>

cyclin H, and MAT 1) (4). When TFIIF associates with the Ω XaV motif in NSs, p62 is degraded, leading to the inhibition of the interferon (IFN) response and enhancing RVFV virulence (5). The mechanism by which RVFV infection inhibits host RNA synthesis and evades viral immune responses involves the competitive binding between NSs and p44. This competition prevents the interaction of XPD (the natural partner of p44 in TFIIF) with p44, and NSs sequesters certain TFIIF subunits within nuclear filamentous structures, leading to the segregation of the XPB/p44 complex and inhibiting the assembly of TFIIF subunits (6). Additionally, RVFV-encoded NSs proteins impact cellular fluidity, cell shape, and cell–cell adhesion by targeting the expression of Abl2 and the host actin cytoskeleton, thereby contributing to RVFV pathogenesis (7).

RVFV is primarily transmitted among animals through mosquito bites. However, for humans, RVFV infection can occur through contact with the blood of infected animals, inhalation or exposure to viral particles, and consumption of raw meat from sick animals (8, 9). This virus causes significant damage to ruminant livestock, resulting in high mortality rates among young newborn animals, widespread abortion in pregnant animals, and severe liver damage, posing a significant threat to animal health (8, 10, 11). Throughout history, RVFV has inflicted substantial harm on animal husbandry. In humans, the initial symptoms of RVFV infection include fever, headache, muscle and joint pain, and in some cases, nausea and vomiting. Conjunctivitis and photophobia may also occur. Severe cases can lead to bleeding, encephalitis, hepatitis, permanent blindness, or even death (12). Although there have been no reported cases of human-to-human transmission of RVFV, it is still considered a highly dangerous zoonotic pathogen. *Aedes* and *Culex* mosquitoes are the primary vectors responsible for the transmission of this disease between animals, as documented in the literature (13).

Given the broad host range of RVFV and the diversity of infected cells, host proteins play a crucial role in RVFV infection across different cell types and species. Identifying the function of these host factors is essential for the development of effective antiviral therapeutics. A genome-wide CRISPR/Cas9 screen revealed that low-density lipoprotein receptor-associated protein 1 (LRP1) is a critical host factor for RVFV infection. Heat shock protein (Grp94) and receptor-associated protein (RAP) were also found to influence RVFV entry by regulating the expression and function of LRP1 (14). The biological significance of LRP1 in RVFV infection was further demonstrated by inhibiting its interaction, which prevented RVFV from entering target cells across various host species. Studies have shown significant homology between the LRP1 protein in certain livestock species, such as cattle, and humans (15), suggesting that LRP1 is highly conserved among different species and may have a consistent function. This could potentially explain why humans are susceptible to RVFV after coming into contact with infected animals. Furthermore, LRP1 is widely expressed, with higher levels observed in the liver, placenta, and brain, which correspond to major sites of disease manifestation during RVFV infection. This highlights the potential of LRP1 as a target for antiviral therapeutics. Interestingly, LRP1 also plays a significant role in Oropouche orthobunyavirus infection (16), suggesting its potential involvement in the host infection process of Bunyaviruses. Further research is needed to explore the precise mechanisms underlying this relationship.

The RVF epidemic has had a significant impact on animal husbandry in areas where the disease is endemic. Therefore,

understanding the host range of RVFV is crucial for preventing RVF outbreaks. Additionally, there is an urgent need for the research and development of effective vaccines and therapeutic drugs. However, the occurrence and progression of RVFV-induced diseases in humans are complex. It is impractical to deeply explore the pathogenesis and efficacy of these diseases in patients, thus biomedical research often relies on animal models as an experimental basis for testing hypotheses. Currently, laboratory infection models are established through virus inoculation, inhalation, or aerosol infection (Table 1). Some experiments use footpad infections to simulate the transmission mode of mosquito bites under realistic conditions. Different studies employ varying infection methods based on their specific research objectives. Furthermore, the choice of animal models depends on the specific research purposes. This review provides a summary of the geographical distribution of natural hosts for RVFV and the application and pathological responses of different animal models. These models are suitable for studying various pathological consequences associated with RVFV infection.

2. Natural hosts

As a zoonotic disease transmitted by animals, extensive research has been conducted on the natural hosts of RVFV. Due to common host factors, viruses have the ability to cross species barriers. The variation in organ damage severity may be attributed to the differential distribution of host factors in different organs. This allows RVFV to exhibit a broad host range and distinct manifestations of the disease. In this review, we have categorized them into rodents, ruminants, non-human primates, and other animals. To provide a visual representation, we have created a map showing the global distribution of RVFV animal hosts (Figure 1). The broad host range of RVFV, coupled with its mosquito-borne transmission characteristics, allows for viral mutation and sustained transmission over extended periods. Although the incidence of RVFV infection varies among different animal species, the detection rate of RVFV and the occurrence of viremia emphasize the crucial role of natural hosts in the prevalence and outbreak of RVFV.

2.1. Rodents

While some studies suggest that wild rodents are not hosts for RVFV (41) most research findings indicate that wild rodents, being natural hosts, play a crucial role in the maintenance and transmission of RVFV. For instance, an ELISA test conducted in Egypt revealed a high RVFV positivity rate of 36.36% in rodents (42). Similarly, Senegal's VNT test identified positive results in 4 out of the 14 rodent species examined, with the highest positivity rate observed in rodents from the low valley region of Senegal (43). It can be inferred that the variance in positivity rates is associated with the humidity levels in the respective regions where these species are found. This correlation is also evident from an ELISA survey conducted in South Africa, which showed an increased rate of rodent infection following heavy rainfall (44). In addition to the wide variety of rodents susceptible to RVFV, their early sexual maturity, rapid reproduction due to large litter sizes, and their ability to inhabit areas where humans or livestock reside make them potential risk factors for the further

TABLE 1 Animal models of RVFV and their pathological manifestations.

Order	Genus or Species	Disease features	Route of exposure	References
Rodent	Mouse	Hepatitis	FP	(17)
		Hepatitis/cerebritis	IP/SC/Aerosol	(18)
		Hepatitis/cerebritis	IP/SC	(19)
		Cerebritis	FP	(20)
		Cerebritis	Aerosol	(21)
	Rat	Hepatitis	IP/SC/Aerosol	(22)
		Hepatitis	IP/SC/Aerosol	(23)
		Hepatitis/cerebritis/eye lesions	Aerosol	(24)
		Hepatitis	IP	(25)
		Eye lesions	SC/Aerosol	(26)
	Gerbil	Cerebritis	SC	(27)
	Hamster	Hepatitis	Aerosol	(28)
		Hepatitis	SC	(29)
Non-human primates	Rhesus monkey	Hepatitis/cerebritis/hemorrhage/fever	IV/IM	(30)
		Hepatitis/fever	Aerosol/IV	(31)
	Marmoset	Hepatitis/haemorrhag/cerebritis/fever	IV/SC/IN	(32)
		Cerebritis/hemorrhage/fever	Aerosol	(33)
	African green monkeys (AGM)	Cerebritis/hemorrhage/fever	Aerosol	(33)
		Cerebritis/hepatitis/hemorrhage/fever	Aerosol	(34)
Ruminantia	Sheep	Hepatitis/abortion	SC	(35)
		Fever/abortion	Inoculated	(36)
	Goats	Fever/hepatitis	SC	(37)
		Viremia	IN/SC	(38)
	Calves	Cerebritis/hepatitis	SC	(10)
	Lambs	Fever/hepatitis	Aerosol	(28)
		Hepatitis	Inoculated	(36)
	Cattle	Hepatitis/fever	IN/ID/IN+ID+SC	(39)
Other mammalia	Ferret	Fever/cerebritis	ID/IN	(40)

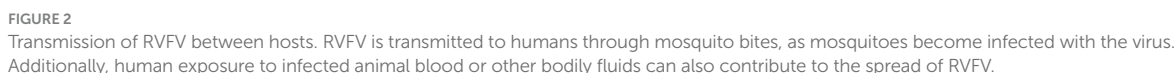
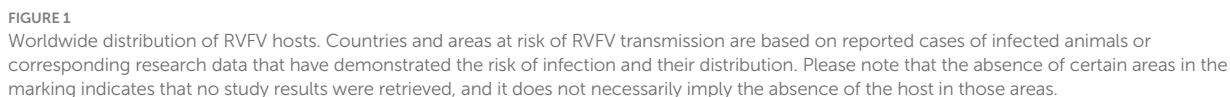
SC, subcutaneous; IP, intraperitoneal; FP, footpad; ID, intradermal; IN, intranasal.

spread of RVFV transmission. HI testing conducted in the Sinai Peninsula has demonstrated RVFV infection among both rodents and local soldiers (45). As human populations expand, areas with lower living standards may struggle to maintain adequate health conditions, leading to increased contact between humans, livestock, and rodents, thereby facilitating virus transmission. A PCR test conducted in Egypt revealed significantly higher RVFV-positive rates among rats in rural areas compared to urban areas (46), indicating an extremely high risk of infection among local rural residents. Therefore, in RVFV-endemic regions, in addition to mosquito control and treatment of sick animals, controlling rodents is also crucial. Recent experimental infections have shown that black rats, despite not exhibiting any pathological manifestations following subcutaneous infection, develop antibodies and experience long-term viremia (47). Another investigation indicated that a higher concentration of the virus in the blood facilitates its spread (48), suggesting that this commonly found rodent species also poses a risk as a host for RVFV. The extensive infection of rodents and their associated pathological reactions have paved the way for rodents to

be used as animal models in the development of RVFV vaccines and the exploration of pathogenesis (Figure 2).

2.2. Ruminants

Ruminants serve as the primary reservoir of RVFV and have a significant impact on economic development following RVFV infection. During the RVFV epidemic in Kenya, ruminants had much higher positivity rates in both antibody tests conducted compared to other wild animals (49, 50). The virus was first isolated from an infected flock of sheep during the 1930 RVF outbreak in East Africa (1). Various factors such as species differentiation, age of infection, and climatic conditions can affect the manifestation of the disease in ruminants. Pregnant female ruminants are particularly prone to having a “miscarriage storm” after being infected with RVFV. This suggests that the virus can cross the placenta and cause an increase in inflammatory chemokines and interferon response, leading to miscarriage.



gender discrepancy is uncertain. RVFV epidemics typically occur in autumn and winter, especially following heavy rains and floods, which create humid conditions that promote mosquito breeding.

Ruminant reproduction plays a significant role in determining the likelihood of a large-scale outbreak following infection, which in turn increases the risk of human infections. A Tanzanian study found that animal infection rates were closely related to human infection rates during epidemics, possibly due to increased local cattle slaughter, which is proportional to the human population (53). RVFV induces different pathologies in ruminants of different species, with cattle having a higher IgG positivity rate than sheep and goats in Cameroon. This may be due to feeding methods as nomadic cattle-raising methods increase the risk of cattle exposure to the virus.

IgM-positive samples and samples with successful RVFV RNA detected by PCR were only found in sheep and cattle, suggesting that goats may have lower susceptibility to the virus (54). A Tunisian survey showed higher antibody positivity rates in cattle and sheep than goats, providing further evidence for this speculation (55). In order to improve the specificity and sensitivity of detection, Gn-based ELISA methods are being increasingly applied to investigations (56). However, studies have shown that viremia peaks 3–4 days after infection in goats to activate innate immunity, and later produces neutralizing antibodies for long-term protection. This indicates that goats also play a role in RVFV maintenance (37).

Animal vaccination programmes are already in place in some areas, and surveys in Egypt have shown lower virus prevalence rates on vaccinated farms (57). However, a sample survey conducted in Rwanda following the implementation of the vaccine programme showed that no animals had been vaccinated, indicating the need for increased vaccine coverage (51). Authorities also need to pay attention to the risk of re-infection by other viruses to avoid adding to the burdens of infected animals (51).

Since researchers re-isolated the virus from camels in 1979, serological studies have shown that camels are susceptible hosts of RVFV (58). Additionally, serological studies of wild ruminants such as giraffes, antelopes, and buffalo have shown their overall susceptibility to RVFV, even though reported symptoms of the virus pandemic in wild ruminants are rare. It is likely that RVFV causes mild subclinical diseases in wild ruminants and maintains long-term low viremia, allowing the virus to continue to spread (50). Three separate ELISA surveys have revealed that the prevalence range of RVFV has expanded to the Middle East through ruminants (Table 2) (60–62). The high positive rate of RVFV detection in ruminants, as indicated by the EFSA Panel on Animal Health and Welfare (AHAW) PCR assay in 2020 on Mayot Island, further demonstrates the effectiveness and severity of RVFV infection in this group of animals. The region is under the jurisdiction of France and has closer trade ties with Europe, which has prompted European countries to be vigilant about the risks associated with the movement of goods (71). Although the RVFV gene is highly conserved, studies have identified some mutated strains in ruminants (72), indicating that ruminants also play a role in the evolution of the virus. This poses challenges in controlling its spread. Therefore, it is crucial for all countries to strengthen animal quarantine efforts at ports in order to effectively prevent the substantial losses that can be caused by the introduction of RVFV.

2.3. Non-human primates

Due to limitations in field investigations, studies on primates have primarily been conducted in laboratory settings. It was only in 1954 that

the presence of RVFV positivity in macaques was discovered during field investigations (70). Laboratory studies have focused on the manifestations of RVFV infection in red monkeys, long-tailed monkeys, white-eyebrowed monkeys, and rhesus monkeys. It was found that rhesus monkeys could develop viremia for up to 12 days after RVFV infection. Baboons infected with RVFV developed fever and viremia for several days (73). Intravenous inoculation of RVFV typically leads to benign viral infections in most rhesus monkeys. However, approximately 20% of cases still develop a hemorrhagic fever syndrome, characterized by extensive hepatic necrosis, disseminated intravascular coagulation, and hemolytic anemia (30). Another experimental infection of rhesus monkeys demonstrated that although all monkeys exhibited high levels of viral infection, the disease manifestations varied. A small proportion of monkeys infected with RVFV showed signs of hemorrhagic fever and eventually died. The remaining animals survived RVFV infection, but some displayed clinical symptoms such as loss of appetite and skin petechiae, while others showed no signs of clinical disease. In deceased macaques, abnormal liver function and coagulation markers were observed early in the infection, while monkeys without clinical manifestations exhibited high levels of IFN, suggesting that early morbidity events are critical factors for survival (74). The genes of non-human primates and humans exhibit a high degree of homology and similarity in terms of morphology and function. As hosts of RVFV, non-human primates serve as an alert for potential infections in humans. Therefore, during virus epidemics, the possibility of human infection should be taken into consideration.

2.4. Other animals

The mammalian host range of RVFV extends beyond ruminants and rodents. Serological tests have shown positive results for pigs and warthogs (66). RVFV has also been isolated from horses (58). In 1987, the virus was isolated from bats in Guinea (67), and in 2021, RVFV infection in bats was identified through PCR testing in Egypt (68). RVFV has been detected in rhinoceros (69), and serological investigations and PCR detection have revealed the infection of zebra, elephants, and rhinos with RVFV (50). A special investigation in 1996 focused on the RVFV positivity rate in carnivorous mammals such as jackals, wild dogs, cheetahs, and lions, and it was found that these animals could serve as natural hosts of RVFV (75). There have been no reported cases of RVFV infections in domestic pets, such as cats and dogs. However, given that many mammals are susceptible to RVFV, it remains uncertain whether domestic pets may play a role in the spread of the virus. Therefore, it is still important to monitor the infection status of pets. A laboratory study conducted in 2018 on North American white-tailed deer found that RVFV infection in these deer was associated with fever, hemorrhagic hepatic necrosis, and moderate to severe hemorrhagic lymphadenopathy, similar to the situation observed in ruminants. However, further attention and study are needed to understand the specific lesions, particularly moderate to severe diffuse hemorrhagic enteritis (76).

In addition to the natural hosts mentioned earlier, there have been studies exploring potential candidates as hosts for RVFV. Some vector mosquitoes of RVFV have been found to feed on amphibian blood (77), and *in vitro* studies have demonstrated the sensitivity of *Xenopus* cells and certain reptile cells to RVFV (78, 79). This suggests that amphibians or reptiles may potentially serve as natural hosts for RVFV. However, it is important to note that although RVFV infection

TABLE 2 Summary of animal hosts for RVFV.

Order	Family	Detection method	Location	References
Rodent	Muridae	HI	Zimbabwe, Egypt, Egypt	(41, 45, 48)
		VNT	Senegal	(43)
		ELISA	Egypt, South Africa	(42, 44)
		PCR	Egypt	(46)
	Sciuridae	VNT	Senegal	(43)
Ruminantia	Bovidae	HI	South Africa	(52)
		VNT	Kenya	(50)
		ELISA	Tanzania, Cameroon, Tunisia, Cameroon	(54, 55, 59)
		PCR	Egypt, Rwanda, Cameroon	(51, 54, 57)
	Caprinae	Virus Isolation	East Africa	(1)
		ELISA	Tunisia, Tanzania, Cameroon, Iran, Iraqi, Saudi Arabia	(53–55, 60–62)
		VNT	Mozambique, Senegal, Uganda, Yemen	(56)
		PCR	Zambia, Uganda, Cameroon, The Democratic Republic of the Congo	(54, 63–65)
	Camelidae	ELISA	Kenya	(49)
		Virus Isolation	Egypt	(58)
Mammalia	Suidae	VNT	South Africa	(66)
	Elephantidae	VNT	Kenya	(50)
	Vespertilionidae	Virus isolation	Guinea	(67)
		PCR	Egypt	(68)
	Equidae	VNT	Kenya	(50)
		Virus isolation	Egypt	(58)
	Rhinoceros	HI	Zimbabwe	(69)
		VNT	Kenya	(50)
Non-human primates	Cercopithecidae	/	Ghana to Angola	(70)
	Chimpanzee	/	Disjunct distribution in western and central Africa	(70)

HI, hemagglutination inhibition; VNT, virus neutralization test; ELISA, enzyme-linked immunosorbent assay; PCR, polymerase chain reaction.

in amphibians and reptiles has not been observed in their natural state, these animals are still at risk of RVFV infection, highlighting the broad host range of the virus.

3. Animal models

Considering the wide range of hosts for RVFV and the potential risk of transmission, further studies are necessary. However, it is important to note that different animal models and inoculation routes are suitable for studying diverse pathological processes related to RVFV. Each animal model possesses its own unique characteristics and advantages. Additionally, changes in hemogram parameters in each animal model are also worth considering (Table 1). As a reference, a summary of animal models for RVFV is provided (Table 1), which investigators can use to identify and select appropriate models based on their experimental requirements.

3.1. Rodents

Rodents are commonly used as animal models to study RVFV. Among rodents, rats, mice, and gerbils are the three main

categories of animal models used. Gerbils, in particular, have been valuable in the study of neurological pathogenesis and can serve as effective animal models (27). However, it is important to note that the diversity of pathological changes observed in rodents following RVFV infection suggests that relying solely on a single rodent species for research may not be sufficient to ensure the reliability of experimental results or meet all experimental requirements.

Rodents are primarily infected with RVFV through direct intranasal injection or aerosol infection (18, 19, 21, 25, 28) (Table 1), as they are intranasally susceptible to the virus. Intraperitoneal injection can also lead to successful infection, but this method differs from the natural transmission route, which involves mosquito bites or contact with contaminated tissues. To simulate the natural infection process and study the status of human infection under more realistic conditions, recent experiments have utilized footpad infection in rodents (17). Different strains of animals exhibit varying pathological changes following RVFV infection, with most rats and mice being suitable for studying liver-related injuries. However, the most severe reactions observed in humans after RVFV infection involve central nervous system (CNS) lesions and permanent blindness caused by ocular lesions. Consequently, efforts have been made to develop rat and mouse models that can be used to study these specific aspects. For instance,

Haley Cartwright et al. found that CC057 strain mice infected *via* footpad can be used to study encephalitis (20). Madeline M. Schwarz et al. demonstrated the tropism of RVFV for Lrp1 in the posterior eye of Sprague Dawley rats, making them suitable for studying uvea, retina, and optic nerve damage (26). Additionally, pregnant rats have been found to be more susceptible to RVFV infection compared to non-pregnant rats. RVFV infection in pregnant rats can lead to intrauterine fetal death and severe congenital abnormalities. During the second trimester, RVFV can directly infect placental chorionic villi in human placental tissue. Pregnant rats can transmit RVFV directly and vertically through the placenta, making them suitable models for studying RVFV-induced abortion, which closely mimics the situation in pregnant humans (80). During the development of animal models, researchers discovered that hamsters can be utilized as an animal model for studying liver lesions caused by RVFV infection (29). This finding further expands the host range of RVFV in rodents. The use of hamsters as an animal model for RVFV research dates back to as early as 1962. Subcutaneous infection in hamsters leads to noticeable clinical symptoms, indicating that hamsters can be effectively employed in the study of RVFV, similar to other rodent models.

3.2. Ruminants

Due to the significant role of ruminants in the maintenance of RVFV, these animals serve as ideal animal models in vaccine studies. Ruminants, such as sheep, goats, and cattle, are commonly used in the development of animal vaccines against RVFV. Given the effects of RVFV on pregnant ruminants, such as liver necrosis and abortion (8), pregnant ewes or cows are often included as separate populations to assess the application range and effects of vaccines during the research and development process. Furthermore, the efficacy of RVFV infection differs among animals of different ages. Newborn sheep or calves are more susceptible to RVFV, emphasizing the need to consider the efficacy and safety of vaccines for both the young animals and their parents, who may be infected with RVFV. Researchers have investigated the efficacy and safety of the four-segmented RVFV (RVFV-4s) vaccine in young sheep, goats, and cattle (11). Additionally, the efficacy of the nonspreading RVFV (NSR) vaccine has been studied specifically in lambs (81). With the vRVFV-4s vaccine, transmission of the virus is not observed in vaccinated animals or in the environment, and the virus does not regain virulence upon animal passage. This vaccine has proven effective in protecting various ruminant species from their corresponding RVFV strains (11). It provides some relief from liver damage in infected pregnant animals and reduces the risk of miscarriage caused by viral infection (36). However, there are notable variations among different species, and the immune response in young sheep and cattle is not entirely satisfactory. Similar to vRVFV-4s, MP-12 does not exhibit viral shedding or transmission (82). However, its use during early pregnancy may lead to partial abortion (83). NSR can reduce viremia in lambs to a level undetectable by viral isolation, thereby protecting them from clinical symptoms, although this effect is not long-lasting. High-precision detection has shown that RVFV can also be transmitted from pregnant ewes to their fetuses, indicating that the vaccine's immunization efficacy has not met expectations. Different

inoculation methods in ruminants result in varying clinical manifestations. In calves, natural RVFV infection primarily leads to liver lesions, while subcutaneous infection tests have revealed encephalomyelitis, lymphatic necrosis, and adrenal gland damage (10). Studies on different routes of infection in cattle and goats have indicated that intranasal infection is more likely to cause neurological damage (38, 39). Neuronal infection in goats has been observed as early as 1 day after infection (38). Although short-term infection is unlikely to be attributed to high levels of viremia breaking through the blood–brain barrier, it is plausible that intranasal infection directly affects neurons. This finding offers a viable direction for future research on neurological lesions caused by RVFV. Furthermore, the immune status of animals after virus infection, including changes in interferon levels, pro-inflammatory factors, antibodies, etc., also influences clinical symptoms and should be given due attention (37). Table 1 provides an overview of the main clinical manifestations and experimental infection routes observed in these ruminant animal models. This information can serve as a valuable reference for future development of animal vaccines.

3.3. Non-human primates

Non-human primates are used as animal models to study the harm of RVFV to the human body due to their high similarity to humans in terms of pathogenesis and clinical manifestations. These animal models serve as valuable tools in the development of vaccines for human use. Despite being expensive and challenging to obtain approval for their use, non-human primates are still essential in studying RVFV-induced neurological diseases. This is because stable encephalitis models are not commonly observed in rodents such as rats, mice, and gerbils, primarily due to age limitations. Rhesus monkeys, as long-term non-human primate models widely used in various viral studies, exhibit phenotypic similarities to humans after RVFV infection. However, due to the low incidence of neurological diseases in rhesus monkeys, they may not be the most suitable models for RVFV studies (30, 31). Studies have shown that African green monkeys and marmosets demonstrate more significant clinical manifestations, including neurological symptoms, when establishing RVFV infection models (32–34). In non-human primates, the varying disease manifestations observed after infection may be attributed to differences in host defense status and the distribution of host factors. This finding holds significant implications for humans as well. Therefore, these non-human primate species are considered more suitable for relevant RVFV studies as animal models (Table 1).

3.4. Other animals

Recently, ferrets have emerged as a potential animal model for studying RVFV. When inoculated intranasally with RVFV, ferrets have shown a high likelihood of developing central nervous system (CNS) diseases, characterized by symptoms such as seizures and ataxia (40). This model is particularly valuable because the RVFV-induced CNS diseases observed in ferrets occur following exposure, thereby mimicking the natural exposure pathway seen in humans. Consequently, the RVFV ferret model can be utilized to investigate

how the virus enters the CNS. In addition, ferrets can also serve as animal models for studying mild self-limited febrile illness caused by RVFV. Although this may not be the most severe symptom, it is still important to consider, as it represents a significant manifestation of human RVFV infection and warrants attention. Therefore, ferrets provide a valuable tool for studying both the CNS effects and mild febrile illness associated with RVFV.

4. Conclusion and prospect

The host range of RVFV infection is determined by host receptors and entry factors. It has been discovered that human LRP1 serves as a receptor for RVFV. However, the conservation of LRP1 protein sequence is relatively low in humans and some RVFV-sensitive animals, suggesting the existence of other receptors in these animals. In mice, sheep, and *Aedes aegypti*, homologs of C-type lectin receptors (CLRs) have been proposed as potential attachment factors or entry receptors in various species (84).

The heterogeneity among hosts in RVFV infection can be attributed to factors such as the efficiency of viral replication in the host and the survival time of infectious viral particles. Studies on host resistance to RVFV have revealed that the viral glycoprotein Gn plays a significant role in triggering immune responses on the surface of the RVFV viral envelope. Gn-specific antibodies are a major component of the RVFV neutralizing antibody response, indicating that the entry of RVFV into the host depends on Gn (85). Therefore, these two critical molecules, Gn and LRP1, can be potential targets for future vaccines and drug development. In addition to inhibiting viral entry, translational arrest and autophagy are also considered integral components of host defense against RVFV (86, 87). Cholesterol can be incorporated into RVFV particles and enhance RVFV infectivity in a polyamine-dependent manner (88). Studies have found that a high-cholesterol diet can lead to liver cholesterol accumulation, and it mainly affects cerebral vessels among the vascular effects, with up-regulation of LDLr and LRP1 detected in cerebral vessels (89). This finding aligns with the liver and brain lesions caused by RVFV infection, but the specific relationship still requires further exploration.

Furthermore, local ecological factors, such as the relative abundance and feeding preferences of vector hosts, can influence the transmission of RVFV among hosts. The prevalence of RVFV is closely linked to ecological and climatic conditions (90). Mosquito species in North America and European *Aedes* mosquitoes have been found to be capable of infecting and transmitting RVFV (91–95). With the impacts of climate change and global trade, these mosquitoes have the potential to spread the virus to Europe and the Americas, posing a significant risk to animal husbandry. Therefore, it is crucial to address and mitigate this risk to prevent irreversible damage. The variation in pathological responses to RVFV infection among different host species is an important consideration in selecting animal models for research. The US Food and Drug Administration recommends testing potential vaccines and treatments in at least two well-established animal models (96). Multiple animal models have been utilized to confirm the efficacy and safety of the RVFV-4s and MP-12 vaccines.

In conclusion, this review highlights the risk of RVFV transmission by providing an overview of its host range. Although an

inactivated vaccine has been developed, it has not yet been licensed for commercial use. Currently, the vaccine is only administered to protect veterinarians and laboratory personnel who may be at high risk of exposure to RVFV. However, the infectivity of RVFV to humans and its potential to cause severe illness or even death cannot be ignored. Therefore, there is still much research needed in the prevention and treatment of RVFV. To provide a reference for future research, this review summarizes the commonly used animal models in RVFV studies and emphasizes the pathological findings associated with RVFV infection in different host models. Presently, the available animal models for studying visual impairment and nervous system damage caused by RVFV are insufficient to meet the demands of scientific research. This poses challenges for the prevention and treatment of these two symptoms. Future model development should focus on these symptoms, adjust research directions, and address the gaps in understanding the immunopathology of such symptoms. Furthermore, it is worth noting that different hosts exhibit variations in their response to RVFV infection. For instance, some animals may develop ocular lesions while others can escape death resulting from liver damage but still experience severe encephalitis. The underlying reasons for these differences, including the distribution of RVFV host factors in various host animals or the existence of alternative antiviral pathways, require further investigation and exploration. Additionally, attention should be given to the similarities between RVFV and other hemorrhagic fever viruses. This includes examining whether there is cross-reactivity between factors involved in mediating the infection of each virus. Such investigations can shed light on the feasibility of combined prevention and treatment strategies.

Author contributions

YX: Writing – original draft. XW: Writing – review & editing. LJ: Writing – review & editing. YZ: Writing – review & editing. YL: Software, Writing – review & editing. FW: Writing – review & editing. LZ: Conceptualization, Writing – review & editing.

Funding

The author(s) declare financial support was received for the research, authorship, and/or publication of this article. This work was supported by grants from National Natural Science Foundation of China (82272306 and 82072270), College Students innovation and entrepreneurship training program of Shandong Province (S202310439074), Taishan Scholars Program (tstp20221142), and Academic Promotion Programme of Shandong First Medical University (2019LJ001).

Conflict of interest

The authors declare that the research was conducted in the absence of any commercial or financial relationships that could be construed as a potential conflict of interest.

The author(s) declared that they were an editorial board member of Frontiers, at the time of submission. This had no impact on the peer review process and the final decision.

Publisher's note

All claims expressed in this article are solely those of the authors and do not necessarily represent those of their affiliated

organizations, or those of the publisher, the editors and the reviewers. Any product that may be evaluated in this article, or claim that may be made by its manufacturer, is not guaranteed or endorsed by the publisher.

References

- Daubney R, Hudson JR, Garnham PC. Enzootic hepatitis or Rift Valley fever. an undescribed virus disease of sheep cattle and man from East Africa. *J Pathol Bacteriol.* (1931) 34:545–79.
- Wright D, Kortekaas J, Bowden TA, Warimwe GM. Rift Valley fever: biology and epidemiology. *J Gen Virol.* (2019) 100:1187–99. doi: 10.1099/jgv.0.001296
- Muller R, Saluzzo JF, Lopez N, Dreier T, Turell M, Smith J, et al. Characterization of clone 13, a naturally attenuated avirulent isolate of Rift Valley fever virus, which is altered in the small segment. *Am J Trop Med Hygiene.* (1995) 53:405–11. doi: 10.4269/ajtmh.1995.53.405
- Kolesnikova O, Radu L, Poterszman A. TFIIF: a multi-subunit complex at the cross-roads of transcription and DNA repair. *Adv Protein Chem Struct Biol.* (2019) 115:21–67. doi: 10.1016/bs.apcsb.2019.01.003
- Cyr N, de la Fuente C, Lecoq L, Guendel I, Chabot PR, Kehn-Hall K, et al. A Ω XaV motif in the Rift Valley fever virus NSs protein is essential for degrading p 62, forming nuclear filaments and virulence. *Proc Natl Acad Sci U S A.* (2015) 112:6021–6. doi: 10.1073/pnas.1503688112
- Le May N, Dubaele S, Proietti De Santis L, Billecocq A, Bouloy M, Egly JM. TFIIF transcription factor, a target for the Rift Valley hemorrhagic fever virus. *Cells.* (2004) 116:541–50. doi: 10.1016/S0092-8674(04)00132-1
- Bamia A, Marcato V, Boissière M, Mansuroglu Z, Tamietti C, Romani M, et al. The NSs protein encoded by the virulent strain of Rift Valley fever virus targets the expression of Abl 2 and the actin cytoskeleton of the host, affecting cell mobility, cell shape, and cell-cell adhesion. *J Virol.* (2020) 95:e01768–20. doi: 10.1128/JVI.01768-20
- Odendaal L, Clift SJ, Fosgate GT, Davis AS. Ovine fetal and placental lesions and cellular tropism in natural Rift Valley fever virus infections. *Vet Pathol.* (2020) 57:791–806. doi: 10.1177/0300985820954549
- LaBeaud AD, Muchiri EM, Ndlovu M, Mwanje MT, Muiruri S, Peters CJ, et al. Inter-epidemic Rift Valley fever virus seropositivity, northeastern Kenya. *Emerg Infect Dis.* (2008) 14:1240–6. doi: 10.3201/eid1408.080082
- Rippy MK, Topper MJ, Mebus CA, Morrill JC. Rift Valley fever virus-induced encephalomyelitis and hepatitis in calves. *Vet Pathol.* (1992) 29:495–502. doi: 10.1177/030098589202900602
- Wichers Schreur PJ, Oreshkova N, van Keulen L, Kant J, van de Water S, Soós P, et al. Safety and efficacy of four-segmented Rift Valley fever virus in young sheep, goats and cattle. *NPJ Vaccines.* (2020) 5:65. doi: 10.1038/s41541-020-00212-4
- Bird BH, Ksiazek TG, Nichol ST, MacLachlan NJ. Rift Valley fever virus. *J Am Vet Med Assoc.* (2009) 234:883–93. doi: 10.2460/javma.234.7.883
- Linthicum KJ, Britch SC, Anyamba A. Rift Valley fever: an emerging mosquito-borne disease. *Annu Rev Entomol.* (2016) 61:395–415. doi: 10.1146/annurev-ento-010715-023819
- Ganaie SS, Schwarz MM, McMillen CM, Price DA, Feng AX, Albe JR, et al. Lrp 1 is a host entry factor for Rift Valley fever virus. *Cells.* (2021) 184:5163–5178.e24. doi: 10.1016/j.cell.2021.09.001
- Bopp NE, Fernández D, Aguilar PV. Closing the rift: discovery of a novel virus receptor. *Cells.* (2021) 184:5084–6. doi: 10.1016/j.cell.2021.09.004
- Schwarz MM, Price DA, Ganaie SS, Feng A, Mishra N, Hoehl RM, et al. Oropouche orthobunyavirus infection is mediated by the cellular host factor Lrp 1. *Proc Natl Acad Sci U S A.* (2022) 119:e2204706119. doi: 10.1073/pnas.2204706119
- Cartwright HN, Barbeau DJ, McElroy AK. Rift Valley fever virus is lethal in different inbred mouse strains independent of sex. *Front Microbiol.* (2020) 11:1962. doi: 10.3389/fmicb.2020.01962
- Smith DR, Steele KE, Shamblin J, Honko A, Johnson J, Reed C, et al. The pathogenesis of Rift Valley fever virus in the mouse model. *Virology.* (2010) 407:256–67. doi: 10.1016/j.virol.2010.08.016
- Batista L, Jouvion G, Simon-Chazottes D, Houzelstein D, Buren-Defranoux O, Boissière M, et al. Genetic dissection of Rift Valley fever pathogenesis: Rvfv 2 locus on mouse chromosome 11 enables survival to early-onset hepatitis. *Sci Rep.* (2020) 10:8734. doi: 10.1038/s41598-020-65683-w
- Cartwright HN, Barbeau DJ, Doyle JD, Klein E, Heise MT, Ferris MT, et al. Genetic diversity of collaborative cross mice enables identification of novel rift valley fever virus encephalitis model. *PLoS Pathog.* (2022) 18:e1010649. doi: 10.1371/journal.ppat.1010649
- Reed C, Lin K, Wilhelmsen C, Friedrich B, Nalca A, Keeney A, et al. Aerosol exposure to Rift Valley fever virus causes earlier and more severe neuropathology in the murine model, which has important implications for therapeutic development. *PLoS Negl Trop Dis.* (2013) 7:e2156. doi: 10.1371/journal.pntd.0002156
- Peters CJ, Slone TW. Inbred rat strains mimic the disparate human response to Rift Valley fever virus infection. *J Med Virol.* (1982) 10:45–54. doi: 10.1002/jmv.1890100107
- Anderson GW Jr, Smith JF. Immunoelectron microscopy of Rift Valley fever viral morphogenesis in primary rat hepatocytes. *Virology.* (1987) 161:91–100. doi: 10.1016/0042-6822(87)90174-7
- Anderson GW Jr, Lee JO, Anderson AO, Powell N, Mangiafico JA, Meadors G. Efficacy of a Rift Valley fever virus vaccine against an aerosol infection in rats. *Vaccine.* (1991) 9:710–4. doi: 10.1016/0264-410X(91)90285-E
- Ritter M, Bouloy M, Vialat P, Janzen C, Haller O, Frese M. Resistance to Rift Valley fever virus in *Rattus norvegicus*: genetic variability within certain 'inbred' strains. *J Gen Virol.* (2000) 81:2683–8. doi: 10.1099/0022-1317-81-11-2683
- Schwarz MM, Connors KA, Davoli KA, McMillen CM, Albe JR, Hoehl RM, et al. Rift Valley fever virus infects the posterior segment of the eye and induces inflammation in a rat model of ocular disease. *J Virol.* (2022) 96:e0111222. doi: 10.1128/jvi.01112-22
- Anderson GW Jr, Slone TW Jr, Peters CJ. The gerbil, *Meriones unguiculatus*, a model for Rift Valley fever viral encephalitis. *Arch Virol.* (1988) 102:187–96. doi: 10.1007/BF01310824
- Miller WS, Demchak P, Rosenberger CR, Dominik JW, Bradshaw JL. Stability and infectivity of airborne yellow fever and rift valley fever viruses. *Am J Hyg.* (1963) 77:114–21.
- Scharton D, Van Wettere AJ, Bailey KW, Vest Z, Westover JB, Siddharthan V, et al. Rift Valley fever virus infection in golden Syrian hamsters. *PLoS One.* (2015) 10:e0116722. doi: 10.1371/journal.pone.0116722
- Peters CJ, Jones D, Trotter R, Donaldson J, White J, Stephen E, et al. Experimental Rift Valley fever in rhesus macaques. *Arch Virol.* (1988) 99:31–44. doi: 10.1007/BF01311021
- Morrill JC, Peters CJ. Mucosal immunization of rhesus macaques with Rift Valley fever MP-12 vaccine. *J Infect Dis.* (2011) 204:617–25. doi: 10.1093/infdis/jir354
- Smith DR, Bird BH, Lewis B, Johnston SC, McCarthy S, Keeney A, et al. Development of a novel nonhuman primate model for Rift Valley fever. *J Virol.* (2012) 86:2109–20. doi: 10.1128/JVI.06190-11
- Hartman AL, Powell DS, Bethel LM, Caroline AL, Schmid RJ, Oury T, et al. Aerosolized rift valley fever virus causes fatal encephalitis in African green monkeys and common marmosets. *J Virol.* (2014) 88:2235–45. doi: 10.1128/JVI.012341-13
- Wonderlich ER, Caroline AL, McMillen CM, Walters AW, Reed DS, Barratt-Boyes SM, et al. Peripheral blood biomarkers of disease outcome in a monkey model of Rift Valley fever encephalitis. *J Virol.* (2018) 92:e01662-17. doi: 10.1128/JVI.01662-17
- Yedloutschnig RJ, Dardiri AH, Mebus CA, Walker JS. Abortion in vaccinated sheep and cattle after challenge with Rift Valley fever virus. *Vet Rec.* (1981) 109:383–4. doi: 10.1136/vr.109.17.383
- Wichers Schreur PJ, Oymans J, Kant J, van de Water S, Kollár A, Dehon Y, et al. A single vaccination with four-segmented rift valley fever virus prevents vertical transmission of the wild-type virus in pregnant ewes. *NPJ Vaccines.* (2021) 6:8. doi: 10.1038/s41541-020-00271-7
- Nfon CK, Marszal P, Zhang S, Weingartl HM. Innate immune response to Rift Valley fever virus in goats. *PLoS Negl Trop Dis.* (2012) 6:e1623. doi: 10.1371/journal.pntd.0001623
- Kroeker AL, Smid V, Embury-Hyatt C, Moffat E, Collignon B, Lung O, et al. RVFV infection in goats by different routes of inoculation. *Viruses.* (2018) 10:709. doi: 10.3390/v10120709
- Kroeker AL, Babiuk S, Pickering BS, Richt JA, Wilson WC. Livestock challenge models of Rift Valley fever for agricultural vaccine testing. *Front Vet Sci.* (2020) 7:238. doi: 10.3389/fvets.2020.00238
- Barbeau DJ, Albe JR, Nambulli S, Tilston-Lunel NL, Hartman AL, Lakdawala SS, et al. Rift Valley fever virus infection causes acute encephalitis in the ferret. *mSphere.* (2020) 5:e00798-20. doi: 10.1128/mSphere.00798-20
- Hoogstraal H, Meegan JM, Khalil GM, Adham FK. The Rift Valley fever epizootic in Egypt 1977–78. 2. Ecological and entomological studies. *Trans R Soc Trop Med Hyg.* (1979) 73:624–9. doi: 10.1016/0035-9203(79)90005-1
- Youssef BZ, Donia HA. The potential role of *Rattus rattus* in enzootic cycle of Rift Valley fever in Egypt. 1-detection of RVF antibodies in *R. rattus* blood samples by both enzyme linked immuno sorbent assay (ELISA) and immuno-diffusion technique (ID). *J Egypt Public Health Assoc.* (2001) 76:431–41.

43. Gora D, Yaya T, Jocelyn T, Didier F, Maoulouth D, Amadou S, et al. The potential role of rodents in the enzootic cycle of Rift Valley fever virus in Senegal. *Microbes Infect.* (2000) 2:343–6. doi: 10.1016/S1286-4579(00)00334-8
44. Pretorius A, Oelofsen MJ, Smith MS, van der Ryst E. Rift Valley fever virus: a seroepidemiological study of small terrestrial vertebrates in South Africa. *Am J Trop Med Hygiene.* (1997) 57:693–8. doi: 10.4269/ajtmh.1997.57.693
45. Kark JD, Aynor Y, Ben Mordechai Y, Ron-Kuper N, Peleg BA, Peters CJ. A serological survey of Rift Valley fever antibodies in the northern Sinai. *Trans R Soc Trop Med Hyg.* (1982) 76:427–30. doi: 10.1016/0035-9203(82)90129-8
46. Youssef BZ, Donia HA. The potential role of *rattus rattus* in enzootic cycle of Rift Valley fever in Egypt 2-application of reverse transcriptase polymerase chain reaction (RT-PCR) in blood samples of *Rattus rattus*. *J Egypt Public Health Assoc.* (2002) 77:133–41.
47. Stoek F, Rissmann M, Ulrich R, Eiden M, Groschup MH. Black rats (*Rattus rattus*) as potential reservoir hosts for Rift Valley fever phlebovirus: experimental infection results in viral replication and shedding without clinical manifestation. *Transbound Emerg Dis.* (2022) 69:1307–18. doi: 10.1111/tbed.14093
48. Swanepoel R, Blackburn NK, Efstratiou S, Condy JB. Studies on Rift Valley fever in some African murids (Rodentia: Muridae). *J Hyg.* (1978) 80:183–96. doi: 10.1017/S0022172400053535
49. Britch SC, Binopal YS, Ruder MG, Kariithi HM, Linthicum KJ, Anyamba A, et al. Rift Valley fever risk map model and seroprevalence in selected wild ungulates and camels from Kenya. *PLoS One.* (2013) 8:e66626. doi: 10.1371/journal.pone.0066626
50. Evans A, Gakuya F, Paweska JT, Rostal M, Akoolo L, Van Vuren PJ, et al. Prevalence of antibodies against Rift Valley fever virus in Kenyan wildlife. *Epidemiol Infect.* (2008) 136:1261–9. doi: 10.1017/S0950268807009806
51. Dutuze MF, Ingabire A, Gafarasi I, Uwituze S, Nzayirambaho M, Christofferson RC. Identification of Bunyamwera and possible other Orthobunyavirus infections and disease in cattle during a Rift Valley fever outbreak in Rwanda in 2018. *Am J Trop Med Hyg.* (2020) 103:183–9. doi: 10.4269/ajtmh.19-0596
52. LaBeaud AD, Cross PC, Getz WM, Glinka A, King CH. Rift Valley fever virus infection in African buffalo (*Syncerus caffer*) herds in rural South Africa: evidence of interepidemic transmission. *Am J Trop Med Hyg.* (2011) 84:641–6. doi: 10.4269/ajtmh.2011.10-0187
53. Sindato C, Karimuribo ED, Vairo F, Misinzio G, Rweyemamu MM, Hamid MMA, et al. Rift Valley fever seropositivity in human and domestic ruminants and associated risk factors in Sengerema, Ilala, and Rufiji districts, Tanzania. *Int J Infect Dis.* (2022) 122:559–65. doi: 10.1016/j.ijid.2022.07.012
54. Sado FY, Tchegnna HS, Kamgang B, Djonabaye D, Nakouné E, McCall PJ, et al. Seroprevalence of Rift Valley fever virus in domestic ruminants of various origins in two markets of Yaoundé, Cameroon. *PLoS Neglect Trop Dis.* (2022) 16:e0010683. doi: 10.1371/journal.pntd.0010683
55. Zouaghi K, Bouattour A, Aounallah H, Surtees R, Krause E, Michel J, et al. First serological evidence of Crimean-Congo hemorrhagic fever virus and Rift Valley fever virus in ruminants in Tunisia. *Pathogens.* (2021) 10:769. doi: 10.3390/pathogens10060769
56. Jäckel S, Eiden M, Balkema-Buschmann A, Ziller M, van Vuren PJ, Paweska JT, et al. A novel indirect ELISA based on glycoprotein Gn for the detection of IgG antibodies against Rift Valley fever virus in small ruminants. *Res Vet Sci.* (2013) 95:725–30. doi: 10.1016/j.rvsc.2013.04.015
57. Mroz C, Gwida M, El-Ashker H, Ziegler U, Homeier-Bachmann T, Eiden M, et al. Rift Valley fever virus infections in Egyptian cattle and their prevention. *Transbound Emerg Dis.* (2017) 64:2049–58. doi: 10.1111/tbed.12616
58. Imam IZ, El-Karamany R, Darwish MA. An epidemic of Rift Valley fever in Egypt. 2. Isolation of the virus from animals. *Bull World Health Organ.* (1979) 57:441–3.
59. Bronsvoort BM, Kelly RE, Freeman E, Callaby R, Bagninbom JM, Ndipl L, et al. Population-based, seroepidemiological study of Rift Valley fever in Cameroonian cattle populations. *Front Vet Sci.* (2022) 9:897481. doi: 10.3389/fvets.2022.897481
60. Aghaa OB, Rhaymah MS. Seroprevalence study of Rift Valley fever antibody in sheep and goats in Ninevah governorate. *Iraqi J Vet Sci.* (2013) 27:53–61. doi: 10.33899/IJVS.2013.82778
61. Al-Afaleq AI, Hussein MF, Al-Naeem AA, Housawi F, Kabati AG. Seroepidemiological study of Rift Valley fever (RVF) in animals in Saudi Arabia. *Trop Anim Health Prod.* (2012) 44:1535–9. doi: 10.1007/s11250-012-0100-x
62. Fakour S, Naserabadi S, Ahmadi E. A serological and hematological study on rift valley fever and associated risk factors in aborted sheep at Kurdistan province in west of Iran. *Comp Immunol Microbiol Infect Dis.* (2021) 75:101620. doi: 10.1016/j.cimid.2021.101620
63. Tshilenge GM, Mulumba MLK, Misinzio G, Noad R, Dundon WG. Rift Valley fever virus in small ruminants in the Democratic Republic of the Congo. *Onderstepoort J Vet Res.* (2019) 86:e1–5. doi: 10.4102/ojvr.v86i1.1737
64. Shoemaker TR, Nyakaruhka L, Balinandi S, Ojwang J, Tumusiime A, Mulei S, et al. First laboratory-confirmed outbreak of human and animal Rift Valley fever virus in Uganda in 48 years. *Am J Trop Med Hyg.* (2019) 100:659–71. doi: 10.4269/ajtmh.18-0732
65. Chambaro HM, Hirose K, Sasaki M, Libanda B, Sinkala Y, Fandamu P, et al. An unusually long rift valley fever inter-epizootic period in Zambia: evidence for enzootic virus circulation and risk for disease outbreak. *PLoS Negl Trop Dis.* (2022) 16:e0010420. doi: 10.1371/journal.pntd.0010420
66. Lubisi BA, Ndouhda PN, Neiffer D, Penrith ML, Sibanda DR, Bastos ADS. Evaluation of a virus neutralisation test for detection of Rift Valley fever antibodies in Suid sera. *Trop Med Infect Dis.* (2019) 4:52. doi: 10.3390/tropicalmed4010052
67. Boiro I, Konstantinov OK, Numerov AD. Isolation of Rift Valley fever virus from bats in the Republic of Guinea. *Bull Soc Pathol Exotique Filiales.* (1987) 80:62–7.
68. Saeed OS, El-Deeb AH, Gadalla MR, El-Soally SAG, Ahmed HAH. Genetic characterization of Rift Valley fever virus in insectivorous bats, Egypt. *Vector Borne Zoonotic Dis.* (2021) 21:1003–6. doi: 10.1089/vbz.2021.0054
69. Anderson EC, Rowe LW. The prevalence of antibody to the viruses of bovine virus diarrhoea, bovine herpes virus 1, rift valley fever, ephemeral fever and bluetongue and to *Leptospira* sp in free-ranging wildlife in Zimbabwe. *Epidemiol Infect.* (1998) 121:441–9. doi: 10.1017/S0950268898001289
70. Pellissier A, Rousselot R. Serological investigation on the incidence of neurotropic viruses in some monkeys in French equatorial Africa. *Bull Soc Pathol Exotique Filiales.* (1954) 47:228–31.
71. Nielsen SS, Alvarez J, Bicout DJ, Calistri P, Depner K, Drewe JA, et al. Rift Valley fever: risk of persistence, spread and impact in Mayotte (France). *EFSA J Eur Food Saf Authority.* (2020) 18:e06093. doi: 10.2903/j.efsa.2020.6093
72. Bird BH, Khristova ML, Rollin PE, Ksiazek TG, Nichol ST. Complete genome analysis of 33 ecologically and biologically diverse Rift Valley fever virus strains reveals widespread virus movement and low genetic diversity due to recent common ancestry. *J Virol.* (2007) 81:2805–16. doi: 10.1128/JVI.02095-06
73. Davies FG, Clausen B, Lund LJ. The pathogenicity of Rift Valley fever virus for the baboon. *Trans R Soc Trop Med Hyg.* (1972) 66:363–5. doi: 10.1016/0035-9203(72)90253-2
74. Morrill JC, Jennings GB, Johnson AJ, Cosgriff TM, Gibbs PH, Peters CJ. Pathogenesis of Rift Valley fever in rhesus monkeys: role of interferon response. *Arch Virol.* (1990) 110:195–212. doi: 10.1007/BF01311288
75. House C, Alexander KA, Kat PW, O'Brien SJ, Mangiafico J. Serum antibody to Rift Valley fever virus in African carnivores. *Ann N Y Acad Sci.* (1996) 791:345–9. doi: 10.1111/j.1749-6632.1996.tb53541.x
76. Wilson WC, Kim JJ, Trujillo JD, Sunwoo SY, Noronha LE, Urbaniak K, et al. Susceptibility of White-tailed deer to Rift Valley fever virus. *Emerg Infect Dis.* (2018) 24:1717–9. doi: 10.3201/eid2409.180265
77. Lutomiah J, Omondi D, Masiga D, Mutai C, Mireji PO, Ongus J, et al. Blood meal analysis and virus detection in blood-fed mosquitoes collected during the 2006–2007 Rift Valley fever outbreak in Kenya. *Vector Borne Zoonotic Dis.* (2014) 14:656–64. doi: 10.1089/vbz.2013.1564
78. Gaudreault NN, Indran SV, Bryant PK, Richt JA, Wilson WC. Comparison of Rift Valley fever virus replication in north American livestock and wildlife cell lines. *Front Microbiol.* (2015) 6:664. doi: 10.3389/fmicb.2015.00664
79. Rissmann M, Lenk M, Stoek F, Szentiks CA, Eiden M, Groschup MH. Replication of Rift Valley fever virus in amphibian and reptile-derived cell lines. *Pathogens.* (2021) 10:681. doi: 10.3390/pathogens10060681
80. McMillen CM, Arora N, Boyles DA, Albe JR, Kujawa MR, Bonadio JE, et al. Rift Valley fever virus induces fetal demise in Sprague-Dawley rats through direct placental infection. *Sci Adv.* (2018) 4:eau9812. doi: 10.1126/sciadv.aau9812
81. Oreshkova N, van Keulen L, Kant J, Moormann RJ, Kortekaas J. A single vaccination with an improved nonspreading Rift Valley fever virus vaccine provides sterile immunity in lambs. *PLoS One.* (2013) 8:e77461. doi: 10.1371/journal.pone.0077461
82. Morrill JC, Mebus CA, Peters CJ. Safety and efficacy of a mutagen-attenuated Rift Valley fever virus vaccine in cattle. *Am J Vet Res.* (1997) 58:1104–9.
83. Hunter P, Erasmus BJ, Vorster JH. Teratogenicity of a mutagenised Rift Valley fever virus (MVP 12) in sheep. *Onderstepoort J Vet Res.* (2002) 69:95–8.
84. Schön K, Lindenwald DL, Monteiro JT, Glanz J, Jung K, Becker SC, et al. Vector and host C-type lectin receptor (CLR)-fc fusion proteins as a cross-species comparative approach to screen for CLR-Rift Valley fever virus interactions. *Int J Mol Sci.* (2022) 23:3243. doi: 10.3390/ijms23063243
85. Wright D, Allen ER, Clark MHA, Gitonga JN, Karanja HK, Hulswit RJG, et al. Naturally acquired Rift Valley fever virus neutralizing antibodies predominantly target the Gn glycoprotein. *iScience.* (2020) 23:101669. doi: 10.1016/j.isci.2020.101669
86. Hopkins KC, Tartell MA, Herrmann C, Hackett BA, Taschuk F, Panda D, et al. Virus-induced translational arrest through 4EBP1/2-dependent decay of 5'-TOP mRNAs restricts viral infection. *Proc Natl Acad Sci U S A.* (2015) 112:E2920–9. doi: 10.1073/pnas.1418805112
87. Moy RH, Gold B, Molleston JM, Schad V, Yanger K, Salzano MV, et al. Antiviral autophagy restricts Rift Valley fever virus infection and is conserved from flies to mammals. *Immunity.* (2014) 40:51–65. doi: 10.1016/j.immuni.2013.10.020
88. Mastrodomenico V, LoMascolo NJ, Cruz-Pulido YE, Cunha CR, Mounce BC. Polyamine-linked cholesterol incorporation in Rift Valley fever virus particles promotes infectivity. *ACS Infect Dis.* (2022) 8:1439–48. doi: 10.1021/acsinfectdis.2c00071

89. Schneider EH, Fitzgerald AC, Ponnampala SS, Dopico AM, Bukiya AN. Differential distribution of cholesterol pools across arteries under high-cholesterol diet. *Biochim Biophys Acta Mol Cell Biol Lipids*. (2022) 1867:159235. doi: 10.1016/j.bbalip.2022.159235
90. Hardcastle AN, Osborne JCP, Ramshaw RE, Hulland EN, Morgan JD, Miller-Petrie MK, et al. Informing Rift Valley fever preparedness by mapping seasonally varying environmental suitability. *Int J Infect Dis*. (2020) 99:362–72. doi: 10.1016/j.ijid.2020.07.043
91. Turell MJ, Wilson WC, Bennett KE. Potential for North American mosquitoes (Diptera: Culicidae) to transmit rift valley fever virus. *J Med Entomol*. (2010) 47:884–9. doi: 10.1093/jmedent/47.5.884
92. Birnberg L, Talavera S, Aranda C, Núñez AI, Napp S, Busquets N. Field-captured *Aedes vexans* (Meigen, 1830) is a competent vector for Rift Valley fever phlebovirus in Europe. *Parasit Vectors*. (2019) 12:484. doi: 10.1186/s13071-019-3728-9
93. Turell MJ, Dohm DJ, Mores CN, Terracina L, Wallethe DL Jr, Hribar LJ, et al. Potential for North American mosquitoes to transmit Rift Valley fever virus. *J Am Mosq Control Assoc*. (2008) 24:502–7. doi: 10.2987/08-5791.1
94. Turell MJ, Britch SC, Aldridge RL, Xue RD, Smith ML, Cohnstaedt LW, et al. Potential for *Psorophora columbiae* and *Psorophora ciliata* mosquitoes (Diptera: Culicidae) to transmit Rift Valley fever virus. *J Med Entomol*. (2015) 52:1111–6. doi: 10.1093/jme/tjv093
95. Turell MJ, Britch SC, Aldridge RL, Kline DL, Boohene C, Linthicum KJ. Potential for mosquitoes (Diptera: Culicidae) from Florida to transmit Rift Valley fever virus. *J Med Entomol*. (2013) 50:1111–7. doi: 10.1603/ME13049
96. Snoy PJ. Establishing efficacy of human products using animals: the US food and drug administration's "animal rule". *Vet Pathol*. (2010) 47:774–8. doi: 10.1177/0300985810372506



OPEN ACCESS

EDITED BY

Annalisa Ciabattini,
University of Siena, Italy

REVIEWED BY

Bikash Sahay,
University of Florida, United States
François Trottein,
Centre National de la Recherche
Scientifique (CNRS), France

*CORRESPONDENCE

Marcelo Freire
✉ mfreire@jcv.org

RECEIVED 23 May 2023

ACCEPTED 11 September 2023

PUBLISHED 19 October 2023

CITATION

Jang H, Matsuoka M and Freire M (2023)
Oral mucosa immunity: ultimate strategy
to stop spreading of pandemic viruses.
Front. Immunol. 14:1220610.
doi: 10.3389/fimmu.2023.1220610

COPYRIGHT

© 2023 Jang, Matsuoka and Freire. This is an open-access article distributed under the terms of the [Creative Commons Attribution License \(CC BY\)](#). The use, distribution or reproduction in other forums is permitted, provided the original author(s) and the copyright owner(s) are credited and that the original publication in this journal is cited, in accordance with accepted academic practice. No use, distribution or reproduction is permitted which does not comply with these terms.

Oral mucosa immunity: ultimate strategy to stop spreading of pandemic viruses

Hyesun Jang¹, Michele Matsuoka¹ and Marcelo Freire^{1,2*}

¹Genomic Medicine and Infectious Diseases, J. Craig Venter Institute, La Jolla, CA, United States,

²Division of Infectious Diseases and Global Public Health Department of Medicine, University of California San Diego, La Jolla, CA, United States

Global pandemics are most likely initiated via zoonotic transmission to humans in which respiratory viruses infect airways with relevance to mucosal systems. Out of the known pandemics, five were initiated by respiratory viruses including current ongoing coronavirus disease 2019 (COVID-19). Striking progress in vaccine development and therapeutics has helped ameliorate the mortality and morbidity by infectious agents. Yet, organism replication and virus spread through mucosal tissues cannot be directly controlled by parenteral vaccines. A novel mitigation strategy is needed to elicit robust mucosal protection and broadly neutralizing activities to hamper virus entry mechanisms and inhibit transmission. This review focuses on the oral mucosa, which is a critical site of viral transmission and promising target to elicit sterile immunity. In addition to reviewing historic pandemics initiated by the zoonotic respiratory RNA viruses and the oral mucosal tissues, we discuss unique features of the oral immune responses. We address barriers and new prospects related to developing novel therapeutics to elicit protective immunity at the mucosal level to ultimately control transmission.

KEYWORDS

oral mucosa, RNA viruses, pandemics, saliva immunity, mucosal vaccine

1 Zoonotic respiratory RNA viruses are linked to global pandemics

Pandemic refers to the explosive outbreaks of communicable diseases on a global scale (1–3). The scale, geographic location, and duration of pandemics are unpredictable (4, 5). Historically, the most devastating pandemics were initiated by cross-species transmission of pathogens, such as Justinian plague (541–542 AD), the Black Death (1347–1351), flu pandemics (Spanish flu in 1918, Asian flu in 1957, Hong Kong flu in 1968, Russian flu 1977, Swine flu in 2009), and the ongoing SARS-CoV-2 COVID-19 pandemics (2019–current) (6–9). Since most human populations are immunologically naive, wildlife pathogens that acquired a susceptibility to humans can spread rapidly (10). Still, cross-species transmission from animal to human is not as common and requires successful adaptation to maintain long-term human to human transmission (11–14). Wolfe et al. summarized five progressive stages of animal microbe's

human adaptation: 1) exclusivity to animals; 2) obtaining non-sustainable animal-to-human transmission; 3) limited human-to-human transmission; 4) sustained human-to-human transmission without the need for an intermediate host (influenza A, SARS, MERS, SARS-CoV-2, *Vibrio cholerae*, and dengue virus); and 5) exclusive circulation in humans (15). As humans encroach into the natural habitats of wildlife and as human population, travel, and trade increases, so does the risk of spillover events (16). Domestic animals serve as intermediate hosts to create novel zoonotic pathogens, increasing the chance of transmission from wildlife (17, 18). Emergence of the pandemic 2009 H1N1 virus (pdm09 H1N1) serves as a prime example where the novel virus was created by a triple genetic reassortment event (influenza genes derived from North American swine, humans, and birds) which most likely occurred in domesticated pigs (19–21). Exceptional mutation rates and short generation times are highly advantageous to RNA viruses, allowing them to adapt to new host systems and break the species barrier by compatibility to host cell receptors, cellular enzyme systems, or tissue tropism (22, 23). Mutation rates of RNA viruses can roughly occur at rates of six orders of magnitude greater than those of their cellular hosts (23). Across multiple studies, a critical part of emerging pathogens (25–44%) in humans is reported to be related to respiratory RNA viruses (24–27).

The global pandemics affecting all five continents almost simultaneously were initiated by zoonotic respiratory RNA viruses including influenza and the coronaviruses. Currently, vaccines are the most efficacious measure to reduce the disease severity and mortality of respiratory viral diseases (28, 29). However, due to the biased immunogenicity to elicit systemic neutralizing antibody response, vaccinations cannot stop the spread of the virus at mucosal surfaces (30–33). Silent spread of viruses among asymptomatic patients can further generate novel escaping mutants (34–37) and impact public health.

2 Salivary droplets as transmission source of zoonotic respiratory RNA viruses

Respiratory RNA viruses primarily infect and replicate at respiratory tracts, and the amplified viruses shed their progeny into mucosal droplets, often spread by coughing or sneezing (38, 39). Considering the poor stability of RNA and viral envelope structure, transmission of aerosolized particles had been, historically, less supported (40). Due to this belief, the efficacy of facial masks was questioned in preventing transmission of the respiratory viruses during the initial phase of the COVID-19 pandemic (41). The role of aerosolized particles in transmission of respiratory particles has been more supported as experiencing explosive incidence of the COVID-19 cases in indoor environments that are poorly ventilated, such as meatpacking factories, cruise ships, and churches (40).

For the transmission of highly attenuated SARS-CoV-2 variant strains, salivary droplets generated during speech have been increasingly considered as a major transmission vehicle for the asymptomatic carriers lacking respiratory symptoms (coughing and

sneezing) (42, 43). While the SARS-CoV-2 virus is considered a respiratory pathogen, the virus is known to replicate in a variety of tissues and organs expressing the ACE2/TMPRSS receptors, including gingival tissues and salivary glands (44).

This is also consistent with human adapted influenza viruses and oral epithelium. It requires galactose linked to α -2,6-sialic acid, abundantly expressed on epithelial cells of the upper respiratory tract, including oropharynx (45). While avian influenza viruses preferentially bind to the α -2,3-SA expressed in the human lower respiratory tract, human adapted zoonotic influenza viruses replicate in the oropharyngeal airway and shed into the salivary droplets. Responsible for the 2009 pandemic, the A/(H1N1)pdm09 virus has been reported to bind to α -2,6-SA and, to a limited extent, to α -2,3-SA (45, 46). In the case of the highly pathogenic avian influenza virus H5N1 viruses, one of the most devastating candidate pandemic virus strains, can also infect and replicate in cells of the nasopharyngeal and oropharyngeal epithelia (47). Influenza is also known to be detected in saliva (48, 49). A recent study showed no significant difference in detection rate of influenza virus detection rate between saliva and nasopharyngeal swabs (48).

In the case of small virus-laden droplets (<30 μ m), highly sensitive laser light scattering observations have revealed that loud speech can emit thousands of oral fluid droplets per second (43). In a closed, stagnant air environment, they disappear from the window of view with time constants in the range of 8 to 14 min, corresponding to droplet nuclei of 4 μ m diameter, or 12 to 21 μ m droplets prior to dehydration (43). Virus-laden droplets less than 30 μ m could even spill over conventional facial masks. Spilled RNA virus particles maintain infectivity for hours in the air or on surfaces and infection virus was still detected up to 28 days later (50). The stability of coronaviruses varied between 1 hour to 24 hours depending on the humidity and temperature (51–55). In the case of animal coronavirus porcine enteric diarrhea virus (PEDV), the viral RNA in air was detectable at 16.1 km (56). Actual evidence of airborne transmission has also been demonstrated in *in vitro* and *in vivo* models. Kormuth et al. used humidity-controlled chambers and identified that the 2009 pandemic influenza A (H1N1) virus in suspended aerosols stationary droplets remain infectious for an hour across a wide range of humidities (23–98%) (57). Through a guinea pig model, transmission of influenza A/Panama/2007/1999 (H3N2) (58) virus through the air was measured as efficient as the fomite transmission (58). Collectively, active shedding of respiratory RNA viruses in saliva can be a major source of transmission from asymptomatic carriers lacking respiratory symptoms. Stability of RNA viruses in the air and potential of airborne transmission shows the ease of transmission of the zoonotic respiratory RNA viruses, emphasizing the need for induction of oral immunity (Figure 1).

3 Induction of oral immunity reduces respiratory viruses spread

The lack of effective measures to prevent entry of viral particles at the mucosal surfaces poses a major challenge in controlling

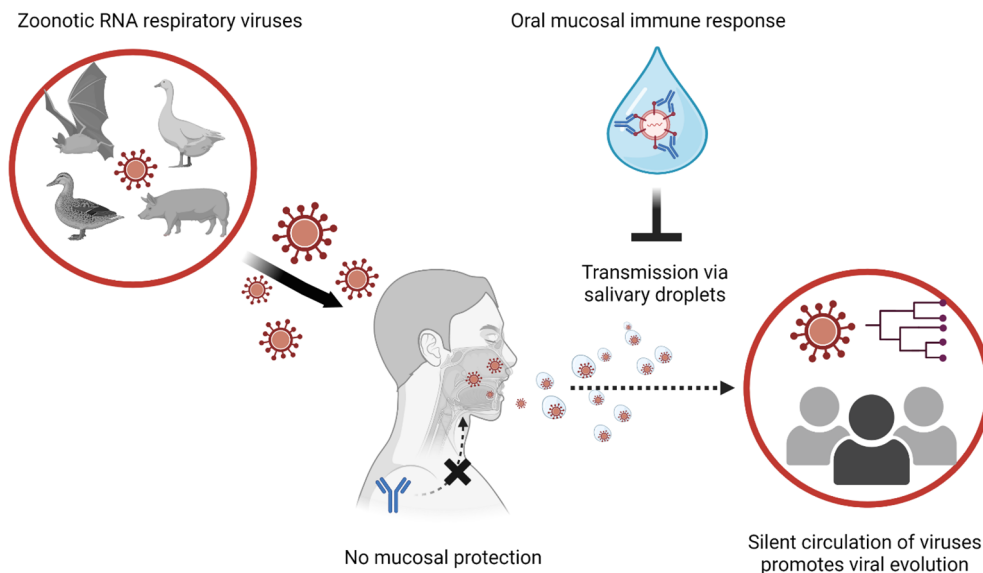


FIGURE 1

Global transmission viral transmission patterns could be interrupted by mucosal immune responses to manage zoonotic RNA respiratory viruses. Novel viral infections to humans are originated from animals. Especially when zoonotic respiratory RNA viruses gain human-to-human transmission capabilities, the novel infectious agent can explosively spread through the immunologically naive human population. In the case of human populations gaining partial immunity to the virus, systemic antibody response reduces the severity of clinical illness and mortality. However, systemic immune response cannot block the infections/transmission of the viruses at the mucosal surfaces (e.g., upper respiratory tract and oral cavity). In transmission of asymptomatic infection without respiratory symptoms (sneezing and coughing), virus-laden salivary droplets can act as major source of viral transmission. Thus, induction of protective immune response at the oral mucosal surface is instrumental to control transmission of the zoonotic respiratory RNA viruses.

zoonotic respiratory viruses. Vaccination is the most effective strategy to control zoonotic respiratory RNA viral disease, significantly lowering the disease severity and case-fatality rate (59–61). However, current vaccines administered via parenteral route cannot directly stimulate the mucosal immune system (29, 62). Systemic antibodies induced by vaccination provide partial protection to subjects but transportation from blood to mucosal epithelia surface is highly restricted to confer protection at mucosal surfaces (63–65). Instead, vaccinated individuals can carry the viruses without apparent symptoms and serve as asymptomatic carriers (66). As viruses are more attenuated and sheds easier without apparent symptoms, vaccination and symptom-based intervention strategies lose their efficacy and the viruses evolve to more divergent escaping mutants (67). The ultimate strategy to end the current pandemic and prevent future pandemics is to control transmission. Current efforts to control variant viruses are to induce sterilizing immunity, which in turn provides protective immune responses at both mucosal and systemic levels (68, 69). In theory, sterilizing immunity aims to induce neutralizing antibodies at the viral entry site, differentiated from the protective immunity which refers to prevention from symptomatic infections. Sterile immunity prevents the viral transmission, including the asymptomatic and presymptomatic carriers (68, 70). At the phase when the viruses are highly attenuated and asymptomatic transmission lacking respiratory symptoms (e.g., coughing or sneezing) is more frequent, induction of neutralizing IgA response at oral mucosa should be considered (43). While the oral immune system is known to be on the frontline of the gastrointestinal tract (GIT) and respiratory tract, it has been relatively less investigated (71–74).

Novel strategies needed to induce oral mucosal immune responses are particularly scarce due to its unique role in preventing entry of external pathogens and hyperactivity to diet or to air exposure.

4 The oral mucosal immune system is driven by a unique features

Oral mucosa is the beginning of the GIT and shares anatomic and histologic characteristics with GIT (75–77). In addition to mucus produced by overall GIT, the oral cavity produces saliva (32, 78). The whole saliva is originally generated from serum exudates and supplemented with highly diverse molecules from mucosal cells, immune cells, and microbes (78). Continuous production and swallowing of saliva provide a mechanical clearance of pathogens (78). Also, saliva contains host defense proteins, primarily responsible for both adaptive and innate humoral immune response at oral mucosa (78).

Oral mucosa, like other mucosal tissues, can be divided into three major layers, epithelia, lamina propria, and specialized lymphoid tissues (visual summary in Figure 2) (73, 75). The epithelial layer of oral mucosa is stratified squamous epithelium, forming a thicker and denser mechanical barrier than the single layer of GIT epithelia (73, 75). The top portion of the oral epithelial layer forms a level of various levels of keratinization according to the anatomical location (73, 75). Some areas, such as pharynx and junctional epithelium at periodontal space, are non-keratinized and serve as a major point for the innate defense and homeostasis in oral microenvironments (79–81). Lamina propria (LP), a loose connective tissue containing blood and

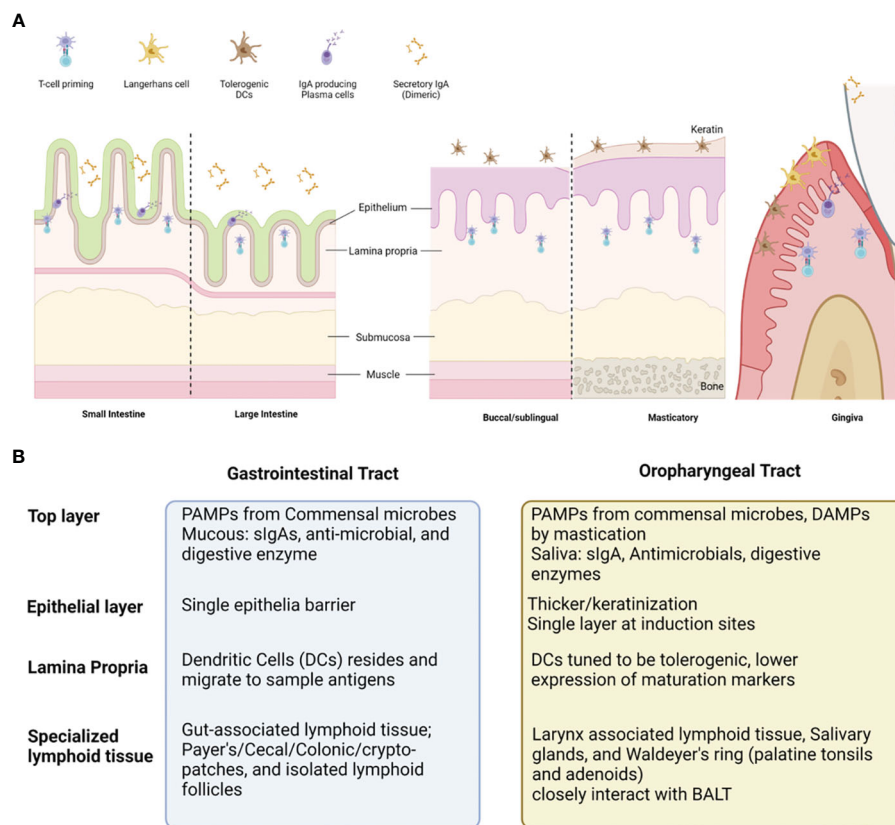


FIGURE 2

Comparison between oral vs gastrointestinal mucosal tissues and the cell populations contributing to overall immunity. Oral mucosa is the initial compartment for gastrointestinal tract (GIT). Overall structure of oral mucosa is like GIT, consisted with the shares common histologic structure; covered with commensal microbes and saliva filled with diverse antimicrobial, enzymes, and secretory IgAs (sIgAs) (A). The top layer, epithelium, lamina propria, and specialized lymphoid tissues present distinct cells and functions according to the GI versus Oral tract (B). Oral cavity presents unique traits (much thicker epithelial layer, presence of keratin layer, and tolerogenic dendritic cells), which can prevent vaccine antigen delivery and induction of virus-specific immune response at oral mucosal surfaces.

lymphatic vessels under epithelial layers, is a major inductive and effector site for immune cells (79). Steady-state dendritic cells (DCs) reside throughout the lamina propria and often migrate to sample auto-, and foreign antigens derived from commensal microbes, dietary components, mastication damage and pathogens (82). The steady-state DCs in oral tissues are tuned to be tolerogenic to most stimuli from the oral microenvironment, expressing low levels of maturation markers (CD80, CD83, and CD86) (83, 84). In certain conditions, such as invasion of pathogenic microbes, dysbiosis, or damage associated with molecular patterns (DAMPs), the DCs are activated and migrate to lymphoid tissues to induce T activation, such as buccal mucosa, salivary glands, and Waldeyer's ring, is located and serves as major site for activation and expansion of lymphocytes (79). Activated antigen-specific IgA secreting B cells or CD8+ T cells relocate to the effector site, such as the epithelium, LP, and salivary glands, to mediate immune response. But mature DCs also limit T cell activation and promote immune tolerance in specific triggers, such as IL-27, IL-10, vitamin A, or ligands of the aryl hydrocarbon receptor (AhR) (85–88).

As the sIgA can block the viral replication cycle at the initial stage, virus specific sIgAs has been thought to be the most potent target to induce sterilizing immunity at mucosal surfaces (70). In oral mucosa,

the sIgA is produced from plasma cells primarily residing in salivary glands and secreted as two monomers linked by a junctional chain via polymeric immunoglobulin receptors (pIgR) at the basolateral membrane of epithelial cells (89–91). In mucosa, the process of class switching to the IgA producing B cell occurs at the lymphoid tissues, such as nasopharyngeal-associated lymphoid tissues (NALT), tear duct associated lymphoid tissue (TALT), and peripheral lymphoid tissues. To elicit antibodies specific to the viral antigen with high affinity, the naive B cells go through the class switch recombination (CSR) by CD40-CD40L ligation in presence of the TGF- β and other co-stimulatory cytokines (IL-4, IL-5, IL-6, IL-10 and IL-21) mediated by CD4+ helper T cells (Th) (91, 92). Meanwhile, naive B cells can activate in response to the continuous stimuli from commensal microbes, metabolites and dietary antigens without involvement of T cells or hypersomatic mutations (93, 94). Two types of antigens have been known to induce the T cell-independent activation (95–97). Type I antigens are typically microbial products (e.g. bacterial LPS or DNA), directly activating B cells through the toll-like receptors on the B cell surface. Type 2 antigens are usually repetitive or highly cross-linked structures found on the surface of encapsulated bacteria, such as polysaccharides or glycolipids. Type II antigens do not have intrinsic activity to stimulate, but accumulation of BCRs and cross-activation of

the receptors can activate B lymphocytes, leading to the production of various cytokines, including interleukin-6 (IL-6) and tumor necrosis factor- α (TNF- α). Type II antigens can only activate mature B cells. Due to the lack of CSR, sIgAs produced by T cell independent processes present low affinity and low specificity to antigens (98). The source of cytokines involved in T cell independent class-switching is thought to come from subsets of innate immune cells, such as innate lymphoid cells (ILCs) (99). In addition to the sIgA response, commensal microbes are instrumental for the induction and/or tolerance of local immune responses (100–102). Oral mucosa possesses the second largest microbial community after the gut (103, 104). The symbiotic interaction between mucosal epithelial linings and microbes is crucial to maintain steady state of the oral mucosa (100–102).

Microbial colonies serve as primary barriers to inhibit the invasion of external microbes (105). Microbes and their metabolites can also modulate the tone of immune response to constant stimulation by the dietary and inhaled antigens (100–102). Metabolites produced from gut microbiota have been shown to directly influence both inflammatory cells (inflammatory Macs (iMacs), DCs, CD4 T helper (Th)1, CD4Th2, Th17, natural killer (NK) T cells, NK cells and neutrophils) and immuno-suppressive cells (e.g., tolerogenic T cells (T_{reg}), regulatory B cells (B_{reg}) and innate lymphocytes (ILCs)) (103). Accumulating evidence reveals that the dysbiosis in oral mucosa also contributes to the disease pathogenesis, especially for the respiratory viral infection (103, 106, 107). It is important to note that the oropharynx is the primary site of viral replication and immune induction and major source of the lung microbiome (103, 108). Also, infection with respiratory viruses, such as the SARS-CoV-2, impacts on enrichment of opportunistic pathobionts in the oral cavity (106, 109, 110). A recent cross-sectional study showed that the COVID-19 patients presented a distinctive microbiome profile, a decrease in the alpha-diversity and bacterial species richness in association with symptom severity (103).

The oral cavity maintains homeostatic inflammatory state, created by microflora. The local microflora habituated on the oral cavity is known to be more than 700 species of bacteria, viruses, fungi, and protozoa (111). The main inhabitants of a healthy oral cavity are gram positive and negative cocci and rods, such as Firmicutes, Bacillus, Proteobacteria and Actinomycetes (111–113). In a homeostatic state, the microbial community acts as a barrier against colonization of foreign agents and aids differentiation/maturation of the oral immune system (114). For example, constant production of bacterial products and damage associated molecular patterns (DAMPs) constantly recruit and stimulate innate immune cells (eg. neutrophil). Also, bacterial products (LPS, DNA, or polysaccharides) serve as antigen to induce T cell independent low affinity sIgA response during normal state. The sIgAs produced from the healthy state play a pivotal role to prevent overt growth of microbiome. Another important regulator of the microbiome is the fibrin (115). Inflammation triggered by the microbiome results in constant fibrin deposition in oral mucosa. The fibrin activates neutrophil effector functions, harnessing overgrowth of bacteria and activating the plasmin-mediated fibrinolysis. Since the homeostatic inflammation is highly

orchestrated by complex interaction among oral mucosa, microbiota, immune cells and clotting factors, dysbiosis and/or tissue damage created by viral infection can significantly impair the oral immune system and promote disease progress from local infection to the systemic illness (103, 115).

5 Induction of protective mucosal immune response is challenging: insights on the oral immunology

The oral mucosa is exposed to a variety of environmental insults, including pathogens, allergens, and toxins (77, 116). The oral mucosa is also the first line of defense against these insults, and it is essential that the oral mucosa is able to mount an effective immune response (77, 116). The immune response at mucosal surfaces is mediated by a variety of cells, including dendritic cells, macrophages, neutrophils, and B cells (117). These cells work together to generate an immune response that is specific to the pathogen or allergen that is being encountered (117). While the oral mucosa is constantly stimulated by foreign intakes, the symbiotic interactions among microbes epithelial cells and immune cells can also send signals to the system including clotting factors and microbiome intrusion (83, 84, 115). Due to the complexity, induction of antigen-specific immune response at the oral mucosal surface requires alternative approaches differentiated from conventional parenteral prophylactic or therapeutic strategies. The induction of mucosal immune responses is a complex process that is not fully understood, however, it is known that a number of factors can influence the ability of the oral mucosa to mount an effective immune response (83, 84, 115). These factors include: (i) the presence of pathogens or allergens; (ii) the integrity of the oral mucosa; (iii) the presence of IgA antibodies; (iv) the presence of cytokines; (v) the presence of regulatory T cells (83, 84, 115, 116). Also, the oral mucosa is home to a variety of commensal bacteria that can interfere with the immune response (83, 84, 115).

The first challenge for inducing mucosal immune response is the multiple mechanical and chemical barriers. Specially, the oral cavity is composed of multiple layers of epithelial cells, most areas covered with keratinized cells, except the inductive sites (pharynx, tonsil, hard/soft palate, buccal-, and sublingual mucosa) (81, 83). Also, the continuous production and swallowing of saliva containing diverse enzymes interferes with stable delivery of vaccine antigens and adjuvants (118). To induce protective immune response, the immunogen needs to overcome such barriers and persist at the site to initiate cascades of immune responses that lead to protection, such as homeostasis and maintenance of health.

The second barrier is to elicit protective immune responses by overcoming oral tolerance without the risk of experiencing hypersensitivity (83, 119, 120). Oral tolerance refers to the process in which the immune system does not respond to orally administered antigens (83, 119). At least two different mechanisms have been identified to mediate development of oral tolerance (83, 119). One mechanism is the induction of regulatory T cells via production of TGF- β but that concomitant retinoic acid signaling

boosted this process by mucosal DCs (119). T cell anergy is another possible mechanism induced in high-dose oral tolerance. Anergic T cells are also known to contribute to oral tolerance (83, 119). One method to circumvent oral tolerance could be to apply antigen in another mucosal route, such as intranasal or sublingual route.

Additional considerations relate to inducing protective oral immune response from by influence of commensal microbes and microbiome derived signals (77, 82). Oral cavity maintains homeostatic inflammatory status against commensal microbiota (77, 121, 122). In oral vaccination, depletion of microbiota significantly reduced Th1 and Th17 response to the heat-labile enterotoxin of enterotoxigenic *Escherichia coli* as adjuvant (LT R192G/L211A) (123). Also, individuals who displayed more diverse gut microbiota tended to exhibit better response to vaccinations (124). In contrast, dysbiosis can result in reduction in vaccine efficacy (125–127). Probiotics have been suggested to enhance IgA and memory T cell response in COVID-19 management (128).

Above issues are the major barrier in developing prophylactic/vaccine strategies to induce oral mucosal immune system and stop the silent spread of the zoonotic respiratory viruses via salivary droplets. Next, we discuss novel approaches targeting influenza, and the SARS-CoV-2 viruses, under clinical trials to prove their efficacy in induction of oral mucosal immunity.

6 Novel approaches inducing mucosal immune response specific to the zoonotic respiratory RNA viruses

6.1 Delivery system

6.1.1 Direct sensitization of oral mucosa

Is the most efficient route to activate resident immune cells and induce antigen-specific IgA response (129). Novel delivery strategies have been designed to overcome multiple mechanical barriers (e.g., keratinized epithelium, clearance system), proteolytic activity of saliva, and tolerogenic mechanism of oral mucosa. A lipid based delivery system (i.e. liposome, lipid nanoparticles, emulsion and immunostimulatory complexes (ISCOMs)) is a promising vehicle, formulating immunogens in water-immiscible lipid, protecting enzymatic digestion, and enhancing absorption into the mucosal surfaces (130, 131). For COVID-19, the lipid nanoparticle-mRNA format was successfully introduced in an intramuscular injection format. To induce oral mucosal immunity to influenza and COVID-19, the lipid-based delivery system has been tested in *in vivo* studies (132–137).

6.1.2 Polymer-based delivery systems

Can increase the contact time of delivered adjuvant/immunogen, provide stability, and adjunctive effects (138, 139). Polymers can be divided into natural (chitosan, gamma polyglutamic acid, hyaluronic acid, and pullulan) and synthetic (PLGA, Polyethyleneimine, poly-ε-caprolactone, PCL, and Polypropylene sulfide). For influenza, the polymer-based vaccines have already been developed and proven their efficacy in animal

models for the mucosal influenza vaccine development (140–144). Also, the polymeric-based nanoparticles system is under development for COVID-19 therapeutics and vaccines (145).

6.1.3 Sublingual vaccination

Is also a method of delivering vaccines directly under the tongue, absorbed by the mucous membranes (118, 146). Similar to sublingual vaccination, buccal vaccination is another method of delivering vaccines directly to the mucous membranes in the mouth (118, 146). However, instead of placing the vaccine under the tongue, the vaccine is placed on the inner cheek or buccal mucosa (118, 146). Both sublingual-, and buccal mucosa contains high level of antigen presenting cells, T-, and B-cells and attractive target as vaccine delivery (118, 146, 147). One potential advantage of buccal vaccination over sublingual vaccination is that it may offer more flexibility in terms of vaccine design and formulation. The buccal mucosa has a larger surface area than the sublingual mucosa, which may allow for the delivery of larger doses of the vaccine or the use of more complex formulations (148). There are ongoing research and development efforts to create sublingual vaccines for influenza and coronavirus (including SARS-CoV-2) (118, 149–151). Previous preclinical studies in animals have shown promising results for sublingual vaccines against influenza and coronaviruses, demonstrating the induction of robust immune responses and protection against infection. However, to date, no sublingual vaccine for influenza or coronavirus has been approved for use in humans. Development of the sublingual vaccines for influenza and coronaviruses remains an active area of research, there have been multiple clinical trials (Table 1).

6.1.4 Microbial display system

Microorganisms, such as virus, bacteria or yeast, can be used as a vaccine delivery system. The microbial display system can leverage their surface proteins as immunostimulants, enhancing immunogenicity of weakly immunogenic vaccine antigens. Also, the *in vitro* cultivation of vehicle microbes enables mass production in a cost-effective way. Bacteria, varial, and fungi have been widely investigated as delivery vehicles. The spore-based system is under clinical trial for the COVID-19 vaccine. (NCT05239923).

6.2 Mucosal vaccines

6.2.1 Live attenuated vaccines (LAV)

AV promote direct sensitization of the mucosal surface and have been the most efficacious way to elicit a protective immune response in the oral mucosa (152, 153). Also, live replicating viruses in epithelia stimulates innate and cell-mediated immunity, serving as a self-adjuvant and preserved from the mucosal clearance system. The LAV can be delivered via a variety of routes, including oral, nasal, and rectal (154). Oral delivery of live attenuated vaccines is particularly effective in inducing mucosal immunity (155–158). This attribute has distinct benefits from the parenterally delivered injectable vaccines, including, high efficacy at oral mucosa, ease of administration, and cost effectiveness (28, 159, 160). Also, the LAV

TABLE 1 Clinical Trials, Study Phase, and Types of Investigations Related to Oral Mucosa.

1	Phase	Study
Novel delivery system		
NCT04334980	Phase I/II	phase 1/2 trial evaluating the safety and immunogenicity of a sublingual influenza vaccine
NCT04625972	Phase I	phase 1 trial evaluating the safety and immunogenicity of a sublingual COVID-19 vaccine
NCT04563702	Phase I	phase 1 trial evaluating the safety and immunogenicity of a buccal COVID-19 vaccine
NCT04644782	Phase II	phase 2 trial evaluating the safety and efficacy of a sublingual COVID-19 vaccine
Live attenuated/vector vaccine candidates		
NCT01982331	Phase II	phase 2 trial evaluating the Reactogenicity, Safety and Immunogenicity of a Live Monovalent A/17/California/66/395 (H2N2) Influenza Vaccine
NCT02480101	Phase II	phase 2 trial evaluating the Reactogenicity, Safety and Immunogenicity of a Live Monovalent A/17/Anhui/2013/61 (H7N9) Influenza Vaccine
NCT01841918	Phase II	phase 2 trial evaluating the Safety and Immunogenicity of Live Attenuated Influenza H5 Candidate Vaccine Strain A/17/Turkey/Turkey/05/133 (H5N2) in Healthy Thai Volunteers
NCT02229357	non-randomized open label	non-randomized open label study evaluating the priming Effects by Pandemic Live Attenuated Influenza Vaccine (LAIV Candidate Vaccine Strain A/17/Turkey/Turkey/05/133 (H5N2)) on the Subsequent Response to Inactivated H5N1 Vaccine in Healthy Thai Volunteers: A Non-Randomized, Open Label Study
NCT03300050	Phase I	phase 1 trial evaluating the Reactogenicity, Safety, and Immunogenicity of a Live Attenuated Universal Influenza Vaccine (cH8/1N1 LAIV) Administered as a Single Priming Dose Followed Three Months Later by a Single Booster Dose of an Inactivated Universal Influenza Vaccine (cH5/1N1 IIV) (Adjuvanted With AS03A or Unadjuvanted) in 18 Through 39 Year-old Healthy Subjects, Contrasted With a Two Dose Schedule of an Inactivated Universal Influenza Vaccine (cH8/1N1 IIV + AS03A Followed Three Months Later by cH5/1N1 IIV + AS03A)
NCT04619628	Phase I	phase 1 trial evaluating the safety and efficacy of a COVI-VAC COVID-19 vaccine
NCT04871737	Phase I	phase 1 trial evaluating the safety and efficacy of a Newcastle disease virus (NDV) vector vaccines expressing the spike protein of SARS-CoV-2
NCT04816019	Phase I	phase 1 trial evaluating the safety and efficacy of a intranasal ChAdOx1 nCoV-19 (AZD1222) COVID-19 vaccine
NCT05007275	Phase I	phase 1 trial evaluating the safety and efficacy of a aerosole ChAdOx1 nCoV-19 (AZD1222) COVID-19 vaccine
NCT04839042	Phase I	phase 1 trial evaluating the safety and efficacy of SC-Ad6-1 COVID-19 vaccine
Second generation vaccine: Adjuvnat-vaccine complex		
NCT05385991	Phase I	phase 1 trial evaluating the Safety and Immunogenicity of the ACM-SARS-CoV-2-beta With ACM-CpG Vaccine Candidate (ACM-001), Administered Intramuscularly or Intranasally as a Booster Dose in Healthy Adults Aged 18 to 55 Years, Who Were Previously Vaccinated Against SARS-CoV-2.
Oral antivirals/antiseptics		
NCT04405570, NCT04405739	Phase II/III	phase 2/3 trial evaluating the ribonucleoside analogue inhibitor of influenza viruses, MK-4482/EIDD-280 for influenza and SARS-CoV-2 viruses
NCT04405570	Phase Iia	phase 2a trial evaluating the Safety, Tolerability and Efficacy of EIDD-2801 to Eliminate SARS-CoV-2 RNA Detection in Persons With COVID-19
NCT04497987	Phase III	phase 3 trial evaluating the Efficacy and Safety of LY3819253 Alone and in Combination With LY3832479 in Preventing SARS-CoV-2 Infection and COVID-19

is free from the issue of delivery since the vaccine virus attaches to the cellular receptor and is internalized into the mucosal epithelial surface. Activation of innate intracellular signaling pathways during internalization can add self-adjuvanting effects, mainly through the pathogen recognition receptor (PRRs) (161). For seasonal influenza, for example, FluMist has been used over decades as an intranasal spray vaccine (162). Also, there have been multiple live vaccine candidates, such as live attenuated vaccine format and or vector

vaccines (163). However, the FluMist could not induce salivary IgA response (164), showing that nasal activation is not always effective.

Multiple live attenuated influenza vaccines have been developed against pandemic influenza strains H5Nx and H7N9 viruses, which is under clinical trials (H2N2: NCT01982331; H7N9: NCT02480101; H5Nx: NCT01841918 and NCT02229357) (165–168). As a next-generation influenza vaccine, a chimeric hemagglutinine-based universal influenza vaccine is also under clinical trial

(NCT03300050) (169). Since this novel antigen does not naturally occur, it can avoid the risk of back-mutation. For COVID-19, the COVI-VAC is under phase I clinical trial (NCT04619628).

6.2.2 Vector vaccines

Live vaccines can be designed by using viral vectors, such as Newcastle disease virus (NV), Vestibulo stomatitis virus (VSV), and adenoviruses (170–172). Viral vectors are genetically engineered to express novel antigens, such as the spike protein of the SARS-CoV-2 virus (170–173). As the LAVs, vector viruses attach and replicate directly on the target mucosal tissue, solving the issues of delivery, dosage, and deposition (174). Also, the replication of vector virus triggers the innate and cell-mediated immune system, providing an adjuvant effect for the vaccine antigen (175). A Newcastle disease virus (NDV) vector vaccine expressing the spike protein of SARS-CoV-2 is currently under phase I clinical study (NCT04871737). A replication-competent chimeric VSV-SARS-CoV-2 vaccine candidate by replacing the VSV glycoprotein (G) gene with a coding sequence for the SARS-CoV-2 Spike glycoprotein (S) (VSVΔG-SARS-CoV-2) also has proven efficacy in a hamster model (176). The ChAdOx1 nCoV-19 (AZD1222), developed by AstraZeneca and first approved as an intramuscular vaccine, is now under phase I clinical trial to be applied as intranasal vaccine (NCT04816019) and aerosols (NCT05007275). The SC-Ad6-1 is another adenovirus vector vaccine from Tetherex Pharmaceuticals Corporation also under phase I clinical trial (NCT04839042).

Novel live vaccine candidates under clinical trials are highly expected to be used to complement limitations of current parenteral vaccines. Their efficacy on stopping transmission of viruses is still an emerging topic in the vaccine industry and more accumulated data will be needed.

6.3 Mucosal adjuvants

Adjuvants are substances an agent that increases specific immune responses to an antigen (177). Mucosal adjuvants can enhance the immunogenicity of vaccines at the mucosal surface, as evidenced in AS03, MF59, and CpG-ODN (178–180). To enhance the immunogenicity of the vaccines at the mucosal surface, novel adjuvant strategies have been suggested, especially for the influenza vaccine (181–186). Novel approaches apply the microbiome and its byproduct as a source of innate signaling to enhance the antiviral immune response in mucosal surfaces. For example, PMAPs from antibiotic-killed bacteria could enhance antiviral-immune response in intranasal mucosa (187, 188). In a hamster model, Mao et al. applied antibiotic-killed intranasal and oral microbes to induce vaccine-specific nasal IgA and serum IgG responses to influenza and SARS-CoV-2 viruses in a dose-dependent manner (189).

Novel vaccines incorporate adjuvant molecules into vaccine candidates to enhance immunogenicity and delivery system. As a second-generation vaccine, the ACM-SARS-CoV-2-beta ACM-CpG vaccine candidate (ACM-001) is under clinical trial (ClinicalTrials.gov identifier: NCT05385991). The vaccine consists of recombinant Beta spike protein co-administered with synthetic

CpG adjuvant. Both components are encapsulated within artificial cell membrane (ACM) polymersomes, synthetic nanovesicles efficiently internalized by antigen-presenting cells, including dendritic cells, enabling targeted delivery of cargo for enhanced immune responses. The ACM vaccine has proven enhanced serum IgG and neutralized response immunogenicity in C57BL/6 mice and Golden Syrian hamsters. In the oral cavity, the ACM-001 vaccination could not reduce the viral peak titer but shortened the viral shedding period (190).

6.4 Direct reduction of viral load by using oral antivirals/antiseptics

While the threat of current and future pandemic respiratory viruses is still ongoing, there has not been an effective strategy to induce oral mucosal immunity, especially to novel viruses. Focusing on reducing transmission of the viral spread through saliva droplets, direct administration of antivirals on the oral mucosa can be a temporary alternative strategy to reduce or block viral shedding at oral mucosa. For example, the ribonucleoside analog inhibitor of influenza viruses, MK-4482/EIDD-2801, reported the efficacy for both influenza and SARS-CoV-2 viral infection (currently in phase II/III clinical trials, NCT04405570 and NCT04405739, respectively). In a ferret model, the MK-4482/EIDD-2801 significantly reduced the replication level of the virus at the upper respiratory tract and completely prevented transmission to the contact controls (191). Molnupiravir is also antiviral under clinical trial (NCT04405570), which completely stopped virus shedding from the COVID-19 outpatients by day five after administration via oral route (192) and also active against other RNA viruses, such as influenza, SARS, and MERS. Paxlovid is also an oral antiviral test for COVID-19, reported to shorten the viral shedding period, but it cannot prevent viral infection (193). Antivirals can also be used as prophylaxis to prevent viral infection in the population with high exposure risk. In the case of the influenza virus, antiviral medications (amantadine and neuraminidase inhibitors) are allowed to be used as chemoprophylaxis in people at high risk of influenza complications and people with severe immune deficiencies or receiving immunosuppressive medications (194).

For SARS-CoV-2, repurposing of antivirals as prophylaxis is currently under clinical trial (study NCT04497987). In a stochastic model of early-phase viral infection, the combination of antivirals that block the viral entry and increase viral clearance was estimated to block the small load of viral inoculum (195). Still, the use of antivirals is highly restricted due to their potential side effects and genotoxicity (196). Also, in a primate model, incomplete use of Remdesivir induced a longer duration of viral shedding (197). The combination of Bromelain and Acetylcysteine (BromAc) is under clinical trial to be used as a nebulized form in Healthy volunteers (198). Bromelain, extracted from the pineapple plant (*Ananas comosus*), contains enzymes that hydrolyze glycosidic bonds in complex carbohydrates and has been shown to remove the spike and hemagglutinin proteins of Semliki Forest virus, Sindbis virus, mouse gastrointestinal coronavirus, hemagglutinating encephalomyelitis virus, and H1N1 influenza viruses (199–201). Acetylcysteine is known to destabilize virion structures by disulfide bridge disruption. The combination use of two molecules unfolds the

molecular structures of complex glycoproteins, thus allowing binding to occur because of the high affinity between RBD and ACE2 (198).

To directly reduce/remove viral particles from the oral cavity, antiseptics are also tested under clinical trials and considered to be used. Povidone Iodine has especially shown its efficacy for the oropharyngeal infection (202–204). Since Povidone Iodine has not shown side effects, While hydrogen peroxide can provide an antiseptic effect plus boost the innate immune response by stimulating toll-like receptor 3; the results have been conflicting on the reduction of viral load at the oral mucosal surface (205).

7 Future directions and synergistic effects from current vaccines and next-generation vaccines

As COVID-19 pandemic is not considered a “public health emergency”, the risk of the virus spreading and evolving into new variant strains persists. Partial immunity provided by parenteral immunization greatly contributed to reducing the disease severity, but cannot fully stop the spread of the virus, constantly producing novel variant viruses. This review summarized unique characteristics of oral mucosal immunity and discussed strategies currently under clinical trials. Induction of the “sterilizing immunity” is not yet achieved, but there have been remarkable advances in understanding of oral mucosal immune system and vaccine/adjuvants. As a temporary measure to reduce active viral replication at oral mucosa, direct application of antiseptics/antivirals are also considered and under clinical trials. Albeit the limitations, current parenteral vaccines are still the most effective strategy to control pandemic viruses at this present, and emerging mucosal strategies are needed. Even though vaccination provides only partial immunity to mask apparent symptoms and contributes to the silent evolution of the zoonotic respiratory RNA viruses, vaccine-induced immunity reduces the viral load and limits the evolution pool of the viruses, which in turn can hamper transmission. In country-scale analyses on the SARS-CoV-2 genome, diversity of the SARS-CoV-2 virus showed an inverse correlation with the mass vaccine rate ($n = 25$ countries, mean correlation coefficient = -0.72 , S.D. = 0.20) and viruses isolated from vaccinated COVID-19 patients presented significantly lower diversity in known B cell epitopes compared to those from unvaccinated COVID-19 patients (2.3-fold, 95% C.I. 1.4–3.7) (206). Also, pre-existing immunity built by parenteral immunization still provides a booster effect to the mucosal immunization. There have been multiple studies proving the combination of current parenteral vaccinations with mucosal vaccines, providing a synergistic effect on both systemic and mucosal responses (207–209).

Current open questions remaining in the mucosal immune response are 1) What is the sensitive, specific, and reproducible analyte to quantify protective mucosal immune response? 2) what is the complete mechanism involved in oral tolerance and hyperactivity? 3) the most efficient and safe delivery/adjuvant system for the oral mucosa, and 4) the oral microbiome which can contribute elicit protective immune responses. The COVID-19 pandemic has been a unique opportunity to explore diverse strategies against respiratory pathogens. Our current real challenge will be a continuous effort and investment in developing novel strategies to provoke mucosal immunity, especially at oral mucosal sites at a populational scale.

Author contributions

HJ conceptualized the topic of the article. HJ and MF contributed to build the outline of the paper. HJ and MF wrote the first draft of the paper and MM contributed manuscript revision. HJ and MM created figures, revised by MF. All authors contributed to the article and approved the submitted version.

Funding

This work was supported in part by The Conrad Prebys Foundation Grant, U.S. Public Health Service Grants NIH R21DE02962 from the National Institute of Dental and Cranial Research (given to MF).

Conflict of interest

The authors declare that the research was conducted in the absence of any commercial or financial relationships that could be construed as a potential conflict of interest.

Publisher's note

All claims expressed in this article are solely those of the authors and do not necessarily represent those of their affiliated organizations, or those of the publisher, the editors and the reviewers. Any product that may be evaluated in this article, or claim that may be made by its manufacturer, is not guaranteed or endorsed by the publisher.

References

- Kelly H. The classical definition of a pandemic is not elusive. *Bull World Health Organ* (2011) 89(7):540–1. doi: 10.2471/BLT.11.088815
- Morens DM, Fauci AS. Emerging pandemic diseases: how we got to COVID-19. *Cell* (2020) 182(5):1077–92. doi: 10.1016/j.cell.2020.08.021
- Madhav N, Oppenheim B, Gallivan M, Mulembakani P, Rubin E, Wolfe N. *Pandemics: Risks, Impacts, and Mitigation*. (Washington, DC: The International Bank for Reconstruction and Development/The World Bank) (2017).
- Morse SS, Mazet JAK, Woolhouse M, Parrish CR, Carroll D, Karesh WB, et al. Prediction and prevention of the next pandemic zoonosis. *Lancet* (2012) 380(9857):1956–65. doi: 10.1016/S0140-6736(12)61684-5
- Batty M. The COVID years: Predictable unpredictability. *Environ Plann B: Urban Analytics City Sci* (2022) 49(1):3–6. doi: 10.1177/23998083211072588
- Pike BL, Saylor KE, Fair JN, Lebreton M, Tamoufe U, Djoko CF, et al. The origin and prevention of pandemics. *Clin Infect Dis* (2010) 50(12):1636–40. doi: 10.1086/652860
- Choudhury PR, Saha T, Goel S, Shah JM, Ganjewala D. Cross-species virus transmission and its pandemic potential. *Bull Natl Salmon Resour Cent* (2022) 46(1):18. doi: 10.1186/s42269-022-00701-7
- Piret J, Boivin G. Pandemics throughout history. *Front Microbiol* (2020) 11:631736. doi: 10.3389/fmicb.2020.631736
- Kilbourne ED. Influenza pandemics of the 20th century. *Emerg Infect Dis* (2006) 12(1):9–14. doi: 10.3201/eid1201.051254
- Dobson A, Foufopoulos J. Emerging infectious pathogens of wildlife. *Philos Trans R Soc Lond B Biol Sci* (2001) 356(1411):1001–12. doi: 10.1098/rstb.2001.0900
- Parrish CR, Holmes EC, Morens DM, Park EC, Burke DS, Calisher CH, et al. Cross-species virus transmission and the emergence of new epidemic diseases. *Microbiol Mol Biol Rev* (2008) 72(3):457–70. doi: 10.1128/MMBR.00004-08
- Nova N. Cross-species transmission of coronaviruses in humans and domestic mammals, what are the ecological mechanisms driving transmission, spillover, and disease emergence? *Front Public Health* (2021) 9:717941. doi: 10.3389/fpubh.2021.717941
- Klempner MS, Shapiro DS. Crossing the species barrier—one small step to man, one giant leap to mankind. *N Engl J Med* (2004) 350(12):1171–2. doi: 10.1056/NEJMp048039
- Webby R, Hoffmann E, Webster R. Molecular constraints to interspecies transmission of viral pathogens. *Nat Med* (2004) 10(12 Suppl):S77–81. doi: 10.1038/nm1151
- Wolfe ND, Dunavan CP, Diamond J. Origins of major human infectious diseases. *Nature* (2007) 447(7142):279–83. doi: 10.1038/nature05775
- Machalaba CC, Loh EH, Daszak P, Karesh WB. Emerging diseases from animals. In: *State of the World 2015: Confronting Hidden Threats to Sustainability*. Washington, DC: Island Press/Center for Resource Economics (2015). p. 105–16.
- Abdelwhab EM, Mettenleiter TC. Zoonotic animal influenza virus and potential mixing vessel hosts. *Viruses* (2023) 15(4). doi: 10.3390/v15040980
- Ellwanger JH, Chies JAB. Zoonotic spillover: Understanding basic aspects for better prevention. *Genet Mol Biol* (2021) 44(1 Suppl 1):e20200355. doi: 10.1590/1678-4685-gmb-2020-0355
- Parrish CR, Murcia PR, Holmes EC. Influenza virus reservoirs and intermediate hosts: dogs, horses, and new possibilities for influenza virus exposure of humans. *J Virol* (2015) 89(6):2990–4. doi: 10.1128/JVI.03146-14
- Shinde V, Bridges CB, Uyeki TM, Shu B, Balish A, Xu X, et al. Triple-reassortant swine influenza A (H1N1) in humans in the United States, 2005–2009. *N Engl J Med* (2009) 360(25):2616–25. doi: 10.1056/NEJMoa0903812
- Garten RJ, Davis CT, Russell CA, Shu B, Lindstrom S, Balish A, et al. Antigenic and genetic characteristics of swine-origin 2009 A(H1N1) influenza viruses circulating in humans. *Science* (2009) 325(5937):197–201. doi: 10.1126/science.1176225
- Woolhouse ME J, Adair K, Brierley L. RNA viruses: A case study of the biology of emerging infectious diseases. *Microbiol Spectr* (2013) 1(1). doi: 10.1128/microbiolspec.OH-0001-2012
- Holmes EC. RNA virus genomics: a world of possibilities. *J Clin Invest* (2009) 119(9):2488–95. doi: 10.1172/JCI38050
- Dong J, Olano JP, McBride JW, Walker DH. Emerging pathogens: challenges and successes of molecular diagnostics. *J Mol Diagn* (2008) 10(3):185–97. doi: 10.2353/jmoldx.2008.070063
- Carrasco-Hernandez R, Jácóme R, López Vidal Y, Ponce de León S. Are RNA viruses candidate agents for the next global pandemic? A review. *ILAR J* (2017) 58(3):343–58. doi: 10.1093/ilar/ilx026
- Jones KE, Patel NG, Levy MA, Storeygard A, Balk D, Gittleman JL, et al. Global trends in emerging infectious diseases. *Nature* (2008) 451(7181):990–3. doi: 10.1038/nature06536
- Alvarez-Munoz S, Upegui-Porras N, Gomez AP, Ramirez-Nieto G. Key factors that enable the pandemic potential of RNA viruses and inter-species transmission: A systematic review. *Viruses* (2021) 13(4). doi: 10.3390/v13040537
- Pollard AJ, Bijker EM. A guide to vaccinology: from basic principles to new developments. *Nat Rev Immunol* (2021) 21(2):83–100. doi: 10.1038/s41577-020-00479-7
- Lavelle EC, Ward RW. Mucosal vaccines - fortifying the frontiers. *Nat Rev Immunol* (2022) 22(4):236–50. doi: 10.1038/s41577-021-00583-2
- Mouro V, Fischer A. Dealing with a mucosal viral pandemic: lessons from COVID-19 vaccines. *Mucosal Immunol* (2022) 15(4):584–94. doi: 10.1038/s41385-022-00517-8
- Houston S. SARS-CoV-2 mucosal vaccine. *Nat Immunol* (2023) 24(1):1. doi: 10.1038/s41590-022-01405-w
- Russell MW, Mestecky J. Mucosal immunity: The missing link in comprehending SARS-CoV-2 infection and transmission. *Front Immunol* (2022) 13:957107. doi: 10.3389/fimmu.2022.957107
- Wang T, Wei F, Liu J. Emerging role of mucosal vaccine in preventing infection with avian influenza A viruses. *Viruses* (2020) 12(8). doi: 10.3390/v12080862
- van de Sandt CE, Kreijtz JHCM, Rimmelzwaan GF. Evasion of influenza A viruses from innate and adaptive immune responses. *Viruses* (2012) 4(9):1438–76. doi: 10.3390/v4091438
- Doherty PC, Turner SJ, Webby RG, Thomas PG. Influenza and the challenge for immunology. *Nat Immunol* (2006) 7(5):449–55. doi: 10.1038/nri1343
- Read AF, Baigent SJ, Powers C, Kgosana LB, Blackwell L, Smith LP, et al. Imperfect vaccination can enhance the transmission of highly virulent pathogens. *PloS Biol* (2015) 13(7):e1002198. doi: 10.1371/journal.pbio.1002198
- Chakraborty C, Sharma AR, Bhattacharya M, Lee SS. A detailed overview of immune escape, antibody escape, partial vaccine escape of SARS-CoV-2 and their emerging variants with escape mutations. *Front Immunol* (2022) 13:801522. doi: 10.3389/fimmu.2022.801522
- Leung NHL. Transmissibility and transmission of respiratory viruses. *Nat Rev Microbiol* (2021) 19(8):528–45. doi: 10.1038/s41579-021-00535-6
- Dhand R, Li J. Coughs and sneezes: their role in transmission of respiratory viral infections, including SARS-CoV-2. *Am J Respir Crit Care Med* (2020) 202(5):651–9. doi: 10.1164/rccm.202004-1263PP
- Wang CC, Prather KA, Sznitman J, Jimenez JL, Lakdawala SS, Tufekci Z, et al. Airborne transmission of respiratory viruses. *Science* (2021) 373(6558). doi: 10.1126/science.abd9149
- Raymond JR. The great mask debate: A debate that shouldn't be a debate at all. *WMJ* (2020) 119(4):229–39.
- Carrouel F, Gadea E, Esparcieux A, Dimet J, Langlois ME, Perrier H, et al. Saliva quantification of SARS-CoV-2 in real-time PCR from asymptomatic or mild COVID-19 adults. *Front Microbiol* (2021) 12:786042. doi: 10.3389/fmicb.2021.786042
- Stadnytskyi V, Bax CE, Bax A, Anfinrud P. The airborne lifetime of small speech droplets and their potential importance in SARS-CoV-2 transmission. *Proc Natl Acad Sci USA* (2020) 117(22):11875–7. doi: 10.1073/pnas.2006874117
- Huang N, Pérez P, Kato T, Mikami Y, Okuda K, Gilmore RC, et al. SARS-CoV-2 infection of the oral cavity and saliva. *Nat Med* (2021) 27(5):892–903. doi: 10.1038/s41591-021-01296-8
- Nicholls JM, Bourne AJ, Chen H, Guan Y, Peiris JSM. Sialic acid receptor detection in the human respiratory tract: evidence for widespread distribution of potential binding sites for human and avian influenza viruses. *Respir Res* (2007) 8(1):73. doi: 10.1186/1465-9921-8-73
- Baldo V, Bertonecello C, Cocchio S, Fonzo M, Pillon P, Buja A, et al. The new pandemic influenza A(H1N1)pdm09 virus: is it really “new”? *J Prev Med Hyg* (2016) 57(1):E19–22.
- Alkie TN, Cox S, Embury-Hyatt C, Stevens B, Pople N, Pybus MJ, et al. Characterization of neurotropic HPAI H5N1 viruses with novel genome constellations and mammalian adaptive mutations in free-living mesocarnivores in Canada. *Emerg Microbes Infect* (2023) 12(1):2186608. doi: 10.1080/22221751.2023.2186608
- Galar A, Catalán P, Vesperinas L, Miguens I, Muñoz I, García-Espona A, et al. Use of saliva swab for detection of influenza virus in patients admitted to an emergency department. *Microbiol Spectr* (2021) 9(1):e0033621. doi: 10.1128/Spectrum.00336-21
- Tsunetsugu-Yokota Y, Ito S, Adachi Y, Onodera T, Kageyama T, Takahashi Y. Saliva as a useful tool for evaluating upper mucosal antibody response to influenza. *PloS One* (2022) 17(2):e0263419. doi: 10.1371/journal.pone.0263419
- Fukuta M, Mao ZQ, Morita K, Moi ML. Stability and infectivity of SARS-CoV-2 and viral RNA in water, commercial beverages, and bodily fluids. *Front Microbiol* (2021) 12:667956. doi: 10.3389/fmicb.2021.667956
- Ijaz MK, Brunner AH, Sattar SA, Nair RC, Johnson-Lussenburg CM. Survival characteristics of airborne human coronavirus 229E. *J Gen Virol* (1985) 66(Pt 12):2743–8. doi: 10.1099/0022-1317-66-12-2743
- van Doremalen N, Bushmaker T, Munster VJ. Stability of Middle East respiratory syndrome coronavirus (MERS-CoV) under different environmental conditions. *Euro Surveill* (2013) 18(38). doi: 10.2807/1560-7917.es2013.18.38.20590
- Pyankov OV, Bodnev SA, Pyankova OG, Agranovski IE. Survival of aerosolized coronavirus in the ambient air. *J Aerosol Sci* (2018) 115:158–63. doi: 10.1016/j.jaerosci.2017.09.009

54. Fears AC, Klimstra WB, Duprex P, Hartman A, Weaver SC, Plante KC, et al. Comparative dynamic aerosol efficiencies of three emergent coronaviruses and the unusual persistence of SARS-CoV-2 in aerosol suspensions. *medRxiv* (2020) 1:4–5. doi: 10.1101/2020.04.13.20063784
55. van Doremalen N, Bushmaker T, Morris D, Holbrook M, Gamble A, Williamson B, et al. Aerosol and surface stability of SARS-CoV-2 as compared with SARS-CoV-1. *N Engl J Med* (2020) [Preprint]. doi: 10.1056/NEJMc2004973
56. Alonso C, Goede DP, Morrison RB, Davies PR, Rovira A, Marthaler DG, et al. Evidence of infectivity of airborne porcine epidemic diarrhea virus and detection of airborne viral RNA at long distances from infected herds. *Vet Res* (2014) 45(1):73. doi: 10.1186/s13567-014-0073-z
57. Kormuth KA, Lin K, Prussin AJ 2nd, Vejerano EP, Tiwari AJ, Cox SS, et al. Influenza virus infectivity is retained in aerosols and droplets independent of relative humidity. *J Infect Dis* (2018) 218(5):739–47. doi: 10.1093/infdis/jiy221
58. Mubareka S, Lowen AC, Steel J, Coates AL, García-Sastre A, Palese P. Transmission of influenza virus via aerosols and fomites in the Guinea pig model. *J Infect Dis* (2009) 199(6):858–65. doi: 10.1086/597073
59. Trovato M, Sartorius R, D'Apice L, Manco R, De Berardinis P. Viral emerging diseases: challenges in developing vaccination strategies. *Front Immunol* (2020) 11, 2130. doi: 10.3389/fimmu.2020.02130
60. Huang YZ, Kuan CC. Vaccination to reduce severe COVID-19 and mortality in COVID-19 patients: a systematic review and meta-analysis. *Eur Rev Med Pharmacol Sci* (2022) 26(5):1770–6. doi: 10.26355/eurrev_202203_28248
61. Olson SM, Newhams MM, Halasa NB, Feldstein LR, Novak T, Weiss SL, et al. Vaccine effectiveness against life-threatening influenza illness in US children. *Clin Infect Dis* (2022) 75(2):230–8. doi: 10.1093/cid/ciab931
62. Correa VA, Portillo AI, De Gaspari E. Vaccines, adjuvants and key factors for mucosal immune response. *Immunol* (2022) 167(2):124–38. doi: 10.1111/imm.13526
63. Hart TK, Cook RM, Zia-Amirhosseini P, Minthorn E, Sellers TS, Maleeff BE, et al. Preclinical efficacy and safety of mepolizumab (SB-240563), a humanized monoclonal antibody to IL-5, in cynomolgus monkeys. *J Allergy Clin Immunol* (2001) 108(2):250–7. doi: 10.1067/mai.2001.116576
64. Peebles RS Jr, Liu MC, Lichtenstein LM, Hamilton RG. IgA, IgG and IgM quantification in bronchoalveolar lavage fluids from allergic rhinitis, allergic asthmatics, and normal subjects by monoclonal antibody-based immunoenzymetric assays. *J Immunol Methods* (1995) 179(1):77–86. doi: 10.1016/0022-1759(94)00275-2
65. Wu H, Pfarr DS, Johnson S, Brewah YA, Woods RM, Patel NK, et al. Development of motavizumab, an ultra-potent antibody for the prevention of respiratory syncytial virus infection in the upper and lower respiratory tract. *J Mol Biol* (2007) 368(3):652–65. doi: 10.1016/j.jmb.2007.02.024
66. Acharya CB, Schrom J, Mitchell AM, Coil DA, Marquez C, Rojas S, et al. Viral load among vaccinated and unvaccinated, asymptomatic and symptomatic persons infected with the SARS-CoV-2 delta variant. *Open Forum Infect Dis* (2022) 9(5):ofac135. doi: 10.1093/ofid/ofac135
67. Gandhi M, Yokoe DS, Havlir DV. Asymptomatic transmission, the Achilles' Heel of current strategies to control Covid-19. *N Engl J Med* (2020) 382(22):2158–60. doi: 10.1056/NEJMe2009758
68. Focosi D, Maggi F, Casadevall A. Mucosal vaccines, sterilizing immunity, and the future of SARS-CoV-2 virulence. *Viruses* (2022) 14(2). doi: 10.3390/v14020187
69. Bouvier NM. The future of influenza vaccines: A historical and clinical perspective. *Vaccines (Basel)* (2018) 6(3). doi: 10.3390/vaccines6030058
70. Wahl I, Wardemann H. Sterilizing immunity: understanding COVID-19. *Immunity* (2022) 55(12):2231–5. doi: 10.1016/j.immuni.2022.10.017
71. Kurashima Y, Kiyono H. Mucosal ecological network of epithelium and immune cells for gut homeostasis and tissue healing. *Annu Rev Immunol* (2017) 35:119–47. doi: 10.1146/annurev-immunol-051116-052424
72. Kurashima Y, Yamamoto D, Nelson S, Uematsu S, Ernst PB, Nakayama T, et al. Mucosal mesenchymal cells: secondary barrier and peripheral educator for the gut immune system. *Front Immunol* (2017) 8:1787. doi: 10.3389/fimmu.2017.01787
73. Boyaka PN, Fujihashi K. 20 - host defenses at mucosal surfaces. In: Rich RR, Fleisher TA, Shearer WT, Schroeder HW, Frew AJ, Weyand CM, editors. *Clinical Immunology, Fifth Edition*. London: Elsevier (2019). p. 285–98.e1.
74. Kiyono H, Yuki Y, Nakahashi-Ouchida R, Fujihashi K. Mucosal vaccines: wisdom from now and then. *Int Immunol* (2021) 33(12):767–74. doi: 10.1093/intimm/dxab056
75. Suárez LJ, Arboleda S, Angelov N, Arce RM. Oral versus gastrointestinal mucosal immune niches in homeostasis and allostasis. *Front Immunol* (2021) 12:705206. doi: 10.3389/fimmu.2021.705206
76. Janeway CA Jr, Travers P, Walport M, Shlomchik MJ. The mucosal immune system. *Garland Sci* (2001).
77. Moutsopoulos NM, Konkel JE. Tissue-specific immunity at the oral mucosal barrier. *Trends Immunol* (2018) 39(4):276–87. doi: 10.1016/j.it.2017.08.005
78. Fábian TK, Hermann P, Beck A, Fejérdy P, Fábian G. Salivary defense proteins: their network and role in innate and acquired oral immunity. *Int J Mol Sci* (2012) 13(4):4295–320. doi: 10.3390/ijms13044295
79. Wu RQ, Zhang DF, Tu E, Chen QM, Chen W. The mucosal immune system in the oral cavity-an orchestra of T cell diversity. *Int J Oral Sci* (2014) 6(3):125–32. doi: 10.1038/ijfos.2014.48
80. Tsukamoto Y, Usui M, Yamamoto G, Takagi Y, Tachikawa T, Yamamoto M, et al. Role of the junctional epithelium in periodontal innate defense and homeostasis. *J Periodontol Res* (2012) 47(6):750–7. doi: 10.1111/j.1600-0765.2012.01490.x
81. Brizuela M, Winters R. *Histology, Oral Mucosa*. (Treasure Island, FL: StatPearls Publishing) (2022).
82. Meghil MM, Cutler CW. Oral microbes and mucosal dendritic cells, “Spark and flame” of local and distant inflammatory diseases. *Int J Mol Sci* (2020) 21(5). doi: 10.3390/ijms21051643
83. Pelaez-Prestel HF, Sanchez-Trincado JL, Lafuente EM, Reche PA. Immune tolerance in the oral mucosa. *Int J Mol Sci* (2021) 22(22). doi: 10.3390/ijms222212149
84. Audiger C, Rahman MJ, Yun TJ, Tarbell KV, Lesage S. The importance of dendritic cells in maintaining immune tolerance. *J Immunol* (2017) 198(6):2223–31. doi: 10.4049/jimmunol.1601629
85. Mascanfroni ID, Yeste A, Vieira SM, Burns EJ, Patel B, Sloma I, et al. IL-27 acts on DCs to suppress the T cell response and autoimmunity by inducing expression of the immunoregulatory molecule CD39. *Nat Immunol* (2013) 14(10):1054–63. doi: 10.1038/ni.2695
86. Zhou F, Broere F, Ganguly D. *Molecular Mechanisms of Dendritic Cell-Mediated Immune Tolerance and Autoimmunity*. (Lausanne, Switzerland: Frontiers Media SA) (2022). 228 p.
87. Battaglia M, Gianfrani C, Gregori S, Roncarolo MG. IL-10-producing T regulatory type 1 cells and oral tolerance. *Ann N Y Acad Sci* (2004) 1029:142–53. doi: 10.1196/annals.1309.031
88. Quintana FJ, Sherr DH. Aryl hydrocarbon receptor control of adaptive immunity. *Pharmacol Rev* (2013) 65(4):1148–61. doi: 10.1124/pr.113.007823
89. Brandtzaeg P, Korsrud FR. Significance of different J chain profiles in human tissues: generation of IgA and IgM with binding site for secretory component is related to the J chain expressing capacity of the total local immunocyte population, including IgG and IgD producing cells, and depends on the clinical state of the tissue. *Clin Exp Immunol* (1984) 58(3):709–18.
90. Kinane DF, Lappin DF, Koulouri O, Buckley A. Humoral immune responses in periodontal disease may have mucosal and systemic immune features. *Clin Exp Immunol* (1999) 115(3):534–41. doi: 10.1046/j.1365-2249.1999.00819.x
91. Boyaka PN. Inducing mucosal IgA: A challenge for vaccine adjuvants and delivery systems. *J Immunol* (2017) 199(1):9–16. doi: 10.4049/jimmunol.1601775
92. Cerutti A. The regulation of IgA class switching. *Nat Rev Immunol* (2008) 8(6):421–34. doi: 10.1038/nri2322
93. Weller S, Braun MC, Tan BK, Rosenwald A, Cordier C, Conley ME, et al. Human blood IgM “memory” B cells are circulating splenic marginal zone B cells harboring a prediversified immunoglobulin repertoire. *Blood* (2004) 104(12):3647–54. doi: 10.1182/blood-2004-01-0346
94. Weller S, Faili A, Garcia C, Braun MC, Le Deist FF, de Saint Basile GG, et al. CD40-CD40L independent Ig gene hypermutation suggests a second B cell diversification pathway in humans. *Proc Natl Acad Sci USA* (2001) 98(3):1166–70. doi: 10.1073/pnas.98.3.1166
95. Jeurissen A, Ceuppens JL, Bossuyt X. T lymphocyte dependence of the antibody response to “T lymphocyte independent type 2” antigens. *Immunol* (2004) 111(1):1–7. doi: 10.1111/j.1365-2567.2003.01775.x
96. Fagarasan S, Kawamoto S, Kanagawa O, Suzuki K. Adaptive immune regulation in the gut: T cell-dependent and T cell-independent IgA synthesis. *Annu Rev Immunol* (2010) 28:243–73. doi: 10.1146/annurev-immunol-030409-101314
97. Suzuki K, Ha SA, Tsuji M, Fagarasan S. Intestinal IgA synthesis: a primitive form of adaptive immunity that regulates microbial communities in the gut. *Semin Immunol* (2007) 19(2):127–35. doi: 10.1016/j.smim.2006.10.001
98. Li Y, Jin L, Chen T. The effects of secretory IgA in the mucosal immune system. *BioMed Res Int* (2020) 2020:2032057. doi: 10.1155/2020/2032057
99. Zheng M, Mao K, Fang D, Li D, Lyu J, Peng D, et al. B cell residency but not T cell-independent IgA switching in the gut requires innate lymphoid cells. *Proc Natl Acad Sci USA* (2021) 118(27). doi: 10.1073/pnas.2106754118
100. Zenobia C, Herpold KL, Freire M. Is the oral microbiome a source to enhance mucosal immunity against infectious diseases? *NPJ Vaccines* (2021) 6(1):80. doi: 10.1038/s41541-021-00341-4
101. Stephen-Victor E, Chatila TA. Regulation of oral immune tolerance by the microbiome in food allergy. *Curr Opin Immunol* (2019) 60:141–7. doi: 10.1016/j.coi.2019.06.001
102. Tordesillas L, Berin MC. Mechanisms of oral tolerance. *Clin Rev Allergy Immunol* (2018) 55(2):107–17. doi: 10.1007/s12016-018-8680-5
103. Soffritti I, D'Accolti M, Fabbri C, Passaro A, Manfredini R, Zuliani G, et al. Oral microbiome dysbiosis is associated with symptoms severity and local immune/inflammatory response in COVID-19 patients: A cross-sectional study. *Front Microbiol* (2021) 12:687513. doi: 10.3389/fmicb.2021.687513
104. Caselli E, Fabbri C, D'Accolti M, Soffritti I, Bassi C, Mazzacane S, et al. Defining the oral microbiome by whole-genome sequencing and resistome analysis: the complexity of the healthy picture. *BMC Microbiol* (2020) 20(1):120. doi: 10.1186/s12866-020-01801-y
105. König J, Wells J, Cani PD, García-Ródenas CL, MacDonald T, Mercenier A, et al. Human intestinal barrier function in health and disease. *Clin Transl Gastroenterol* (2016) 7(10):e196. doi: 10.1038/ctg.2016.54

106. Gupta A, Bhanushali S, Sanap A, Shekatkar M, Kharat A, Raut C, et al. Oral dysbiosis and its linkage with SARS-CoV-2 infection. *Microbiol Res* (2022) 261:127055. doi: 10.1016/j.micres.2022.127055
107. Tada A, Senpuku H. The impact of oral health on respiratory viral infection. *Dent J* (2021) 9(4). doi: 10.3390/dj9040043
108. Bassis CM, Erb-Downward JR, Dickson RP, Freeman CM, Schmidt TM, Young VB, et al. Analysis of the upper respiratory tract microbiotas as the source of the lung and gastric microbiotas in healthy individuals. *MBio* (2015) 6(2):e00037. doi: 10.1128/mBio.00037-15
109. Yamamoto S, Saito M, Tamura A, Prawisuda D, Mizutani T, Yotsuyanagi H. The human microbiome and COVID-19: A systematic review. *PloS One* (2021) 16(6): e0253293. doi: 10.1371/journal.pone.0253293
110. Wu Y, Cheng X, Jiang G, Tang H, Ming S, Tang L, et al. Author Correction: Altered oral and gut microbiota and its association with SARS-CoV-2 viral load in COVID-19 patients during hospitalization. *NPJ Biofilms Microbiomes* (2021) 7(1):90. doi: 10.1038/s41522-021-00262-z
111. Lu M, Xuan S, Wang Z. Oral microbiota: A new view of body health. *Food Sci Hum Wellness* (2019) 8(1):8–15. doi: 10.1016/j.fshw.2018.12.001
112. Segata N, Haake SK, Mannon P, Lemon KP, Waldron L, Gevers D, et al. Composition of the adult digestive tract bacterial microbiome based on seven mouth surfaces, tonsils, throat and stool samples. *Genome Biol* (2012) 13(6):R42. doi: 10.1186/gb-2012-13-6-r42
113. Mark Welch JL, Rossetti BJ, Rieken CW, Dewhirst FE, Borisy GG. Biogeography of a human oral microbiome at the micron scale. *Proc Natl Acad Sci USA* (2016) 113(6):E791–800. doi: 10.1073/pnas.1522149113
114. Deo PN, Deshmukh R. Oral microbiome: Unveiling the fundamentals. *J Oral Maxillofac Pathol* (2019) 23(1):122–8. doi: 10.4103/jomfp.JOMFP_304_18
115. Silva LM, Doyle AD, Greenwell-Wild T, Dutzan N, Tran CL, Abusleme L, et al. Fibrin is a critical regulator of neutrophil effector function at the oral mucosal barrier. *Science* (2021) 374(6575):eab15450. doi: 10.1126/science.abl5450
116. Şenel S. An overview of physical, microbiological and immune barriers of oral mucosa. *Int J Mol Sci* (2021) 22(15). doi: 10.3390/ijms22157821
117. Mann ER, Li X. Intestinal antigen-presenting cells in mucosal immune homeostasis: crosstalk between dendritic cells, macrophages and B-cells. *World J Gastroenterol* (2014) 20(29):9653–64. doi: 10.3748/wjg.v20.i29.9653
118. Jahan N, Archie SR, Shoyab AA, Kabir N, Cheung K. Recent approaches for solid dose vaccine delivery. *Sci Pharm* (2019) 87(4):27. doi: 10.3390/scipharm87040027
119. Commins SP. Mechanisms of oral tolerance. *Pediatr Clin North Am* (2015) 62(6):1523–9. doi: 10.1016/j.pcl.2015.07.013
120. Van der Weken H, Cox E, Devriendt B. Advances in oral subunit vaccine design. *Vaccines (Basel)* (2020) 9(1). doi: 10.3390/vaccines9010001
121. Kleinstein SE, Nelson KE, Freire M. Inflammatory networks linking oral microbiome with systemic health and disease. *J Dent Res* (2020) 99(10):1131–9. doi: 10.1177/0022034520926126
122. Belkaid Y, Hand TW. Role of the microbiota in immunity and inflammation. *Cell* (2014) 157(1):121–41. doi: 10.1016/j.cell.2014.03.011
123. Hall JA, Bouladoux N, Sun CM, Wohlfert EA, Blank RB, Zhu Q, et al. Commensal DNA limits regulatory T cell conversion and is a natural adjuvant of intestinal immune responses. *Immunity* (2008) 29(4):637–49. doi: 10.1016/j.immuni.2008.08.009
124. Eloe-Fadros EA, McArthur MA, Seekatz AM, Drabek EF, Rasko DA, Szein MB, et al. Impact of oral typhoid vaccination on the human gut microbiota and correlations with s. Typhi-specific immunological responses. *PloS One* (2013) 8(4): e62026. doi: 10.1371/journal.pone.0062026
125. Nadeem S, Maurya SK, Das DK, Khan N, Agrewala JN. Gut dysbiosis thwarts the efficacy of vaccine against mycobacterium tuberculosis. *Front Immunol* (2020) 11:726. doi: 10.3389/fimmu.2020.00726
126. Campillo-Gimenez L, Rios-Covian D, Rivera-Nieves J, Kiyono H, Chu H, Ernst PB. Microbial-driven immunological memory and its potential role in microbiome editing for the prevention of colorectal cancer. *Front Cell Infect Microbiol* (2021) 11:752304. doi: 10.3389/fcimb.2021.752304
127. Lynn DJ, Pulendran B. The potential of the microbiota to influence vaccine responses. *J Leukoc Biol* (2018) 103(2):225–31. doi: 10.1189/jlb.5MR0617-216R
128. Singh K, Rao A. Probiotics: A potential immunomodulator in COVID-19 infection management. *Nutr Res* (2021) 87:1–12. doi: 10.1016/j.nutres.2020.12.014
129. Huang M, Zhang M, Zhu H, Du X, Wang J. Mucosal vaccine delivery: A focus on the breakthrough of specific barriers. *Acta Pharm Sin B* (2022) 12(9):3456–74. doi: 10.1016/j.apsb.2022.07.002
130. Calderón-Colón X, Zhang Y, Tiburzi O, Wang J, Hou S, Raimondi G, et al. Design and characterization of lipid nanocarriers for oral delivery of immunotherapeutic peptides. *J BioMed Mater Res A* (2022) 111(7). doi: 10.1002/jbm.a.37477
131. Li M, Kaminskis LM, Marasini N. Recent advances in nano/microparticle-based oral vaccines. *J Pharm Investig* (2021) 51(4):425–38. doi: 10.1007/s40005-021-00537-9
132. Sia ZR, He X, Zhang A, Ang JC, Shao S, Seffouh A, et al. A liposome-displayed hemagglutinin vaccine platform protects mice and ferrets from heterologous influenza virus challenge. *Proc Natl Acad Sci USA* (2021) 118(22). doi: 10.1073/pnas.2025759118
133. Dhakal S, Cheng X, Salcido J, Renu S, Bondra K, Lakshmanappa YS, et al. Liposomal nanoparticle-based conserved peptide influenza vaccine and monosodium urate crystal adjuvant elicit protective immune response in pigs. *Int J Nanomed* (2018) 13:6699–715. doi: 10.2147/IJN.S178809
134. Sato-Kaneko F, Yao S, Lao FS, Shpigelman J, Messer K, Pu M, et al. A novel synthetic dual agonistic liposomal TLR4/7 adjuvant promotes broad immune responses in an influenza vaccine with minimal reactogenicity. *Front Immunol* (2020) 11:1207. doi: 10.3389/fimmu.2020.01207
135. Gregoriadis G. Liposomes and mRNA: Two technologies together create a COVID-19 vaccine. *Med Drug Discov* (2021) 12:100104. doi: 10.1016/j.medidd.2021.100104
136. Schoenmaker L, Witzigmann D, Kulkarni JA, Verbeke R, Kersten G, Jiskoot W, et al. mRNA-lipid nanoparticle COVID-19 vaccines: Structure and stability. *Int J Pharm* (2021) 601:120586. doi: 10.1016/j.ijpharm.2021.120586
137. Liu T, Tian Y, Zheng A, Cui C. Design strategies for and stability of mRNA-lipid nanoparticle COVID-19 vaccines. *Polymers* (2022) 14(19). doi: 10.3390/polym14191915
138. Chen G, Zhao B, Ruiz EF, Zhang F. Advances in the polymeric delivery of nucleic acid vaccines. *Theranostics* (2022) 12(9):4081–109. doi: 10.7150/thno.70853
139. Vasquez-Martinez N, Guillen D, Moreno-Mendieta SA, Sanchez S, Rodriguez-Sanoja R. The role of mucoadhesion and mucopenetration in the immune response induced by polymer-based mucosal adjuvants. *Polymers* (2023) 15(7). doi: 10.3390/polym15071615
140. Dhakal S, Renu S, Ghimire S, Shaan Lakshmanappa Y, Hogshead BT, Feliciano-Ruiz N, et al. Mucosal immunity and protective efficacy of intranasal inactivated influenza vaccine is improved by chitosan nanoparticle delivery in pigs. *Front Immunol* (2018) 9:934. doi: 10.3389/fimmu.2018.00934
141. Chowdhury MYE, Kim TH, Uddin MB, Kim JH, Hewawaduge CY, Ferdowsi Z, et al. Mucosal vaccination of conserved sM2, HA2 and cholera toxin subunit A1 (CTA1) fusion protein with poly gamma-glutamate/chitosan nanoparticles (PC NPs) induces protection against divergent influenza subtypes. *Vet Microbiol* (2017) 201:240–51. doi: 10.1016/j.vetmic.2017.01.020
142. Okamoto S, Matsuura M, Akagi T, Akashi M, Tanimoto T, Ishikawa T, et al. Poly(gamma-glutamic acid) nano-particles combined with mucosal influenza virus hemagglutinin vaccine protects against influenza virus infection in mice. *Vaccine* (2009) 27(42):5896–905. doi: 10.1016/j.vaccine.2009.07.037
143. Singh M, Briones M, O'Hagan DT. A novel bioadhesive intranasal delivery system for inactivated influenza vaccines. *J Control Release* (2001) 70(3):267–76. doi: 10.1016/S0168-3659(00)00330-8
144. Song L, Xiong D, Song H, Wu L, Zhang M, Kang X, et al. Mucosal and systemic immune responses to influenza H7N9 antigen HA1-2 co-delivered intranasally with flagellin or polyethyleneimine in mice and chickens. *Front Immunol* (2017) 8:326. doi: 10.3389/fimmu.2017.00326
145. Charelli LE, de Mattos GC, de Jesus Sousa-Batista A, Pinto JC, Balbino TA. Polymeric nanoparticles as therapeutic agents against coronavirus disease. *J Nanopart Res* (2022) 24(1):12. doi: 10.1007/s11051-022-05396-5
146. Kraan H, Vrieling H, Czerkinsky C, Jiskoot W, Kersten G, Amorij JP. Buccal and sublingual vaccine delivery. *J Control Release* (2014) 190, 580–92. doi: 10.1016/j.jconrel.2014.05.060
147. Kweon MN. Sublingual mucosa: A new vaccination route for systemic and mucosal immunity. *Cytokine* (2011) 54(1):1–5. doi: 10.1016/j.cyto.2010.12.014
148. Paris AL, Colomb E, Verrier B, Anjuere F, Monge C. Sublingual vaccination and delivery systems. *J Control Release* (2021) 332:553–62. doi: 10.1016/j.jconrel.2021.03.017
149. Shim BS, Choi YK, Yun CH, Lee EG, Jeon YS, Park SM, et al. Sublingual immunization with M2-based vaccine induces broad protective immunity against influenza. *PloS One* (2011) 6(11):e27953. doi: 10.1371/journal.pone.0027953
150. Kim H, Kim JK, Song H, Choi J, Shim B, Kang B, et al. Preliminary study about sublingual administration of bacteria-expressed pandemic H1N1 influenza vaccine in miniature pigs. *J Microbiol* (2014) 52(9):794–800. doi: 10.1007/s12275-014-4289-4
151. Kim Y, Park IH, Shin J, Choi J, Jeon C, Jeon S, et al. Sublingual dissolving microneedle (SLDMN)-based vaccine for inducing mucosal immunity against SARS-CoV-2. *Adv Healthc Mater* (2023):e2300889. doi: 10.1002/adhm.202300889
152. Nizard M, Diniz MO, Roussel H, Tran T, Ferreira LC, Badoual C, et al. Mucosal vaccines: novel strategies and applications for the control of pathogens and tumors at mucosal sites. *Hum Vaccin Immunother* (2014) 10(8):2175–87. doi: 10.4161/hv.29269
153. Shakra AK, Chowdhury MYE, Tao W, Gill HS. Mucosal vaccine delivery: Current state and a pediatric perspective. *J Control Release* (2016) 240:394–413. doi: 10.1016/j.jconrel.2016.02.014
154. Anggraeni R, Ana ID, Wihadmyatami H. Development of mucosal vaccine delivery: an overview on the mucosal vaccines and their adjuvants. *Clin Exp Vaccine Res* (2022) 11(3):235–48. doi: 10.7774/cevr.2022.11.3.235
155. Johnson S, Martinez CI, Tedjakusuma SN, Peinovich N, Dora EG, Birch SM, et al. Oral vaccination protects against severe acute respiratory syndrome coronavirus 2 in a Syrian hamster challenge model. *J Infect Dis* (2022) 225(1):34–41. doi: 10.1093/infdis/jiab561
156. Basak S, Kang HJ, Lee SH, Chu KB, Moon EK, Quan FS. Influenza vaccine efficacy induced by orally administered recombinant baculoviruses. *PloS One* (2020) 15(5):e0233520. doi: 10.1371/journal.pone.0233520

157. Mettelman RC, Allen EK, Thomas PG. Mucosal immune responses to infection and vaccination in the respiratory tract. *Immunity* (2022) 55(5):749–80. doi: 10.1016/j.immuni.2022.04.013
158. Hellfritzsch M, Scherließ R. Mucosal vaccination via the respiratory tract. *Pharmaceutics* (2019) 11(8). doi: 10.3390/pharmaceutics11080375
159. Minor PD. Live attenuated vaccines: Historical successes and current challenges. *Virol* (2015) 479–480:379–92. doi: 10.1016/j.virol.2015.03.032
160. Belshe RB, Edwards KM, Vesikari T, Black SV, Walker RE, Hultquist M, et al. Live attenuated versus inactivated influenza vaccine in infants and young children. *N Engl J Med* (2007) 356(7):685–96. doi: 10.1056/NEJMoa065368
161. Pulendran B, Ahmed R. Immunological mechanisms of vaccination. *Nat Immunol* (2011) 12(6):509–17. doi: 10.1038/ni.2039
162. Shannon I, White CL, Nayak JL. Understanding immunity in children vaccinated with live attenuated influenza vaccine. *J Pediatr Infect Dis Soc* (2020) 9 (Supplement_1):S10–4. doi: 10.1093/jpids/piz083
163. Alu A, Chen L, Lei H, Wei Y, Tian X, Wei X. Intranasal COVID-19 vaccines: From bench to bed. *EBioMed* (2022) 76:103841. doi: 10.1016/j.ebiom.2022.103841
164. Ponzio TA, Sanders JW. The salivary gland as a target for enhancing immunization response. *Trop Dis Travel Med Vaccines* (2017) 3:4. doi: 10.1186/s40794-017-0047-z
165. Ortiz JR, Spearman PW, Goepfert PA, Cross K, Buddy Creech C, Chen WH, et al. Safety and immunogenicity of monovalent H7N9 influenza vaccine with AS03 adjuvant given sequentially or simultaneously with a seasonal influenza vaccine: A randomized clinical trial. *Vaccine* (2022) 40(23):3253–62. doi: 10.1016/j.vaccine.2022.03.055
166. Pitisuttithum P, Boonnak K, Chammanchanunt S, Puthavathana P, Luvira V, Lersamran H, et al. Safety and immunogenicity of a live attenuated influenza H5 candidate vaccine strain A/17/Turkey/Turkey/05/133 H5N2 and its priming effects for potential pre-pandemic use: a randomised, double-blind, placebo-controlled trial. *Lancet Infect Dis* (2017) 17(8):833–42. doi: 10.1016/S1473-3099(17)30240-2
167. Isakova-Sivak I, Stukova M, Erofeeva M, Naykhin A, Donina S, Petukhova G, et al. H2N2 live attenuated influenza vaccine is safe and immunogenic for healthy adult volunteers. *Hum Vaccin Immunother* (2015) 11(4):970–82. doi: 10.1080/21645515.2015.1010859
168. Liebowitz D, Gottlieb K, Kolhatkar NS, Garg SJ, Asher JM, Nazareno J, et al. Efficacy, immunogenicity, and safety of an oral influenza vaccine: a placebo-controlled and active-controlled phase 2 human challenge study. *Lancet Infect Dis* (2020) 20(4):435–44. doi: 10.1016/S1473-3099(19)30584-5
169. Nachbagauer R, Feser J, Naficy A, Bernstein DI, Guptill J, Walter EB, et al. A chimeric hemagglutinin-based universal influenza virus vaccine approach induces broad and long-lasting immunity in a randomized, placebo-controlled phase I trial. *Nat Med* (2021) 27(1):106–14. doi: 10.1038/s41591-020-1118-7
170. García-Sastre A. Mucosal delivery of RNA vaccines by Newcastle disease virus vectors. *Curr Res Immunol* (2022) 3:234–8. doi: 10.1016/j.crimmu.2022.10.001
171. Fathi A, Dahlke C, Addo MM. Recombinant vesicular stomatitis virus vector vaccines for WHO blueprint priority pathogens. *Hum Vaccin Immunother* (2019) 15(10):2269–85. doi: 10.1080/21645515.2019.1649532
172. Sakurai F, Tachibana M, Mizuguchi H. Adenovirus vector-based vaccine for infectious diseases. *Drug Metab Pharmacokin* (2022) 42:100432. doi: 10.1016/j.dmpk.2021.100432
173. Sun W, Leist SR, McCroskery S, Liu Y, Slamanig S, Oliva J, et al. Newcastle disease virus (NDV) expressing the spike protein of SARS-CoV-2 as a live virus vaccine candidate. *EBioMed* (2020) 62:103132. doi: 10.1016/j.ebiom.2020.103132
174. Travieso T, Li J, Mahesh S, Mello JDFRE, Blasi M. The use of viral vectors in vaccine development. *NPJ Vaccines* (2022) 7(1):75. doi: 10.1038/s41541-022-00503-y
175. Chiale C, Marchese AM, Furuya Y, Robek MD. Virus-based vaccine vectors with distinct replication mechanisms differentially infect and activate dendritic cells. *NPJ Vaccines* (2021) 6(1):138. doi: 10.1038/s41541-021-00400-w
176. Espeseth AS, Yuan M, Citron M, Reiserova L, Morrow G, Wilson A, et al. Preclinical immunogenicity and efficacy of a candidate COVID-19 vaccine based on a vesicular stomatitis virus-SARS-CoV-2 chimera. *EBioMed* (2022) 82:104203. doi: 10.1016/j.ebiom.2022.104203
177. Pulendran B, Arunachalam P S, O'Hagan DT. Emerging concepts in the science of vaccine adjuvants. *Nat Rev Drug Discov* (2021) 20(6):454–75. doi: 10.1038/s41573-021-00163-y
178. New RRC. Formulation technologies for oral vaccines. *Clin Exp Immunol* (2019) 198(2):153–69. doi: 10.1111/cei.13352
179. Wilkins AL, Kazmin D, Napolitani G, Clutterbuck EA, Pulendran B, Siegrist CA, et al. AS03- and MF59-adjuvanted influenza vaccines in children. *Front Immunol* (2017) 8:1760. doi: 10.3389/fimmu.2017.01760
180. Iho S, Maeyama JI, Suzuki F. CpG oligodeoxynucleotides as mucosal adjuvants. *Hum Vaccin Immunother* (2015) 11(3):755–60. doi: 10.1080/21645515.2014.1004033
181. Ichinohe T, Watanabe I, Ito S, Fujii H, Moriyama M, Tamura SI, et al. Synthetic double-stranded RNA poly(I:C) combined with mucosal vaccine protects against influenza virus infection. *J Virol* (2005) 79(5):2910–9. doi: 10.1128/JVI.79.5.2910-2919.2005
182. Spinner JL, Oberoi HS, Yorgensen YM, Poirier DS, Burkhart DJ, Plante M, et al. Methylglycol chitosan and a synthetic TLR4 agonist enhance immune responses to influenza vaccine administered sublingually. *Vaccine* (2015) 33(43):5845–53. doi: 10.1016/j.vaccine.2015.08.086
183. Aina I, Ichinohe T, Tamura SI, Kurata T, Sata T, Tashiro M, et al. Zymosan enhances the mucosal adjuvant activity of poly(I:C) in a nasal influenza vaccine. *J Med Virol* (2010) 82(3):476–84. doi: 10.1002/jmv.21694
184. Skountzou I, Martin M del P, Wang B, Ye L, Koutsouanos D, Weldon W, et al. Salmonella flagellins are potent adjuvants for intranasally administered whole inactivated influenza vaccine. *Vaccine* (2010) 28(24):4103–12. doi: 10.1016/j.vaccine.2009.07.058
185. Sjölander S, Drane D, Davis R, Beezum L, Pearce M, Cox J. Intranasal immunisation with influenza-ISCOR induces strong mucosal as well as systemic antibody and cytotoxic T-lymphocyte responses. *Vaccine* (2001) 19(28–29):4072–80. doi: 10.1016/S0264-410X(01)00110-4
186. Bracci L, Canini I, Puzelli S, Sestili P, Venditti M, Spada M, et al. Type I IFN is a powerful mucosal adjuvant for a selective intranasal vaccination against influenza virus in mice and affects antigen capture at mucosal level. *Vaccine* (2005) 23(23):2994–3004. doi: 10.1016/j.vaccine.2004.12.006
187. Matsuo K, Yoshikawa T, Asanuma H, Iwasaki T, Hagiwara Y, Chen Z, et al. Induction of innate immunity by nasal influenza vaccine administered in combination with an adjuvant (cholera toxin). *Vaccine* (2000) 18(24):2713–22. doi: 10.1016/S0264-410X(00)00055-4
188. Gopinath S, Kim MV, Rakib T, Wong PW, van Zandt M, Barry NA, et al. Topical application of aminoglycoside antibiotics enhances host resistance to viral infections in a microbiota-independent manner. *Nat Microbiol* (2018) 3(5):611–21. doi: 10.1038/s41564-018-0138-2
189. Nagai M, Moriyama M, Ichinohe T. Oral bacteria combined with an intranasal vaccine protect from influenza A virus and SARS-CoV-2 infection. *MBio* (2021) 12(4):e0159821. doi: 10.1128/mBio.01598-21
190. Lam JH, Shivhare D, Chia TW, Chew SL, Sinsinbar G, Aw TY, et al. Artificial cell membrane polymersome-based intranasal beta spike formulation as a second generation Covid-19 vaccine. *ACS Nano* (2022) 16(10):16757–75. doi: 10.1021/acsnano.2c06350
191. Cox RM, Wolf JD, Plemper RK. Therapeutically administered ribonucleoside analogue MK-4482/EIDD-2801 blocks SARS-CoV-2 transmission in ferrets. *Nat Microbiol* (2021) 6(1):11–8. doi: 10.1038/s41564-020-00835-2
192. Fischer WA 2nd, Eron JJ Jr, Holman W, Cohen MS, Fang L, Szczyk LJ, et al. A phase 2a clinical trial of molnupiravir in patients with COVID-19 shows accelerated SARS-CoV-2 RNA clearance and elimination of infectious virus. *Sci Transl Med* (2022) 14(628):eab17430. doi: 10.1126/scitranslmed.abl7430
193. Zhong W, Jiang X, Yang X, Feng T, Duan Z, Wang W, et al. The efficacy of paxlovid in elderly patients infected with SARS-CoV-2 omicron variants: Results of a non-randomized clinical trial. *Front Med* (2022) 9, 980002. doi: 10.3389/fmed.2022.980002
194. CDC. *Influenza antiviral medications: Summary for clinicians*. Centers for Disease Control and Prevention, National Center for Immunization and Respiratory Diseases (NCIRD, online source). (2022). Available at: <https://www.cdc.gov/flu/professionals/antivirals/summary-clinicians.htm>.
195. Czuppon P, Débarre F, Gonçalves A, Tenaillon O, Perelson AS, Guedj J, et al. Success of prophylactic antiviral therapy for SARS-CoV-2: Predicted critical efficacies and impact of different drug-specific mechanisms of action. *PLoS Comput Biol* (2021) 17(3):e1008752. doi: 10.1371/journal.pcbi.1008752
196. Zhou S, Hill CS, Sarkar S, Tse LV, Woodburn BMD, Schinazi RF, et al. β -d-N4-hydroxycytidine inhibits SARS-CoV-2 through lethal mutagenesis but is also mutagenic to mammalian cells. *J Infect Dis* (2021) 224(3):415–9. doi: 10.1093/infdis/jiab247
197. Kim KS, Iwanami S, Oda T, Fujita Y, Kuba K, Miyazaki T, et al. Incomplete antiviral treatment may induce longer durations of viral shedding during SARS-CoV-2 infection. *Life Sci Alliance* (2021) 4(10). doi: 10.26508/lsa.202101049
198. Akhtar J, Quémès V, Pillai K, Kepenekian Y, Badar S, Mekki AH, et al. The combination of bromelain and acetylcysteine (BromAc) synergistically inactivates SARS-CoV-2. *Viruses* (2021) 13(3). doi: 10.3390/v13030425
199. Amini A, Masoumi-Moghaddam S, Morris DL. *Utility of Bromelain and N-Acetylcysteine in Treatment of Peritoneal Dissemination of Gastrointestinal Mucin-Producing Malignancies*. (Kapandriti, Greece: Springer) (2016). 229 p.
200. Schlegel A, Schaller J, Jentsch P, Kempf C. Semliki Forest virus core protein fragmentation: its possible role in nucleocapsid disassembly. *Biosci Rep* (1993) 13(6):333–47. doi: 10.1007/BF01150478
201. Greig AS, Bouillant AM. Binding effects of concanavalin A on a coronavirus. *Can J Comp Med* (1977) 41(1):122–6.
202. Lim NA, Teng O, Ng CYH, Bao LXY, Tambyah PA, Quek AML, et al. Repurposing povidone-iodine to reduce the risk of SARS-CoV-2 infection and transmission: a narrative review. *Ann Med* (2022) 54(1):1488–99. doi: 10.1080/07853890.2022.2076902
203. Naqvi SHS, Citardi MJ, Cattano D, Ostrosky-Zeichner L, Knackstedt MI, Karni RJ. Povidone-iodine solution as SARS-CoV-2 prophylaxis for procedures of the upper aerodigestive tract: a theoretical framework. *J Otolaryngol Head Neck Surg* (2020) 49(1):77. doi: 10.1186/s40463-020-00474-x
204. Kanagalingam J, Feliciano R, Hah JH, Labib H, Le TA, Lin JC. Practical use of povidone-iodine antiseptic in the maintenance of oral health and in the prevention and treatment of common oropharyngeal infections. *Int J Clin Pract* (2015) 69(11):1247–56. doi: 10.1111/ijcp.12707

205. Mateos-Moreno MV, Mira A, Ausina-Márquez V, Ferrer MD. Oral antiseptics against coronavirus: *in-vitro* and clinical evidence. *J Hosp Infect* (2021) 113:30–43. doi: 10.1016/j.jhin.2021.04.004
206. Mueller S. *Challenges and Opportunities of mRNA Vaccines Against SARS-CoV-2: A Multidisciplinary Perspective*. (New York, USA: Springer Nature) (2023). 439 p.
207. Mao T, Israelow B, Peña-Hernández MA, Suberi A, Zhou L, Luyten S, et al. Unadjuvanted intranasal spike vaccine elicits protective mucosal immunity against sarbecoviruses. *Science* (2022) 378(6622):eabo2523. doi: 10.1126/science.abo2523
208. Yang Z, Zhao Q, Gao YA, Zhang W. Combined oral and intravenous immunization stimulates strong igA responses in both systemic and mucosal compartments. *PloS One* (2016) 11(12):e0168037. doi: 10.1371/journal.pone.0168037
209. Tsunetsugu-Yokota Y, Ishige M, Murakami M. Oral attenuated *Salmonella enterica* serovar Typhimurium vaccine expressing codon-optimized HIV type 1 Gag enhanced intestinal immunity in mice. *AIDS Res Hum Retroviruses* (2007) 23(2):278–86. doi: 10.1089/aid.2006.0098



OPEN ACCESS

EDITED BY

Sophie Gryseels,
University of Antwerp, Belgium

REVIEWED BY

Francesco Cerutti,
Ospedale Amedeo di Savoia, Italy
Satya Ranjan Dash,
KIIT University, India

*CORRESPONDENCE

Tavis K. Anderson
✉ tavis.anderson@usda.gov

RECEIVED 09 May 2023

ACCEPTED 06 November 2023

PUBLISHED 04 December 2023

CITATION

Zeller MA, Arendsee ZW, Smith GJD and
Anderson TK (2023) classLog: Logistic
regression for the classification of
genetic sequences.
Front. Virol. 3:1215012.
doi: 10.3389/fviro.2023.1215012

COPYRIGHT

© 2023 Zeller, Arendsee, Smith and
Anderson. This is an open-access article
distributed under the terms of the [Creative
Commons Attribution License \(CC BY\)](#). The
use, distribution or reproduction in other
forums is permitted, provided the original
author(s) and the copyright owner(s) are
credited and that the original publication in
this journal is cited, in accordance with
accepted academic practice. No use,
distribution or reproduction is permitted
which does not comply with these terms.

classLog: Logistic regression for the classification of genetic sequences

Michael A. Zeller^{1,2}, Zebulun W. Arendsee³,
Gavin J.D. Smith^{1,4} and Tavis K. Anderson^{3*}

¹Programme in Emerging Infectious Diseases, Duke - National University of Singapore Medical School, Singapore, Singapore, ²Iowa State University Veterinary Diagnostic Laboratory, Iowa State University, Ames, IA, United States, ³Virus and Prion Research Unit, National Animal Disease Center, USDA-ARS, Ames, IA, United States, ⁴Centre for Outbreak Preparedness, Duke - National University of Singapore Medical School, Singapore, Singapore

Introduction: Sequencing and phylogenetic classification have become a common task in human and animal diagnostic laboratories. It is routine to sequence pathogens to identify genetic variations of diagnostic significance and to use these data in realtime genomic contact tracing and surveillance. Under this paradigm, unprecedented volumes of data are generated that require rapid analysis to provide meaningful inference.

Methods: We present a machine learning logistic regression pipeline that can assign classifications to genetic sequence data. The pipeline implements an intuitive and customizable approach to developing a trained prediction model that runs in linear time complexity, generating accurate output rapidly, even with incomplete data. Our approach was benchmarked against porcine respiratory and reproductive syndrome virus (PRRSv) and swine H1 influenza A virus (IAV) datasets. Trained classifiers were tested against sequences and simulated datasets that artificially degraded sequence quality at 0, 10, 20, 30, and 40%.

Results: When applied to a poor-quality sequence data, the classifier achieved between >85% to 95% accuracy for the PRRSv and the swine H1 IAV HA dataset and this increased to near perfect accuracy when using the full dataset. The model also identifies amino acid positions used to determine genetic clade identity through a feature selection ranking within the model. These positions can be mapped onto a maximum-likelihood phylogenetic tree, allowing for the inference of clade defining mutations.

Discussion: Our approach is implemented as a python package with code available at <https://github.com/flu-crew/classLog>.

KEYWORDS

classification, machine learning, logistic regression, taxonomy, automation

1 Introduction

Classification of pathogens has become a routine task in modern veterinary diagnostics (1). Classification of the infectious agent is a critical diagnostic step that allows for an informed decision on vaccination regimens and biosecurity measures that may be considered to clear a pathogen outbreak (2–4). Currently genetic classification is performed using phylogenetic methods such as maximum-likelihood and neighbor joining (2, 5, 6). These methods are effective at classifying sequences and inferring relationships between taxa, but the time and skill required to execute and interpret analyses may impact their application in routine high-throughput activities. While diagnosticians are interested in the transmission and history of disease, the most pressing need is to provide a classification of data. Consequently, methods that do not conduct computationally intensive phylogenetic inference for inferring ancestry and genomic epidemiology are required.

Phylogenetic placement (PP) methods are one solution to the problem of accurately assigning lineage designations to taxa. PP places a given taxa onto a reference tree without recomputing the topology and lineage designations are subsequently inferred based on the proximity to annotated taxa in the tree. PP methods are advantageous in that they can interpolate lineage within a broad context (between species) and narrow context (specific clades within a subtype). Multiple phylogenetic placement software are available such as the pplacer suite (7), RAPPAS (8), EPA-ng (9), and Nextclade (10). While PP methods are invaluable for research, there is still room for other methodologies to provide fast and accurate lineage assignments without the requirement for a robust reference tree topology.

Machine learning has been recognized as a viable method for classifying sequences (4, 11). Differing from PP methods, machine learning approaches do not need a reference tree for classification. Genetic divergence over time leads to distinguishable genetic patterns within monophyletic clades that are linearly separable across aligned amino acid positions. This linear separability lends itself well to supervised machine learning methods such as logistic regression and random forest classification. Logistic regression based on aligned sequences is used as the primary means of automated classification for influenza A viruses (IAV) in swine that are processed within the FLUture database (12). Similarly, porcine reproductive and respiratory syndrome virus (PRRSV) amino acid sequence data have been classified to genetic lineage using random forest, k-nearest neighbor, support vector machines, and multilayer perceptron methods (4). Decision tree machine learning approaches have been introduced to classify avian IAV sequences and SARS-CoV-2 sequences successfully at multiple taxonomical levels (13, 14). PangoLEARN, a random forest model, currently supplements the pangolin classification system for SARS-CoV-2 (11). However, despite machine learning appearing to be an effective approach for classification, few of these algorithms are user-friendly with intuitive generalized software that has been publicly released.

This manuscript introduces a general-purpose software application, classLog, that can train sequence classifiers based on user-labelled training data for use in classification of unknown

sequences. The method used by the program leverages logistic regression, a parametric method of classification that runs in linear time complexity. Application of classLog provides a routine and robust way to integrate classification into pipelines where speed is necessary and there is no interest in inferring historical context of the sequences. Through decoupling the classification step from the inference of the history of the virus, this manuscript presents a method of classification that is rapid, accurate, and suitable for high-throughput pipelines.

2 Methods

2.1 Curation of swine H1 IAV and PRRSV North America datasets

We compiled two datasets to test the utility of our classification pipeline: porcine reproductive and respiratory syndrome virus (PRRSV) and influenza A virus (IAV) in swine. We restricted the swine IAV to H1 subtype hemagglutinin (HA) genes from the United States collected between 2015 to 2021: these data were curated and annotated by genetic clade by the Influenza Research Database (2, 15). These lineages were delineated based on a rule system applied to a maximum-likelihood phylogeny. Briefly, lineages were designated as statistically supported phylogenetic clusters when they contained more than 10 taxa, had statistical support > 70%, and the average pairwise distance between and within clades was >7% and < 7% respectively. Sequences sampled between 2015–2019 were used as a training set (n=3510), while 2020 and later sequences were extracted as a test set (n=163) (Figure 1B). For PRRSV sequences, we extracted the curated ORF5 gene sequence data provided by (3), and extracted and assigned the genetic clade for each sequence from the GenBank accession's feature information. The genetic lineage delineations for PRRSV were also based on a maximum-likelihood phylogeny, with monophyletic lineages identified as those with strong statistical support and were designated using ClusterPicker (16). The dataset was further refined by removing all “Type 1” European sequences, sequences that were not the full coding region, i.e., not equal to 603 or 606 nucleotides in length, and the remaining sequences were translated. The final dataset of 3047 annotated sequences were randomly split into training and test sets, using 80% (n=2,483) and 20% (n=609) of the sequences respectively (Figure 1A).

The datasets were split differently to simulate two distinct uses of the classifier. IAV data was split temporally to simulate classifying new data, while PRRSV sequences were split randomly to simulate filling in classifications from a mixed set.

2.2 Simulated Sequencing Errors and Removing Informative Features

Gene sequences retrieved from Sanger sequencing, next generation, and third generation sequencing methods are not always complete, and there may be ambiguities and gaps in the data (17–19). These errors impact the estimation of the multiple

sequence alignment that may subsequently decrease the accuracy of classification (20, 21). To mimic decreasing quality of sequences, a python script was created to randomly generate a number of indices for replacement with an ambiguous 'X'. Subsequently, the X's were removed from the sequence to generate incomplete, unaligned sequences. Test set sequences were degraded at 0%, 10%, 20%, 30%, and 40% prior to classification. While more robust simulations of sequence degradation exist (22), the replication and implication of these methods is beyond the scope of this manuscript.

2.3 Constructing classLog: the general sequence classifier

Sequence classification was implemented as a one-versus-rest logistic regression classifier, with a general outline provided (Supplemental Figure 1). Input for classification requires an aligned nucleotide or amino acid FASTA file, with definition lines specifying the classification classes using character delimiters, e.g., A/swine/Iowa/A02636475/2022|1B.2.2.1, where '|' delimits the phylogenetic clade from the strain name. The binary features of this model are the presence or absence of an amino acid at a specific position within the alignment. An optional feature selection process, which selects the most relevant sequence positions for classification, was implemented using a tree classifier that ranks binary features by GINI importance so that the user may restrict the prediction model to the most important features (23). To facilitate the reusability of the classification scheme, the first sequence, feature labels, trained model, and class names are exported using a standard python pickle file format. The first sequence in the pickle file is used for pairwise alignment of unknown sequences to ensure there is consistency between query sequence alignment positions and the model feature positions. During prediction, a matrix of the presence or absence of nucleotides or amino acids at specific alignment positions is created, which is then fed to the model for

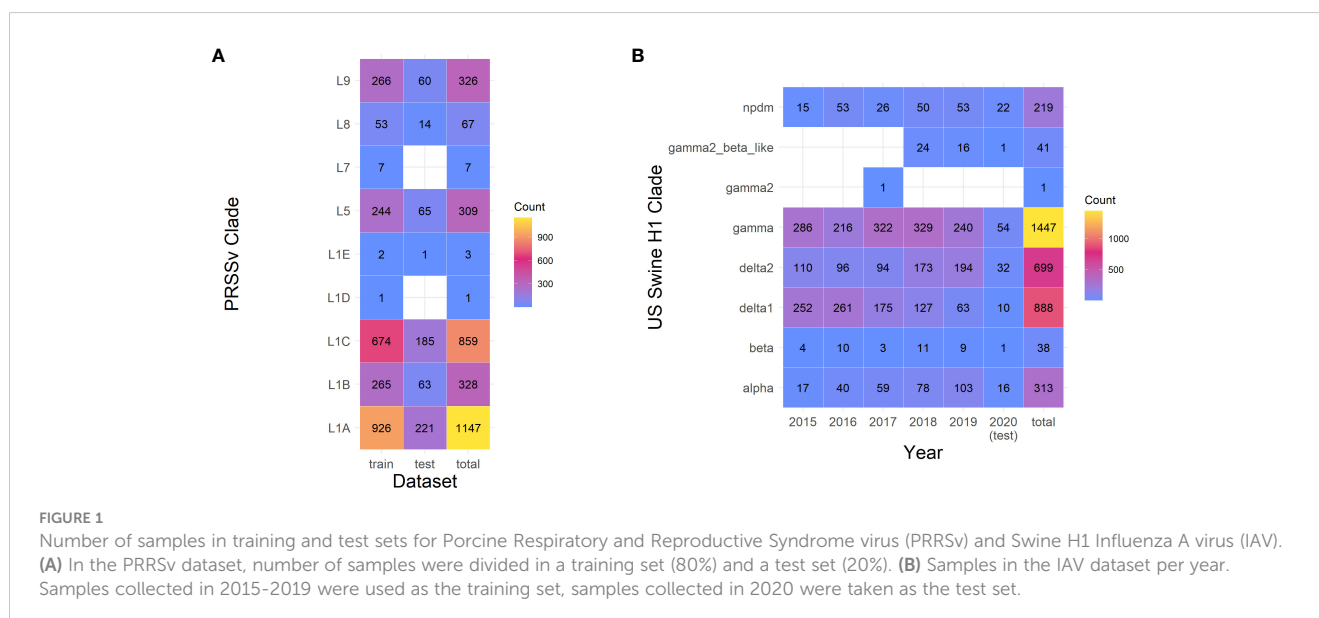
prediction. For user submitted query sequences, the predicted classification is assigned and reported using classification names derived from the user-annotated classification fasta file used in training.

A prediction threshold option was included within the classifier to provide support for predicted classes on unknown data. Classifications with a score less than the threshold are rejected, and classified into an 'unknown' category (default value of 85%). The threshold criteria can have a direct effect on the performance of classification.

For validation, the general classifier was trained using 100%, 20%, 10%, 5%, 1%, and 0.5% of the available features within the H1 IAV and the PRRSV training datasets. For the H1 IAV sequence dataset, this resulted in 2439, 487, 243, 121, 24, and 12 features respectively. For the PRRSV dataset, this resulted in 686, 137, 68, 34, 6, and 3 features. Each classifier was used to classify the 0%, 10%, 20%, 30%, and 40% test set sequences that had been generated to reflect sequencing errors and misalignment.

2.4 Simplifying feature identification in query sequences using a Needleman-Wunsch pairwise alignment algorithm

An intrinsic challenge to the implementation of the machine learning classification process was correctly assigning the positions to new genetic sequences. To overcome this challenge without keeping the original alignment, a heuristic was applied such that the first sequence from the training set was saved and stored, and subsequent classification attempts would be pairwise aligned to recover the positions. To increase the speed and keep calculations within a tractable time for computation, a Needleman-Wunsch dynamic programming alignment algorithm (24) with affine gap penalties and a BLOSUM90 substitution matrix (25) was implemented in C++ and exported as a python library using python bindings.



2.5 Measuring the performance of the classifier on swine H1 IAV and PRRSv North America dataset classification

The performance of the classifiers was measured under the metrics of accuracy, macro precision, macro recall, and macro F1 (26–28). From a confusion matrix M where true classification is assigned along the y-axis and the predicted class is assigned along the x-axis, the precision and recall equations can be generalized as follows:

$$Precision_i = \frac{M_{ii}}{\sum_j M_{ji}} \quad (1)$$

$$Recall_i = \frac{M_{ii}}{\sum_j M_{ij}} \quad (2)$$

$$F1_i = 2 \frac{Precision_i \times Recall_i}{(Precision_i + Recall_i)} \quad (3)$$

$$Precision_{macro} = \frac{1}{n} \sum_i Precision_i \quad (4)$$

$$Recall_{macro} = \frac{1}{n} \sum_i Recall_i \quad (5)$$

$$F1_{macro} = \frac{1}{n} \sum_i F1_i \quad (6)$$

These metrics were taken for each classifier applied to the 0%, 10%, 20%, 30%, and 40% test set sequences with the results plotted using ggplot2 (29) in R v3.959 (30).

Runtime performance was benchmarked using the Linux `usr/bin/time` program provided from Ubuntu v20.04LTS running within the Windows Subsystem Linux v2 (Supplemental Table 1). A second non-comparable benchmark approach that used existing phylogenetic placement approaches was run using pplacer and RAPPAS with the same test sets described above (Supplemental Table 2). The reference trees provided to the phylogenetic placement programs were paraphyletically pruned to 200 taxa using smot v1.0.0 (31) to more realistically simulate a phylogenetic placement scenario. Accuracy from either PP method was not tested as sufficient validation has been given in the originating and subsequent publication (7, 8).

2.6 Visualization of swine H1 IAV and PRRSv North America dataset using ordination and phylogenetic analysis

Sequences from both datasets were aligned using MAFFT v7.487 (32). The pairwise number of differences between each sequence were extracted from the alignment using Geneious Prime 2022 (33). These distances were ordinated into two-dimensional space using metric multidimensional scaling. Each

ordination was colored first by the designated genetic clade, and then by a genetic motif consisting of the amino acids of the top two ranking amino acid positions. Amino acid position rank was calculated as the sum of GINI importance given by the extra tree classifier for each amino acid position, i.e., the two most important amino acids in determining the classification of the query sequence.

To identify the biological basis of the H1 swine IAV and PRRSv classifications, maximum likelihood trees were inferred for each dataset. Sequences were aligned using MAFFT v7.487 (32), and trees were inferred using IQ-TREE v1.6.12 (34). The PRRSv dataset was analyzed using a BLOSUM62 amino acid substitution model, while the IAV dataset was analyzed using the FLU amino acid substitution model (35). Statistical support was determined using the rapid bootstrap algorithm with 1,000 bootstraps, and the support was displayed on the branch of the resultant trees. Each tree was colored along the backbone by the phylogenetic clade, while the tips were annotated and colored by the top two ranking amino acid positions determined using GINI importance.

3 Results

3.1 classLog performance on H1 swine IAV and PRRSv observed and simulated data

A classLog classifier was trained on PRRSv ORF5 sequences collected and classified to lineage (3), dividing the dataset into 80% training and 20% testing. The classifier performed perfectly correct when trained with 10% of features ($n=68$) of the total features with no sequence degradation (Figure 2A). At 10% sequence degradation (20aa), 10% of the features were able to achieve an accuracy of 97%. At 20% sequence degradation (40aa), 10% of the features were sufficient to achieve 88% accuracy, though increasing the number of features did not improve accuracy. Accuracy rapidly decreased at 30% sequence degradation (60aa), with 10% of the features achieving 69% correct classifications. At 40% sequence degradation (80aa) the greatest accuracy achieved was 42%.

A classLog classifier was trained on H1 swine sequences present in IRD collected between 2015 to 2019 and was tested on 136 test sequences from 2020. The classifier performed perfectly correct when trained with as few as 12 features (0.5%) when there was no sequence degradation (Figure 2B). At 10% sequence degradation (56 aa), 5% of the features (121 features) were needed to achieve perfect accuracy. At 20% sequence degradation (112 aa), 10% of the features (243 features) were sufficient to achieve perfect accuracy. At 30% sequence degradation (170aa), 10% of the features were sufficient to achieve 93% correct classifications, although 20% of features (487 features) only achieved 82% correct classification. At 40% sequence degradation (227aa), there was a steep decline in the accuracy, falling below 60% across the board.

For both datasets, precision was consistently higher than recall (Figure 2). This is a consequence of rejecting classifications below the 85% scoring threshold and classifying them as 'unknown,' i.e., the number of false positives decreased while increasing false negatives.

3.2 Using classLog to identify genetic features of biological relevance

The pairwise differences between the test set sequences were used to ordinate points in two-dimensional space (Figure 3). The ordination of both the PRRSV ORF5 and swine H1 IAV datasets were colored by their original designated clades, and by the motif formed by the amino acids present at the top two features ranked by GINI importance (Supplemental Figures 2, 3). This manuscript uses the top two features as the number of amino acid combinations above two exceeds the number of distinct colors available on the pallet; but lower ranked features are important to discriminate between phylogenetic clades. Qualitatively, the ordination demonstrated separation between distant genetic lineages such as the H1 1A classical swine lineage versus the H1 1B human seasonal lineage (Figure 2C; 2). However, sequences within some closely related genetic clades within the same lineage appeared to have overlap when assessed in a two-dimensional ordination. Within the PRRSV data (Figure 2B), the top two ranked amino acid positions (170, 172) corresponded well with the classified genetic clades suggesting that these positions may be clade defining mutations. For example, L1A has primarily the EE motif, L1B has EN, and L1C has DG. These divisions were not exclusive as L5, L8, L9 also have the EE motif that was exclusively within the L1A, and more features may need to be accounted for to discriminate between these clades. The top two positions of the swine H1 IAV dataset were 159 and 158 (H1 numbering, 17AA signal peptide removed) (Figure 2D), with a relatively high number of amino acid polymorphisms between those two positions. While some clades were well matched to one or two motifs, some clades such as the 1A alpha were highly varied in the motifs they carried, suggesting that other features position with a lower rank may better segregate this clade from the other clades. These data can be generated by extracting the features and their rankings using the classLog algorithm.

3.3 Congruency between phylogenetic classification, classLog predictions, and model features

Maximum-likelihood trees were inferred for the PRRSV ORF5 and swine H1 IAV HA test datasets. The backbones of the phylogenetic trees were colored by the assigned genetic lineage, while the tips were labeled and colored by the motif formed by the two amino acid positions that had the highest cumulative GINI importance. For the PRRSV ORF5 dataset (Figure 4A: positions 170 and 172), the majority of L1B motifs were represented by an EN and L1C by DG. L1A, L5, L8, and L9 were also represented by EE at 170 and 172, suggesting that despite good concordance between the inferred phylogeny and the classLog predicted clade, this was being driven by features outside of these two positions.

For the swine H1 HA dataset (Figure 4B), the two most important features identified by classLog were positions 159 and 158. The majority of the 1B delta1a clade was primarily represented by GK, the 1B delta2 by SN, and 1A pandemic09 by KA. Three distinct motifs were identified within the 1A gamma clade, KT, NT, and ST, with RT interspersed. The 158T at was distinct enough to serve as a general rule to separate diversity within the 1A gamma clade. The remaining major H1 clade, 1A alpha, was associated with a significant amount of motif diversity, exhibiting GK, GR, KA, SA, SK and RR. The high amount of motif diversity is suggestive that another set of features may be used by the classifier for identifying this clade.

4 Discussion

Applications of machine learning present computationally efficient ways of classifying genetic sequences without relying on traditional phylogenetic methods. The direct utility of machine

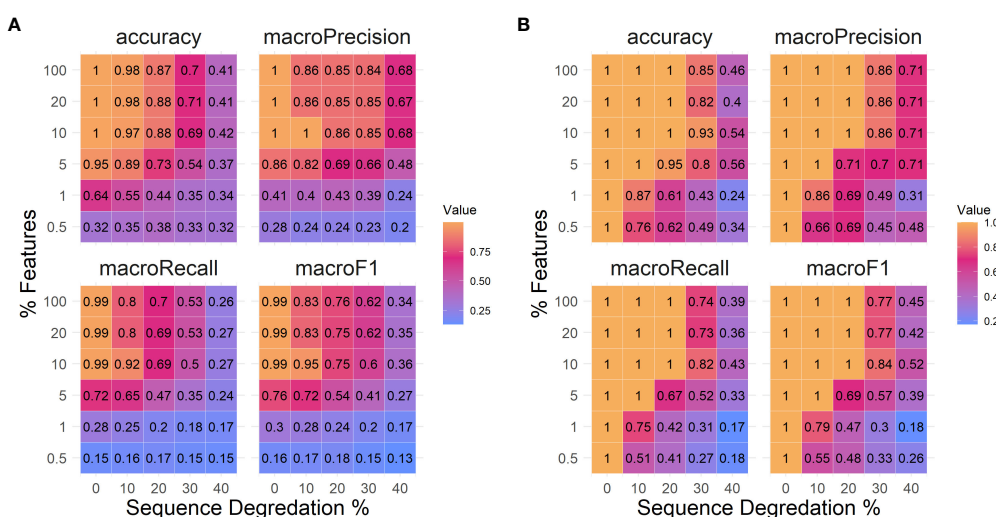
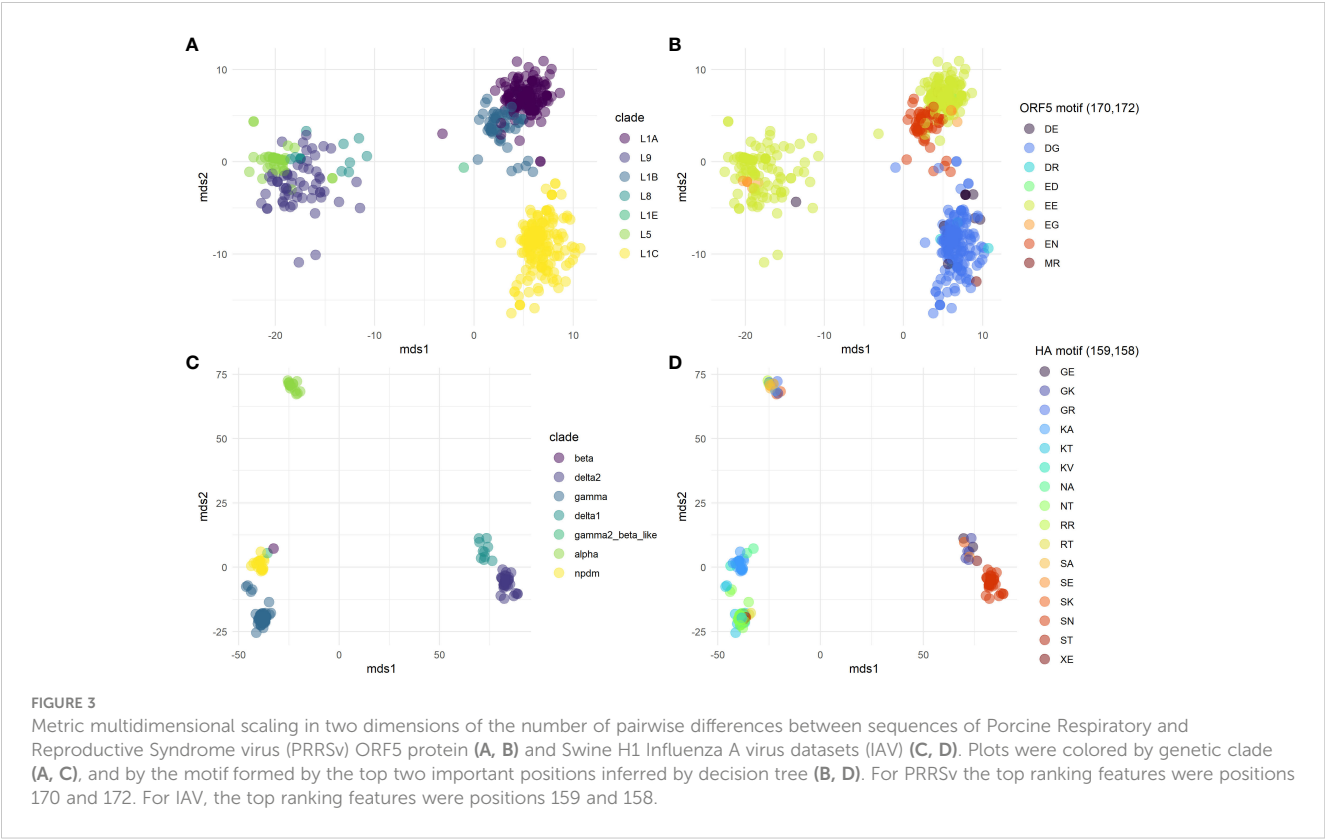


FIGURE 2

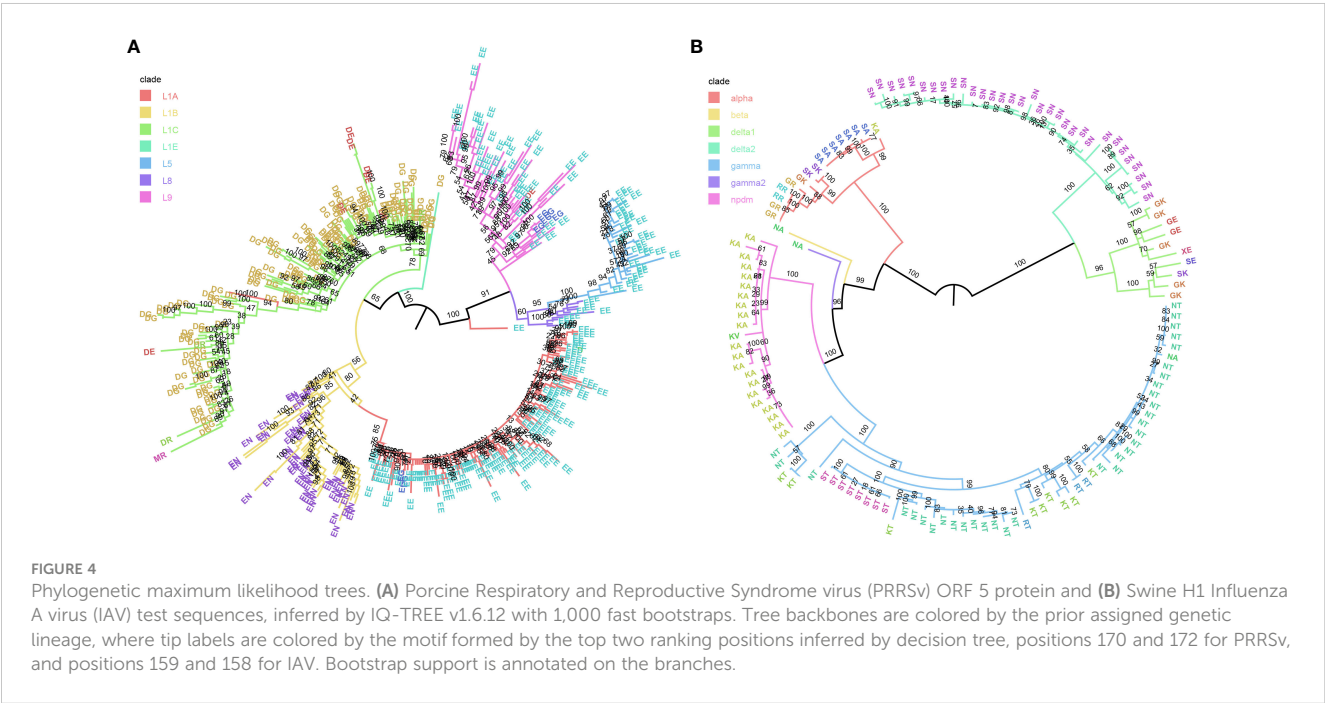
Measures of logistic regression classifier performance in the metrics of accuracy, precision, recall, and F1 scoring. (A) Porcine Respiratory and Reproductive Syndrome virus and (B) Swine H1 Influenza A virus datasets. Each metric was measured over simulated sequence degradation of 0%, 10%, 20%, 30% and 40%, as well as with classifiers using 0.5%, 1%, 5%, 10%, 20%, and 100% of the available features for classification.



learning methods is in high-throughput diagnostic processes, where the primary objective is to assign classification and there is not an immediate interest in inferring the evolutionary history of the sequence in question. By decoupling the classification process from phylogenetic method, complexity and computational time are reduced. Machine learning methods have the additional benefit of being highly portable and reproducible with minimal effort once

an initial prediction model is trained. Our command line interface, classLog, represents a user-friendly and validated tool that can ingest annotated genetic sequences, train a classification model, and generate predictions and associated confidence scores without extensive computational and machine learning training.

Logistic regression was chosen to ensure scalability with linear time complexity, fast computational runtime, and for simple model



interpretability. These factors allow classLog to function as a lightweight component in classification pipelines. Moreover, many genetic lineage classification schemes frequently depend on phylogenetic relationships to delineate lineages, which is effectively a form of clustering by similarity. Consequently, linear separability emerges when significant genetic divergence exists between designated lineages. Although other machine learning methods such as neural networks can learn complex relationships and patterns, within the narrow context of lineage classification, logistic regression is generally sufficient. Taxonomic classification of virus sequence data is typically performed via either phylogenetic methods or through similarity-based approaches such as BLAST. Phylogenetic methods can be computationally complex: simple techniques such as neighbor joining have a cubic time complexity, but more statistically robust techniques have a higher range of complexity and runtime. BLAST overcomes these complexity issues, but there is a necessity for a curated database of sequences, and large databases can be difficult to update and share. In general, machine learning models can overcome both limitations as they offer both reasonable time complexity and space complexity for classification; and if an adequate dataset is used to generalize a model during training, the subsequent model may be reused without maintaining or training input reference datasets. In recognition of these strengths, machine learning approaches are being used (11, 14), but a generalized application has not yet been created.

classLog can be applied for rapid classification of genomic data either on site or in field settings. The advent of rapid and portable sequencing such as minION Nanopore technologies has resulted in the generation of thousands of sequences with a critical need to identify what they are, and whether the sample represents an “unknown.” The classLog program can be easily adopted as part of a light-weight pipeline that can be used to do classification on the fly in the field (36). The execution of classLog does not require significant computational resources, and our testing was conducted on regular Windows and MacOS laptops. Consequently, it can easily be integrated within mobile diagnostic stations that are functional within remote locations that may have minimal access to extensive computational resources or trained personnel (37, 38).

A consequence of field genomic epidemiology and the integration of Nanopore technology has been an increase in sequence error rate relative to traditional Sanger sequencing (39, 40). Our testing with classLog on simulated datasets, where we introduced sequence errors, suggested that the inaccuracies do not dramatically reduce the accuracy of classification using this machine learning method. It was noted that the classification failure within the H1 sequence dataset occurred proportionally to the number of samples present in the training dataset. As the sequence errors increased, misclassifications began to occur first in the sequences that had the least clade representation in the training set. It is likely that if there are more samples present in the training data to represent a specific clade, then the prediction model was better able to generalize the clade. This indicates one potential

drawback of classLog, and that user-curated training datasets must remain large enough for optimal classifier performance. classLog performs within the narrow context of classification, assigning clades within a species, although it can quickly segregate unrelated sequences by specifying them as “unknown”. An alternate approach to generating large, curated datasets when attempting to classify multiple species could be the application of phylogenetic placement algorithms or using advanced machine learning models beyond logistic regression. Logistic regression is a parametric model that performs well on linearly separable classifications. In cases where the data are not linearly separable and that have limited training data, non-parametric models like random forest or neural networks may perform significantly better, potentially provide easy to understand biological context to feature rankings (41, 42), but require more computational time and effort.

Benchmarks of classLog runtime demonstrate that the combined training and classification time is fast, with each test case presenting a combined time under a minute (Supplementary Table 1). While the conditions of the test are not directly comparable to the testing of pplacer and RAPPAS, it can be noted that the total runtime of classLog is less than both PP methods when finding a solution to the same classification problem. It is notable that once the RAPPAS database is built, the placement of taxa onto a tree is very rapid, although the memory usage is higher. However, it is important to note that the use-cases of classLog compared to PP methods differs: classLog is designed specifically to assign lineages within a narrow scope of genetic diversity within a single species. Comparatively, both pplacer and RAPPAS can function with multiple species and additionally infer topology. The difference in the use-cases for the tools makes comparison only valid for the subset of problems where the tools overlap.

classLog is a method of creating light weight classifiers that can assign taxonomic classifications rapidly with minimal user curation and training. The implementation of this classification methodology can benefit diagnostic labs by saving computational run time associated with current phylogenetic classification approaches and can be easily customized to work for different pathogens. An additional benefit is the identification of critical genetic features associated with clade classifications: these features are likely clade defining mutations and can be used to form hypotheses to investigate the gene to phenotype link (43–45) and other functional studies. A benefit of machine learning approaches is that the results are also more directly interpretable as they are given as an assignment, rather than needing to be inferred from a tree. The culmination of these benefits offers a more streamlined approach to taxonomic assignment in a diagnostic setting.

Data availability statement

Publicly available datasets were analyzed in this study. This data can be found here: <https://github.com/flu-crew/classLog>.

Author contributions

MZ conceived the study. MZ, ZA, and TKA programmed the code. MZ, GS and TKA conceptualized the framework for testing. All authors tested the program. MZ and TA wrote the manuscript. All authors contributed to the article and approved the submitted version.

Funding

The author(s) declare financial support was received for the research, authorship, and/or publication of this article. This work was supported in part by: the U.S. Department of Agriculture (USDA) Agricultural Research Service [ARS project number 5030-32000-231-000-D]; the National Institute of Allergy and Infectious Diseases, National Institutes of Health, Department of Health and Human Services [contract numbers 75N93021C00015 and 75N93021C00016]; the USDA Agricultural Research Service Research Participation Program of the Oak Ridge Institute for Science and Education (ORISE) through an interagency agreement between the U.S. Department of Energy (DOE) and USDA Agricultural Research Service [contract number DE-AC05-06OR23100]; the SCINet project of the USDA Agricultural Research Service [ARS project number 0500-00093-001-00-D]; and the Duke-NUS Signature Research Program funded by the Ministry of Health, Singapore. The funders had no role in study design, data collection and interpretation, or the decision to submit the work for publication. Mention of trade names or commercial products in this article is solely for the purpose of providing specific information and does not imply recommendation or endorsement by the USDA, DOE, or ORISE. USDA is an equal opportunity provider and employer.

References

- Shi M, Lam TT-Y, Hon C-C, Hui RK-H, Faaborg KS, Wennblom T, et al. Molecular epidemiology of PRRSV: a phylogenetic perspective. *Virus Res* (2010) 154:7–17. doi: 10.1016/j.virusres.2010.08.014
- Anderson TK, Macken CA, Lewis NS, Scheuermann RH, Van Reeth K, Brown IH, et al. A phylogeny-based global nomenclature system and automated annotation tool for H1 hemagglutinin genes from swine influenza A viruses. *mSphere* (2016) 1:e00275–00216. doi: 10.1128/mSphere.00275-16
- Paploski I, Corzo C, Rovira A, Murtaugh MP, Sanhueza JM, Vilalta C, et al. Temporal dynamics of co-circulating lineages of porcine reproductive and respiratory syndrome virus. *Front Microbiol* (2019) 10:2486. doi: 10.3389/fmicb.2019.02486
- Kim J, Lee K, Rupasinghe R, Rezaei S, Martínez-López B, Liu X. Applications of machine learning for the classification of porcine reproductive and respiratory syndrome virus sublineages using amino acid scores of ORF5 gene. *Front Veterinary Sci* (2021) 8:13. doi: 10.3389/fvets.2021.683134
- Chang J, Anderson TK, Zeller MA, Gauger PC, Vincent AL. octoFLU: automated classification for the evolutionary origin of influenza A virus gene sequences detected in US swine. *Microbiol resource announcements* (2019) 8:e00673–00619. doi: 10.1128/MRA.00673-19
- Turakhia Y, Thornlow B, Hinrichs AS, De Maio N, Gozashti L, Lanfear R, et al. Ultrafast Sample placement on Existing tRees (USHER) enables real-time phylogenetics for the SARS-CoV-2 pandemic. *Nat Genet* (2021) 53:809–16. doi: 10.1038/s41588-021-00862-7
- Matsen FA, Kodner RB, Armbrust E. pplacer: linear time maximum-likelihood and Bayesian phylogenetic placement of sequences onto a fixed reference tree. *BMC Bioinf* (2010) 11:1–16. doi: 10.1186/1471-2105-11-538
- Linard B, Swenson K, Pardi F. Rapid alignment-free phylogenetic identification of metagenomic sequences. *Bioinformatics* (2019) 35:3303–12. doi: 10.1093/bioinformatics/btz068
- Barbera P, Kozlov AM, Czech L, Morel B, Darriba D, Flouri T, et al. EPA-ng: massively parallel evolutionary placement of genetic sequences. *Systematic Biol* (2019) 68:365–9. doi: 10.1093/sysbio/syy054
- Aksamentov I, Roemer C, Hodcroft EB, Neher RA. Nextclade: clade assignment, mutation calling and quality control for viral genomes. *J Open Source software* (2021) 6:3773. doi: 10.21105/joss.03773
- O'toole Á, Scher E, Underwood A, Jackson B, Hill V, McCrone JT, et al. Assignment of epidemiological lineages in an emerging pandemic using the pangolin tool. *Virus Evol* (2021) 7:veab064. doi: 10.1093/ve/veab064
- Zeller MA, Anderson TK, Walia RW, Vincent AL, Gauger PC. ISU FLU ture: a veterinary diagnostic laboratory web-based platform to monitor the temporal genetic patterns of Influenza A virus in swine. *BMC Bioinf* (2018) 19:397. doi: 10.1186/s12859-018-2408-7
- Randhawa GS, Soltysiak MP, El Roz H, De Souza CP, Hill KA, Kari L. Machine learning using intrinsic genomic signatures for rapid classification of novel pathogens: COVID-19 case study. *PLoS One* (2020) 15:e0232391. doi: 10.1371/journal.pone.0232391
- Humayun F, Khan F, Fawad N, Shamas S, Fazal S, Khan A, et al. Computational method for classification of avian influenza A virus using DNA sequence information and physicochemical properties. *Front Genet* (2021) 12:10. doi: 10.3389/fgene.2021.599321

Acknowledgments

We gratefully acknowledge pork producers, swine veterinarians, and laboratories for participating in the USDA Influenza A Virus in Swine Surveillance System and publicly sharing sequences.

Conflict of interest

The author(s) TKA declared that they were an editorial board member of Frontiers, at the time of submission. This had no impact on the peer review process and the final decision.

The remaining authors declare that the research was conducted in the absence of any commercial or financial relationships that could be construed as a potential conflict of interest.

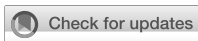
Publisher's note

All claims expressed in this article are solely those of the authors and do not necessarily represent those of their affiliated organizations, or those of the publisher, the editors and the reviewers. Any product that may be evaluated in this article, or claim that may be made by its manufacturer, is not guaranteed or endorsed by the publisher.

Supplementary material

The Supplementary Material for this article can be found online at: <https://www.frontiersin.org/articles/10.3389/fviro.2023.1215012/full#supplementary-material>

15. Zhang Y, Aevermann BD, Anderson TK, Burke DF, Dauphin G, Gu Z, et al. Influenza Research Database: An integrated bioinformatics resource for influenza virus research. *Nucleic Acids Res* (2017) 45:D466–74. doi: 10.1093/nar/gkw857
16. Ragonnet-Cronin M, Hodcroft E, Hue S, Fearnhill E, Delpech V, Brown AJ, et al. Automated analysis of phylogenetic clusters. *BMC Bioinf* (2013) 14:317. doi: 10.1186/1471-2105-14-317
17. Shendure J, Ji H. Next-generation DNA sequencing. *Nat Biotechnol* (2008) 26:1135–45. doi: 10.1038/nbt1486
18. Schirmer M, D'Amore R, Ijaz UZ, Hall N, Quince C. Illumina error profiles: resolving fine-scale variation in metagenomic sequencing data. *BMC Bioinf* (2016) 17:1–15. doi: 10.1186/s12859-016-0976-y
19. Pfeiffer F, Gröber C, Blank M, Händler K, Beyer M, Schultze JL, et al. Systematic evaluation of error rates and causes in short samples in next-generation sequencing. *Sci Rep* (2018) 8:1–14. doi: 10.1038/s41598-018-29325-6
20. Wang L-S, Leebens-Mack J, Wall PK, Beckmann K, Depamphilis CW, Warnow T. The impact of multiple protein sequence alignment on phylogenetic estimation. *IEEE/ACM Trans Comput Biol Bioinf* (2009) 8:1108–19. doi: 10.1109/TCBB.2009.68
21. Smirnov V, Warnow T. Phylogeny estimation given sequence length heterogeneity. *Systematic Biol* (2021) 70(2):268–82. doi: 10.1093/sysbio/syaa058
22. Machado DJ, Castroviejo-Fisher S, Grant T. Evidence of absence treated as absence of evidence: The effects of variation in the number and distribution of gaps treated as missing data on the results of standard maximum likelihood analysis. *Mol Phylogenet Evol* (2021) 154:106966. doi: 10.1016/j.ympev.2020.106966
23. Breiman L, Friedman J, Stone CJ, Olshen RA. *Classification and regression trees*. Boca Raton, FL: CRC press (1984).
24. Needleman SB, Wunsch CD. A general method applicable to the search for similarities in the amino acid sequence of two proteins. *J Mol Biol* (1970) 48:443–53. doi: 10.1016/0022-2836(70)90057-4
25. Henikoff S, Henikoff JG. Amino acid substitution matrices from protein blocks. *Proc Natl Acad Sci* (1992) 89:10915–9. doi: 10.1073/pnas.89.22.10915
26. Yang Y, Liu X. A re-examination of text categorization methods, in: *SIGIR '99: proceedings of the 22nd annual international ACM SIGIR conference on research and development in information retrieval*. New York, NY, United States: Association for Computing Machinery (1999) pp. 42–9. Available at: <https://dl.acm.org/doi/proceedings/10.1145/312624>.
27. Jiao Y, Du P. Performance measures in evaluating machine learning based bioinformatics predictors for classifications. *Quantitative Biol* (2016) 4:320–30. doi: 10.1007/s40484-016-0081-2
28. Opitz J, Burst S. Macro f1 and macro f1. *arXiv preprint arXiv:1911.03347*. (2019). doi: 10.48550/arXiv.1911.03347
29. Wickham H. *ggplot2: elegant graphics for data analysis*. New York: Springer Publishing (2016).
30. R Core Team. *R: A language and environment for statistical computing*. Oxford, UK: Oxford Academic (systemic biology) (2015).
31. Arendsee ZW, Vincent AL, Anderson TK. smot: A python package and CLI tool for contextual phylogenetic subsampling. *J Open Source Softw* (2020) 7(80):4193. doi: 10.21105/joss.04193
32. Katoh K, Standley DM. MAFFT multiple sequence alignment software version 7: improvements in performance and usability. *Mol Biol Evol* (2013) 30:772–80. doi: 10.1093/molbev/mst010
33. Kears M, Moir R, Wilson A, Stones-Havas S, Cheung M, Sturrock S, et al. Geneious Basic: an integrated and extendable desktop software platform for the organization and analysis of sequence data. *Bioinformatics* (2012) 28:1647–9. doi: 10.1093/bioinformatics/bts199
34. Nguyen L-T, Schmidt HA, Von Haeseler A, Minh BQ. IQ-TREE: a fast and effective stochastic algorithm for estimating maximum-likelihood phylogenies. *Mol Biol Evol* (2015) 32:268–74. doi: 10.1093/molbev/msu300
35. Dang CC, Le QS, Gascuel O, Le VS. FLU, an amino acid substitution model for influenza proteins. *BMC evolutionary Biol* (2010) 10:1–11. doi: 10.1186/1471-2148-10-99
36. Rambo-Martin BL, Keller MW, Wilson MM, Nolting JM, Anderson TK, Vincent AL, et al. Influenza A virus field surveillance at a swine-human interface. *MSphere* (2020) 5:e00822–00819. doi: 10.1128/mSphere.00822-19
37. Hoenen T, Groseth A, Rosenke K, Fischer RJ, Hoenen A, Judson SD, et al. Nanopore sequencing as a rapidly deployable Ebola outbreak tool. *Emerging Infect Dis* (2016) 22:331. doi: 10.3201/eid2202.151796
38. Quick J, Loman NJ, Duraffour S, Simpson JT, Severi E, Cowley L, et al. Real-time, portable genome sequencing for Ebola surveillance. *Nature* (2016) 530:228–32. doi: 10.1038/nature16996
39. Laver T, Harrison J, O'Neill P, Moore K, Farbos A, Paszkiewicz K, et al. Assessing the performance of the oxford nanopore technologies minion. *Biomolecular detection quantification* (2015) 3:1–8. doi: 10.1016/j.bdq.2015.02.001
40. Delahaye C, Nicolas J. Sequencing DNA with nanopores: Troubles and biases. *PLoS One* (2021) 16:e0257521. doi: 10.1371/journal.pone.0257521
41. Sun H, Yang J, Zhang T, Long L-P, Jia K, Yang G, et al. Using sequence data to infer the antigenicity of influenza virus. *MBio* (2013) 4:e00230–00213. doi: 10.1128/mBio.00230-13
42. Zeller MA, Gauger PC, Arendsee ZW, Souza CK, Vincent AL, Anderson TK. Machine learning prediction and experimental validation of antigenic drift in H3 influenza A viruses in swine. *MSphere* (2021) 6:e00920–00920. doi: 10.1128/mSphere.00920-20
43. Koel BF, Burke DF, Bestebroer TM, van der Vliet S, Zondag GC, Vervaeke G, et al. Substitutions near the receptor binding site determine major antigenic change during influenza virus evolution. *Science* (2013) 342:976–9. doi: 10.1126/science.1244730
44. Lewis NS, Anderson TK, Kitikoon P, Skepner E, Burke DF, Vincent AL. Substitutions near the hemagglutinin receptor-binding site determine the antigenic evolution of influenza A H3N2 viruses in US swine. *J Virol* (2014) 88:4752–63. doi: 10.1128/JVI.03805-13
45. Abente EJ, Santos J, Lewis NS, Gauger PC, Stratton J, Skepner E, et al. The molecular determinants of antibody recognition and antigenic drift in the H3 hemagglutinin of swine influenza A virus. *J Virol* (2016) 90:8266–80. doi: 10.1128/JVI.01002-16



OPEN ACCESS

EDITED BY

Sarah J. Edwards,
Commonwealth Scientific and Industrial
Research Organisation (CSIRO), Australia

REVIEWED BY

Hong Dong,
The Ohio State University, United States
Enric M. Mateu,
Autonomous University of Barcelona, Spain

*CORRESPONDENCE

Constantinos S. Kyriakis
✉ csk@auburn.edu

RECEIVED 13 July 2023

ACCEPTED 16 November 2023

PUBLISHED 18 December 2023

CITATION

Neasham PJ, Pliasis VC, North JF, Johnson C,
Tompkins SM and Kyriakis CS (2023)
Development and characterization of an
immortalized swine respiratory cell line for
influenza A virus research.
Front. Vet. Sci. 10:1258269.
doi: 10.3389/fvets.2023.1258269

COPYRIGHT

© 2023 Neasham, Pliasis, North, Johnson,
Tompkins and Kyriakis. This is an open-access
article distributed under the terms of the
[Creative Commons Attribution License \(CC BY\)](#).
The use, distribution or reproduction in other
forums is permitted, provided the original
author(s) and the copyright owner(s) are
credited and that the original publication in this
journal is cited, in accordance with accepted
academic practice. No use, distribution or
reproduction is permitted which does not
comply with these terms.

Development and characterization of an immortalized swine respiratory cell line for influenza A virus research

Peter J. Neasham^{1,2}, Vasilis C. Pliasis^{1,2}, J. Fletcher North^{1,2},
Celeste Johnson¹, S. Mark Tompkins^{2,3} and
Constantinos S. Kyriakis^{1,2,3*}

¹Department of Pathobiology, College of Veterinary Medicine, Auburn University, Auburn, AL, United States, ²Emory-UGA Center of Excellence for Influenza Research and Surveillance (CEIRS), Atlanta, GA, United States, ³Center for Vaccines and Immunology, University of Georgia, Athens, GA, United States

Introduction: Swine serve as an important intermediate host species for generating novel influenza A viruses (IAVs) with pandemic potential because of the host's susceptibility to IAVs of swine, human and avian origin. Primary respiratory cell lines are used in IAV research to model the host's upper respiratory tract *in vitro*. However, primary cell lines are limited by their passaging capacity and are time-consuming for use in industry and research pipelines. We were interested in developing and characterizing a biologically relevant immortalized swine respiratory cell line that could be used for efficient propagation and characterization of swine IAV isolates.

Methods: Lung tissue for the generation of primary swine respiratory cells were isolated from the bronchi of an 8-week-old Yorkshire/Hampshire pig, which were immortalized by transduction of the SV40 T antigen using a lentivirus vector. The transduction of the SV40 T antigen was confirmed by Real Time RT-PCR in cells passaged greater than twenty times.

Results: Immortalized swine respiratory cells expressed primarily $\alpha 2,6$ sialic acid receptors and were susceptible to both swine and human IAVs, with swine viruses exhibiting higher replication rates. Notably, infection with a swine H3N2 isolate prompted increased IL-6 and IL-1 α protein secretion compared to a seasonal human H3N2 virus. Even after 20 passages, the immortalized cells maintained the primary respiratory cell phenotype and remained permissive to IAV infection without exogenous trypsin.

Discussion: In summary, our developed immortalized swine respiratory cell line offers an alternative *in vitro* substrate for studying IAV replication and transmission dynamics in pigs, overcoming the limitations of primary respiratory cells in terms of low passage survivability and cost.

KEYWORDS

swine, influenza A virus, primary respiratory cells, immortalized respiratory cells, cells characterization

Introduction

Influenza A viruses (IAV) are enveloped, negative sensed RNA viruses with a single stranded and segmented genome, which belong to the *Orthomyxoviridae* family. Wild birds serve as the natural host reservoir for IAV. However, IAV has a relatively wide host range and has been isolated in both avian and mammalian species including: domesticated birds, humans, swine,

canines, equines, felines, and aquatic mammals. The ability of IAV to jump multiple species barriers is enabled by the segmented nature of the IAVs genome, which enables reassortment of whole gene segments between co-infecting IAV strains and lack of a proofreading mechanism enabling rapid drift of the viruses surface glycoproteins (1).

In mammalian hosts, IAV is known to cause respiratory disease. IAV enters into respiratory tract and enters into primarily respiratory epithelial cells that express glycoprotein receptors that terminate with sialic acids (SA). The SA is attached to a galactose molecule, which provides a recognition site for the receptor binding domain (RBS) of the IAV haemagglutinin (HA) protein, facilitating receptor mediated endocytosis. The HA protein can bind to SA receptors in either an 2,3 or 2,6 linked configuration. Strains of avian-origin preferentially bind to host cells in an 2,3 configuration, whilst mammalian-origin strains preferentially bind in an 2,6 configuration (2–6). The distribution of SA receptors is implicated as a host range factor that IAVs must overcome to cross species barriers.

In the human and swine hosts, the distribution of α 2,3 and α 2,6 linked SA are similar in the respiratory tract (7–9). However, IAVs encoding solely human (hu) origin gene segment are isolated from swine during passive surveillance (10–13). This suggests that reverse zoonotic transmission of IAVs at the human/swine interface is not solely dependent on SA distribution of the host, and multiple host and viral factors are involved with the ability of the IAV to efficiently transmit and replicate within the swine host (14).

Cell lines are often used in IAV research to propagate and to assess the transmission and replicatory potential of novel isolates within a particular host for pandemic preparation. Primary respiratory epithelial cell lines are currently the gold-standard cellular model for assessing the physical properties of IAV strains and can be fully differentiated in an air–liquid interface (ALI) system to produce a pseudostratified epithelium, containing ciliated cells and goblet cells, that models the respiratory structure and architecture of the hosts lungs *in vitro* (3, 15–18). However, primary cell lines are limited by the low number of passages before reaching senescence, susceptibility to contamination and verification of the absence of pathogens, high cost of reagents needed to grow and maintain the cells in ALI, donor-to-donor variability, availability of host tissue, and the time taken to fully differentiate the cells (3–4 weeks in ALI). Consequently, immortalized respiratory cell lines are used as an alternative cellular model to study the properties of IAV isolates to a susceptible host. However, immortalized respiratory cell lines may have altered physical properties to the primary host cell. This includes losing the ability to secrete proteases necessary for IAV entry into the host cell and differentiate. Immortalized swine tracheal (siTEC) and nasal epithelial (siNEC) cells have been previously developed by transducing the SV40-T antigen using a lentivirus vector (19). The siTEC and siNEC cell lines were permissive to H1N1, H1N2, and H3N2 IAV strains and retained the functional characteristics of the primary cells (19).

In this study, we developed an immortalized swine bronchial epithelial cell line for IAV research by introducing Simian Virus 40 (SV40-T) antigen into primary swine respiratory cells harvested from the bronchi of an 8 weeks old porcine reproductive and respiratory virus (PRRSv) and IAV seronegative pig. Porcine bronchial epithelial cells (PBEC) have been immortalized by delivering human telomerase reverse transcriptase (h-TERT), to extend the replicative capacity of cells through telomerase extension (20). However, our primary

objective was to establish an immortalized swine bronchial epithelial cell line via transduction of SV40-T antigen.

The immortalized swine respiratory cells appeared mostly of epithelial origin and retained morphological characteristics of the swine primary cells. In addition, both primary and immortalized swine respiratory cells were permissive to human (huIAV) and swine (swIAV) IAVs of H1N1, H1N2, and H3N2 subtypes that most predominantly circulate at the human/swine interface and modelled host restriction of wholly human-origin H3N2 observed in the swine host. Our results suggest that the immortalized swine respiratory cells could be used as an appropriate immortalized cellular model for the lower respiratory tract of the swine host and may serve as a tool to study the transmission and replicatory potential of novel IAV strains.

Materials and methods

Cell culture and virus stocks

Madin-Darby canine kidney (MDCK) cells were cultured in Dulbecco's modified Eagles' medium (DMEM) (Invitrogen), supplemented with 10% fetal bovine serum (FBS) and 1% penicillin–streptomycin. The MDCK cells were maintained at 37°C in a 5% CO₂ atmosphere. Influenza A viruses used in this study were propagated in MDCK cells (ATCC). Virus titers were quantified by TCID₅₀ and calculated using the Reed and Muench method (21).

Harvesting, isolation, and immortalization of primary respiratory swine cells

Lung tissue for the isolation of swine respiratory cells were collected from an 8 weeks-old Yorkshire/Hampshire pig. Lung tissue was rinsed in phosphate-buffered saline (PBS) and sections from the bronchi were sliced into small pieces. The sliced bronchial tissue was incubated for 2 h with 800 U collagenase at 37°C and 5% CO₂. Following collagenase digestion, respiratory cells were strained through a 70 μ m cell strainer and centrifuged. The cell pellet was washed twice with PBS and cells were seeded onto collagen coated flasks. Cells were incubated for 24 h at 37°C and 5% CO₂ in DMEM/F12 supplemented with FBS, retinoic acid, bovine pituitary extract (BPE), epidermal growth factor, cholera toxin, transferrin, insulin, and penicillin/streptomycin (growth media). Following the 24 h incubation, non-adherent cells were transferred to rat-tail collagen (Corning) coated flask and cultured until fully confluent.

At passage four, primary swine respiratory cells were plated in growth media onto rat-tail collagen coated 6-well plates (1×10^5). Once the cells reached 70% confluence, the growth media was removed, and cells were washed with PBS. Target primary swine respiratory cells were infected and incubated overnight at 37°C and 5% CO₂ with 10^7 Lenti-SV40T vector (abm) in the presence of 10 μ g/mL polybrene. Following the overnight incubation, supernatant from lentivirus infected swine cells was removed, and cells were washed with PBS. Fresh growth media was added to the cells, which were incubated for 72 h at 37°C and 5% CO₂. Immortalized swine respiratory cells were passaged >20 times and successful transduction of the SV40 T antigen gene into the immortalized swine respiratory

cells was confirmed by quantitative reverse transcription polymerase chain reaction (RT-qPCR) using SV40 T antigen targeting primers 5' ACTGAGGGGCCTGAAATGA, 5' GACTCAGGGCATGAAAC AGG. Swine respiratory cells were confirmed of swine origin using swine GAPDH targeting primers 5' ACCCAGAAGACTGTGGATGG and 5' ACGCCTGCTTCACACCTTC.

Immunofluorescent staining and confocal microscopy

Immortalized (P20) and primary (P6) swine respiratory cells were seeded (1×10^5) into 6-well plates to 70–80% confluency onto coverslips coated with rat-tail collagen (Corning) and inoculated with either control/PBS, A/TX/12/H3N2 or A/swine/MN/12/H3N2 at an MOI of 0.1 diluted in PBS (–/–). At 24 hpi, cells were washed twice and fixed using 4% paraformaldehyde and permeabilised with 0.5% TritonX/PBS for 30 min. The cells were blocked in 10% goat serum with PBS/Tween20 for 1 h prior to staining with the primary antibodies:

Cytokeratin 18 staining

Immortalized and primary swine respiratory cells were incubated for 1 h with anti-cytokeratin 18 mouse monoclonal antibody (Abcam) (1:200).

Vimentin staining

Immortalized and primary swine respiratory cells were incubated for 1 h with anti-vimentin rabbit monoclonal antibody (Abcam) (1:400).

Lectin staining

Immortalized and primary swine respiratory cells were incubated for 1 h with biotinylated *Maackia amurensis* lectin I and II (Vector® Laboratories) (1:800), to stain α 2,3-linked SA receptors or fluorescein isothiocyanate (FITC)-conjugated *Sambucus nigra agglutinin* (Vector® Laboratories) (1,200) to stain for α 2,6-linked SA receptors.

Influenza A virus staining

Immortalized swine respiratory cells were incubated for 45 min with anti-alpha tubulin (1:800), anti-beta-tubulin (1:200), and anti-influenza A nucleoprotein (1:500).

After staining with the appropriate primary antibodies, cells were washed 3× with PBS/Tween20 and stained with secondary antibodies: goat anti-mouse Alexa Fluor 546 (Invitrogen) (1:400), goat anti-rabbit Alexa Fluor 488 (Invitrogen) (1:400) or goat anti-mouse FITC (1:400). Coverslips were transferred to slides and mounted using slowfade mounting medium (Invitrogen). The slides were visualized using ECHO revolve fluorescent microscope (ECHO A Bico Company, San Diego, CA). All captured images were edited and process using FIJI software (22).

Influenza A virus infections

Immortalized (P24) swine respiratory cells were seeded (1×10^5) onto 6-well plates and cultured in growth media onto rat-tail collagen (Corning) coated 6-well plates until 80% confluency. Cells were then washed in PBS and inoculated with a panel of hu- and swIAVs (Table 1) at an MOI of 0.1 diluted in PBS (–/–). Following IAV inoculation, cells were incubated for 2 h at 37°C and 5% CO₂ before washing cells with PBS and replacing the inoculum with fresh FBS free growth media. The inoculated cells were incubated at 37°C and 5% CO₂ until the appropriate end point of collection (0-, 24-, 48-, 72-hpi). At this point, cell supernatant was harvested and IAV was quantified by TCID₅₀ and calculated using the Reed and Muench method as previously described. Samples were analyzed using three biological replicates from each time point.

Quantification of cytokine/chemokine secretion from primary and immortalized swine respiratory cells

Supernatant from primary (P6) and immortalized (P24) swine respiratory cell inoculated with either A/TX/12/H3N2 or A/swine/MN/12/H3N2 at an MOI of 0.1 harvested at –24 and –48 hpi was analyzed for IL-1 α , IL-6, and IL-8 secretion using the MILLIPLEX MAP Porcine Cytokine/Chemokine Magnetic Bead panel per manufacture's instruction (EMD Millipore Corporation, Billerica, MA).

Statistics

Statistical analysis was performed using GraphPad Prism 9.3.1. A two-way ANOVA was used to identify significance differences between IL-1 α , IL-6, and IL-8 secreted from the immortalized (P24) and primary (P6) swine respiratory cells that were either mock infected (PBS), or inoculated independently with A/TX/12/H3N2 or A/swine/MN/12/H3N2. To determine the percentage of vimentin positive cells in the immortalized (P20) and primary (P6) swine respiratory cell lines, IF images taken on the ECHO revolve fluorescent microscope (ECHO A Bico Company, San Diego, CA) were processed using FIJI software and vimentin positive cells were counted and subtracted from the number of DAPI positive cells ($n = 3$).

Results

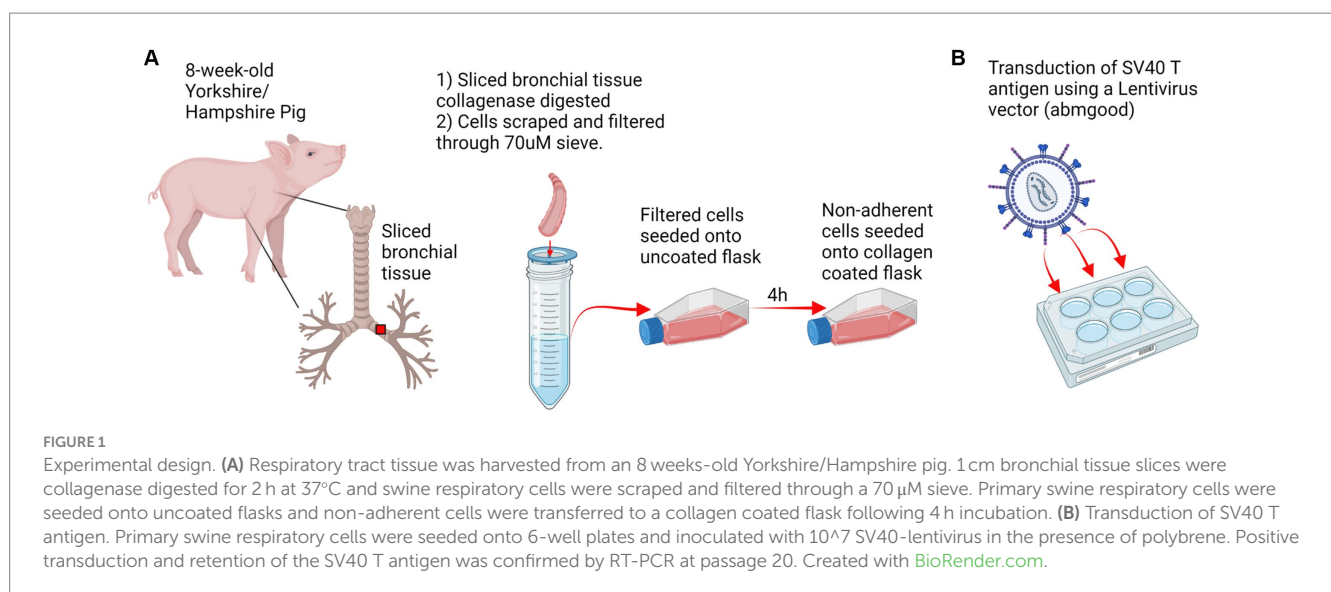
Immortalized swine respiratory cells maintain functional properties of primary cell counterparts

Primary swine respiratory cells were isolated from the bronchi of an 8 weeks old Yorkshire/Hampshire and immortalized by transduction of the SV40-T antigen following 4 successful passages (Figure 1). The immortalized swine respiratory cells were successfully passaged >20 times, whilst primary swine respiratory cells failed to proliferate at P16. SV40 T antigen retention in the immortalized swine respiratory cells was confirmed by rt-qPCR, with a mean SV40-T

TABLE 1 Immortalized swine respiratory cells are permissible to hu and swIAV strains of H1N1, H1N2, and H3N2 subtypes.

Virus name	Abbreviation	Subtype	Origin	Virus Titer 24 hpi	Virus Titer 48 hpi	Virus Titer 72 hpi	Area under curve
				(log10 TCID ₅₀ /mL)	(log10 TCID ₅₀ /mL)	(log10 TCID ₅₀ /mL)	
A/Puerto Rico/8/1934	A/PR8/1935	H1N1	Human	4.88 ± 0.22	6.21 ± 0.29	5.22 ± 0.11	329 ± 11.09
A/New Caledonia/20/99	A/NewCal/1999	H1N1	Human	4.77 ± 0.27	6.11 ± 0.11	5.55 ± 0.22	327.9 ± 9.90
A/Brisbane/10/2007	A/Bris/2007	H3N2	Human	3.83 ± 0.16	5.22 ± 0.11	4.61 ± 0.05	272.6 ± 5.97
A/Perth/16/2009	A/Perth/2009	H1N1	Human	2.38 ± 0.39	3.89 ± 0.11	2.78 ± 0.27	183.9 ± 13.27
A/CA/07/2009	A/CA/2009	H1N1	Human/pdm	4.77 ± 0.11	6.05 ± 0.27	6.5 ± 0.5	337.8 ± 13.61
A/Victoria/361/2011	A/VIC/2011	H3N2	Human	4.55 ± 0.05	5.33 ± 0.16	3.77 ± 0.39	282.6 ± 9.77
A/TX/50/2012	A/TX/2012	H3N2	Human	3.6 ± 0.05	4.6 ± 0.05	1.17 ± 0.16	211.1 ± 4.11
A/swine/MN/A01125993/2012	A/swine/MN/2012	H3N2	Swine	7.34 ± 0.05	7.44 ± 0.11	6.89 ± 0.11	438.5 ± 4.33
A/Hong Kong/4081/2014	A/HK/2014	H3N2	Human	3.11 ± 0.11	3.88 ± 0.22	1.67 ± 0.16	181.8 ± 8.09
A/swine/NC/KH1552516/2016	A/swine/NC/2016	H3N2	Swine	3.55 ± 0.46	6.28 ± 0.14	7.05 ± 0.24	320.5 ± 15.74
A/WI/588/2019	A/WI/2019	H1N1	Human/pdm	4.6 ± 0.05	6.05 ± 0.27	5.94 ± 0.24	327.2 ± 9.68
A/swine/GA/27480/2019	A/swine/GA/2019	H1N2	Swine	5.55 ± 0.11	7.55 ± 0.22	7.83 ± 0.16	408.5 ± 8.09

Replication kinetics of H1N1, H1N2, and H3N2 hu and swIAV subtypes in immortalized swine respiratory cells. Immortalized swine respiratory cells were seeded onto rat-tail collagen coated 6-well and inoculated independently with H1N1 or H3N2 huIAVs, or H1N2, or H3N2 swIAV strains at an MOI of 0.1. Supernatant was harvested at 0-, 24-, 48-, and 72 h post infection and IAV titers were measured by TCID₅₀. The averages of three replicates. ± represents standard error ($n = 3$).



antigen Cq value of 27.7 ($n = 3$) in cells passaged 20 times (Supplementary Table S1). Visually, immortalized swine respiratory cells maintained the morphological features of primary swine respiratory epithelial cells, such as, possessing the ability to form tight-junctions and a cobble-stone like appearance (Figure 2). The primary and immortalized swine respiratory cells expressed both $\alpha 2,3$ and $\alpha 2,6$ linked SA receptors, which are an important host restriction factor for IAV entry into the host cell (Figure 3). Both primary and immortalized cell lines expressed $\alpha 2,6$ linked SA receptors at a higher abundance compared to $\alpha 2,3$ linked SA receptors (Figure 3). In addition, the immortalized swine respiratory cells appeared to be mostly of epithelial origin, which was demonstrated by the majority of visualized cells expressing the epithelial marker cytokeratin 18 (Figure 4).

Staining with the epithelial-mesenchymal transition and fibroblast marker vimentin, demonstrated that the isolated primary swine respiratory cells contained a high percentage (56.7%) of contaminating cells (Supplementary Figure S1). However, following trypsin-treatment and immortalization via SV40-T antigen transduction, we observed a decrease in the mean percentage of vimentin positive cells (32.08%), which was maintained up to 20 passages (Supplementary Figure S1).

We evaluated the permissibility of either cell lines to IAV's of mammalian origin, given the similar distribution of SA receptors to the swine hosts respiratory tract. Both primary and immortalized swine respiratory cell lines were permissive to A/TX/2012/H3N2 (Figure 5A), pdm A/CA/2009/H1N1 (Figure 5B) huIAV strains, A/

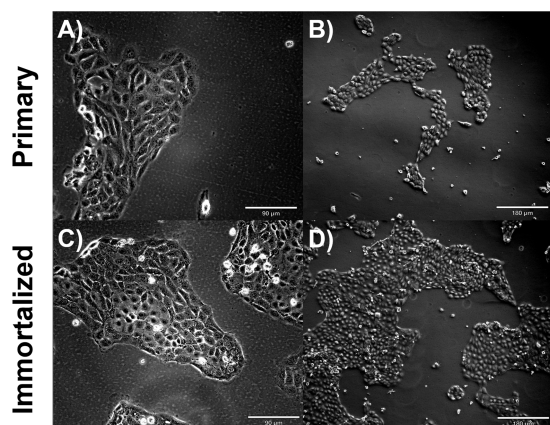


FIGURE 2
Immortalized and primary swine respiratory cell phenotype. Immortalized and primary swine respiratory cells were seeded onto collagen coated flasks and incubated at 37°C and 5% CO₂ for 2 days. Bright field primary respiratory cells at P6 (A) Magnification x10, Scale Bar 90 μm, (B) Magnification x20, Scale Bar 180 μm. Bright field primary swine respiratory cells at P20 (C) Magnification x10, Scale Bar 90 μm (D) Magnification x20, Scale Bar 180 μm.

swine/GA/2019/H1N2 (Figure 5C), and A/swine/MN/2012/H3N2 swIAV strains (Figure 5D). However, A/TX/2012/H3N2 replicated to lower titers compared to the other panel of IAV strains, which was most pronounced at 72-hpi (Figure 5A). This trend was reflected in both the primary and immortalized swine respiratory cell lines, which suggests that the host specificity of swine respiratory cells was not impacted by immortalization via SV40 T antigen transduction.

Immortalized swine respiratory cells are permissible to IAV strains of human and swine H1N1, H1N2, and H3N2 subtypes

The viral replication kinetics of both human and swine-origin strains were evaluated to assess the permissiveness of the immortalized cells to IAV strains of H1N1, H1N2, and H3N2 subtypes. The panel of strains were selected to represent IAV subtypes that commonly circulate at the human/swine interface. The immortalized swine respiratory cells were permissible to the entire panel of IAV strains, regardless of IAV host-origin or subtype (Table 1). However, we did measure differences in the ability of individual strains to replicate within the immortalized cell line. Generally, huIAV H3N2 strains

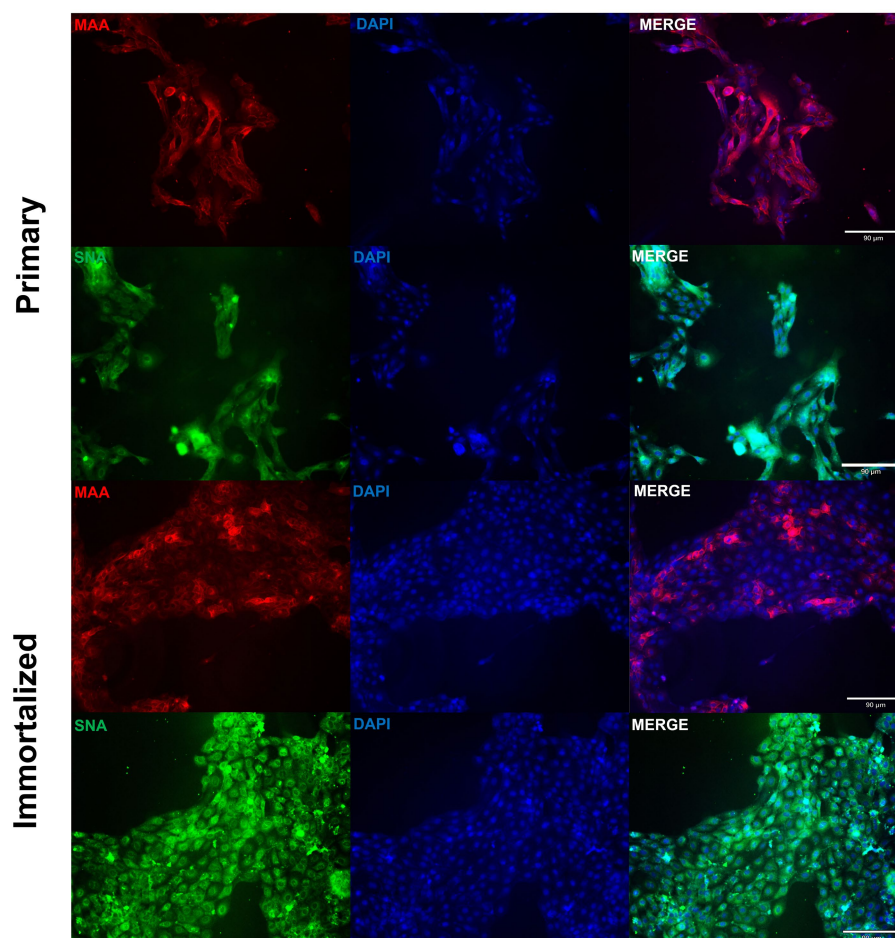


FIGURE 3
Primary and immortalized swine respiratory cells express α2,6 sialic acid receptors. Primary (P6) and immortalized swine respiratory (P20) cells were seeded onto 6-well rat-tail collagen coated coverslips and stained with DAPI (blue) and either *Maackia amurensis* (MAA, red) or *Sambucus nigra* agglutinin (SNA, green) lectins. Magnification x10, Scale Bar 90 μm.

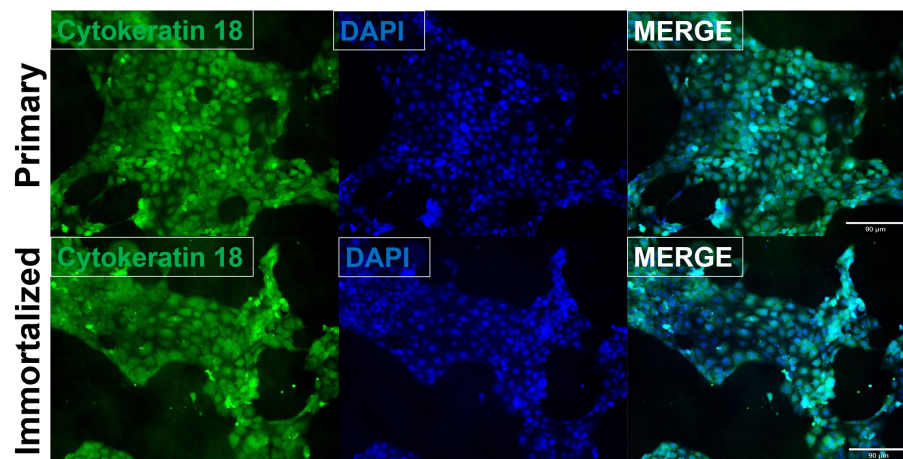


FIGURE 4

Immortalized swine respiratory cells are primarily of epithelial origin. Following harvesting, isolation, and immortalization, both the primary (P6) and immortalized (P20) swine respiratory cells were seeded onto 6 well rat-tail collagen coated coverslips and stained for cytokeratin 18 (green) and DAPI (blue). Magnification $\times 10$.

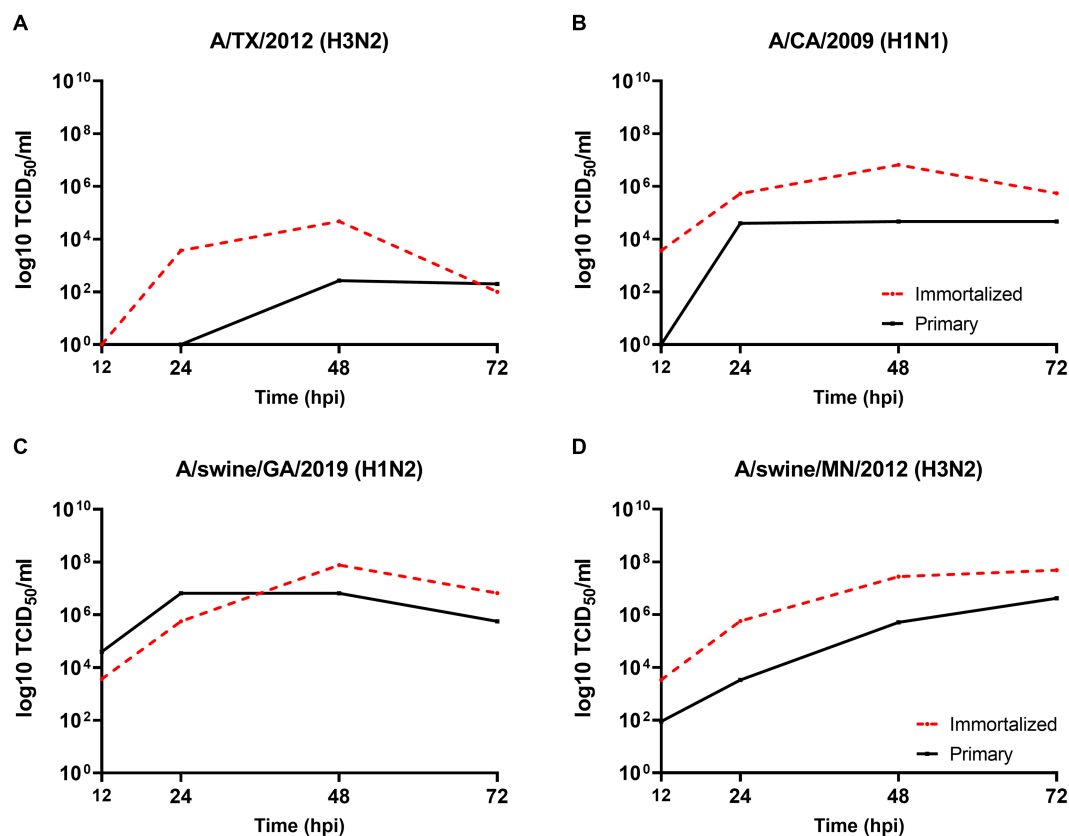


FIGURE 5

Primary and immortalized swine respiratory cells are permissible to hu- and swIAVs. Primary (solid black line) and Immortalized (dashed red line) respiratory swine cells (P6 and P24 respectively), were seeded onto 6-well rat-tail collagen coated coverslips and inoculated independently with either A/TX/2012/H3N2 (A), A/CA/2009/H1N1 (B), A/swine/GA/2019/H1N2 (C), or A/swine/MN/2012/H3N2 (D) at an MOI of 0.1. Supernatant was harvest, 12-, 24-, 48-, and 72-hpi and viral titers were quantified by TCID₅₀.

replicated poorly within the immortalized swine respiratory cell compared to swIAVs. The highest difference between peak titers were measured between A/swine/GA/2019/H1N2 (7.83 TCID₅₀/mL), and

A/TX/2012/H3N2 (1.17 TCID₅₀/mL) at 72-hpi. Whilst the greatest difference in area under curve (AUC) was observed between A/swine/MN/2012/H3N2 (438.5), and the A/HongKong/2014/H3N2 huIAV

strain (181.8). Overall, the replication kinetics of the panel of IAVs imply that the swIAVs replicate more efficiently in the immortalized swine respiratory cells, which provides evidence of swine host specificity.

We observed no differences in the viral titers and AUC values between A/CA/2009/H1N1 (pdm strain), A/NewCal/1999/H1N1 (pre-pandemic strain), and A/WI/2019/H1N1 (post-pandemic-like strain) at 24-, 48-, and 72-hpi (Table 1).

Wholly huIAV H3N2 strains replicate poorly and produce a mild pro-inflammatory cytokine response in immortalized swine respiratory cells

From the panel of H1N1, H1N2, and H3N2 hu and sw-origin IAVs evaluated in the immortalized swine respiratory cells (Table 1), we selected A/TX/2012/H3N2 and A/swine/MN/2012/H3N2 strain, encoding the triple reassortment internal gene (TRIG) cassette, to compare the replication and pro-inflammatory responses between wholly huIAV and swIAV H3N2 strains. Using immunohistochemistry, we were unable to visualize A/TX/2012/H3N2 nucleoprotein (NP) at 24-hpi (Figure 6). Although, both the A/TX/2012/H3N2 and A/swine/MN/2012/H3N2 NP protein was visualized at 72-hpi (Figure 6). This showed that there was a delay in the replication of the wholly huIAV H3N2 strain, compared to the TRIG swIAV H3N2 strain in the immortalized swine respiratory cells.

We evaluated IL-1 α , IL-6, and IL-8 pro-inflammatory cytokine protein production from the immortalized swine respiratory cells following independent inoculation from either A/TX/2012/H3N2 or A/swine/MN/2012/H3N2. There was no significant difference in production of IL-1 α , IL-6, and IL-8 between the A/TX/2012/H3N2 and A/swine/MN/2012/H3N2 infected immortalized swine respiratory cells at 24-hpi (Figures 7D–F). Whilst IL-1 α and IL-6 secretion was significantly higher at 48-hpi when infected with A/swine/MN/2012/H3N2 (Figures 7D,E). Additionally, IL-6 and IL-8 secretion was significantly higher at 48-hpi following inoculation from either A/TX/2012/H3N2 or A/swine/MN/2012/H3N2 compared to the control (Figures 7E,F).

Discussion

The development of an immortalized swine respiratory cell line is a useful tool for the assessment of novel IAV isolates from the field. Swine are an important natural and intermediate reservoir host species and are considered the ‘mixing vessel’ for the reassortment of co-infecting IAV strains in a singular host, leading to the generation of novel strains which may pose a pandemic threat to humans. This is partially due to the highly diverse pool of currently circulating IAV strains in the swine host, which increases the potential combinations of novel strains evolving. In addition, many of the circulating strains incorporate wholly human IAV gene segments into their genome and generate novel strains that possess the molecular tools to transmit and replicate within the human host. The gold-standard *in vitro* model for assessing the pandemic potential of novel isolates at the human/swine interface includes primary respiratory epithelial cells isolated from the host and fully differentiated in ALI. However, given the time taken to

fully differentiate the primary cell lines, we were interested in developing an immortalized respiratory epithelial cell line that maintained the characteristic of the primary swine host. This would enable a more efficient pipeline for identifying the transmission and replication success of novel IAV isolates within the swine host and fast-track the development of vaccines against highly virulent strains.

In this study, we harvested and isolated respiratory cells from the bronchi of an 8 weeks-old Yorkshire/Hampshire swine and immortalized the cell line by delivering the SV40-T antigen to the isolated primary cells. We demonstrated that immortalized swine respiratory cell lines were primarily of epithelial origin, as indicated through expression of CK18, which has been used as a marker for respiratory epithelial cells and simple epithelia (23). In addition, staining for potential contaminating cells, such as, fibroblasts and epithelial-mesenchymal transitioning (EMT) cells, revealed that there was a decrease in the percentage of contaminating cells following immortalization via SV40 T antigen transduction (Supplementary Figure S1). However, we were unable to develop a pure population of immortalized swine bronchial epithelial cells and our mixed immortalized swine respiratory cell line contained approximately 30% of undesired fibroblastic or EMT cells.

We demonstrated that both the primary and immortalized swine respiratory cells expressed both α 2,3 and α 2,6 SA receptors in a similar distribution to what is observed in the lower respiratory tract of the swine host (2, 4, 9). Since, the primary and immortalized swine respiratory cells expressed α 2,6 SA, we proposed that both the primary and immortalized cell lines would be permissible to mammalian IAVs and would be an appropriate model to assess strains isolated at the human/swine interface. We measured the replication kinetics of four IAV isolates in both the primary and immortalized swine respiratory cell lines, which included the wholly human-origin A/TX/12/H3N2 huIAV, A/CA/09/H1N1 pandemic strain (pdm09) belonging to the pandemic clade (1A.3.3.2), A/swine/GA/19/H1N2 delta 2 clade (1B.2.1), and A/swine/MN/12/H3N2 swIAVs (Figure 4). The primary swine respiratory cells were permissible to all tested huIAV and swIAVs. However, A/TX/12/H3N2 huIAV replicated to lower titers and for a reduced time in comparison to either of the tested swIAVs, or A/CA/09/H1N1 that originated from the swine host. We hypothesized that this phenomenon observed within the primary swine respiratory cells was due to a lack of adaptation of the huIAV to the swine respiratory cells leading to a robust innate immune response to prevent viral replication. Additionally, we observed similar replication kinetics of the four IAVs in the immortalized swine respiratory cells. Although, the trends observed with the IAV titers were mostly exaggerated in the immortalized swine respiratory cell line, which we theorize could be caused by the immortalization process selecting for a more homogeneous cellular population. In future studies, it would be interesting to further characterize the immortalized cellular population and identify molecular determinants that are selected for during SV40-T antigen immortalization. In addition, to characterize the innate immune responses within sub-populations of immortalized swine respiratory cells that enable enhanced replication of hu- and swIAVs.

We assessed the replication kinetics of an extensive panel of H1N1, H1N2, and H3N2 hu- and swIAVs isolated between 1999 and 2019 in the immortalized swine respiratory cells. All isolates used in the study were permissible in the immortalized swine respiratory cells without the need of trypsin protease to enable IAV entry in the

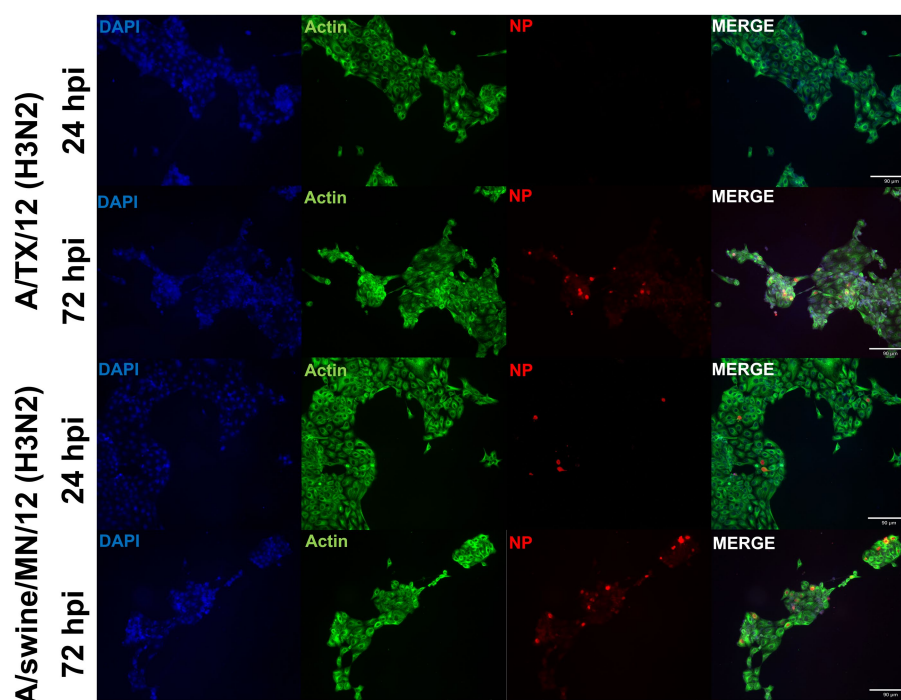


FIGURE 6

Human-origin H3N2 strain replicates poorly in immortalized swine respiratory cells compared to swIAV H3N2 counterpart. Immortalized swine respiratory cells (P20) were seeded onto 6-well rat-tail collagen coated coverslips and inoculated independently with either A/swine/MN/12/H3N2 or A/TX/2012.H3N2 at an MOI of 0.1. At 24 hpi, coverslips were stained with NP (red), alpha/beta actin (green), and DAPI (blue). Magnification $\times 10$, Scale Bar 90 μm .

host cell. This implies that protease secretion was not lost following SV40-T antigen immortalization. Mostly, H3N2 huIAVs replicated poorly in the immortalized swine respiratory cells compared to H1N1 or H3N2 strains encoding gene segments of swine-origin. This poor replication of wholly huIAV H3N2 strains has been observed experimentally in the swine host and requires further investigation from both a host and viral standpoint. Surprisingly, we observed similar replication titers and total AUC curve values between pre-pdm09 A/NewCal/99/H1N1, pdm09 A/CA/09/H1N1, and post-pdm09 A/WI/19/H1N1 strains. The pdm strain was a novel reassortment of IAV gene segments of human, classical swine, and avian origin, which was first transmitted to the human host in early 2009. The A/CA/2009/H1N1 strain was able to efficiently transmit between humans, leading to a global pandemic outbreak (24). Accordingly, we were surprised to observe no significant differences between the replication kinetics of A/NewCal/99/H1N1 and A/CA/09/H1N1 in the immortalized swine respiratory cells. However, this observation may highlight limitations in utilizing solely *in vitro* assays to model the complex physiology and immunity of the swine host, which includes multiple physical barriers and cell types that determine the infectivity of IAV within the swine host. Additionally, previous studies have investigated the effects of temperature on the replication kinetics of huIAVs and swIAVs within swine host cells, which we did not address in this study (11, 25). It would be of interest to assess host body temperature and its role as a host factor that IAVs must overcome to efficiently replicate within primary and immortalized swine respiratory cells. In addition, to assess whether temperature influences the replication kinetics of IAVs possessing a specific arrangement of internal gene constellations.

We were interested in measuring the differential pro-inflammatory response of the cell line following inoculation of either hu- or swIAVs. This was because of the differences observed between the replication kinetics of H3N2 subtypes in the immortalized swine respiratory cells (Table 1). In this study, we tested and compared A/TX/12/H3N2 huIAV and A/swine/MN/12/H3N2 swIAV, isolated from the same year and of the same subtype. We found that there was a significant increase in the production of IL-1 α and IL-6 following inoculation of A/swine/MN/12/H3N2 at 48 hpi, compared to inoculation from A/TX/12/H3N2, and no significant difference in the secretion of IL-8 at 24 and 48 hpi (Figure 7). Previously, it has been demonstrated that fibroblasts secrete IL-6, and under specific conditions, IL-1 α (26, 27). Consequently, it is essential to note that the observed increase in IL-6 and IL-1 α following IAV inoculation may have been influenced by the proportion of contaminating cells in the primary and immortalized swine respiratory cell lines developed in this study. Nevertheless, despite this potential influence, we observed a significant increase in IL-1 α and IL-6 production following inoculation with the swIAV H3N2 strain compared to the huIAV H3N2 counterpart (Figure 7). In the future, we want to further assess the cytokine production from the immortalized swine respiratory cell line inoculated with a broader panel of hu- and swIAVs. In addition, to extend the assessment of time points to compare the kinetics of secreted cytokines (28, 29).

Conclusion

We have developed an immortalized swine respiratory cell line that retained most of the characteristics of its primary swine

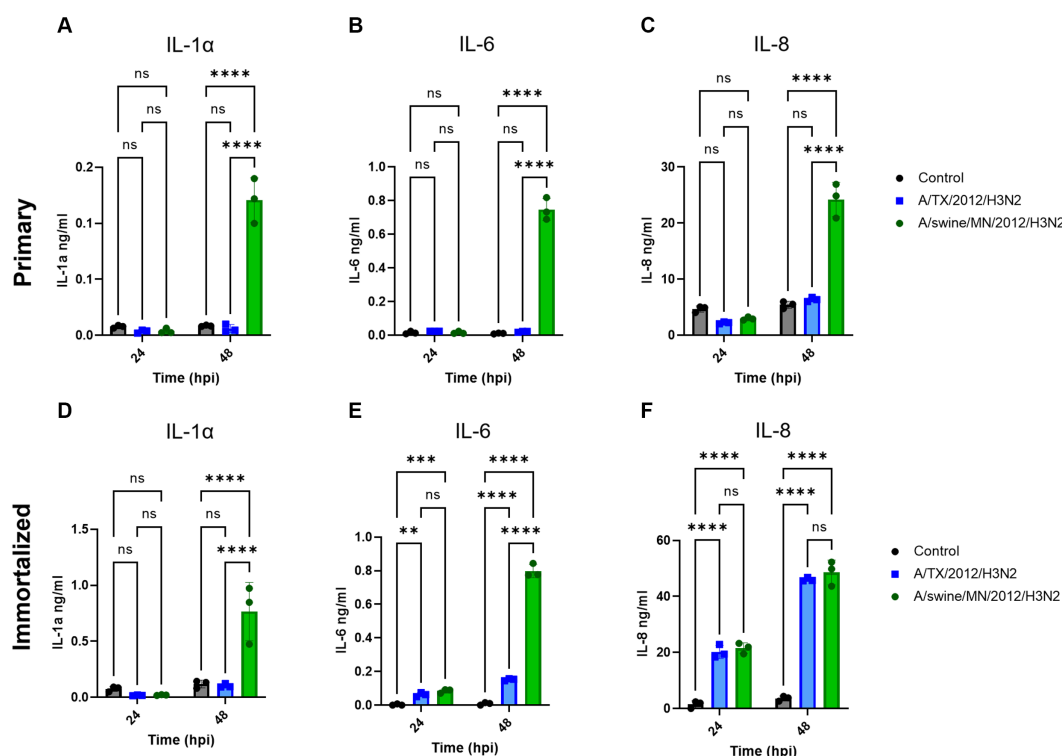


FIGURE 7

swIAV of H3N2 subtype promotes robust pro-inflammatory cytokine secretion in both immortalized and primary swine respiratory cells. Immortalized (P24) and primary (P6) swine respiratory cells were seeded onto 6-well collagen coated plates and inoculated independently with either control/PBS (black), A/TX/2012/H3N2 (blue), or A/swine/MN/2012/H3N2 (green) at an MOI of 0.1. Supernatant harvested from either primary or immortalized cells at -24 and -48 hpi was tested for (A,D) IL-1α, (B,E) IL-6, and (C,F) IL-8 cytokine/chemokine secretion with MILLIPEX. Statistical analysis was performed by a two-way ANOVA test. **, $p < 0.01$; ***, $p < 0.001$; ****, $p < 0.0001$; ns, no statistical difference. Error bars represent standard deviation ($n = 3$).

respiratory cell counterpart. The immortalized swine respiratory cell line was still permissive to IAVs at passage 24 and did not require the addition of exogenous trypsin for IAV inoculation, which is mostly observed in primary epithelial cell lines that have undergone airlift in an ALI (9, 30, 31). It is important to continue to identify potential applications for the immortalized swine respiratory cell line for IAV research. In this study, we did not assess whether the isolated primary and immortalized swine respiratory cells could fully differentiate in the ALI system, which warrants investigation because the isolated cell were mostly of epithelial origin. This would provide more flexibility for the researcher to study IAV infectivity in an appropriate model that maintains the biological functionality of the swine hosts lower respiratory tract.

Data availability statement

The raw data supporting the conclusions of this article will be made available by the authors, without undue reservation.

Ethics statement

Ethical approval was not required for the studies on humans in accordance with the local legislation and institutional requirements

because only commercially available established cell lines were used. The animal study was approved by Auburn University Institutional Animal Care and Use Committee (IACUC). The study was conducted in accordance with the local legislation and institutional requirements.

Author contributions

PN: Conceptualization, Formal analysis, Investigation, Methodology, Validation, Visualization, Writing – original draft, Writing – review & editing. VP: Investigation, Methodology, Writing – review & editing. JN: Investigation, Methodology, Writing – review & editing. CJ: Investigation, Methodology, Writing – review & editing. MT: Conceptualization, Supervision, Writing – review & editing. CK: Conceptualization, Data curation, Funding acquisition, Investigation, Methodology, Resources, Supervision, Validation, Writing – original draft, Writing – review & editing.

Funding

The author(s) declare financial support was received for the research, authorship, and/or publication of this article. This work was funded by the NIH/NIAID Centers of Excellence for Influenza Research and Surveillance (CEIRS) contract HHSN272201400004C

and the Auburn University Alabama Agricultural Experiment Station (AAES).

Acknowledgments

The authors would like to thank Madelyn Krunkosky, graduate student at the lab of Mark Tompkins (currently Senior Research Scientist at Q2 Solutions) for sharing her primary cell culture protocols. This work was funded by the NIH/NIAID Centers of Excellence for Influenza Research and Surveillance (CEIRS) contract HHSN272201400004C and the Auburn University Alabama Agricultural Experiment Station (AAES).

Conflict of interest

The authors declare that the research was conducted in the absence of any commercial or financial relationships that could be construed as a potential conflict of interest.

References

- Shao W, Li X, Goraya MU, Wang S, Chen JL. Evolution of influenza A virus by mutation and re-assortment. *Int J Mol Sci.* (2017) 18:81650. doi: 10.3390/ijms18081650
- Nicholls JM, Bourne AJ, Chen H, Guan Y, Peiris JS. Sialic acid receptor detection in the human respiratory tract: evidence for widespread distribution of potential binding sites for human and avian influenza viruses. *Respir Res.* (2007) 8:73. doi: 10.1186/1465-9921-8-73
- Oshansky CM, Pickens JA, Bradley KC, Jones LP, Saavedra-Ebner GM, Barber JP, et al. Avian influenza viruses infect primary human bronchial epithelial cells unconstrained by sialic acid alpha2,3 residues. *PLoS One.* (2011) 6:e21183. doi: 10.1371/journal.pone.0021183
- Trebbien R, Larsen LE, Viuff BM. Distribution of sialic acid receptors and influenza A virus of avian and swine origin in experimentally infected pigs. *Virol J.* (2011) 8:434. doi: 10.1186/1743-422X-8-434
- Baum LG, Paulson JC. Sialyloligosaccharides of the respiratory epithelium in the selection of human influenza virus receptor specificity. *Acta Histochem Suppl.* (1990) 40:35–8.
- Imai M, Kawaoka Y. The role of receptor binding specificity in interspecies transmission of influenza viruses. *Curr Opin Virol.* (2012) 2:160–7. doi: 10.1016/j.coviro.2012.03.003
- Scholtissek JMP. Practise, Pigs as 'mixing vessels' for the creation of new pandemic influenza. *Med Princ Pract.* (2004) 2:65–71. doi: 10.1159/000157337
- Ma W, Kahn RE, Richt J. AJJom, research gmaijob. The pig as a mixing vessel for influenza viruses: human and veterinary implications. *J Mol Genet Med.* (2009) 3:158. doi: 10.4172/1747-0862.1000028
- Nelli RK, Kuchipudi SV, White GA, Perez BB, Dunham SP, Chang KC. Comparative distribution of human and avian type sialic acid influenza receptors in the pig. *BMC Vet Res.* (2010) 6:4. doi: 10.1186/1746-6148-6-4
- Mo JS, Abente EJ, Cardenas Perez M, Sutton TC, Cowan B, Ferreri LM, et al. Transmission of human influenza A virus in pigs selects for adaptive mutations on the HA gene. *J Virol.* (2022) 96:e0148022. doi: 10.1128/jvi.01480-22
- Rajao DS, Abente EJ, Powell JD, Bolton MJ, Gauger PC, Arruda B, et al. Changes in the hemagglutinin and internal gene segments were needed for human seasonal H3 influenza A virus to efficiently infect and replicate in swine. *Pathogens.* (2022) 11:90967. doi: 10.3390/pathogens11090967
- Landolt GA, Karasin AI, Phillips L, Olsen CW. Comparison of the pathogenesis of two genetically different H3N2 influenza A viruses in pigs. *J Clin Microbiol.* (2003) 41:1936–41. doi: 10.1128/JCM.41.5.1936-1941.2003
- Nelson MI, Wentworth DE, Culhane MR, Vincent AL, Viboud C, LaPointe MP, et al. Introductions and evolution of human-origin seasonal influenza A viruses in multinational swine populations. *J Virol.* (2014) 88:10110–9. doi: 10.1128/JVI.01080-14
- Rajao DS, Vincent AL, Perez DR. Adaptation of human influenza viruses to swine. *Front Vet Sci.* (2019) 5:347. doi: 10.3389/fvets.2018.00347
- Bateman AC, Karamanska R, Busch MG, Dell A, Olsen CW, Haslam SM. Glycan analysis and influenza A virus infection of primary swine respiratory epithelial cells: the importance of NeuAc2-6 glycans. *J Biol Chem.* (2010) 285:34016–26. doi: 10.1074/jbc.M110.115998
- Bateman AC, Busch MG, Karasin AI, Olsen CW. Infectivity phenotypes of H3N2 influenza A viruses in primary swine respiratory epithelial cells are controlled by sialic acid binding. *Influenza Other Respir Viruses.* (2012) 6:424–33. doi: 10.1111/j.1750-2659.2012.00333.x

The author(s) declared that they were an editorial board member of Frontiers, at the time of submission. This had no impact on the peer review process and the final decision.

Publisher's note

All claims expressed in this article are solely those of the authors and do not necessarily represent those of their affiliated organizations, or those of the publisher, the editors and the reviewers. Any product that may be evaluated in this article, or claim that may be made by its manufacturer, is not guaranteed or endorsed by the publisher.

Supplementary material

The Supplementary material for this article can be found online at: <https://www.frontiersin.org/articles/10.3389/fvets.2023.1258269/full#supplementary-material>

- Ibricevic A, Pekosz A, Walter MJ, Newby C, Bataille JT, Brown EG, et al. Influenza virus receptor specificity and cell tropism in mouse and human airway epithelial cells. *J Virol.* (2006) 80:7469–80. doi: 10.1128/JVI.02677-05
- Seo SH, Goloubeva O, Webby R, Webster RG. Characterization of a porcine lung epithelial cell line suitable for influenza virus studies. *J Virol.* (2001) 75:9517–25. doi: 10.1128/JVI.75.19.9517-9525.2001
- Meliopoulos V, Cherry S, Wohlgenuth N, Honce R, Barnard K, Gauger P, et al. Primary swine respiratory epithelial cell lines for the efficient isolation and propagation of influenza A viruses. *J Virol.* (2020) 94:20. doi: 10.1128/JVI.01091-20
- Xie X, Gan Y, Pang M, Shao G, Zhang L, Liu B, et al. Establishment and characterization of a telomerase-immortalized porcine bronchial epithelial cell line. *J Cell Physiol.* (2018) 233:9763–76. doi: 10.1002/jcp.26942
- Muench HRJAH. A simple method of estimating 50 per cent end points. *American Journal of Epidemiology* (1938) 27:493–497. doi: 10.1093/oxfordjournals.aje.a118408
- Schindelin J, Arganda-Carreras I, Frise E, Kaynig V, Longair M, Pietzsch T, et al. Fiji: an open-source platform for biological-image analysis. *Nat Methods.* (2012) 9:676–82. doi: 10.1038/nmeth.2019
- Kuburich NA, den Hollander P, Pietzsch T, Mani SA. Vimentin and cytokeratin: good alone, bad together. *Semin Cancer Biol.* (2022) 86:816–26. doi: 10.1016/j.semcancer.2021.12.006
- Smith GJ, Vijaykrishna D, Bahl J, Lycett SJ, Worobey M, Pybus OG, et al. Origins and evolutionary genomics of the 2009 swine-origin H1N1 influenza A epidemic. *Nature.* (2009) 459:1122–5. doi: 10.1038/nature08182
- Massin P, Kuntz-Simon G, Barbezange C, Deblanc C, Oger A, Marquet-Blouin E, et al. Temperature sensitivity on growth and/or replication of H1N1, H1N2 and H3N2 influenza A viruses isolated from pigs and birds in mammalian cells. *Vet Microbiol.* (2010) 142:232–41. doi: 10.1016/j.vetmic.2009.10.012
- Carty SE, Buresh CM, Norton JA. Decreased IL-6 secretion by fibroblasts following repeated doses of TNF alpha or IL-1 alpha: post-transcriptional gene regulation. *J Surg Res.* (1991) 51:24–32. doi: 10.1016/0022-4804(91)90065-t
- Yang ML, Wang CT, Yang SJ, Leu CH, Chen SH, Wu CL, et al. IL-6 ameliorates acute lung injury in influenza virus infection. *Sci Rep.* (2017) 7:43829. doi: 10.1038/srep43829
- Bakre AA, Jones LP, Murray J, Reneer ZB, Meliopoulos VA, Cherry S, et al. Innate antiviral cytokine response to swine influenza virus by swine respiratory epithelial cells. *J Virol.* (2021) 95:e0069221. doi: 10.1128/JVI.00692-21
- Hauser MJ, Dlugolenski D, Culhane MR, Wentworth DE, Tompkins SM, Tripp RA. Antiviral responses by swine primary bronchoepithelial cells are limited compared to human bronchoepithelial cells following influenza virus infection. *PLoS One.* (2013) 8:e70251. doi: 10.1371/journal.pone.0070251
- Bottcher E, Matrosovich T, Beyerle M, Klenk HD, Garten W, Matrosovich M. Proteolytic activation of influenza viruses by serine proteases TMPRSS2 and HAT from human airway epithelium. *J Virol.* (2006) 80:9896–8. doi: 10.1128/JVI.01118-06
- Bateman AC, Karasin AI, Olsen CW. Differentiated swine airway epithelial cell cultures for the investigation of influenza A virus infection and replication. *Influenza Respir Viruses.* (2013) 7:139–50. doi: 10.1111/j.1750-2659.2012.00371.x



OPEN ACCESS

EDITED BY

Sarah J. Edwards,
Commonwealth Scientific and Industrial
Research Organization (CSIRO), Australia

REVIEWED BY

Paul Selleck,
Australian Animal Health Laboratory (CSIRO),
Australia
Florescia Celeste Mansilla,
CONICET Institute of Virology and
Technological Innovations (IVIT), Argentina

*CORRESPONDENCE

Ted M. Ross
✉ Rosst7@ccf.org

RECEIVED 31 August 2023

ACCEPTED 28 November 2023

PUBLISHED 19 December 2023

CITATION

Núñez IA, Jang H, Huang Y, Kelvin A and
Ross TM (2023) Influenza virus immune
imprinting dictates the clinical outcomes in
ferrets challenged with highly pathogenic avian
influenza virus H5N1.
Front. Vet. Sci. 10:1286758.
doi: 10.3389/fvets.2023.1286758

COPYRIGHT

© 2023 Núñez, Jang, Huang, Kelvin and Ross.
This is an open-access article distributed under
the terms of the [Creative Commons Attribution
License \(CC BY\)](https://creativecommons.org/licenses/by/4.0/). The use, distribution or
reproduction in other forums is permitted,
provided the original author(s) and the
copyright owner(s) are credited and that the
original publication in this journal is cited, in
accordance with accepted academic practice.
No use, distribution or reproduction is
permitted which does not comply with these
terms.

Influenza virus immune imprinting dictates the clinical outcomes in ferrets challenged with highly pathogenic avian influenza virus H5N1

Ivette A. Núñez^{1,2}, Hyesun Jang¹, Ying Huang¹, Alyson Kelvin³ and
Ted M. Ross^{1,2*}

¹Center for Vaccines and Immunology, University of Georgia, Athens, GA, United States, ²Department of Infectious Diseases, University of Georgia, Athens, GA, United States, ³Vaccine and Infectious Disease Organization (VIDO), University of Saskatchewan, Saskatoon, SK, Canada

Zoonotic transmission of H5N1 highly pathogenic avian influenza virus (HPAIV) into the human population is an increasing global threat. The recent 2022 HPAIV outbreak significantly highlighted this possibility, increasing concern in the general population. The clinical outcomes of H5N1 influenza virus exposure can be determined by an individual's primary influenza virus infection (imprinting) or vaccination status. Immunological imprinting with Group 1 - (H1N1, H2N2, and H2N3) increases survival rates following H5N1 viral infection compared to Group 2 - (H3N2) imprinted individuals. Vaccination against H5N1 influenza viruses can offer protection to at-risk populations; however, stockpiled inactivated H5N1 influenza vaccines are not readily available to the public. We hypothesize that the immunological response to vaccination and subsequent clinical outcome following H5N1 influenza virus infection is correlated with the immunological imprinting status of an individual. To test this hypothesis, our lab established a ferret pre-immune model of disease. Naïve ferrets were intranasally inoculated with seasonal influenza viruses and allowed to recover for 84 days prior to H5N1 virus infection. Ferrets imprinted following H1N1 and H2N3 virus infections were completely protected against lethal H5N1 influenza virus challenge (100% survival), with few to no clinical symptoms. In comparison, H3N2 influenza virus-imprinted ferrets had severe clinical symptoms, delayed disease progression, and a sublethal phenotype (40% mortality). Consecutive infections with H1N1 influenza viruses followed by an H3N2 influenza virus infection did not abrogate the immune protection induced by the original H1N1 influenza virus infection. In addition, ferrets consecutively infected with H1N1 and H2N3 viruses had no clinical symptoms or weight loss. H3N2 pre-immune ferrets were vaccinated with a broadly reactive H5 HA-based or H1 NA-based vaccine (Hu-CO 2). These ferrets were protected against H5N1 influenza virus challenge, whereas ferrets vaccinated with the H1N1 wild-type CA/09 rHA vaccine had similar phenotypes as non-vaccinated H3N2-imprinted ferrets with 40% survival. Overall, Group 2 imprinted ferrets, which were vaccinated with heterologous Group 1 HA vaccines, had redirected immune responses to Group 1 influenza viral antigens and rescued a sublethal phenotype to complete protection.

KEYWORDS

H5N1, pre-immunity, influenza imprinting, universal influenza vaccine, highly pathogenic avian H5N1 influenza A virus

1 Introduction

Primary influenza virus infection elicits a life-long imprint on the immune system, which further dictates serological and cellular immune responses upon re-infection (1). This imprinting, also known as “antigenic sin” (2) or “antigenic seniority” (3) is thought to dampen the serological response against subsequent infection with heterologous viral strains. Subsequent infection with influenza viruses recall antibody responses against shared antigens, even if the original antigen becomes a secondary or lesser component (4). The term original antigenic sin (OAS) has been correlated with negative effects, such that recall responses are targeted toward antigenic epitopes that have undergone antigenic drift, and recognition of the drift variant is lost (5). There is an ineffective cross-reactive immune response to new viral strains while maintaining protective antibody titers to the primary infection strain (6, 7). Some studies have shown that repeated vaccination results in a diminished antibody response to viral antigens (8, 9). However, these studies measured antibody protection through hemagglutinin inhibition assay (HAI) that only measures the antibody response against the hemagglutinin (HA) head to block sialic acid binding. Repeated vaccination can elicit antibody responses against HA-stem regions, which are not detectable via HAI (10). Following viral infection or seasonal vaccination, there is a pre-immune status that often narrows antibody cross-reactivity to influenza viruses. This is dependent on the age or date of birth of the individual (3, 11–13) but does not inhibit the immune response to unique influenza virus strains.

Although the induction of pre-immunity with seasonal influenza viruses has been previously investigated, the effects of pandemic H5N1 avian influenza virus (AIV) vaccination on a seasonal pre-immune background in ferrets are less well understood. There is an age-related response against H5N1 viral infection in humans with incidence and mortality due to H5N1 infection being highest in individuals born between the years 1957 and 2009 (14). Older adults with no record of prior exposure to AIV had heterotypic antibodies against H9N2 and H5N1 viruses (15). People immunized with seasonal influenza vaccines during the seasons between 2006 and 2011 had increased cross-protective antibodies (15). Out of the 174 participants, 25 had seroconverted levels of antibodies to the H5N1 (A/Vietnam/1194/2004) virus after seasonal influenza vaccination. However, out of those who had seroconverted only 1.1% had HAI antibody titers above 1:40 (15). It is speculated that because of the age of the individuals (74–79 mean age), they had been exposed to viruses similar to the Spanish influenza virus (H1N1 virus). This data is in agreement with the epidemiological study performed by Gostic et al. (14) that suggested individuals born after 1957 were most susceptible to H5N1 viral morbidity and were most likely to be imprinted with H3N2 viruses (14). This study found that primary infections of the seasonal influenza virus correlated with protection against the same influenza HA group, which is determined phylogenetically. Influenza virus HA proteins are antigenically divided into two groups: group 1, which contains viral subgroups H1, H5, and H2, and group 2, which contains H3, H7, and H9 (16). Individuals born before 1957, who were most likely imprinted with a group 1 influenza virus (H1N1) had lower case incidences of H5N1 (group 1) viral infection (14). Pre-immunity with group 1 or group 2 viruses leaves a long-lasting effect on the immunological response against exposure to heterologous viruses. This pre-immune status will ultimately influence

pre-pandemic vaccination strategies and must be investigated in order to produce a successful H5N1 vaccine.

The development of a protective avian influenza vaccine has proven to be a difficult task. A pandemic avian influenza vaccine should be capable of inducing long-lasting memory response, neutralizing titers, cross-clade protection, and cellular and humoral responses in the occurrence of an outbreak. Human clinical trials with avian influenza vaccinations have shown varying results and complications. Avian influenza vaccines delivered as inactivated viruses are a safe approach to immunizing naïve populations but can also have negative setbacks. Inactivated vaccines take 6 months to produce and can often result in limited immunogenicity and elicit a poor cellular immune response (17). Inactivated vaccines are also often grown in eggs, which introduces a large amount of egg proteins and can sometimes have vaccine reactogenicity, especially in people who are younger than 23 years of age (18). Egg viral growth can also introduce glycosylation that is normally not present in the wild-type strain of the virus and can result in a vaccine that is not protective against circulating strains (19). The growth of HPAI viruses is also highly lethal to embryos and is often difficult to propagate safely in eggs (17). Most inactivated vaccines for H5N1 are poorly immunogenic and require at least two doses to elicit a long-lasting immune response (17). Unadjuvanted inactivated split virus and sub-unit H5N1 vaccines elicit neutralizing antibody titers in only 58% of individuals who are vaccinated (20). Antibody titers in these recipients decreased substantially 6 months after their second dose (20). The recipients were therefore offered a third dose to boost their antibody response, and protective titers were seen in 78 and 67% depending on the dose (21). Other studies have shown that the combination of inactivated influenza and adjuvant can induce a long-lasting response; however, the vaccine doses were very high, and neutralizing antibody titers were highest in children aged 6 months to 17 years of age (22, 23). Recombinant protein-based vaccines have shown promising results; rHA vaccines are well tolerated but do not easily elicit neutralizing antibodies after two doses (24). The current pre-pandemic vaccine that is stockpiled is a subvirion vaccine with recombinant H5N1 HA derived from the A/Vietnam/1203/2004 virus. Although this vaccine was well tolerated, it only induced neutralizing titers in 43% of the participants (20). Heterologous prime-boost regimens performed with this sub-unit vaccine, however, have been seen to induce cross-clade protection, specifically to clade 2.3.4.4 viruses (25, 26). However, there are still challenges to providing protection against highly variable and rapidly diverging strains of avian influenza viruses and a limited number of antigens that can be stockpiled.

In order to test vaccine efficacy and pre-immunity, an influenza model must be utilized. Fitch ferrets are commonly used as influenza experimental models. Although mice are most commonly used for influenza research, they lack clinical symptoms that follow influenza infection such as fever, sneezing, nasal discharge, and inflammation (27). The ferret is the only animal that displays clinical symptoms that are similar to those of humans. Ferrets were discovered as influenza models in 1933; they can be infected with influenza A viruses that do not require adaptation (28). Ferrets can also transmit influenza viruses to susceptible cage mates and carry the α -2,6 linked sialic acid receptors in their upper respiratory tract, which helps transmit the virus via airborne droplets (29, 30). Because of the extensive nature of housing ferrets, sample sizes for experimental purposes are often small

($n = 4-5$). The investigation of pandemic viruses such as H5N1 and H7N9 has increased the use of ferrets in influenza studies.

The effect of pre-immunity on pandemic vaccination has not yet been investigated. As previously mentioned, pre-immune status greatly determines an individual's antibody production and repertoire and must be considered when developing a vaccine for pandemic preparedness. This study aimed to determine the protective response of group 1 vs. group 2 pre-immunity on H5N1 infection and the responses to vaccination depending on pre-immunity. Monovalent HA or NA recombinant proteins were used to vaccinate pre-immune ferrets prior to challenge. Specifically, the chimeric HA protein named Human COBRA 2 (computationally optimized broadly reactive antigen) was tested in H3N2 pre-immune ferrets in an attempt to offer complete protection. Our results show that ferrets that were convalescent for group 1 seasonal influenza virus maintained an antibody repertoire that was capable of neutralizing HPAI H5N1 virus challenge. Ferrets that were imprinted with a group 2 virus were not 100% protected against infection compared to the group 1 imprinted cohort. Sequential infection with the group 1 and group 2 viruses did not inhibit the imprinting effect and protection against H5N1 challenge.

2 Methods

2.1 Virus-like particle vaccine preparation

Mammalian 293T HEK cells were transfected with each of three plasmids expressing the influenza neuraminidase A/Thailand/01/2004 (H5N1), the HIV p55 Gag sequences, and Human COBRA HA expressing plasmids on previously described mammalian expression vectors. After 72 h of incubation at 37°C, supernatants from transiently transfected cells were collected, centrifuged to remove cellular debris, and filtered through a 0.22- μ m-pore-size membrane. Mammalian-derived VLPs were purified and sedimented by ultracentrifugation on a 20% glycerol cushion at 27,000 rpm for 4 h at 4°C. VLPs were resuspended in phosphate-buffered saline (PBS), and the total protein concentration was assessed by a conventional bicinchoninic acid assay. The hemagglutination activity of each preparation of VLPs was determined by adding an equal volume of Horse red blood cells (RBCs) to a V-bottom 96-well plate, followed by incubation with serially diluted volumes of VLPs for 60 min at room temperature.

2.2 Recombinant protein vaccine preparation

Soluble recombinant HA or NA was also produced for vaccination. The HA/NA gene cassettes expressing wild type or Human COBRA HA recombinant protein were cloned into mammalian DNA expression plasmid pcDNA 3.1/Zeo(+)vector (Thermo Fisher Scientific) and were synthesized by Genewiz (South Plainfield, NJ). The plasmid was transformed into a TOP10 bacterial cell line and was purified using Zympure maxi-prep. The HA1 fragment, which contained a KPNI site was removed from the plasmid and was moved into an acceptor vector containing the Hu-CO2 HA2 domain. The final gene of the HA protein contained an extracellular domain that was terminally fused with the trimeric domain of T4 fibrin, an

AviTag sequence, and a hexahistidine affinity tag for purification (31). Each DNA plasmid containing either wild-type or COBRA antigens was transiently transfected into an Expi293F HEK suspension cell line (Thermo Fisher Scientific) and was allowed to incubate for 72 h at 37°C (5% CO₂). Supernatants were collected and tested for protein expression through BCA and Western Blot (His tag antibody). The cells were then pelleted down and the supernatant was purified for protein collection. Soluble HA protein was purified via AKTA Pure System using HisTrap columns following the manufacturer's protocol. Eluted fractions were pooled and purified, protein concentration was tested using an anti-HIS tag antibody (Biolegend, San Diego, CA, United States) using SDS-PAGE and Western blot (32).

2.3 Determination of hemagglutinin protein content in VLPs

Protein concentration was determined by MicroBCA™ Protein Assay Kit (Thermo Fisher Scientific; Pittsburgh, PA, United States). HA concentration was determined by western blot and densitometry. Purified VLPs were prepared in standard total protein amounts and were electrophoresed on 10% SDS-PAGE gel and transferred to a PVDF membrane. The blot was probed with an anti-HA clade 1 influenza A virus (Immune Technology Corporation; New York, NY, United States) monoclonal antibody. HA-antibody complexes were detected using a goat anti-mouse IgG conjugated to horse radish peroxidase (HRP) (Southern Biotech; Birmingham, AL, United States). HRP was detected by chemiluminescent substrate Clarity™ Western ECL substrate (Bio-Rad Laboratories; Hercules, CA, United States). The density of WT HA bands was used to calculate a standard curve and the density of the purified VLPs was interpolated using the results from the WT HA. Experiments were performed in duplicates. The density of bands was determined using myImageAnalysis™ Software (Thermo Fisher Scientific, Waltham, MA, United States).

2.4 Viruses

H1N1, H3N2, and H2N3 viruses were obtained through the Influenza Reagents Resource (IRR), BEI Resources, or the CDC or were provided by Sanofi-Pasteur. Viruses were passaged once under the same growth conditions as they were received in embryonated chicken eggs with the instructions provided by the WHO. Titers of virus lots were determined with both guinea pig and turkey erythrocytes and divided into aliquots for single-use applications. Viruses used to infect ferrets were as follows: H1N1: A/Singapore/6/1986 (A/Sing/86, 1×10^6 pfu/mL), A/California/07/2009 (A/CA/09) and A/AA/Marton/1943 (A/Mar/43). H3N2: A/Panama/2007/1999 (A/Pan/99, 1×10^6 pfu/mL), A/Port Chalmers/1/1973 (A/PC/73), A/Hong Kong/1/1968 (A/HK/68), A/Texas/50/2012 (A/TX/12). H2N3: A/Swine/Missouri/4296424/2006 (A/sw/MO/06). H5N1: A/Vietnam/1203/2004 (A/VN/04, 1×10^5 pfu/mL).

2.5 Animal studies

Fitch ferrets (*Mustela putorius furo*, female and male, 6 to 12 months of age), were de-scented and purchased from Triple F

Farms (Sayre, PA) or sent to us by our collaborator Dr. Alyson Kelvin from Dalhousie University. Ferrets were pair housed in stainless-steel cages (Shor-line Kansas City, KS) containing Sani-Chips laboratory animal bedding (P. J. Murphy Forse Products, Montville, NJ). Ferrets were provided with Teklad Global Ferret Diet (Harlan Teklad, Madison WIS) and freshwater *ad libitum*. The University of Georgia Institutional Animal Care and Use Committee approved all experiments, which were conducted in accordance with the National Research Council's *Guide for the Care and Use of Laboratory Animals*, The Animal Welfare Act, and the CDC/NIH *Biosafety in Microbiological and Biomedical Laboratories guide*. In order to determine negative immunological status, ferrets were bled 2 weeks prior to study initiation, and RDE-treated sera were tested for hemagglutinin inhibition assay-detectable antibodies against a panel of seasonal influenza viruses (H1N1, H3N2, H5N1, H5N2, H5N6, H5N8) and influenza B viruses (data not shown). Ferrets ($n=6-8$) were intranasally inoculated with an H1N1 seasonal isolate or an H3N2 isolate. Animals were monitored for weight loss, loss of activity, nasal discharge, sneezing, and diarrhea and were allowed to recover for a predetermined time of 84 days. The recovery date was empirically determined prior to this study (unpublished) and since has been used in multiple models of pre-immunity (9–12). Ferrets were tested on days 30, 45, 60, and 84 post-infection for infection and vaccine immunogenicity. Ferrets that recovered within 30–45 days did not experience viral infection or elicit antibodies against vaccine-specific antigens when immunized. Serum HAI titers tested 60 days post-infection showed significantly reduced reactivity, and by day 84, pre-immunized ferrets elicited vaccine-antigen-specific antibodies and experienced viral infection post-inoculation, which was determined by weight loss, fevers, and clinical symptoms. On day 84, ferrets were vaccinated with either VLP, rHA antigens, or inactivated seasonal influenza vaccine intramuscularly. Two weeks following vaccination, ferrets were bled to assess the serological antibody response against homologous and heterologous avian influenza strains. If antibody titers are not elicited after one vaccination, ferrets may have to be boosted for a second time. Vaccines consisted of 15 µg or rHA formulated with Addavax™ adjuvant at a 1:1 ratio. Four weeks after final vaccination, ferrets were challenged intranasally with 1×10^4 or 1×10^5 plaque-forming units (PFU) of the highly pathogenic H5N1 virus A/VN/2004 (Clade 1) in a volume of 0.5 mL in each nostril for a total infection volume of 1 mL. Ferrets were monitored daily for weight loss, disease signs, and death for 14 days after infection. Individual body weights, sickness scores, and death were recorded for each group on each day after inoculation. Sickness scores were determined by evaluating activity (0 = normal, 1 = alert and active with stimulation, 2 = alert but not active after stimulation, 3 = not alert or active after stimulation), nasal discharge (0 = absent, 1 = present), sneezing (0 = absent, 1 = present), decreased food intake (0 = absent, 1 = present), diarrhea (0 = absent, 1 = present), dyspnea (0 = absent, 1 = present), and neurological symptoms (0 = absent, 3 = present). Nasal washes were conducted on day 3 after inoculation. Washes were collected and stored at -80°C until use. The experimental endpoint was defined as >25% weight loss, development of neurological symptoms, or an activity score of 3 (not active or alert after stimulation). All H5N1 influenza virus studies were performed under high-containment biosafety level 3 enhanced conditions (BSL3+). All procedures were in accordance with the NRC Guide for the Care and Use of Laboratory Animals, the Animal Welfare 3,046 B.M. Giles,

T.M. Ross / Vaccine 29 (2011) 3043–3,054 Act, and the CDC/NIH Biosafety in Microbiological and Biomedical Laboratories.

2.6 Elisa

Immulon 4HBX plates (Thermo Fisher) were coated overnight at 4°C with cH6/1 in carbonate buffer (pH 9.4) at $0.5 \mu\text{g/mL}$ containing $5 \mu\text{g/mL}$ fraction V bovine serum albumin (BSA [Equitech-Bio, Kerrville, TX]; $50 \mu\text{L/well}$) in a humidified chamber. The plates were then blocked with $200 \mu\text{L/well}$ of ELISA blocking buffer (PBS containing 0.2% BSA plus 0.1% bovine gelatin and 0.05% Tween 20) for 1.5 h at 37°C . Serum samples were serially diluted in blocking buffer, and the plates were incubated overnight at 4°C . The plates were washed three times with PBS-Tween (PBS-T, 0.05%). Then, $100 \mu\text{L/well}$ of biotinylated goat anti-ferret IgG H&L HRP (Cambridge, MA) diluted at 1:10000 in blocking buffer was added, and the plates were incubated for 1 h at 37°C . The plates were washed four times with PBS-T. Then, $100 \mu\text{L}$ of ABTS [2,2-Azinobis-(3-ethylbenz thiazolinesulfonic acid); AMRESCO, Solon, OH] substrate with 0.16% H_2O_2 was added, and the plates were incubated at 37°C for 25 min. Colorimetric conversion was terminated by the addition of 5% SDS ($50 \mu\text{L/well}$), and the optical density was measured at 414 nm using a spectrophotometer (BioTek, Winooski, VT). After subtraction of the background, endpoint titers were determined as the reciprocal dilution of the last well, which had an OD414 above the mean OD414 plus three times the standard deviations of naïve animal sera.

2.7 Plaque assays

Plaque assays were performed in a high-level biosafety containment facility. Lung samples and nasal wash samples taken on day 3 post-infection were snap frozen and kept at -80°C until processing. Lungs were homogenized using a plunger and $0.2 \mu\text{m}$ strainer. Madin-Darby canine kidney (MDCK) cells were seeded 24 h prior to use at (5×10^5) in each well of a six-well plate. The nasal wash and lung homogenate samples were diluted (final dilution factors of 100 to 10^6) and overlaid on the cells in $200 \mu\text{L}$ of Dulbecco's modified Eagle medium supplemented with penicillin–streptomycin, followed by incubation for 1 h in 37°C with 5% CO_2 . Samples were removed, the cells were washed twice, and the medium was replaced with 2 mL of L15 medium plus 0.8% agarose (Cambrex, East Rutherford, NJ), followed by further incubation for 72 h at 37°C with 5% CO_2 . The agarose was removed and discarded. The cells were fixed with 10% buffered formalin for 10 min and then stained with 1% crystal violet for 5 min. The plates were then thoroughly washed in distilled water to remove excess crystal violet before being air-dried; the number of plaques was then counted, and the number of PFU per milliliter was calculated.

2.8 H&E staining

To assess the viral replication and pathological effect of infection, mice ($n=3$) were euthanized 3 days post-infection. The right lung lobes were taken for viral plaques and the incision was clamped with a hemostat; a 22-gauge needle was then used to puncture the apex of the

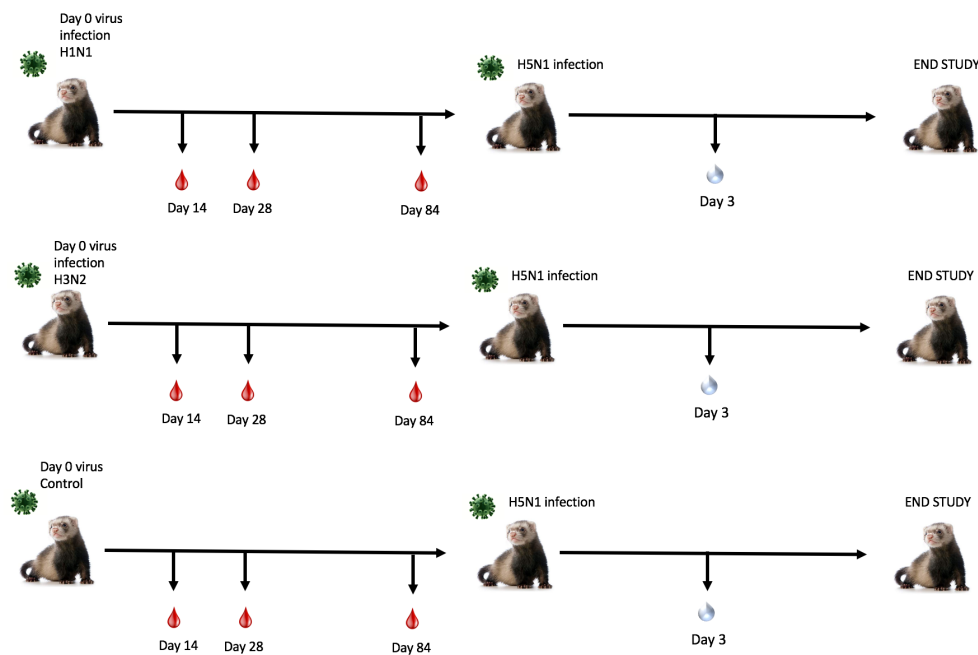


FIGURE 1

Schematic representation of pre-immune ferret study. Naïve fitch ferrets (*Mustela putorius furo*, female) 6–8 months of age were intranasally infected with a Group 1 influenza virus (H1N1 A/Sing/86), Group 2 influenza virus (H3N2 A/Pan/99), or PBS (control) and were monitored for 14 days following infection. Sera was collected to test for antibody responses on days 14, 28, and 84 post-preimmunization. Ferrets were allowed to recover for 84 days post-challenge. Ferrets were transported into a high-level biocontainment facility for H5N1 challenge with VN/04 (1×10^5 pfu/ml) and were monitored daily for weight loss and clinical symptoms. On day 3 post-challenge, ferrets were briefly anesthetized, and nasal wash specimens were taken to test for viral titers. The study was terminated 14 days post-challenge.

heart and sterile PBS was perfused throughout the mouse for 2–3 min. After the blood was efficiently removed from the lungs, 10% formalin was then perfused to fix the left lobes. Lungs were removed and placed into formalin for 1 week prior to paraffin embedding. Mouse lungs were embedded into paraffin and were cut using a Leica microtome. Transverse $5 \mu\text{m}$ sections were placed onto Apex superior adhesive glass slides (Leica biosystem Inc., IL, United States), which were coated for a positive charge, and were processed for H&E staining. Sections were deparaffinized in Xylene and hydrated using different concentrations of ethanol (100, 95, 80, and 75%) for 2 min each. Deparaffinized and hydrated lung sections were stained with Hematoxylin (MilliporeSigma, MA, United States) for 8 min at RT, differentiated in 1% acid alcohol for 10 s, and then counterstained with Eosin (Millipore sigma, MA, United States) for 30 s; slides were dehydrated with 95 and 100% ethanol, cleared by Xylene, and mounted using Permount® mounting media (Thermo Fisher Scientific, MA, United States).

3 Results

3.1 Influenza group imprinting determines disease and survival in a pre-immune ferret model

To determine the effect of seasonal influenza A virus imprinting on pandemic H5N1 infection, naïve female ferrets ($n=6$) were intranasally inoculated (imprinted) with either an H1N1 influenza virus (A/Sing/86), an H3N2 influenza virus (A/Pan/99), or PBS as a

control (Figure 1). Following seasonal influenza virus inoculation, ferrets were allowed to convalesce for 84 days and were then transported to a high-level animal biosafety facility (ABSL-3).

Ferrets were briefly anesthetized and intranasally challenged with the H5N1 influenza virus, VN/04 (1×10^5 pfu). Weights and clinical scores were observed daily until ferrets reached a humane endpoint or until the end of the study (Figure 1). Ferrets that were previously inoculated with A/Sing/86 (H1N1) experienced little weight loss and had no clinical signs for 14 days following H5N1 viral infection (Figures 2A,B). However, ferrets that were imprinted with seasonal influenza virus A/Pan/99 (H3N2) experienced significant weight loss and developed multiple clinical symptoms as early as 6 days post H5N1 challenge (Figures 2A,B). Symptoms in this group including lethargy, weight loss, and neurological symptoms resulted in humane euthanasia (Figure 2C). H3N2 influenza virus-imprinted ferrets began to succumb to disease on day 6 post-challenge (Figure 2C), ultimately having a 66% lethality rate. Weight loss comparison between H1N1 and H3N2 influenza virus-imprinted ferrets was statistically significant between day 3 and day 6 post-challenge (Figure 2F). Ferrets that were inoculated with PBS in-lieu of seasonal influenza virus experienced significant weight loss (Figure 2A) and severe clinical symptoms (Figure 2B) and ultimately resulted in 100% mortality (Figure 2C) within 10 days following H5N1 influenza virus inoculation.

Sera collected from convalescent ferrets immediately prior to A/VN/04 viral challenge were tested for antibody reactivity against the HA protein of the A/VN/04 viral challenge strain in an ELISA binding assay (Figure 2D). Four out of six ferrets imprinted with the H1N1 virus had cross-reactive antibody titers against the HA of the H5N1

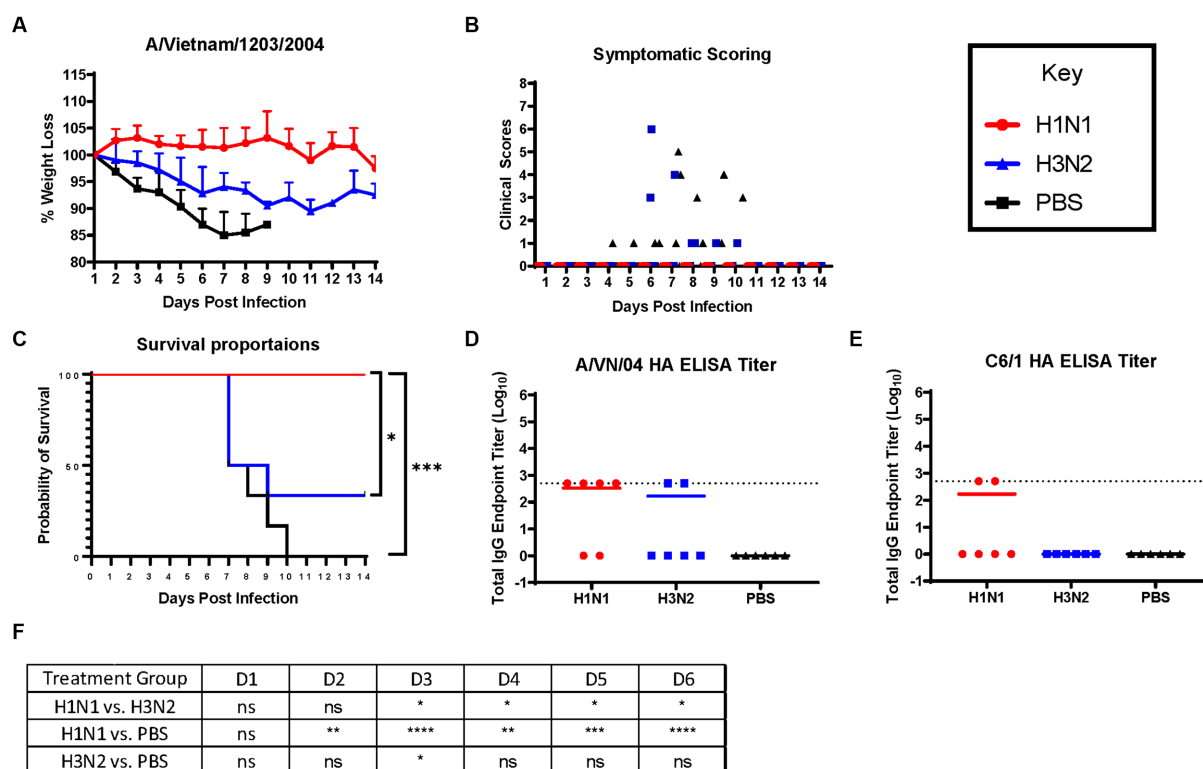


FIGURE 2

H1N1 imprinting provides complete protection against H5N1 challenge in naïve female ferrets. Survival was assessed in each pre-immune group and control. (A) Bodyweight curve of re-immunized female fitch ferrets. A/Sing/86 (H1N1), A/Pan/99 (H3N2), and control (PBS). (B) Clinical scores were recorded for each ferret following challenge. (C) Survival curves obtained following H5N1 HPAI challenge. Statistical analysis performed on PRISM™ software using Log-rank Mantel-Cox test (H1N1 vs. PBS, $p = 0.0004$, H3N2 vs. PBS, $P = ns$, H1N1 vs. H3N2, $p = 0.0178$). (D) Detection of rHA VN/04 antibodies in pre-immune ferret sera collected on day 84 pre-infection. (E) Detection of rHA C6/1 antibodies in pre-immune ferret sera collected on day 84 pre-infection. (F) Statistical analysis of body weight loss between imprinting groups post-exposure performed on PRISM™ software using two-way ANOVA. Statistical differences were indicated as asterisks: * $p < 0.05$, ** $p < 0.01$, *** $p < 0.001$, **** $p < 0.0001$; ns, no significance.

viral challenge strain A/VN/04 (Figure 2D), whereas only two ferrets imprinted with the H3N2 influenza virus had cross-reactive antibodies against the A/VN/04 HA protein. Interestingly, the two ferrets that had A/VN/04 HA cross-reactive antibodies survived challenge against the A/VN/04 H5N1 virus (Figures 2C,D). Additional ELISA assays confirmed seroconversion to the pre-immune challenge strains 14 days after inoculation (Supplementary Figure S1). To elucidate the mechanisms of antibody protection against H5N1 viral challenge, ferret sera were tested for binding antibodies against chimeric HA protein C6/1. Binding was detected against the specific HA chimeric protein with cross-reactive stalk antibodies. Only two ferrets from the H1N1 imprinted group had HAI titers against the C6/1 chimeric HA protein. From this preliminary data, we conclude that influenza virus group imprinting determines the ability to recall cellular immune responses and mount a protective response against pandemic H5N1 challenge that does not include an anti-stem binding antibody.

3.2 Sequential infection with a group 2 virus does not inhibit group 1 influenza virus imprinting

Next, ferrets were sequentially infected with Group 2 HA (H3N2) influenza viruses to determine whether the memory response of

Group 1 HA (H1N1)-imprinted ferrets was skewed and deterred protection against pandemic H5N1 infection. This study also utilized distinct H1N1 and H3N2 influenza viral strains to further test the hypothesis of influenza viral Group 1 HA imprinting eliciting cross-reactive protection against Group 1 HPAI viral challenge and that protection is not based on specific H1N1 strains. Male naïve ferrets ($n = 12$) were inoculated with either A/Mar/43 viral strain (H1N1) or A/HK/68 viral strain (H3N2) or were sequentially infected first with A/Mar/43, then A/HK/68 30 days later. Ferrets in all groups were allowed to convalesce for 60 days following the last intranasal infection and were moved into a high-level ABSL-3 facility prior to challenge with H5N1 influenza virus, A/VN/04 (Figure 3). Similar to the previous study, ferrets that were imprinted with an H1N1 influenza virus had no weight loss (Figure 4A), no clinical symptoms (Figure 4B), and no mortality (Figure 4C) following H5N1 influenza viral challenge. Ferrets that were imprinted with an H3N2 influenza virus had severe and statistically significant weight loss (Figure 4A) and increased clinical scores (Figure 4B) and had 100% mortality (Figure 4C) within 7 days following H5N1 influenza viral challenge. H3N2 influenza virus-imprinted ferrets had severe signs of disease that reached humane endpoints prior to losing 20% of their original weight (Figures 4A,B). Most noticeably, H3N2 influenza virus-imprinted ferrets developed neurological symptoms, extreme lethargy, and hind limb paralysis prior to losing 75% of their original body

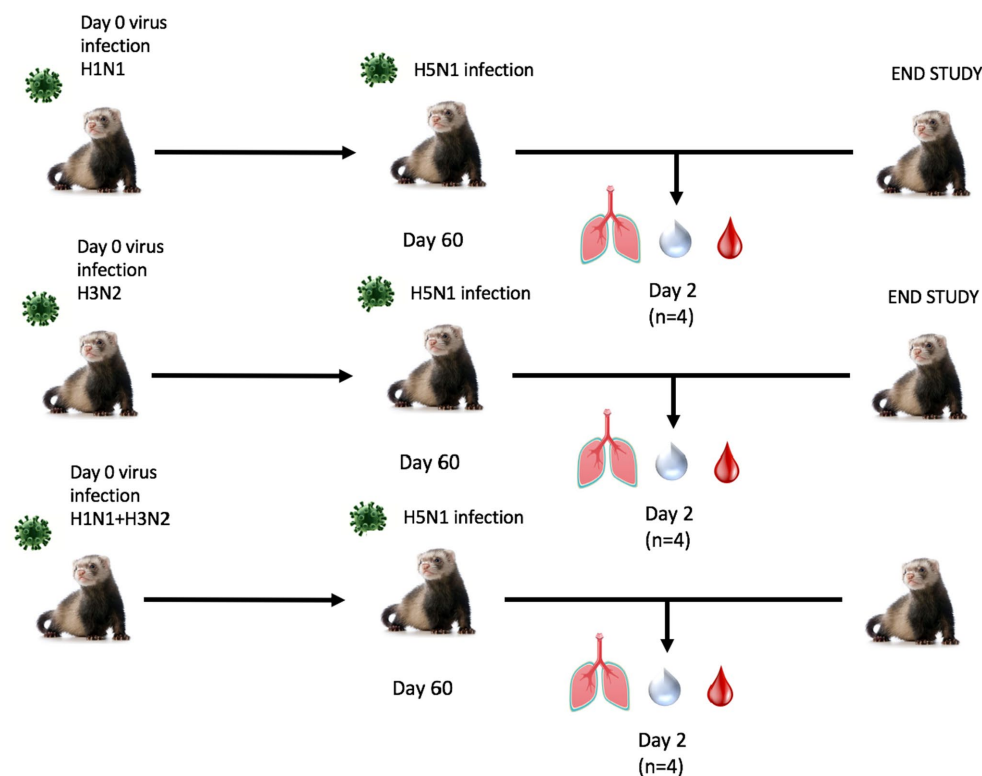


FIGURE 3

Schematic representation of secondary pre-immune ferret study. Male fitch ferrets ($n = 12$) were intranasally infected with live virus at 4–6 months of age using either H1N1 (A/Mar/43), H3N2 (A/HK/68), or both in a sequential infection. Sequentially infected ferrets were allowed to recover for 30 days between challenges. All groups recovered for 60 days and were challenged intranasally using highly pathogenic avian influenza (HPAI) H5N1 A/VN/04 (PFU 1×10^6). Studies using HPAI were performed in a BSL3 select agent accredited facility. Ferrets were monitored for 14 days following challenge.

weight (Figure 4B) and had a range of viral titers collected from nasal wash samples (Figure 4D). Similar to H1N1 influenza virus-imprinted ferrets, H1N1 influenza virus infection followed by H3N2 influenza virus infection had little to no weight loss (Figure 4A) and no clinical symptoms (Figure 4B), and there was no mortality (Figure 4C). There was no statistical significance in ferret weights between H1N1 and H3N2 pre-immune groups on day 1 post-infection (Figure 4F). However, ferrets administered H1N1 followed by H3N2 influenza viruses and ferrets infected with H3N2 virus only had statistically lower weights on days 2–5 PI than ferrets infected with H1N1 influenza viruses only (Figure 4F). This analysis between weight curves suggests that sequentially inoculated ferrets experienced greater weight gain compared to the H1N1 pre-immunized group (Figure 4F). It is important to note here that the age of the male ferrets in this group, 4–6 months, influences weight curves as younger ferrets commonly gain weight throughout an experiment, whereas adult ferrets' weight is stabilized. Therefore, the lack of weight gain in young ferrets can also be indicative of disease.

Nasal washes from all ferrets ($n = 12$) were collected on day 3 post-challenge to determine viral titers in the nasal cavity. As expected, only ferrets that were imprinted with the H3N2 virus were found to contain measurable virus in the nasal wash specimens (Figure 4D). In addition to nasal washes, ferrets from each group ($n = 4$) were humanely euthanized and lung punches were taken from the upper and lower quadrants of the right lungs. Plaque assays were performed to determine viral titers; upper and lower lung punches taken from

ferrets pre-immunized with the H1N1 influenza virus or sequentially infected with the H1N1 and H3N2 influenza viruses had no viral lung titers (Figure 4E). However, punches taken from H3N2 influenza virus-infected ferrets had high titers in both upper and lower quadrants (Figure 4E).

Serological data taken from a subset of ferrets ($n = 4$) was tested for cross-reactive antibodies against A/VN/04-HA and C6/1-HA recombinant protein. H1N1 pre-immunized ferret sera contained detectable antibody titers against the A/VN/04-HA protein, whereas H3N2 pre-immune ferrets did not contain detectable antibody titers against A/VN/04 HA (Supplementary Figure S2A). Sera tested against the chimeric C6/1 stalk protein revealed no significant differences between pre-immune groups (Supplementary Figure S2B), further solidifying our hypothesis that HA-stalk antibodies do not aid in the protection against heterosubtypic H5N1 viral challenge.

3.3 Group 1 HA from H2N3 virus provides protection from heterosubtypic challenge of A/VN/04 H5N1 virus

Although ferrets with pre-existing immunity to H1N1 influenza viruses are protected against H5N1 influenza virus challenge, further determination of group 1 HA viral inoculation elicits protective immune responses against H5N1 viral challenge. Female ferrets (6–8 months) were pre-immunized with either an

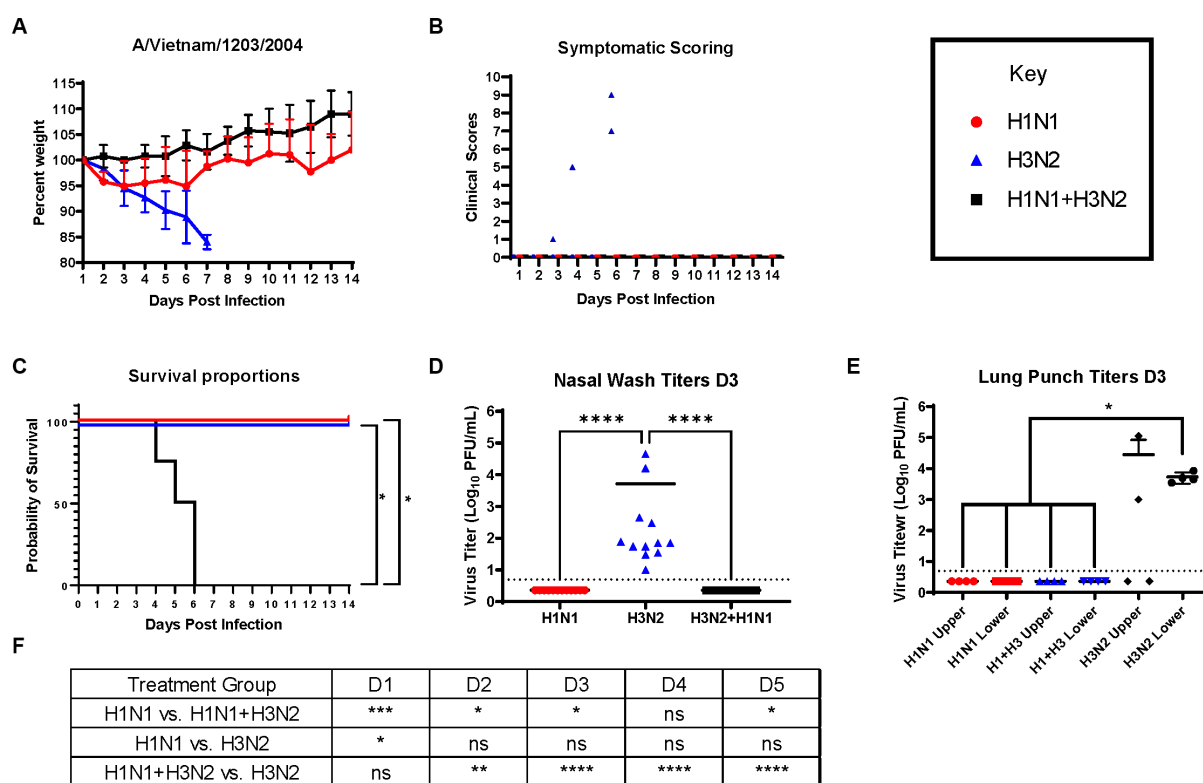


FIGURE 4

Sequential infection with a group 2 HA influenza virus does not deter primary group 1 imprinting protection. (A) Bodyweight curve of pre-immunized male fitch ferrets, $n = 12$ per group. (B) Clinical scores were recorded daily for each ferret following challenge. (C) Survival curves were obtained following H5N1 HPAI challenge. Statistical analysis performed on PRISM™ using Log-rank Mantel-Cox test (H1N1 vs. H1N1 + H3N2, $p = 0.0091$, H1N1 vs. H3N2, $P = ns$, H3N2 vs. H1N1 + H3N2, $p = 0.0091$). (D) Nasal wash samples taken on Day 2 PI tested for detectable viral titers using plaque assay (plaque forming units = PFU). Statistical analysis was performed on PRISM™ using one-way ANOVA non-parametric Kruskal-Wallis test ($p < 0.0001$). Dunn's multiple comparison test analysis was calculated and the results are indicated on the graph as asterisks: * $p < 0.05$, ** $p < 0.01$, *** $p < 0.001$, **** $p < 0.0001$; ns, no significance. (E) Lung punch samples taken on Day 2 PI tested for detectable viral titers using plaque assay (plaque-forming units = PFU). Statistical analysis was performed on PRISM™ using one-way ANOVA non-parametric Kruskal-Wallis test ($p < 0.0038$). Dunn's multiple comparison test analysis was calculated and the results are indicated on the graph as asterisks: * $p < 0.05$, ** $p < 0.01$, *** $p < 0.001$, **** $p < 0.0001$; ns, no significance. (F) Statistical analysis of body weight loss between day 1 and day 5 post-infection (PI) performed on PRISM™ using two-way ANOVA. Statistical differences were calculated and indicated as asterisks: * $p < 0.05$, ** $p < 0.01$, *** $p < 0.001$, **** $p < 0.0001$; ns, no significance.

H3N2 (A/PC/73, $n = 3$), H2N3 (sw/MO/06, $n = 4$), or sequential vaccination of H1N1 then H2N3 (A/CA/09 and A/sw/MO/06, $n = 4$) and were allowed to recover for 84 days prior to challenge with H5N1 virus (Figure 5). Aligning with previous data, pre-immune H3N2 viral ferrets experienced significant weight loss compared to H2N3 (group 1) pre-immunized ferrets (Figures 6A,E). H3N2 pre-immune ferrets displayed a 33% mortality rate following H5N1 viral challenge (Figure 6B). However, H2N3-imprinted ferrets experienced no significant weight loss and all survived challenge, along with H1N1 and H2N3 sequentially infected ferrets (Figure 6B). Statistical analysis of weight loss using two-way-ANOVA ($p = 0.0007$) and Tukey's multiple comparisons showed significant weight differences between H3N2 and H2N3 and/or H1 + H2 pre-immune groups on Day 6–Day 9 post-infection (Figure 6F).

H3N2 influenza virus-infected ferrets were vaccinated with Hu-CO-2 virus-like particle vaccines formulated with Addavax™. Four weeks following the last boost, ferrets were intranasally challenged with the H5N1 virus. There were no observable clinical symptoms, weight loss (Figure 6C), or mortality (Figure 6D) following challenge. Sera taken from Ferrets had an increase in HAI activity

against the A/VN/04 virus on days 84 and 140 following vaccination (Figure 6E).

3.4 Recombinant protein vaccination protects ferrets from lethal challenge with H5N1 virus

While ferrets imprinted with group 1 influenza viruses can induce protective immune responses against H5N1 challenge, the exact mechanism of protection is unclear. To better understand this phenomenon, both female and male ferrets were pre-immunized with an H3N2 influenza virus (A/TX/12) and then vaccinated with HA or NA protein vaccines followed by challenge with an H5N1 A/VN/04 influenza virus (1×10^5 pfu/ml) (Figure 7).

Pre-immune ferrets vaccinated with A/CA/09-HA rapidly lost weight and by day 5 post-infection, 50% of the ferrets had died, which was similar to mock vaccinated ferrets except that all the ferrets died between days 3 and 9 post-infection (Figures 8A,B). Ferrets vaccinated with either HA from A/VN/04 or Hu-CO 2 all survived challenge (Figure 8B). However, ferrets vaccinated with

Pre-immunity/Priming	Vaccination	Challenge Virus
H2N3	Hu-CO2	A/Vietnam/1203/2004 H5N1
	Control	
H3N2	Hu-CO2	
	Control	
H1N1/H2N3	Hu-CO2	
	Control	

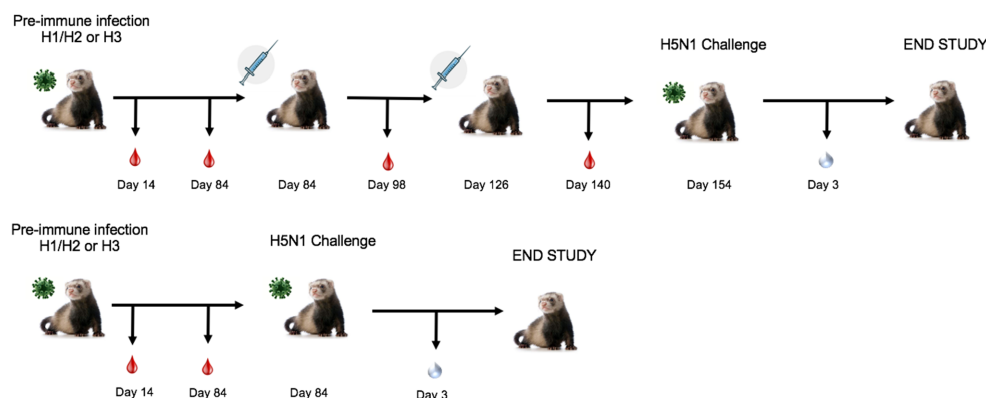


FIGURE 5

Schematic representation of tertiary pre-immune ferret study. Female fitch ferrets aged 9–12 months were intranasally infected with either an H3N2 virus (A/PC/73, $n = 8$), H2N3 (A/sw/MO/06), or a sequential infection of H1N1 + H2N3 (A/CA/09 followed by A/sw/MO/06). Ferrets were then intramuscularly vaccinated on a prime–boost regimen with either a Hu-CO 2 VLP formulated with Addavax™ adjuvant or PBS (control). Then, 28 days following vaccination, all groups were challenged intranasally using highly pathogenic avian influenza (HPAI) H5N1 A/VN/04 (PFU 1×10^5). Studies using HPAI were performed in a BSL-3 select agent accredited facility. Ferrets were monitored for 9 days following challenge.

Hu-CO-2 rHA had less than 5% weight loss, whereas ferrets vaccinated with A/VN/04 rHA lost between 10 and 15% of their original body weight. Ferrets pre-immune to H3N2 influenza viruses that were mock vaccinated had neurological signs or were found to be moribund before they reached the 75% weight cut-off and experienced high clinical scores (Figure 8C) with high viral nasal wash titers in control group ferrets (Figure 8D), whereas vaccinated ferrets had no significant viral nasal wash titers (Figure 8D).

On day 3 post-challenge, lung punches were collected from the upper and lower quadrants of each lung. All ferrets had detectable influenza virus in both upper and lower lung quadrants. Control and A/CA/09-HA-vaccinated ferrets had the highest upper quadrant viral lung titers (Figure 8E). Ferrets vaccinated with A/VN/04-HA had lower viral titers in the upper respiratory tract compared to Control and A/CA/09-HA-vaccinated ferrets.

Ferrets seroconverted to the pre-immune strain A/TX/12 (Supplementary Figure S3), as well as all the vaccines used to vaccinate each ferret (Supplementary Figure S3D). Sera collected from ferrets with A/VN/04-HA protein had detectable IgG anti-A/CA/09-HA antibodies and A/CA/09-HA-vaccinated ferrets had antibodies against A/VN/04-HA; however, these antibodies were not protective in challenge (Supplementary Figure S3B). Histological samples taken 3 days following infection showed that ferrets vaccinated with the Hu-CO 2 vaccine had lower cellular infiltrates when compared to A/CA/09- and A/VN/04-vaccinated ferrets (Supplementary Figure S4), and all three vaccine groups improved lung pathology in comparison to unvaccinated H3N2 primed controls (Supplementary Figure S4D).

4 Discussion

Overall, there are patterns of influenza group imprinting that affect the clinical outcomes of H5N1 virus infections in the ferret model of disease. This study found that group 1 HA influenza A viruses (IAV) elicited heterosubtypic protection against lethal challenge of highly pathogenic avian influenza virus (HPAIV) H5N1 (Figures 2C, 4C, 6B). This data correlates with multiple studies predicting the heterosubtypic immune response elicited by group 1 viruses against group 1 pandemic strains. Specifically, heterosubtypic immunity has been well established in mouse and ferret models of disease (33–37). In lethal challenge studies, naïve female BALB/c mice intranasally inoculated with PR8 (H1N1) virus and subsequently challenged with X31 (H3N2 virus) experienced accelerated viral clearance in the lungs 5 days after challenge (34). However, PR8-priming did not offer complete protection from X31-induced disease in these mice (34). A similar study performed in mice evaluated the heterologous protection of a recombinant influenza virus containing internal influenza B genes and neuraminidase and HA from H1 or H3 virus (35). Mice inoculated with the recombinant B-H1 virus exhibited enhanced protection against H5N1 viral challenge, whereas mice primed with the B-H3 virus or influenza B virus displayed higher morbidity and lower survival rates (35).

The hypothesis of influenza group-dependent imprinting and immunity is further established using Ferret disease models, as they are considered the gold standard for influenza virus infection. In this study, ferrets that received the H3N2 A/Sing/86 virus were afforded partial protection against mortality, whereas male ferrets inoculated

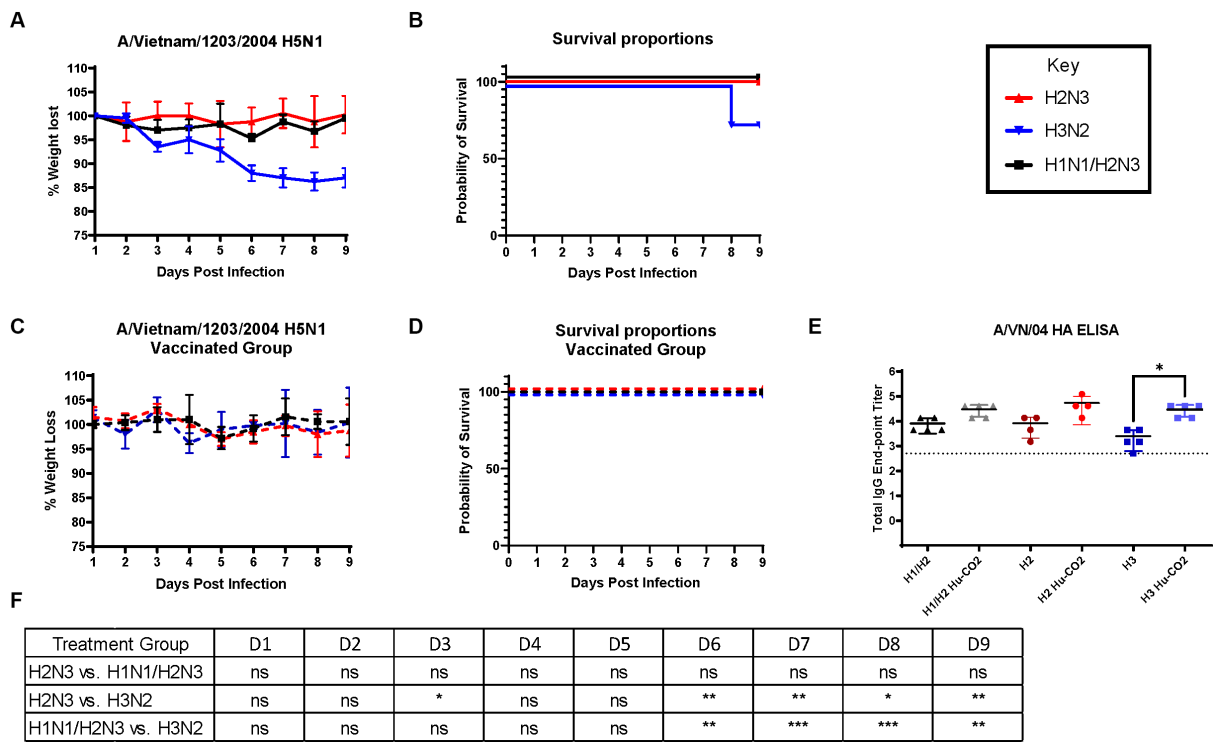


FIGURE 6
Influenza H2 imprinting protects ferrets from HPAI lethal challenge. **(A)** Bodyweight curve of pre-immunized female fitch ferrets, $n = 4$ per group. **(B)** Survival curves were obtained following H5N1 HPAI challenge. **(C)** Bodyweight curves of vaccinated pre-immunized female fitch ferrets, $n = 4$ per group. **(D)** Survival curves of vaccinated ferrets obtained following H5N1 HPAI challenge. **(E)** Statistical analysis of body weight loss between imprinting groups post-exposure performed on PRISM™ using two-way ANOVA. Statistical differences were calculated and indicated as asterisks: * $p < 0.05$, ** $p < 0.01$, *** $p < 0.001$, **** $p < 0.001$; ns, no significance.

Imprinting Virus	Vaccination	Challenge Virus
H3N2	CA/09 HA	H5N1 A/Vietnam/1203/2004
	VN/04 HA	
	Hu-CO-2	
	PBS/Control	

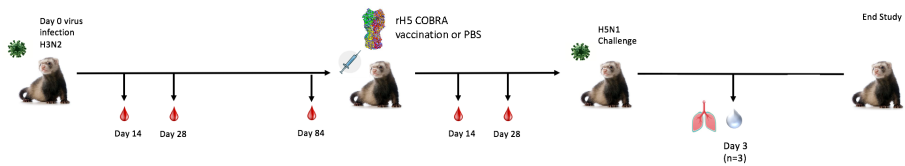


FIGURE 7
Schematic representation of H3N2 pre-immune vaccine study. Female fitch ferrets aged 9–12 months were intranasally infected using the H3N2 (A/TX/12) virus for pre-immune imprinting. After 84 days, ferrets were intramuscularly vaccinated with rHA formulated with Addavax™. Vaccines contained either A/CA/09-HA, A/VN/-4-HA, Hu-CO 2-HA, or PBS (control). Then, 28 days following vaccination, all groups were challenged intranasally using highly pathogenic avian influenza (HPAI) H5N1 A/VN/04 (PFU 1×10^5). Studies using HPAI were performed in a BSL-3 select agent accredited facility. Ferrets were monitored for 14 days following challenge. **(E)** Ferret serum collected on day 84 and day 140 was tested for total IgG reactivity against A/VN/04 HA antigen in an ELISA assay. Limit of detection for this assay is represented by dotted line. **(F)** (previously E).

with H3N2 strain A/HK/68 all succumbed to disease within 6 days following challenge. It is important to note here that although the dosage of the virus was slightly increased to compensate for the increased mass of the male ferret, the same viral strain and passage were used. In hindsight, a similar study should be performed in female

ferrets inoculated with the A/HK/68 strain to correlate mortality and sex differences. This, however, does not lead us to believe that the H3N2 virus strain A/HK/68 would elicit significant protective heterosubtypic immunity to the extent of group 1 HA imprinting. Previous studies involving H3N2 virus pre-immunity also display

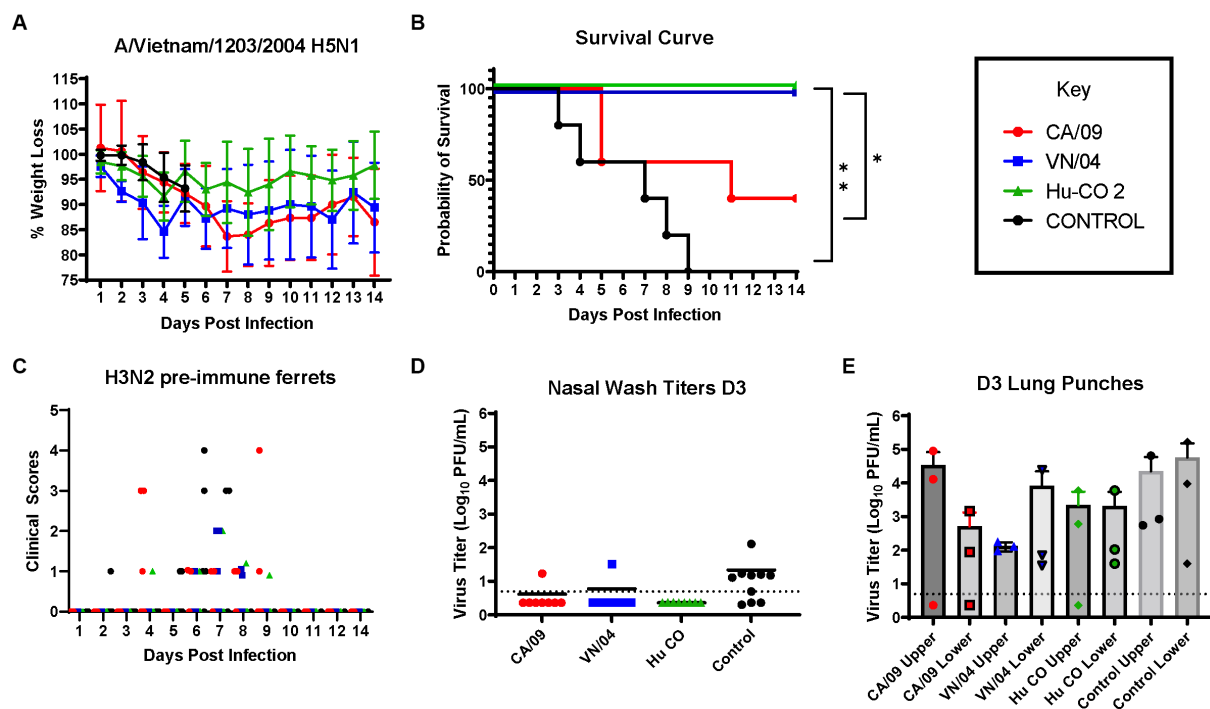


FIGURE 8

H3N2 pre-immune ferrets vaccinated with Human-COBRA 2 HA are rescued from lethal challenge with HPAI virus. (A) Bodyweight curve of pre-immunized control ($n = 10$) and vaccinated female fitch ferrets, $n = 8$ per vaccine group. (B) Survival curves obtained following H5N1 HPAI challenge. Statistical analysis performed on PRISM™ software using Log-rank Mantel-Cox test (Hu-Co 2 or A/VN/04 vs. A/CA/09, $p = 0.0486$, Hu-Co2 or A/VN/04 vs. PBS, $p = 0.0018$). (C) Clinical Scores were recorded for each ferret following H5N1 challenge. (D) Nasal wash samples obtained from anesthetized ferrets on Day 3 PI were tested for detectable viral titers using plaque assay (PFU, plaque forming units). (E) Lung-punch samples taken on Day 2 PI were tested for detectable viral titers using plaque assay (PFU, plaque forming units).

varying results with different H3N2 strains (36, 37). Ferrets inoculated with A/Victoria/361/2011 H3N2 virus and subsequently challenged with the H5N1 virus all succumbed to systemic disease and encephalitis (37). However, ferrets made pre-immune with H3N2 strain A/Perth/16/2009 all survived challenge and experienced lower viral replication and weight loss and fewer clinical symptoms compared to PBS control (36).

The protective effects of group 1 HA imprinting did not falter, however, differing with the viral H1N1 strains both in this study and previous studies (36, 37). Male ferrets primed with H1N1 strain A/Mar/43 showed complete protection from clinical symptoms following viral challenge. This was also true for group 1 HA strain A/sw/MO/06 (H2N3)-primed ferrets, where lethal challenge with the H5N1 virus resulted in no weight loss or clinical symptoms. The investigation of H2 pre-immunity is especially relevant in the context of vaccine preparedness for the elderly population. The influenza virus strain H2N2 circulated from 1957 to 1968, resulting in the Asian Flu pandemic in East Asia (33). During this pandemic, an estimated 1.1 million deaths occurred worldwide (33). Individuals born during this time have also shown decreased severe clinical outcomes against H5N1 virus infection (14). Utilizing this strain not only strengthens influenza group-dependent immunity but also removes the possible effects of matching neuraminidase-induced antibodies against avian-derived N1.

Although group 1 HA-primed ferrets were protected from H5N1 virus-induced disease, the exact mechanism of protection is not well understood. We first thought to investigate the generation of

neutralizing HA stem antibodies following pre-immunity as a protective mechanism against disease. Influenza HA-stem antibodies are commonly studied due to their therapeutic potential against IAV disease and are often targeted for vaccine design due to their conserved epitopes (33, 38–41). The chimeric HA protein containing an H6 head and H1 stalk was utilized in this study to detect HA stalk binding IgG in pre-immune ferret sera, assuming the sera would not contain cross-reactive Abs binding the H6 HA head. Although there were many ferrets that contained cross-reactive stem IgG, there was no correlation between HA-stalk Ab and reduced clinical symptoms (Figure 2E and Supplementary Figure S3C). Previous mouse studies have found a positive correlation with stalk-reactive IgG levels and heterologous virus protection (42). However, the lack of cross-reactive antibodies has been documented in pre-immune ferrets models of disease (34).

In the absence of cross-reactive antibodies, protection against heterologous strains of influenza can be attributed to cellular immunity. T-cell-mediated memory responses against heterologous viral challenge have been studied in ferret models of disease (43, 44). Naïve ferrets imprinted with H1N1 IAV experienced decreased viral shedding and clinical symptoms following H3N2 viral infection but were not entirely protected from disease (43). Ferrets inoculated with H1N1 influenza viruses lacked serum antibodies against the H3N2 virus but had a peak in interferon gamma-secreting T cells 11 days following H3N2 viral challenge (43). In ferrets receiving live attenuated influenza vaccine (LAIV) in human studies, live attenuated influenza vaccination (LAIV) in young children elicits both

serological and cellular immunity (45). LAIV mimics influenza viral infection and induces robust CD4+ and CD8+ T-cell activation, which cannot be achieved through TIV (45). Testing serum IgG antibodies in pre-immune ferrets provides a small insight into the mechanism of protection of group 1 imprinted ferrets against H5 challenge. Cellular or humoral responses against neuraminidase or matrix proteins were not studied here. However, it is clear that Group 1 H2-imprinted ferrets lacking a matching neuraminidase (N3) offered complete protection from H5N1 virus morbidity and mortality.

In attempts to remedy the lack of complete protection from H3N2 viral inoculation, ferrets were intramuscularly vaccinated with monovalent wildtype rHA or with the Human COBRA 2 vaccine. Vaccinated ferrets did not experience clinical symptoms or mortality following challenge. This was also true for the rHA A/VN/04-vaccinated ferrets. This may lead to the conclusion that monovalent strains of vaccination are equally efficacious to chimeric-COBRA rHA. This, however, can be disproven by decades-long research showing the broad reactivity of Hu-CO2 against variant strains of H5 in multiple animal models of disease (32, 46–50). From here, we can conclude that the H3N2 group 2 imprinting can be rescued by pandemic vaccination of a chimeric H5 HA protein expressing Hu-CO 2 or through vaccination with a matching monovalent strain. It is also important to note that the monovalent rHA vaccines were tested using a one-shot regimen in order to simulate dose sparing in pandemic vaccination. Interestingly, 60% of A/CA/09 HA-vaccinated ferrets died and had clinical symptoms similar to H3N2 mock-vaccinated ferrets (Figures 8B,C). This could be due to the low immunogenicity of the A/CA/09 HA protein; however, IgG titers from A/CA/09 HA-vaccinated ferrets had similar IgG titers to A/CA/09 HA and Hu-Co-2 rHA-vaccinated ferrets, which all survived H5N1 influenza virus challenge (Supplementary Figure S3). This further reiterates the lack of correlation between cross-reactive Abs to the challenge strain and protection.

These immune imprinting effects play a role in the development of a universal influenza vaccine. Many studies have led to the speculation that an individual's birth year and subsequent viral imprinting determine the trajectory of future antibody responses to vaccination (12, 14, 33, 34). Therefore, vaccine studies performed in animal models lacking pre-immunity greatly delay the progression of designing a universal influenza virus vaccine. Vaccine studies in naïve ferret models have resulted in narrowly binding Ab repertoires, lacking the breadth and strength of responses in previously infected/pre-immune ferrets (51, 52). Vaccination in a naïve immunological background may also result in increased clinical symptoms following pandemic strain H1N1 A/CA/09 viral challenge, suggesting that vaccination in the absence of primary infection leads to the development of non-neutralizing antibodies (35).

The current H5N1 viral outbreak continues to devastate animal populations including poultry, wild birds, and wild mammals. The individuals responsible for maintaining poultry populations for food and survival are at imminent risk of contracting disease. In addition, the increased incident rate of H5N1 spillover into the human population increases the probability of viral mutation and spread, as has been seen

in reports in Ecuador, Cambodia, and Chile (53–55). Vaccine design and implementation should be a top priority for pandemic preparedness, and the development of an immunogenic universal H5 vaccine will have to consider the pre-immune status of the individuals in question. The specific aims of universal influenza vaccine coverage include the following: 1. all influenza A and B viruses independent of the NA subtype; 2. historical and future influenza strains; 3. pandemic influenza strains; and 4. protection from zoonotic spillover (56, 57). These goals can be achieved by implementing a chimeric HA vaccine that targets conserved epitopes shared throughout H5 viral clades, addressing the problematic accelerated evolution of the H5 virus HA protein. In this study, we demonstrated the protective effects of group 1 influenza pre-immunity against H5N1 viral challenge, and the variable effects of group 2 H3N2 pre-immunity that can be rescued with a one-dose vaccination using a highly immunogenic broadly reactive HA antigen Human COBRA 2 formulated with adjuvant. The efficacy of the H5 Human COBRA 2 vaccine and its predecessors will continue to be investigated in animal models of disease (46), and further studies will be conducted to access immunogenicity in a pre-immunological background against new variant H5 viral strains.

Data availability statement

The raw data supporting the conclusions of this article will be made available by the authors, without undue reservation.

Ethics statement

The animal study was approved by Leanne Alworth-University of Georgia IACUC Office of Research Director. The study was conducted in accordance with the local legislation and institutional requirements.

Author contributions

IN: Conceptualization, Data curation, Formal analysis, Investigation, Methodology, Writing – original draft, Writing – review & editing. HJ: Investigation, Methodology, Project administration, Supervision, Writing – review & editing. YH: Methodology, Validation, Writing – review & editing. AK: Conceptualization, Methodology, Project administration, Resources, Writing – review & editing. TR: Conceptualization, Funding acquisition, Project administration, Resources, Supervision, Visualization, Writing – review & editing.

Funding

The author(s) declare financial support was received for the research, authorship, and/or publication of this article. This work was supported by National Institute of Allergy and Infectious Diseases (NIAID), U.S. National Institutes of Health (NIH), Department of Health and Human Services contract 75N93019C00052 (TR); University of Georgia (US) grant UGA-001 (TR); Georgia Research Alliance (US) grant GRA-001 (TR).

Acknowledgments

The authors would like to thank Zachary Beau Reneer for providing technical assistance and Jeff Ecker and Spencer Pierce for the production of recombinant proteins. We acknowledge the staff at the University of Georgia-Animal Resources for their excellent care of the animals used in this study and the Animal Health Research Center at the University of Georgia for the upkeep and maintenance of the BSL-3 facilities.

Conflict of interest

The authors declare that the research was conducted in the absence of any commercial or financial relationships that could be construed as a potential conflict of interest.

References

- de St Fazekas G, Webster R. Disquisitions on original antigenic sin. II. Proof in lower creatures. *J Exp Med.* (1966) 124:347–61. doi: 10.1084/jem.124.3.347
- Francis T. On the doctrine of original antigenic sin. *Proc Am Philos Soc.* (1960) 104:572–8.
- Lessler J, Riley S, Read JM, Wang S, Zhu H, Smith GJD, et al. Evidence for antigenic seniority in influenza A (H3N2) antibody responses in southern China. *PLoS Pathog.* (2012) 8:e1002802. doi: 10.1371/journal.ppat.1002802
- Francis T Jr. The current status of the control of influenza. *Ann Intern Med.* (1955) 43:534–8. doi: 10.7326/0003-4819-43-3-534
- Huang K-YA, Rijal P, Schimanski L, Powell TJ, Lin TY, McCauley JW, et al. Focused antibody response to influenza linked to antigenic drift. *J Clin Invest.* (2015) 125:2631–45. doi: 10.1172/JCI81104
- Davenport FM, Hennessy AV. A serologic recapitulation of past experiences with influenza A; antibody response to monovalent vaccine. *J Exp Med.* (1956) 104:85–97. doi: 10.1084/jem.104.1.85
- Hennessy A, Davenport F, Francis T. Studies of antibodies to strains of influenza virus in persons of different ages in sera collected in a postepidemic period. *J Immunol.* (1955) 75:401–9. doi: 10.4049/jimmunol.75.5.401
- Thompson MG, Naleway A, Fry AM, Ball S, Spencer SM, Reynolds S, et al. Effects of repeated annual inactivated influenza vaccination among healthcare personnel on serum hemagglutinin inhibition antibody response to a/Perth/16/2009 (H3N2)-like virus during 2010–11. *Vaccine.* (2016) 34:981–8. doi: 10.1016/j.vaccine.2015.10.119
- Kosikova M, Li L, Radvak P, Ye Z, Wan XF, Xie H. Imprinting of repeated influenza A/H3 exposures on antibody quantity and antibody quality: implications on seasonal vaccine strain selection and vaccine performance. *Clin Infect Dis.* (2018) 67:1523–32. doi: 10.1093/cid/ciy327
- Dhar N, Kwatra G, Nunes MC, Cutland C, Izu A, Nachbagauer R, et al. Hemagglutinin stalk antibody responses following trivalent inactivated influenza vaccine immunization of pregnant women and association with protection from influenza virus illness. *Clin Infect Dis.* (2019) 71:1072–9. doi: 10.1093/cid/ciz927
- Fonville JM, Wilks S, James SL, Fox A, Ventresca M, Aban M, et al. Antibody landscapes after influenza virus infection or vaccination. *Science.* (2014) 346:996–1000. doi: 10.1126/science.1256427
- Nuñez IA, Carlock MA, Allen JD, Owino SO, Moehling KK, Nowalk P, et al. Impact of age and pre-existing influenza immune responses in humans receiving split inactivated influenza vaccine on the induction of the breadth of antibodies to influenza A strains. *PLoS One.* (2017) 12:e0185666. doi: 10.1371/journal.pone.0185666
- Davenport FM, Hennessy AV, Francis T. Epidemiologic and immunologic significance of age distribution of antibody to antigenic variants of influenza virus. *J Exp Med.* (1953) 98:641–56. doi: 10.1084/jem.98.6.641
- Gostic KM, Ambrose M, Worobey M, Lloyd-Smith JO. Potent protection against H5N1 and H7N9 influenza via childhood hemagglutinin imprinting. *Science.* (2016) 354:722–6. doi: 10.1126/science.aag1322
- Sanz I, Rojo S, Tamames S, Eiros J, Ortiz de Lejarazu R. Heterologous humoral response against H5N1, H7N3, and H9N2 avian influenza viruses after seasonal vaccination in a European elderly population. *Vaccine.* (2017) 35:17. doi: 10.3390/vaccines5030017
- Russell RJ, Kerry PS, Stevens DJ, Steinhauer DA, Martin SR, Gamblin SJ, et al. Structure of influenza hemagglutinin in complex with an inhibitor of membrane fusion. *Proc Natl Acad Sci.* (2008) 105:17736–41. doi: 10.1073/pnas.0807142105

Publisher's note

All claims expressed in this article are solely those of the authors and do not necessarily represent those of their affiliated organizations, or those of the publisher, the editors and the reviewers. Any product that may be evaluated in this article, or claim that may be made by its manufacturer, is not guaranteed or endorsed by the publisher.

Supplementary material

The Supplementary material for this article can be found online at: <https://www.frontiersin.org/articles/10.3389/fvets.2023.1286758/full#supplementary-material>

- Baz M, Luke CJ, Cheng X, Jin H, Subbarao K. H5N1 vaccines in humans. *Virus Res.* (2013) 178:78–98. doi: 10.1016/j.virusres.2013.05.006
- Nicholson K, Tyrrell D, Harrison P, Potter CW, Jennings R, Clark A, et al. Clinical studies of monovalent inactivated whole virus and subunit A/USSR/77 (H1N1) vaccine: serological responses and clinical reactions. *J Biol Stand.* (1979) 7:123–36. doi: 10.1016/S0092-1157(79)80044-X
- Zost SJ, Parkhouse K, Gumina ME, Kim K, Diaz Perez S, Wilson PC, et al. Contemporary H3N2 influenza viruses have a glycosylation site that alters binding of antibodies elicited by egg-adapted vaccine strains. *Proc Natl Acad Sci.* (2017) 114:12578–83. doi: 10.1073/pnas.1712377114
- Treanor JJ, Campbell JD, Zangwill KM, Rowe T, Wolff M. Safety and immunogenicity of an inactivated subvirion influenza A (H5N1) vaccine. *N Engl J Med.* (2006) 354:1343–51. doi: 10.1056/NEJMoa055778
- Zangwill KM, Treanor JJ, Campbell JD, Noah DL, Ryea J. Evaluation of the safety and immunogenicity of a booster (third) dose of inactivated subvirion H5N1 influenza vaccine in humans. *J Infect Dis.* (2008) 197:580–3. doi: 10.1086/526537
- Chotpitayasonondh T, Thisyakorn U, Pancharoen C, Pepin S, Nougarede N. Safety, humoral and cell mediated immune responses to two formulations of an inactivated, split-virion influenza A/H5N1 vaccine in children. *PLoS One.* (2008) 3:e4028. doi: 10.1371/journal.pone.0004028
- Nolan T, Richmond PC, Formica NT, Höschler K, Skeljo MV, Stoney T, et al. Safety and immunogenicity of a prototype adjuvanted inactivated split-virus influenza A (H5N1) vaccine in infants and children. *Vaccine.* (2008) 26:6383–91. doi: 10.1016/j.vaccine.2008.08.046
- Treanor JJ, Wilkinson BE, Masseoud F, Hu-Primmer J, Battaglia R, O'Brien D, et al. Safety and immunogenicity of a recombinant hemagglutinin vaccine for H5 influenza in humans. *Vaccine.* (2001) 19:1732–7. doi: 10.1016/S0264-410X(00)00395-9
- Levine MZ, Holiday C, Liu F, Jefferson S, Gillis E, Bellamy AR, et al. Cross-reactive antibody responses to novel H5Nx influenza viruses following homologous and heterologous prime-boost vaccination with a Prepandemic stockpiled A (H5N1) vaccine in humans. *J Infect Dis.* (2017) 216:S555–9. doi: 10.1093/infdis/jix001
- Sun X, Belser JA, Pulit-Penaloza JA, Creager HM, Guo Z, Jefferson SN, et al. Stockpiled pre-pandemic H5N1 influenza virus vaccines with AS03 adjuvant provide cross-protection from H5N2 clade 2.3. 4.4 virus challenge in ferrets. *Virology.* (2017) 508:164–9. doi: 10.1016/j.virol.2017.05.010
- Oh DY, Hurt AC. Using the ferret as an animal model for investigating influenza antiviral effectiveness. *Front Microbiol.* (2016) 7:80. doi: 10.3389/fmicb.2016.00080
- Smith W, Andrewes CH, Laidlaw PP. A virus obtained from influenza patients. *Lancet.* (1933) 222:66–8. doi: 10.1016/S0140-6736(00)78541-2
- Jia N, Barclay WS, Roberts K, Yen HL, Chan RY, Lam AKY, et al. Glycomic characterisation of respiratory tract tissues of ferrets: implications for its use in influenza virus infection studies. *J Biol Chem.* (2014) 289:28489–504. doi: 10.1074/jbc.M114.588541
- Ng P, Böhm R, Hartley-Tassell L, Steen JA, Wang H, Lukowski SW, et al. Ferrets exclusively synthesize Neu5Ac and express naturally humanized influenza A virus receptors. *Nat Commun.* (2014) 5:5750. doi: 10.1038/ncomms6750
- He W, Mullarkey CE, Duty JA, Moran TM, Palese P, Miller MS. Broadly neutralizing anti-influenza virus antibodies: enhancement of neutralizing potency in polyclonal mixtures and IgA backbones. *J Virol.* (2015) 89:3610–8. doi: 10.1128/JVI.03099-14

32. Bar-Peled Y, Huang J, Nuñez IA, Pierce SR, Ecker JW, Ross TM, et al. Structural and antigenic characterization of a computationally-optimized H5 hemagglutinin influenza vaccine. *Vaccine*. (2019) 37:6022–9. doi: 10.1016/j.vaccine.2019.08.062
33. Widge AT, Hofstetter AR, Houser KV, Awan SF, Chen GL, Burgos Florez MC, et al. An influenza hemagglutinin stem nanoparticle vaccine induces cross-group 1 neutralizing antibodies in healthy adults. *Sci Transl Med*. (2023) 15:eade4790. doi: 10.1126/scitranslmed.ade4790
34. le Sage V, Jones JE, Kormuth KA, Fitzsimmons WJ, Nturibi E, Padovani GH, et al. Pre-existing heterosubtypic immunity provides a barrier to airborne transmission of influenza viruses. *PLoS Pathog*. (2021) 17:e1009273. doi: 10.1371/journal.ppat.1009273
35. Francis ME, McNeil M, Dawe NJ, Foley MK, King ML, Ross TM, et al. Historical H1N1 influenza virus imprinting increases vaccine protection by influencing the activity and sustained production of antibodies elicited at vaccination in ferrets. *Vaccine*. (2019) 37:133. doi: 10.3390/vaccines7040133
36. Park SJ, Kim EH, Pascua PNQ, Kwon HI, Lim GJ, Decano A, et al. Evaluation of heterosubtypic cross-protection against highly pathogenic H5N1 by active infection with human seasonal influenza virus or trivalent inactivated vaccine immunization in ferret models. *J Gen Virol*. (2014) 95:793–8. doi: 10.1099/vir.0.058636-0
37. Bissel SJ, Wang G, Carter DM, Crevar CJ, Ross TM, Wiley CA. H1N1, but not H3N2, influenza virus infection protects ferrets from H5N1 encephalitis. *J Virol*. (2014) 88:3077–91. doi: 10.1128/JVI.01840-13
38. Andrews SF, Cominsky LY, Shimberg GD, Gillespie RA, Gorman J, Raab JE, et al. An influenza H1 hemagglutinin stem-only immunogen elicits a broadly cross-reactive B cell response in humans. *Sci Transl Med*. (2023) 15:eade4976. doi: 10.1126/scitranslmed.ade4976
39. Andrews SF, Raab JE, Gorman J, Gillespie RA, Cheung CSF, Rawi R, et al. A single residue in influenza virus H2 hemagglutinin enhances the breadth of the B cell response elicited by H2 vaccination. *Nat Med*. (2022) 28:373–82. doi: 10.1038/s41591-021-01636-8
40. Fukuyama H, Shinnakasu R, Kurosaki T. Influenza vaccination strategies targeting the hemagglutinin stem region. *Immunol Rev*. (2020) 296:132–41. doi: 10.1111/immr.12887
41. Moin SM, Boyington JC, Boyoglu-Barnum S, Gillespie RA, Cerutti G, Cheung CSF, et al. Co-immunization with hemagglutinin stem immunogens elicits cross-group neutralizing antibodies and broad protection against influenza A viruses. *Immunity*. (2022) 55:2405–2418.e7. doi: 10.1016/j.immuni.2022.10.015
42. Carreño JM, Strohmeier S, Kirkpatrick Roubidoux E, Hai R, Palese P, Krammer F. H1 hemagglutinin priming provides long-lasting heterosubtypic immunity against H5N1 challenge in the mouse model. *MBio*. (2020) 11:e02090-20. doi: 10.1128/mBio.02090-20
43. Gooch KE, Marriott AC, Ryan KA, Yeates P, Slack GS, Brown PJ, et al. Heterosubtypic cross-protection correlates with cross-reactive interferon-gamma-secreting lymphocytes in the ferret model of influenza. *Sci Rep*. (2019) 9:2617. doi: 10.1038/s41598-019-38885-0
44. Marriott AC, Gooch KE, Brown PJ, Ryan KA, Jones NJ, Merredew N, et al. Severity of heterosubtypic influenza virus infection in ferrets is reduced by live attenuated influenza vaccine. *NPJ Vaccines*. (2021) 6:43. doi: 10.1038/s41541-021-00306-7
45. Carter NJ, Curran MP. Live Attenuated Influenza Vaccine (FluMist®; Fluzent™). *Drugs*. (2011) 71:1591–622. doi: 10.2165/11206860-000000000-00000
46. Nuñez IA, Huang Y, Ross TM. Next-generation computationally designed influenza hemagglutinin vaccines protect against H5Nx virus infections. *Pathogens*. (2021) 10:1352. doi: 10.3390/pathogens10111352
47. Giles BM, Ross TM. A computationally optimized broadly reactive antigen (COBRA) based H5N1 VLP vaccine elicits broadly reactive antibodies in mice and ferrets. *Vaccine*. (2011) 29:3043–54. doi: 10.1016/j.vaccine.2011.01.100
48. Giles BM, Bissel SJ, DeAlmeida DR, Wiley CA, Ross TM. Antibody breadth and protective efficacy are increased by vaccination with computationally optimized hemagglutinin but not with polyvalent hemagglutinin-based H5N1 virus-like particle vaccines. *Clin Vaccine Immunol*. (2012) 19:128–39. doi: 10.1128/CVI.05533-11
49. Giles BM, Crevar CJ, Carter DM, Bissel SJ, Schultz-Cherry S, Wiley CA, et al. A computationally optimized hemagglutinin virus-like particle vaccine elicits broadly reactive antibodies that protect nonhuman primates from H5N1 infection. *J Infect Dis*. (2012) 205:1562–70. doi: 10.1093/infdis/jis232
50. Bertran K, Kassa A, Criado MF, Nuñez IA, Lee DH, Killmaster L, et al. Efficacy of recombinant Marek's disease virus vectored vaccines with computationally optimized broadly reactive antigen (COBRA) hemagglutinin insert against genetically diverse H5 high pathogenicity avian influenza viruses. *Vaccine*. (2021) 39:1933–42. doi: 10.1016/j.vaccine.2021.02.075
51. Skarupka AL, Bebin-Blackwell A-G, Sumner SF, Ross TM. Universal influenza virus neuraminidase vaccine elicits protective immune responses against human seasonal and pre-pandemic strains. *J Virol*. (2021) 95:e0075921. doi: 10.1128/JVI.00759-21
52. Skarupka AL, Zhang X, Blas-Machado U, Sumner SF, Ross TM. Multi-influenza HA subtype protection of ferrets vaccinated with an N1 COBRA-based neuraminidase. *Viruses*. (2023) 15:184. doi: 10.3390/v15010184
53. WHO. (2023). *Human infection caused by avian influenza a(H5) – Ecuador WHO. INT*. World Health Organization. WHO. Human infection caused by avian influenza A(H5) - Ecuador WHO.int/emergencies/diseaseoutbreaknews: World Health Organization; 2023 [Accessed 21 Aug 2023].
54. CDC. (2023). Human Infection with highly pathogenic avian influenza A(H5N1) virus in Chile CDC.GOV: Center for Disease Control and Prevention. Available at: <https://www.cdc.gov/flu/avianflu/spotlights/2022-2023/chile-first-case-h5n1-addendum.htm> (Accessed Aug 21, 2023).
55. WHO. (2023). Avian Influenza A (H5N1) – Cambodia WHO.INT. World Health Organization. [updated February 26, 2023]. Available at: <https://www.who.int/emergencies/disease-outbreak-news/item/2023-DON445> (Accessed Aug 21, 2023)
56. Huang P, Sun L, Li J, Wu Q, Rezaei N, Jiang S, et al. Potential cross-species transmission of highly pathogenic avian influenza H5 subtype (HPAI H5) viruses to humans calls for the development of H5-specific and universal influenza vaccines. *Cell Discov*. (2023) 9:58. doi: 10.1038/s41421-023-00571-x
57. Nachbagauer R, Krammer F. Universal influenza virus vaccines and therapeutic antibodies. *Clin Microbiol Infect*. (2017) 23:222–8. doi: 10.1016/j.cmi.2017.02.009

Frontiers in Veterinary Science

Transforms how we investigate and improve
animal health

The third most-cited veterinary science journal,
bridging animal and human health with a
comparative approach to medical challenges. It
explores innovative biotechnology and therapy for
improved health outcomes.

Discover the latest Research Topics

[See more →](#)

Frontiers

Avenue du Tribunal-Fédéral 34
1005 Lausanne, Switzerland
frontiersin.org

Contact us

+41 (0)21 510 17 00
frontiersin.org/about/contact

